University College London

Department of Chemistry

Faculty of Mathematical and Physical Sciences (MAPS)

Polymers from Food Wastes

SANDRA ALINE SANCHEZ VAZQUEZ

Submitted in fulfilment of the requirements for the degree of

Doctor of Philosophy

Supervisors:

Prof. Julian R. G. Evans

Prof. Helen C. Hailes

London, United Kingdom **2014**

"Success is not final, failure is not fatal: it is the courage to continue that counts."

Winston Churchill

"Sólo triunfa en el mundo quien se levanta y busca las circunstancias y las crea si no las encuentra."

George Bernard Shaw

"En vérité, le chemin importe peu, la volonté d'arriver suffit à tout."

Albert Camus

Acknowledgments

I want to thank my supervisors; Prof. J. Evans for giving me the opportunity to work with him, for his suggestions and support during this time and to Prof. H. Hailes for her advice and support during this project.

I also greatly appreciate the assistance from Mr Phil Hayes and Mr. David Webb, the technical staff in the Turner Lab, for their time and guidance in the use of GC and FT-IR instruments. And to Mr. Martin Vickers who helped and taught me how to use the XRD equipment.

I want to acknowledge the financial support of the National Council of Science and Technology of Mexico (abbreviated CONACYT) which allowed me to opportunity to come to England and accomplish these studies.

To my parents and sister to whom I owe this success and which words are not enough to express my gratitude towards them for all their patience and encouragement during these three years. I would also like to thank the Fagnoni family for taking care of me and looking at me as part of their family. A special gratitude to Eugenia Ramirez, Georgios Kalopitas and Jose Antonio Lopez for their patience and support.

Declaration of work

I, Sandra Aline Sanchez Vazquez confirm that the work presented in this thesis is my own. Where information has been derived from other sources, I confirm that this has been indicated in the thesis.

Abstract

The first part focuses on the conversion of limonene to dimethylstyrene in order to produce polymeric materials. Limonene was dehydrogenated over a palladium catalyst with an anhydrous solvent and base using copper chloride as oxidant under argon atmosphere at 120 °C. Solvent, base, catalyst and reaction conditions were varied in an attempt to improve conversion to DMS. The conditions for conversion to dimethylstyrene without by-products were established. Alternative and cheaper bases and catalysts were identified. It was observed that 69% of the polymer obtained was insoluble in organic solvents while the soluble part had an average M_W of 3800.

The second part focuses on the polymerization of chlorogenic acid, a potato waste product, by enzyme-based solution polymerization as a potential biomaterial. Three environments were used: (i) phosphate buffer pH7 and methanol, (ii) unbuffered water-methanol, and (iii) aqueous buffer pH7 with poly(ethylene glycol) template. To compare and understand this reaction, chlorogenic analogues were studied. Phenol polymerized to high yields in all environments. 2,3-dihydroxybenzoic acid, catechol and 2,4-dihydroxybenzoic acid polymerized to moderately high yield in (i). Caffeic acid polymerised with 23% yield in (ii) but both caffeic acid and chlorogenic acid produced higher yields when the templating method (iii) was used.

The third part of the project focused on the polymerization of oleic acid obtained from mango seed butter. Oleic acid was first purified from mango butter, then esterificated using 1,3-propanediol, resorcinol and orcinol. The resulting di-esters were epoxidized and crosslinking reactions were attempted using anhydride and amine curing agents. All polymers obtained were in form of waxes and dissolved in organic solvents, with the expection of epoxidized resorcinol di-ester cured using phenylenediamine.

Finally a study of the interaction of all the monomers with montmorillonite clay was made. Chlorogenic acid and oleic acid intercalated into the unmodified clay layers while an organoclay was used with D-limonene and dimethylstyrene to obtain intercalation.

Abbreviations

1P	Proven resources from oil
ALA	12-aminolauric acid
BHF	Bis(hydroxymethyl)-furan
DET	Diethylenetriamine
DFF	Diformylfuran
DHBA	Dihydroxybenzoic acid
DCC	Dicyclohexylcarbodiimide
DCM	Dichloromethane
DM	Dry matter
DMAP	4-(dimethylamino)pyridine
DMF	Dimethylfuran
DMS	Dimethylstyrene
EOA	Epoxidized oleic acid
FAO	Food and Agricultural Organization of the United Nations
FDCA	Furan-dicarboxylic acid
FT-IR	Fourier Transformation - Infrared
GC	Gas chromatography
HA	Hydroxyalkanoate
HD	Hydroxydecanoate
HDPE	High density polyethylene
HHH	Hydroxyhexanoate
HMF	Hydrocymethylfurfural
HO	Hydroxyoctanoate
HV	Hydroxyvalerate
IEA	International Energy Agency
INAO	Institut National des Appellations d'Origine
LLDPE	Linear low-density polyethylene
Mcl	Medium chain length
MEG	Monoethylene glycol
MMT	Montmorillonite
MS	Methylstyrene
NFE	Nitrogen Free Extract

NMR	Nuclear Magnetic resonance
ORF	Open reading frames
PBS	Poly(butylene succinate)
PBT	Polybutylene succinate
PBTA	Poly(butylene terepthalate)
PCL	Polycaprolactone
PE	Polyethylene
PEG	Polyethylene glycol
PHA	Polyhydroxyalkanoates
PHB	Polyhydroxybutyrate
PHBV	Poly(3-hydroxybutyrate-co-3-hydroxyvalerate)
Pi	Phosphate buffer
PLA	Poly lactic acid
PP	Polypropylene
PPD	ρ-phenylenediamine
PS	Polystyrene
PVC	Polyvinyl chloride
PVOH	Polyvinyl alcohol
RACOD	Rapidly Acidifying Chemical Oxygen Demand
SEC	Size Exclusion Chromatography
TPS	Thermoplastic strach
USDA	United States Department of Agriculture
XRD	X-ray Diffraction

Contents

Acknowledgments 2
Abstract 3
Abbreviations 4
List of Figures 11
List of Tables 15
List of Schemes 17
Aims 19
1. Introduction 20
1.1 Economic context 20
1.2 Economic sustainability of bio-polymers 24
1.3 Definitions 30
1.4 Biogenesis considerations 32
1.5 A survey of the sources, amounts and constitution of food wastes 33
1.5.1 Potato waste 35
1.5.2 Corn stover 37
1.5.3 Mango seed 39
1.5.4 Citrus' fruit waste 40
1.5.5 Grape waste 43
1.5.6 Pumpkin seed 45
1.5.7 Sugar bagasse 46
1.5.8 Coffee waste 48
1.5.9 Banana waste 49
1.5.10 Avocado seed 51
1.5.11 Carrot waste 52
1.5.12 Peanut husk 54
1.5.13 Cereals straw 55
1.5.14 Animal waste 56
1.6 Strategies for production of biopolymers from food waste 58
1.6.1 Biomass-sourced polymers 59
1.6.1.1 Starch 60
1.6.1.2 Cellulose 62
1.6.1.3 Chitin 64
1.6.1.4 Lignin 66

1.6.1.5 Proteins 68
1.6.1.6 Plant oils 69
1.6.1.7 Sugars 71
1.6.2 Industrial biotechnology (White biotechnology) 72
1.6.2.1 Poly(β-hydroxyalkanoate)s - PHAs 73
1.6.2.2 Poly(β-hydroxybutyrate), PHB 74
1.6.2.3 Poly(hydroxybutyrate-co-hydroxyvalerate), PHBV 74
1.6.2.4 Poly(β-hydroxyalkanoate) copolymers 75
1.6.2.5 Polylactic acid - PLA (Poly(α-hydroxy acid)) 76
1.6.2.6 Enzymatic polymerization 78
1.6.3 Transgenic Plants 80
1.7 Fibres and other reinforcements 81
1.8 Biodegradation of polymers from food waste 82
1.9 D-limonene 85
1.9.1 Description, synthesis, extraction and applications. 85
1.9.2 Catalytic reaction over palladium 87
1.9.3 Production of ρ-cymene from D-limonene 88
1.9.4 Polymerization and copolymerization reactions 89
1.9.5 Other uses of D-limonene in polymerization processes 93
1.10 Chlorogenic acid 94
1.10.1 Description, synthesis and applications 94
1.10.2 Presence in potato waste and its extraction 96
1.10.3 Enzymatic oxidative polymerization 97
2. Experimental Procedure 99
2.1 Materials 99
2.2 Equipment 101
2.2.1 Gas chromatography (GC) 101
2.2.2 Fourier Transformation-Infrared (FT-IR) spectroscopy 101
2.2.3 Nuclear Magnetic Resonance (NMR) spectroscopy 101
2.2.4 X-ray Diffraction (XRD) 102
2.2.5 Viscometer and temperature stabilisation 102
2.2.6 Ultrasonic probe 102
2.2.7 Thermal analysis 102
2.3 Polymerization of citrus waste derivatives 103

2.3.1 Synthesis of monomer 103
2.3.2 Polymerization of DMS 105
2.3.3 Measurement of viscosity 106
2.4 Polymerization of potato waste derivatives 106
2.4.1 Enzymatic polymerization in pH 7 phosphate solution with methanol 107
2.4.2 Enzymatic polymerization in aqueous solution with methanol 108
2.4.3 Enzymatic template polymerization in water-soluble polymer. 108
2.5 Polymerization of oleic acid from mango seed butter 109
2.5.1 Separation of oleic acid 109
2.5.2 Esterification of oleic acid 109
2.5.3 Epoxidation of oleic acid and di-esters. 110
2.5.4 Polymerization of di-esters using curing agents. 110
2.6 Interaction of monomers with clay. 111
2.6.1 Modification of clay 111
3. Results and Discussion of Citrus Waste Experiments 112
3.1 Synthesis of DMS monomer 112
3.1.1 Initial conditions 114
3.1.2 Effect of water 114
3.1.3 Effect of base 116
3.1.4 Effect of temperature 117
3.1.5 Effect of reactant quantities 117
3.1.6 Effect of solvent 118
3.1.7 Effect of different palladium complexes 119
3.1.8 Study of reaction profile 120
3.2 Poly-dimethylstyrene 124
3.3 Addition of clay 126
3.3.1 XRD study of monomer interactions with montmorillonite clay 127
3.3.2 XRD study of monomers interaction with modified clay with L-lysine 128
3.3.3 XRD study of monomer interactions with organoclay (Cloisite 10A) 130
3.4 Summary of results 131
4. Results and Discussion of Potato Waste Experiments. 133
4.1 Enzymatic polymerization in pH 7 phosphate solution with methanol 133
4.1.1 Phenol 134
4.1.2 Caffeic acid 135

4.1.3 Chlorogenic acid 136
4.1.4 2,3-Dihydroxybenzoic acid (2,3-DHBA) 136
4.1.5 1,2-Dihydroxybenzene 139
4.1.6 2,4-Dihydroxybenzoic acid (2,4-DHBA) 140
4.1.7 3,5-Dihydroxybenzoic acid (3,5-DHBA) 143
4.1.8 Summary of results 146
4.2 Enzymatic polymerization in aqueous solution with methanol 147
4.2.1 Phenol 148
4.2.2 Caffeic acid 149
4.2.3 Chlorogenic acid 151
4.2.4 2,3-Dihydroxybenzoic acid 152
4.2.5 1,2-Dihydroxybenzene 152
4.2.6 2,4- and 3,5-Dihydroxybenzoic acid 154
4.2.7 Summary of results 154
4.3 Enzymatic template polymerization in water-soluble polymer. 155
4.3.1 Phenol 155
4.3.2 Caffeic acid 158
4.3.3 Chlorogenic acid 159
4.3.3 Summary of results 160
4.4 Addition of clay - XRD study of monomers with MMT clay 160
4.5 Thermal analysis 161
4.5.1 Melting points 162
4.5.2 Differential Scanning Calorimetry analysis 163
5. Results and Discussion of Mango Seed Butter Experiments. 165
5.1 Separation of oleic acid from mango seed butter 165
5.2 Esterification of oleic acid 167
5.3 Epoxidation of oleic acid and di-esters 169
5.4 Characterization of the products obtained from curing reaction. 171
5.4.1 Anhydride curing agent 171
5.4.2 Amine curing agent 174
5.5 Addition of clay 180
5.5.1 XRD study of monomers with pure montmorillonite clay. 180
5.5.2 XRD study of monomers with DET, ALA and PPD modified clay 181
5.5.3 XRD study of monomers with L-lysine modified clay 182

5.5.4 XRD study of oleic acid with Cloisite 10A 182
5.5.5 Summary of results 183
6. Conclusion 184
7. Future work 187
Appendix 1. Physico-chemical properties of D-limonene 189
Appendix 2. Ways to produce limonene oxide 190
Appendix 3. Diagram of the ink-jet printer valve 192
Appendix 4. Mango butter specifications. 193
Appendix 5. Wacker type process 194
Appendix 6. Techniques deployed in this research 194
1. Gas Chromatography (GC) 194
2. Fourier Transformation – Infrared (FT-IR) spectroscopy 195
3. Nuclear Magnetic Resonance (NMR) 196
4. X-ray Diffraction (XRD) 198
5. Differential Scanning Calorimetry (DSC) 200
References 202

List of Figures

Figure 1. Twenty six year oil price..... 22
Figure 2. World comparison of bio-based polymer production capacities in 2011..... 25
Figure 3. Expected development of bio-based polymer production until 2020..... 29
Figure 4. Expected development of bio-based polymer production in Europe until 2020 29
Figure 5. Corn stover structure 38
Figure 6. Scheme for conventional white wine production 44
Figure 7. Industrial process for fuel ethanol production from sugarcane bagasse. 48
Figure 8. Schematic pathways for industrial meat and by-products. 57
Figure 9. A schematic chart of the categories of biomass-sourced polymers showing the direct and indirect paths to hydrophobicity 58
Figure 10. A representation production cycles for biodegradable polymers from reference 59
Figure 11. Structure of starch..... 60
Figure 12. Structure of Cellulose..... 62
Figure 13. Monomers which form lignin complex structure 66
Figure 14. Basic structure of natural triglycerides..... 70
Figure 15. Synthetic routes for biopolymer production from plant oils..... 70
Figure 16. Main structures of furfural derivatives..... 71
Figure 17. Monomers derived from 5-Hydroxymethylfurfuran 72
Figure 18. Structures of Aliphatic Polyesteres..... 73
Figure 19. HRP catalytic reaction..... 80
Figure 20. Classification of natural fibres..... 82
Figure 21. Degradation pathways. 84
Figure 22. D-limonene chemical structure..... 85
Figure 23. Citrus oil manufacturing process.. 86
Figure 24. Diagram of the enzymatic oxidative polymerization of chlorogenic acid. 98
Figure 25. Method for polymerization of citrus waste and the formation of nanocomposites . 103
Figure 26. GC analysis from reaction..... 104
Figure 27. Calibration graphs for the gas chromatography technique. 104
Figure 28. Method for polymerization of potato waste and the formation of nanocomposites 107
Figure 29. Method for the polymerization of oleic acid from mango seed butter..... 109
Figure 30. Other bases for the D-limonene palladium-catalyzed dehydrogenation.....116
Figure 31. Reaction profile of the conversion of DMS from D-limonene..... 120
Figure 32. Reaction profile using double the amount of oxidant and base..... 121
Figure 33. Reaction profile: triple amount base and double amount of catalyst and oxidant... 121
Figure 34. Reaction profile while changing the amounts of base, catalyst and oxidant. 122
Figure 35. Kinematic viscosity of polymers at different concentrations on toluene solutions . 125

Figure 36. X-ray diffraction of a) clay + toluene and b) clay + dimethylstyrene 127
Figure 37. Structures similar to DMS 127
Figure 38. XRD results from the interaction of clay with a) D-limonene, b) α-methylstyrene, c) 4-methylstyrene and d) styrene..... 128
Figure 39. Schematic diagram: L-lysine interaction with clay and overall exchange reaction. 129
Figure 40. XRD spectrum of a)clay+L-lysine and clay-lysine with b)DMS c)D-limonene..... 129
Figure 41. XRD spectrum of organoclay with a) as received, b) with DMS and D-limonene, c) D-limonene and 4-methylstyrene and d) with DMS and styrene. 131
Figure 42. FT-IR spectrum of (A) phenol monomer and (B) polyphenol obtained at pH 7 (methanol: Pi buffer, 1:1)..... 134
Figure 43. ^{1}H NMR spectrum of polyphenol obtained by solution polymerization at pH 7 (methanol: Pi buffer, 1:1)..... 135
Figure 44. Monomers selected to further understand the polymerization reaction..... 136
Figure 45. FT-IR of A)2,3-dihydroxybenzoic acid monomer and B)Poly 2,3-dihydroxybenzoic acid obtained at pH 7 (methanol: Pi buffer, 1:1)..... 137
Figure 46. ^{1}H NMR spectrum of A) 2,3-dihydroxybenzoic acid monomer and B) Poly 2,3-dihydroxybenzoic acid obtained at pH 7 (methanol: Pi buffer, 1:1)..... 138
Figure 47. ^{13}C NMR of A) 2,3-dihydroxybenzoic acid and B)Poly 2,3-dihydroxybenzoic acid obtained at pH 7 (methanol: Pi buffer, 1:1). 138
Figure 48. FT-IR of A) 1,2-Dihydroxybenzene B) Poly 1,2-Dihydroxybenzene obtained at pH7. (methanol: Pi buffer, 1:1)..... 140
Figure 49. FT-IR of A)2,4-dihydroxybenzoic acid monomer and B)Poly 2,4-dihydroxybenzoic acid obtained at pH 7 (methanol: Pi buffer, 1:1)..... 141
Figure 50. ^{1}H NMR spectrum of A) 2,4-dihydroxybenzoic acid monomer and B) Poly 2,4-dihydroxybenzoic acid obtained at pH 7 (methanol: Pi buffer, 1:1)..... 142
Figure 51. ^{13}C NMR of A)2,4-dihydroxybenzoic acid and B)Poly 2,4-dihydroxybenzoic acid obtained at pH 7 (methanol: Pi buffer, 1:1). 142
Figure 52. FT-IR of A)3,5 Dihydroxybenzoic acid monomer and B)Poly-3,5-dihydroxybenzoic acid obtained at pH 7 (methanol: Pi buffer, 1:1)..... 143
Figure 53. ^{1}H NMR spectrum of A) 3,5-dihydroxybenzoic acid monomer and B) Poly 3,5-dihydroxybenzoic acid obtained at pH 7 (methanol: Pi buffer, 1:1)..... 144
Figure 54. ^{13}C NMR of A) ,5-dihydroxybenzoic acid and B)Poly 3,5-dihydroxybenzoic acid obtained at pH 7 (methanol: Pi buffer, 1:1). 145
Figure 55. FT-IR spectrum of (A) polyphenol obtained by phosphate buffer with methanol, (B) polyphenol obtained by aqueous solution with methanol and (C) phenol monomer.148
Figure 56.^{1}H NMR spectrum of polyphenol obtained by aqueous solution with methanol. 149
Figure 57. FT-IR spectrum of (A) caffeic acid monomer and (B) polycaffeic acid obtained by aqueous solution with methanol 150

Figure 58. FT-IR spectrum of (A) chlorogenic acid monomer and (B) poly(chlorogenic acid) obtained by aqueous solution with methanol. 151
Figure 59. FT-IR spectrum of (A) 2,3 Dihydroxybenzoic acid (B) Poly 2,3-dihydroxybenzoic acid obtained by aqueous solution with methanol. 153
Figure 60. Comparison of FT-IR spectra. A) Poly 1,2-dihydroxybenzoic acid in phosphate buffer, B) poly 1,2-dihydroxybenzoic acid in aqueous solution. 153
Figure 61. ^{1}H NMR spectra of polyphenols obtained by enzymatic template polymerization A)Polyphenol obtained using PEG as template and B)Polyphenol without PEG 156
Figure 62. FT-IR spectra of polyphenols obtained by enzymatic polymerization using A)PEG as template, B)without using PEG, C)phosphate solution with methanol and D)PEG .. 157
Figure 63. FT-IR spectra of polycaffeic acids obtained by enzymatic polymerization using A) PEG as template, B) without using PEG and C) phosphate solution with methanol 158
Figure 64. FT-IR spectra of polychlorogenic acids obtained by enzymatic polymerization using A)PEG as template, B)without using PEG and C)phosphate solution with methanol ... 159
Figure 65. X-ray diffraction spectra of the A) clay with methanol and B) clay with ethanol... 161
Figure 66. XRD spectra of A) clay with caffeic and B) clay with chlorigenic acid..... 161
Figure 67. DSC thermograms of A)PEG, B)phenol, polyphenol with C)PEG and D)no PEG. 163
Figure 68. DSC thermograms of A) PEG, B) caffeic acid, C) polycaffeic acid with PEG and D) polycaffeic acid without PEG..... 164
Figure 69. DSC thermograms of A) PEG, B) chlorogenic acid, C) polychlorogenic acid with PEG and D) chlorogenic acid without PEG..... 164
Figure 70. Binary phase diagram for a saturated and an unsaturated fatty acid. 165
Figure 71. FT-IR spectrum of oleic acid obtained from mango seed butter. 166
Figure 72. ^{1}H NMR spectrum of oleic acid separated from mango seed butter..... 167
Figure 73. FT-IR spectrum of oleic acid di-ester from a)oleic acid, b)1,3-propanediol, c)orcinol and c) resorcinol 168
Figure 74. ^{1}H NMR spectrum of oleic acid di-ester from a) 1,3-propanediol, b) orcinol and c) resorcinol 168
Figure 75. ^{1}H NMR spectrum of epoxide from a)oleic acid, b)1,3-propanediol di-ester, c)orcinol di-ester and d) resorcinol di-ester..... 170
Figure 76. FT-IR spectrum of polymers obtained of epoxidized oleic acid at a) 165 °C for 3h and b) 200 °C for 1h 173
Figure 77. ^{1}H NMR spectrum of polymers obtained of epoxidized oleic acid at a) 200 °C for 1h and b) 165 °C for 3h, where n = degree of polymer 174
Figure 78. Products obtained from curing reaction with amine crosslink agents. 175
Figure 79. FT-IR spectra of products from a)1,3-propanediol di-ester/DET, b)1,3-propanediol di-ester/PPD, c)Orcinol di-ester/DET, d)Orcinol di-ester/PPD, e)Resorcinol di-ester/DET and f) Resorcinol di-ester/PPD 176

Figure 80. ^{1}H NMR spectra of a)ρ-phenylenediamine(PPD) and b)diethylenetriamine(DET) 176
Figure 81. ^{1}H NMR spectra of a) 1,3-propanediol det, b) 1,3-propanediol ppd, c) orcinol det, d) orcinol ppd, e) resorcinol det and f) resorcinol ppd 179
Figure 82. X-ray traces of pure clay, oleic acid-clay and epoxide-clay. 181
Figure 83. X-ray traces of modified clays and their mixture with epoxidized oleic acid. 181
Figure 84. X-ray diffraction traces of L-lysine modified clay with oleic acid and epoxide 182
Figure 85. X-ray trace of organoclay with oleic acid. 183
Figure 86. Possible pathways for the oxidation of limonene with V_2O_5/TiO_2 catalyst 190
Figure 87. Schematic diagram of gas chromatography system components. 195
Figure 88. Schematic diagram of an FT-IR instrument 196
Figure 89. Schematic diagram of an NMR instrument 197
Figure 90. Schematic diagram of the probe inside the NMR instrument 198
Figure 91. Bragg's law 198
Figure 92. X-ray diffractometer configuration 199
Figure 93. Optical arrangement in the X-ray diffractometer 200
Figure 94. Schematic diagram of an DSC instrument 201
Figure 95. (A) DSC curve example (B) Generalized DSC curve for a polymer 201

List of Tables

Table 1. Comparison in energy use for the production of TPS and PE. ... 26
Table 2. Comparison in energy use for the production of PLA and petrochemical polymers. ... 27
Table 3. Comparison in energy use for the production of PLA and petrochemical polymers. ... 27
Table 4. Bio-based polymers, producing companies in Europe and production capacities. ... 28
Table 5. Substances found in the industrial food wastes ... 34
Table 6. Substances found in the industrial food wastes. ... 34
Table 7. Production of potato ... 36
Table 8. Structures of potato polyphenols and chlorogenic acid isomers. ... 36
Table 9. World's corn production ... 37
Table 10. Chemical composition of corn stover ... 38
Table 11. World production of Mango ... 39
Table 12. Chemical composition of mango almond. ... 39
Table 13. Profile of fatty acids in mango almond ... 40
Table 14. World citrus production ... 41
Table 15. Chemical composition of citrus' peel. ... 41
Table 16. Percentages of constituent in citrus peel oils ... 42
Table 17. Main grape producers ... 43
Table 18. Fatty acids founded in grape seed oil ... 44
Table 19. Phenolic substances in grape seeds. ... 45
Table 20. Word production of pumpkins ... 45
Table 21. Fatty acids in pumpkin seed oil ... 46
Table 22. World production of sugar cane ... 46
Table 23. Chemical composition of sugar cane bagasse. ... 47
Table 24. Coffee world production. ... 48
Table 25. Chemical composition of coffee waste. ... 49
Table 26. World production of bananas. ... 50
Table 27. (a) Constitution of banana peel and (b) mineral content of banana peel. ... 50
Table 28. World production of avocado ... 51
Table 29. Aproximate composition of the avocado seed. ... 51
Table 30. Fatty acids found in the avocado seed. ... 52
Table 31. World production of carrot. ... 53
Table 32. Chemical composition and natural antioxidants of carrot by-products ... 53
Table 33. Peanut husk composition. ... 54
Table 34. Cereals production. ... 55
Table 35. Chemical composition of wheat straw. ... 56
Table 36. PHA structures ... 74

Table 37. Renewable sources and Microorganisms used for PLA production. 77
Table 38. PLA characteristic properties 78
Table 39. Enzymes, their specific reactions and polymers they can produce. 79
Table 40. Differences between enzymatic and non-enzymatic degradation 83
Table 41. Chlorogenic acid present in aerial and subterranean tubers of two potato genotypes. 96
Table 42 . Distribution of chlorogenic acid in potato..... 96
Table 43. Details of reagents and materials used for experiments on the polymerization of derivatives of D-limonene. 99
Table 44. Details of reagents and materials used for experiments on the polymerization of chlorogenic acid and analogues. 100
Table 45. Details of reagents and materials used for experiments on the polymerization of oleic acid from mango seed butter. 100
Table 46. Effect of water on conversion and selectivity 115
Table 47. Effect of base on conversion and selectivity 116
Table 48. Effect of temperature on conversion and selectivity. 117
Table 49. Effect in the amount of reactants. 118
Table 50. Effects of solvent. 119
Table 51. Effect of catalyst..... 120
Table 52. Calculated intrinsic viscosity and molecular weight of the polymers obtained 126
Table 53. Summary of results from citrus waste experiments for synthesis of monomer 132
Table 54. Results from the enzymatic polymerization at pH 7 (methanol: Pi buffer, 1:1)..... 146
Table 55. Results from the enzymatic polymerization in aqueous solution with methanol of phenol and derivatives. 154
Table 56. Results from the enzymatic template polymerization using PEG and HRP of phenol and derivatives 160
Table 57. Melting point of the polymers obtained from potato waste. 162
Table 58. Epoxidation of oleic acid and di-esters summary 169
Table 59. Summary of results from epoxide/amine curing reactions. 178
Table 60. Summary of results for clay interaction with oleic acid and epoxidized oleic acid. . 183
Table 61. Epoxidation of D-limonene by microbial biotransformation 191

List of Schemes

Scheme 1. Hydrolysis of starch into sugars 62
Scheme 2. Hydrolysis of cellulose into glucose 64
Scheme 3. Chitin and chitosan chemical structure 65
Scheme 4. A) monomer for the synthesis of polyesters and polyethers. B) linear polyetherification of monoaromatic monomer from lignin 67
Scheme 5. Oxidative pathways for lignin biodegradation 68
Scheme 6. Synthesis of furfural 71
Scheme 7. PHBV pathway synthesis. 75
Scheme 8. Biosynthesis of PHA copolymers. 76
Scheme 9. PLA polymerization 77
Scheme 10 . General biological hydrolytic degradation by enzymes 83
Scheme 11. Mechanism of cyclization of geranyl diphosphate to limonene 85
Scheme 12. Hydrogenation, isomerisation & dehydrogenation of D-limonene over Pd 87
Scheme 13 . Reaction of D-limonene dehydrogenation through electron-transfer oxidation. 89
Scheme 14 . Polymerization of D-limonene. 89
Scheme 15. Mechanism for the polyalkylene sulphide made of D-limonene. 90
Scheme 16 . Mechanism for the copolymerization of limonene with acrylonitrile. 90
Scheme 17. Mechanism for the copolymerization of limonene with methyl methacrylate. 91
Scheme 18. Mechanism for the 1:2 copolymerization. 91
Scheme 19 . Mechanism for the copolymerization of limonene with maleimides. 92
Scheme 20. Copolymerization of *trans*- and *cis*- limonene oxide and CO_2 using β-diiminate zinc acetate complexes 92
Scheme 21 . Mechanism for the polymerization of dicyclopentadiene with monoterpenes using a ruthenium initiator. 93
Scheme 22. Chlorogenic acid chemical structure 94
Scheme 23. Chemical formation of chlorogenic acid precursor 94
Scheme 24 . Pathways for the biosynthesis of chlorogenic acid. 95
Scheme 25. D-limonene liquid phase palladium catalyzed dehydrogenation from Horrillo's work 112
Scheme 26. Reaction of liquid-phase palladium catalyzed dehydrogenation of D-limonene into DMS 113
Scheme 27. Reactions involved in the liquid-phase palladium catalyzed dehydrogenation of D-limonene into DMS 113
Scheme 28. Improved reaction for D-limonene dehydrogenation 123
Scheme 29. Polymerization of dimethylstyrene 124

Scheme 30. Polymer structure of polyphenol. 133
Scheme 31. Polymer structure of poly 2,3-dihydroxybenzoic acid 139
Scheme 32. Polymer structure of poly 1,2-Dihydroxybenzene 140
Scheme 33. Polymer structure of poly 2,4-Dihydroxybenzoic acid 143
Scheme 34. Polymer structure of poly 3,5-dihydroxybenzoic acid 145
Scheme 35. Xu's work results on caffeic acid polymerization. 147
Scheme 36. Polymer structure of poly(caffeic acid) 151
Scheme 37. Polymer structure of poly(chlorogenic acid) 152
Scheme 38. Reaction for esterification and epoxidation reactions 171
Scheme 39. The mechanism reaction of oleic acid with anhydride 172
Scheme 40. Proposed routes for limonene biotransformation. 191

Aims

The aim of this project was to synthesise hydrophobic polymers from plant oils which are obtained from food waste. This extinguishes the conflict over land use that results when biomass is used for non-food applications such as biofuel or chemical feedstock. The next stage was to study the interaction between the biopolymers obtained with mineral platelet reinforcements, such as montmorillonite clay, with the intention to combine them in order to deliver composites. The objective was to find the proper conditions and reinforcement to create composites which have mechanical properties in the range suitable for engineering applications, for example but not exclusively, in the automotive industry.

This project will pave the way for nanocomposites based on polymers that are derived from plant oils and are therefore independent of mineral oil stock and have an environmental premium. Clay reinforcement has the capability to exfoliate to ~1 nm silicate layers and thus provide high aspect ratio reinforcement. This means the reinforcing phase, unlike carbon or glass fibre, also incurs a low carbon cost and the project is therefore in the vanguard of a new generation of engineering materials with nearly zero embodied carbon.

Part of the work uses limonene as the biomass source as it is present in citrus peels and can be obtained as an industrial product. The other part uses chlorogenic acid which is the major component of the phenolic compounds found in potato waste. In addition, the author devised and supervised a project on the polymerization of oleic acid obtained from mango seed (conducted by Miss Yingxue Hu).

The use of biomass in high technology industries also helps to rebalance the industrial and agricultural sectors of the economy of a country, most notably where rapid industrialisation has resulted in urbanisation and agricultural unemployment. Unlike the use of biomass in fuel replacement, a close link can develop between the agricultural raw material supplier and the industrial converter as both seek to modify their processes with a common aim.

1. Introduction

As the mineral oil price increases to accommodate new extraction techniques, the commercial viability of biomass as a source of chemical feedstock begins to emerge from an obscurity that has prevailed since the 1960s. This could have transformative effects on industrial chemistry.

The increase in oil price and a future evolution of regulatory measures addressing climate change will encourage industries to seek independence from fossil fuels and to use biomass resources. Additionally, the use of food waste as a raw material realigns industrial and agricultural sectors and does not incur conflict over land use. It provides new opportunities for food-producing countries.

Therefore, the outline of this introduction follows firstly an economic study of the research viability of biomass resources as raw materials and the possible sustainability for these materials. Secondly a proper definition of all the terms applied for materials obtained from biomass sources is given. Thirdly a description is provided of how the available quantities of compounds derived from food waste can be assessed by the classification of metabolites. Section 1.4 consists of a survey of the current global food-waste resource. Section 1.5 demonstrates how these resources could be used in the generation of hydrophobic polymers.

The main body of this thesis comprises detailed researches on the chosen substances for this project, D-limonene and chlorogenic acid. Detailed research on oleic acid was made by Miss Yingxue Hu. Subsequently, in section 1.10 there is a small description of the techniques used in this research.

1.1 Economic context

In setting out the context for sustainable materials it is important to establish the motivational factors, controversial and uncertain as they are at present. It is not universally accepted that substitutes for fossil fuels are needed because they are "running out": the economic situation is less dramatic and the transition is likely to be quite smooth. The upper bound for stored carbon is set by the high CO_2 content of the second atmosphere from which carbon was fixed by life forms into limestone and buried carbon. Estimates of these distributions, based partly on the isotopic distribution of ^{13}C and ^{12}C between marine sediments and photosynthesised biomass respectively[1] indicate that the reservoir of carbonate is 60 Zg and that carbon in rock is present at 15

Zg.[2] One of the best assessments of oil reserve data from a disinterested perspective is provided by Vacal Smil of the University of Manitoba.[3] There is a long history of claims that peak oil production has passed, each of which is followed by new resource discoveries. Smil suggested that the estimated ultimate recovery is about 3 Tb but his publication preceded several large discoveries, notably the Bakken Formation announcement in 2008. The USGS report[4] shows that the Bakken holds 6 x 10^8 m^3 of technically recoverable oil alone (~26 EJ). Globally, proven reserves (1P) are about 1.3 x 10^{12} barrels (2.1 x 10 ^{11} m^3 or 8 ZJ). Reserves of the three fossil fuels are 31 ZJ with oil and gas making up 40%.[5] An optimistic assessment of the European oil and gas supply futures has also been made by Aguilera[6] and the indications are that shortages of fossil fuels are not imminent.

The wider picture is that as the oil price increases (Figure 1) due to novel extraction techniques, new technologies such as coal-to-liquid, gas-to-liquid and methane hydrate extraction will become economically viable, i.e. the expected price level minus the costs of development and production leave a profit acceptable to the producer. For this reason, the liberation of fossil carbon into the atmosphere is unlikely to be arrested by resource depletion. The huge investment by China in coal to liquid fuel conversion[7] has been temporarily curtailed but similar technologies mean that there is likely to be no shortage of coal-sourced, synthetic liquid fuels. Although many reserves of coal, oil, clathrates or gas are not economically recoverable at present, technical and market circumstances have been changing. The extraction of methane from clathrates, for example, is beginning to be assessed.[8] Increase in the oil price (Figure 1) stimulates both vigorous exploration and new extraction technologies but also entirely new fossil carbon fuel sources. Each of these presents a 'learning' or 'experience' curve in the form of a logarithmic decrease in price with time and output.[9] The importance of the learning curve in determining investment decisions in alternative energy technologies is emphasised in a University of Melbourne report[10] which explores the decreasing costs of photovoltaic, wind and solar concentrating energy collection as a function of deployment.

A rise in oil price also provides a market stimulus for biomass sourced fuels such as bioethanol and biodiesel and for chemicals and polymer production, each associated with its own learning curve. This offers a prospect of sustainability in materials. The free market, responding to a combination of oil price rises and the evolution of regulatory measures to address climate change may therefore encourage the materials industries to use the biomass resource.

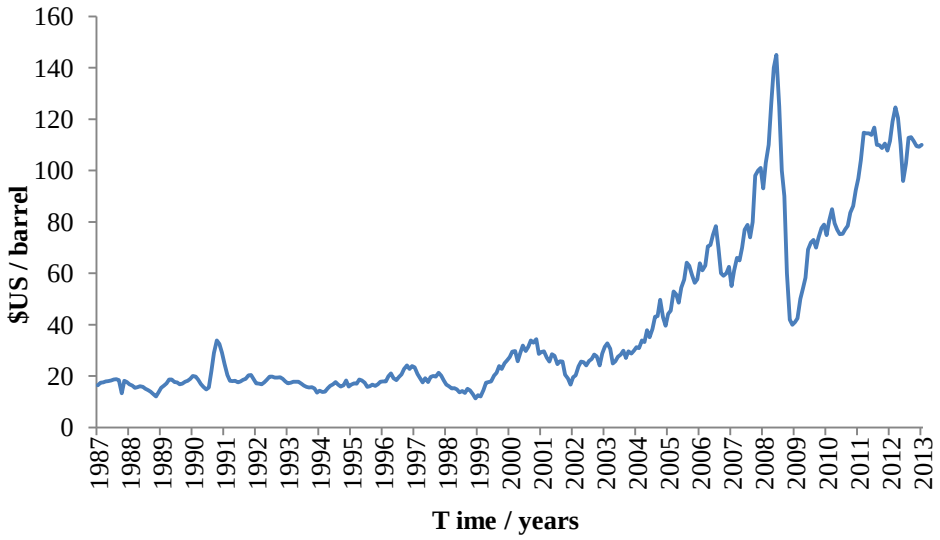

Figure 1. Twenty six year oil price (Brent Crude spot price): the upward trend invites new business from biomass processors but the instability inhibits such investment.[11]

The short term motivational factor in seeking independence from fossil fuels is based on political instability and political interference in the free market. A UK Government report[12] sets out these perceived threats and a 2010 report defines the emergency responses in terms of International Energy Agency (IEA) policy on stockpiling.[13] But this is a short term measure. The wider and longer term issue is climate change associated with the steady increase of atmospheric carbon dioxide which is at present closely linked to economic activity. The feedback effects of warming include loss of polar albedo and liberation of methane from the melting of frozen soils.[14-16] The global effects on health have been clearly defined[17] and the security issues anticipated[18] so that there is a strong societal motivation to launch now those remediation technologies which have a long technical lead-time. The commercial motivation in the context of lead-time is more complex as discussed below.

The polymer materials community has responded to environmental issues in several ways, notably through recycling schemes and the introduction of biodegradable packaging but perhaps the greatest response is the growth of interest in a materials science and technology that uses ‘no new carbon’ and therefore makes use of biomass in order to preserve economic growth.[19] In the last decade there has been renewed and growing interest in biomass-sourced hydrophilic polymers, particularly as reinforcing fibres in polymer composites where they can deliver a 2:1 modulus mismatch,[20-23] but also as bulk polymers in their own right. Moreover the various routes to the synthesis of

hydrophobic polymers are being explored and extended and several reviews have appeared that address both classes of polymer.[24-27] These ideas are not new. In 1940, Henry Ford patented a car body shell made from a soybean-based polymer supported on a tubular steel frame.[28] It saved one third of the weight of a steel body and Ford believed it was safer. Ford had a complex relationship with his farming roots and saw the car as a way to combine industrial and agricultural enterprises. This aspect of Ford's vision is by no means irrelevant today. The sectorization of economies, particularly between industry and agriculture is reflected in the relative wealth of nations with agriculturally-based economies tending to be poorer and the prospect for biomass-sourced polymers represents a 'synthesis' in more ways than one and a paradigm for the emerging idea of 'integrated' or 'balanced sector economics'.

Carbon emissions trading tends to favour the developed nations because the baseline is set by current emissions and it seems increasingly likely that large trading blocks that have been active in emissions control will be prompted to enforce policy on others through climate change trading regulations such as import taxation on embedded fossil carbon. This might be set at levels that are informed by available technology so that if it is possible, within a trading block, to build a car with a carbon output of 50 g/km, the import tariff threshold might be set at 100 g/ km. Similar restrictions would apply to the import of materials, again informed by what is possible in large scale production operations. Research in biomass materials is therefore both a preparation for tomorrow's markets and an influence on the regulations that will shape them. It seems that competition between manufacturers, in the context of climate change, is going to become partly about regulation setting.

This project focuses on synthetic pathways to engineering polymers that begin with industrial food waste. These starting materials avoid the conflict of land use between food crops and raw material crops that has been problematic in the development of biofuels.[29,30] The prospective increase in reliance on biomass is controversial: Patzek argues forcefully[31] that a one-to-one replacement is impossible but the local situation is more complex; regions of sub-Saharan Africa and China for example have land areas that could be deployed for agriculture, which can be viewed as a form of solar energy harvesting, particularly in the context of crops bred or modified for enhanced survival. Changes to oil price and to environmental regulations may therefore conspire together to change the role of agriculture in supplying food, materials and fuel.

The enterprises that benefit from these new markets will be those which have done the preparative work and shortened their technical lead-time with respect to their

competitors once the market summons them. As such, the lead time of a product matters not for its own sake, but because once a rival firm begins the process of working towards production or reducing its own lead times it takes the competitive advantage. It is for this reason that a firm is only likely to be motivated to begin work on a new technology where it believes that technology will deliver sufficient profit and where it believes current lead times must reduce in order to remain competitive and in some cases gain first mover advantage. In this instance, first mover advantage is likely to be enjoyed by the firm with the technological leadership to capture the emerging market first and may therefore enjoy high profit margins and monopoly-like status. Already a significant number of companies have established a foothold in this market and are developing their expertise based on long term market assessments.[32] The properties of biopolymers presently on the market are summarized by Endres.[33] Nova-Institute GmbH and Bioplastics Magazine have published the 2012/2013 International Business Directory for innovative bio-based plastics and composites in which they list the major suppliers of biopolymers in the world.[32] These surveys indicate that the market is beginning to summon biomass resources for polymer production.

1.2 Economic sustainability of bio-polymers

In this section, the author explores the comparison of petroleum-derived and biomass-derived polymer materials in terms of both the raw material cost and the processing costs.

Polymers are produced as by-products of liquid petroleum and natural gas liquid refining. Worldwide, 4% of the oil consumption is destined to plastic production.[34] In 2010, in the United States of America, 2.7 % of the total petroleum consumption was used by the plastic and resins industry for the production of polymers. Throughout the conversion process of oil to polymers during that year, 11.7 Gm^3 of natural gas were used as fuel and feedstock and 65 billion kilowatt-hours were employed. This is equivalent to 1.7 % of the total U.S.A. natural gas and electricity consumption, respectively. About 1% of the total U.S.A. petroleum consumption was used to generate this amount of energy.[35]

During 2011, the total worldwide production of polymers was of 235 Tg from which 3.5 Tg were biopolymers, representing 1.5% of the overall production. These were produced by 247 biopolymer producing companies with plants at 363 different locations. According to an economic study made by Germany´s nova-Institute, it is

expected that by 2020 the biopolymer production capacity will reach around 12 Tg and will represent 3% of the total polymer production.[36]

At present, bio-based polymer production and investment is concentrated in Asia and America although the main consumption is in Europe (Figure 2). This is due to the accessibility to the feedstock and favourable political framework in Asia and South America compared to the extant lack of support from the European community for their production. However, as mentioned previously in the economic context in section 1.1, it is expected that future regulatory measures and new research developments will create a key driver for their production. Indeed even with the as yet unfavourable political framework, this year the first European PLA industrial-scale plant is expected to be inaugurated while facilities for bio-PET production in Europe, from Plant PET Technology Collaborative (PTC) had been announced for 2015.[37]

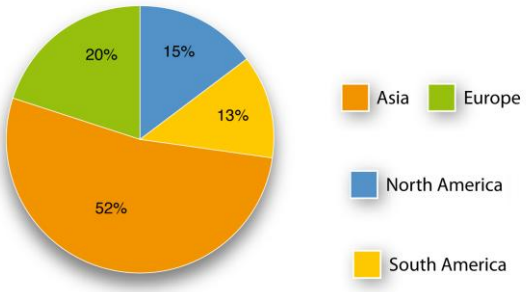

Figure 2. World comparison of bio-based polymer production capacities in 2011. Reproduced from nova-Institute report (not counting cellulose acetate and thermosets).[36]

For the moment starch polymers are one of the most dominant bio-based polymers on the market. Around 50% is used for the production of co-polymers. Packaging is the main application for this bio-based polymer and around 75% is used for this industry. A study of the energy needed for the production of starch polymers and their petrochemical counterpart (polyethylene) indicated that for the starch polymer pellets the energy required was from 25 to 75 % below that required by the petrochemical polymer, with the exception of eutrophication starch polymers (Table 1).This indicates a favourable result for the development of bio-based polymer in the market, with expectations that these numbers will improve as technology, processes and blending possibilities develop in the future years.[38]

Table 1. Comparison in energy use for the production of TPS and PE.[38]

	Non-renewable energy kW-h /kg		
	Petrochemical polymer 50% LLDPE + 50% HDPE	Bio-based polymer	Energy saved
TPS	21.1	6.9	14.2
TPS + 15% PVOH	21.1	6.9	14.2
TPS + 52,5% PCL	21.1	13.3	7.8
TPS + 60% PCL	21.1	14.4	6.7
Starch polymer foam grade	21.1	9.4	11.7
Starch polymer film grade	21.1	15	6.1

TPS = thermoplastic starch, PE = polyethylene, LLDPE = linear low-density polyethylene, HDPE = high-density polyethylene, PVOH = polyvinyl alcohol, PCL = polycaprolactone.

In the case of poly-lactic acid, the first attempts to become sustainable started in the early 1990s when Dupont, Coors, Chronopol and Cargill developed programmes to explore possible applications and continuous processes for production. During 2011, 180 Pg of PLA were produced worldwide by 25 companies at 30 locations: nevertheless NatureWorks, with their plants in USA and Thailand, was the main producer with 78% of the total production.[39]

The final cost in PLA production mainly depends in the efficiency of the fermentation process in order to produce the monomer. During 2003, this process occupied around 45% of Cargill Dow's total cost.[38] Therefore PLA production will only be properly sustainable in the polymer market when the cost of lactic acid (monomer) production decreases and is able to contend against the price of ethylene. Nevertheless, the total non-renewable energy needed for the production of PLA is below to those needed for some petrochemical polymers even though the process energy requirement is higher, as shown in Table 2. This energy requirement can be modified once the technology improves the process production. To give an example, after an optimisation in lactic acid production, around 10% of energy could be saved while further use of lignocellulostic feedstock as source for fermentation and energy production (biorefinery) could decrease by 46% the energy needed in the process.[38] This can give an opportunity for a future competitiveness of PLA in the polymer market.

Table 2. Comparison in energy use for the production of PLA and petrochemical polymers.[38]

	Non-renewable energy kW-h /kg		
	Process energy	Feedstock energy	Total energy
PLA	15	0	15
PLA optimised	13.6	0	13.6
PLA biorefinery	8.1	0	8.1
HDPE	8.6	13.6	22.2
PET (bottle grade)	10.6	10.8	21.4
Nylon 6	22.5	10.8	33.3

As for PHA, the main obstacle for its bulk manufacture is the high production cost. The high prices are due to the high costs of the raw materials and the purification process from the fermentation, which take from 20-25% and 30-35% of the total cost of the production cost, respectively.[38] Moreover, the energy required for the production process is three times higher than that for petrochemical polymers, which doesn't offer any opportunity for the industrial production of this biopolymer. However the total energy requirement for the production of PHA (from fermentation) is lower than that of polystyrene (PS) while when compared to the HPDE energy, the difference is minimal. (Table 3) The low yields and efficiencies plus the high cost of production are the biggest drawbacks for its large-scale production and for this reason PHA success in the market is arrested until these are improved.

Table 3. Comparison in energy use for the production of PLA and petrochemical polymers.[38]

	Non-renewable energy kW-h /kg		
	Process energy	Feedstock energy	Total energy
PHA grown in corn plants	25	0	25
PHA by bacterial fermentation	22.5	0	22.5
HDPE	8.6	13.6	22.2
PET (bottle grade)	10.6	10.8	21.4
PS (general purpose)	10.8	13.3	24.2

Another example is Bio-PET, a partially derived bio-based polymer with chemically identical structure to its petrochemical counterpart, which is not yet produced in Europe but has already a high level of production in Asia and South America. For instance, Teijin and Indorama Venture located in Asia have a production capacity of 100 and 300 Gg, respectively. Whereas bio-monoethylene glycol (MEG), precursor of the PEG, is produced by JBF Industries in Brazil, Indian Glycols LTD and

Greencol Taiwan, with a total production capacity of 775 Gg. Approximately 620 Gg were used for bio-PET production during 2011.[36]

At the same time, the market for bio-based polyurethanes and polyamides is stable and increasing as the construction and automotive sector are expanding the demand of these products. The continuous supply needed in the market provides sustainability for these materials.[40,41]

Moreover, co-polymers between fossil- and bio- based polymers are also found in the market, such as amide-modified poly(butylene terepthalate) (PBTA) or polybutylene succinate (PBT). It is expected that with the development and research in the area of bio-based polymers, the biocomponent increases in the copolymers composition. On the other hand, developments in the creation of bio-based routes to the precursors (1,4-butanediol for PBT) and/or polymers (PLA and PHA) are beginning to establish the commercial feasibility for biopolymers to the industry.

To illustrate the development of the bio-polymer industry at present, Table 4 shows the number of producing companies in Europe and their differences in production after a period of two years. It can be observed that the major development was for starch blends while the production of PHA diminished by 79%. The other bio-based polymers showed no alteration in the production capacity, while the total amount of bio-based polymers produced in Europe had an increase of 20%.

Table 4. Bio-based polymers, producing companies in Europe and production capacities.[37]

Bio-based polymers	Producing companies in 2013**	Production capacities in 2011* /Mg	Production capacities in 2013** /Mg
PLA	7	8.22	8.23
Starch blends	7	217	279
PHA	7	50	10.05
PA	7	16	16
PBAT	1	74	74
PBT	1	0	<50
PUR	3	39.45	39.45
Total		354.72	426.78

* Source: Report Market Study on Bio-based Polymers in the World, 2013-3
** Source: Bio-based Polymers Producer Database, 2013-07

The dynamic evolution of bio-based polymer production until 2020 has been predicted thanks to an international market study made by Germany's nova-Institute, which encompasses market data, trend reports and company profiles of worldwide bio-based polymers. The forecasted results are shown in Figure 3. It foresees that Europe's

share in production will decrease from 20% to 14%, North America's from 15% to 13%, while Asia and South America will increase from 52% to 55% and from 13% to 18%, respectively. It projects a bio-PET production of 5 Tg, a 50 and 80% bio-based share in PBAT and PBS respectively and a quadruple increase in PHA and PLA production, being of 800 Gg production of PLA by 2020.[36]

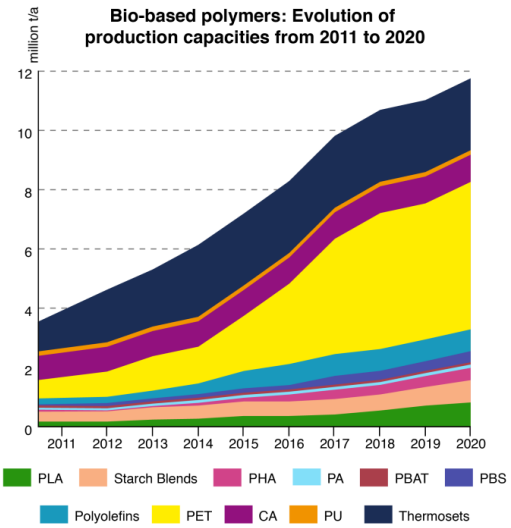

Figure 3. Expected development of bio-based polymer production until 2020 by Germany nova-Institute.[36]

When referring specifically to Europe, the development is mainly focused on starch blends while PHA usage is small and faces a decrease in its production, as seen on Table 1. This behaviour is not expected to change later according to the Germany nova-Institute report.[42] Figure 4 shows the predicted development in Europe for bio-polymers where it can be seen that PHA and polyamides are not expected to grow but to keep in constant production capacity while starch blends and bio-PET will occupy most of the European market.

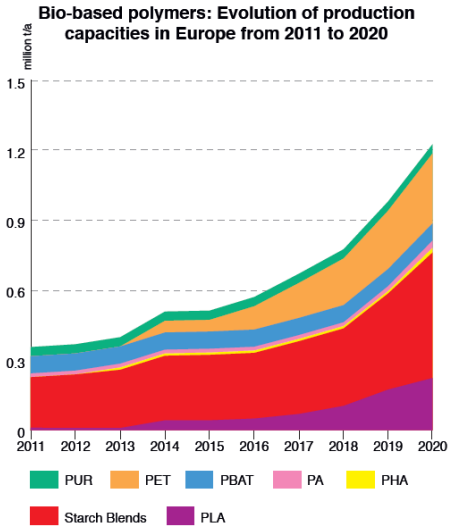

Figure 4. Expected development of bio-based polymer production in Europe until 2020 by Germany nova-Institute. (not counting cellulose acetate and thermosets). [42]

Clearly an assessment of the overall production costs of biomass-derived polymers needs to consider both the raw material price and the energy costs for production. In moving from petroleum-based to biomass-based materials, the former may decrease but the latter increase. Since both are indirectly related to mineral oil price for which there is a background increase overlaid by instability (Figure 1), there is a general expectation that the market will look more favourably on biomass polymers as time passes. However, the example of PHA should be a warning that there can be exceptions to this general rule. It is beyond the scope of this work to conduct a rigorous cost analysis for the production of polymers from food-waste but the cost analyses for existing biopolymers shown above indicate that the costs balance in some cases. It is possible that this thesis is written at a transitional stage in the emergence of the market for food-waste derived polymers.

1.3 Definitions

The term *biopolymers* generally refers to polymers that have been fully synthesised by living organisms and there are three main subsets: polysaccharides, polynucleotides and polypeptides. Indeed, ASTM D6866 defines *biopolymers* as polymers produced by living organisms, that is, polymers synthesised in nature by enzyme-catalyzed chain growth polymerization reactions by complex metabolic processes in the cells of organism during their growth cycles.[43] They are also referred to as *natural polymers.* A somewhat more general definition includes three categories (i) those extracted directly from raw materials, (ii) those produced by chemical synthesis from bio-derived monomers or precursors and (iii) those produced by microorganisms or genetically modified bacteria. This extension to the definition muddies the water and leads to confusion in the meaning of '*biopolymer'*. The three meanings are distinct from the synthesis/processing viewpoint although from the economic and environmental viewpoint they may be indistinguishable. In some cases, the end product might be indistinguishable from that derived from mineral oil except by isotopic assay: the dehydration of bio-ethanol as a source for polyethylene is an example.[44] The emphasis of this work is on polymers that are synthesised from feedstocks that derive from biomass rather than from mineral oil and most therefore fall into the second of these definitions, more specifically we address the category of biomass-*sourced hydrophobic polymers* although these are necessarily placed in the context of other biomass-sourced polymers.

When used as materials, particularly as structural materials, biopolymers are sometimes referred to as *bioplastics*. Most *bioplastics* are degradable and some can be composted such that they are both *renewable* and *biodegradable* making them *sustainable* materials. The term *bioplastic* is therefore unsuitable for hydrophobic polymers derived from biomass that are intended for long term structural applications resisting photo- and bio-degradation. The term *agro-polymer* meaning a renewable and compostable polymer derived from plants is almost a synonym for *biopolymer*. In contrast the term *biomaterial* is normally used in a medical context with quite a different meaning: 'any material that is used in conjunction with living tissue to augment repair for example as a prosthetic device or in wound management'. Some biopolymers can be used as biomaterials because of their steady decomposition *in-vivo* to non-toxic products.

A *bio-based product* is a material derived in whole or in part from biomass resources. Two methods to measure the bio-based content of a material are specified in the ASTM D6866 standard which measures the $^{14}C/^{12}C$ ratio to determining the amount of carbon in products derived from contemporary as opposed to fossil sources.

There is increasing interest in the production of environmentally benign composites designated *biocomposites* or *green composites* from *biopolymeric* matrices and natural fibres which provide alternatives for oil-sourced polymers and glass or carbon fibres respectively. An example is the development of a composite of poly(lactic acid) (PLA) and agricultural by-products which contains a high quantity of cellulose-based fibres such as wheat straw, soy stalk and corn stover.[45] As agricultural residues are from 8 to 10 times cheaper than agricultural fibres, the goal is to create cheap sustainable injection moulded composites with superior properties such as low density, renewability and biodegradability.

The term *white technology*, or *white biotechnology*, is an alternative for *industrial biotechnology* and refers to the use of biotechnology in the chemical industry for the production of fuels or materials employing, *inter alia*, cells and enzymes.

1.4 Biogenesis considerations

The available quantities of compounds derived from food waste can be assessed by classification of metabolites. In the traditional classification, primary metabolites are small molecules essential for the development, growth and reproduction of an organism that are formed by catabolism-degradation pathways and anabolism-synthesis pathways. These metabolic pathways are common across all organisms. Primary metabolites include sugars, amino acids, nucleotides, acyl lipids and 'simple' fatty acids. They are relatively few in number and have a wide distribution across many species.

Other metabolic pathways exist that generate secondary metabolites that on initial inspection appear to have no essential utility. They are formed via secondary metabolism pathways that may be switched on by certain stimuli such as defence, attraction and uv protection, enabling, for example, a species to establish an ecological niche with a plant defence compound or attractant. Many secondary metabolites currently have unknown function. They are extremely diverse in structure, tend to be classified by biosynthetic origin and are invariably found in small quantities in a limited number of species within a phylogenetic group. They are broadly classified into alkaloids, terpenes, glycosides, phenols, polyketides and fatty acid derived products and non-ribosomal peptides. Larger molecules include DNA, RNA, biopolymers, and proteins are often excluded from the classification.

The line between primary and secondary metabolites is not clear cut, for example some steroids that have an essential structural role can be classed as primary metabolites. Also the biopolymer lignin is the second most abundant organic material in plants. Although it is essential for structural purposes, it is considered not as a primary metabolite but a secondary metabolite. Primary metabolites are considered to be involved in the essential metabolic processes for basic cell metabolism, while secondary metabolites affect the interaction between organisms and the environment. The metabolisms are closely related as primary metabolites are frequently the starting materials for secondary metabolite production, such as amino acids for alkaloid production, acetates for polyketide and terpene synthesis and shikimate for the synthesis of aromatics. The widely used categorisation of compounds into the broad primary and secondary metabolite groups has recently been revisited because too many important chemicals do not fit into either of these two groups, such as carotenoids and some lipids.[46]

Within the primary and second metabolites, there is wide diversity of chemical types with similar physicochemical characteristics. Chemists and materials scientists who are accustomed to the extensive heterogeneity of the mineral stock, on first approaching the biomass resource are justified in asking: Given the huge diversity of species, why are there so few high yield primary metabolite types? The classification of metabolites into primary and secondary first proposed by Kössel is also questioned partly because of its lack of evolutionary base and lack of insight into metabolism.[46] In evolutionary terms, the primary metabolic pathways were established at an early stage and it became harder to improve upon them; evolutionary convergence may have strengthened the canalization. It is argued therefore that the derived properties of biomolecular activity and physicochemical behaviour of primary metabolites provides an alternative classification under 'basic integrated metabolism' together with 'supported metabolism'.

In general, the primary metabolites that are obtained commercially are high volume-low value bulk chemicals such as simple fatty acids. Secondary metabolites however, since they are found in smaller quantities, can be difficult to isolate and exhibit a range of bioactivities have a higher commercial value and find applications as fine chemicals and pharmaceuticals. Examples include morphine, cocaine, quinine and limonene. Structurally many possess multiple chiral centres and rings and are difficult to synthesise chemically at low cost.

1.5 A survey of the sources, amounts and constitution of food wastes

Food waste totals 1.3 Pg annually.[47] As the technology of food-processing develops, the pre-consumer food losses tend to decrease but in the developed countries, consumer food waste tends to be greater. At present many of these wastes are uneconomically used and are often disposed of in the local environment, causing pollution issues.

The agro-industrial wastes that are available in large amounts include among others, citrus skin and pulp (orange, grapefruit, mandarin/tangerine, lemon, lime), seed waste (mango, grape, pumpkin), skin (potato and banana), peanut husk, coffee, sugar bagasse and straw. These wastes contain high contents of organic matter and, as seen in Tables 5 and 6, they are rich in ash, fat, fibre, protein and carbohydrates that can be used in several secondary applications. There is a global research effort to investigate new profitable uses.

Table 5. Substances found in the industrial food wastes

	Peanut Husk[48] wt.% DM	Potato [49,50] wt.% DM	Mango seed [51] wt.%	Sugar Bagasse [52] wt.% DM	Citrus peel [53-55]				
					Grapefruit wt.%	Lemons wt.%	Lime wt.%	Orange wt.% DM	Mandarin wt.% DM
Moisture			40.5		8.2	10.6	10.1		
Protein	7.39	10.2	1.43	0.5	4.9	9.3	9.7	9.1 ± 0.4	7.5 ± 0.2
Fatty acids		0.40	4.92					4.0 ± 0.2	1.6 ± 0.1
Fiber	26.2	2.40	3.96		11.9	14.9	14.4		
Lignin				24.8				7.5 ± 0.6	8.6 ± 0.8
Cellulose	22.5		48.19		27.8			37.1 ± 3.1	22.6 ± 2.2
Lipids		0.06							
Hemicellulose	18.33							11.0 ± 1.1	6.0 ± 0.6
Starch		67.5							
Sugar		0.7						9.6 ± 0.2	10.1 ± 0.5
Pectin				0.7				23.0 ± 2.1	16.0 ± 1.2
Ash	7.79				4.2	5.2	5.1	2.6 ± 0.1	5.1 ± 0.2
Ether extract[a]	6.31		0.83	3.9	1.1	2.8	2.9		
NFE[b]	52.4				69.6	67.8	67.9		

[a] Ether extract is the method used to determine the content of lipids (fat and oil) in feedstuffs.[56]

[b] Nitrogen free extract (NFE) is an estimate of soluble carbohydrates like crude starch and sugar content of a feed. This content is not analytically determined, but is calculated by difference with the equation: % NFE = % Dry Matter – (% Ether extracts (Fatty acids) + % Crude protein + % Ash + % Crude Fibre), the estimation of NFE accumulates all the errors that exist in the analysis of the other components.[56,57]

Table 6. Substances found in the industrial food wastes.

	Coffee[58]		Avocado seed [59]	Wheat straw [60]	Banana peel [61]	Corn stover [62]	Carrot [63-65]		
	Pulp	Husk					Pomace	Peel	Leaf
	wt.% DM		wt.%	wt.% DM	wt.% DM	wt.% DM	wt.% DM	wt.% DM	wt.%
Moisture			56.0 ± 2.6						7.2 ± 0.1
Protein	10	9.2	2.0 ± 0.2	7.8 ± 2.2	7.9		8.4 ± 0.2	9.7 ± 0.3	15.2 ± 0.5
Fatty acids	2.5	2			11.6				
Fiber	18		5.1 ± 1.1	54.6 ± 0.6	7.7		63.5 ±1.5	45.5 ±0.4	12.0 ± 0.3
Lignin				4.2 ± 1.3		11.0 ± 1.8			
Carbohydrates [a]	50	57.8	33.2 ± 2.7		59.5	27.8 ± 2.8	19.3	33.0 ±0.8	52.7 ± 0.7
Cellulose				28.0 ± 0.6					
Lipids			1.9 ± 0.3			32.0 ± 2.6	1.1 ± 0.1	1.5 ± 0.1	
Hemicellulose				22.3 ± 0.8					
Starch									
Sugar									
Pectin		12.4				7.8 ± 1.6			
Ash			1.9 ± 0.2		13.4		7.7 ±0.01	10.3 ±0.3	10.5 ± 0.3
NFE [b]									2.5 ± 0.1

[a] The data for carbohydrates is not subdivided. [b] Nitrogen free extract (NFE) is an estimate of soluble carbohydrates like crude starch and sugar content of a feed. This content is not analytically determined, but is calculated by difference with the equation: % NFE = % Dry Matter – (% Ether extracts (Fatty acids) + % Crude protein + % Ash + % Crude Fibre), the estimation of NFE accumulates all the errors that exist in the analysis of the other components.[56,57]

The most common current uses are as inexpensive cattle feed or crop fertilizer but other applications make use of food wastes as renewable sources of pectins, natural fibres, oils and as a culture medium for fungi. They are also used for the production of renewable energy from combustion or as methane and biogas or biofuel sources. The food waste biomass resource could be categorized by the major available component but

this taxonomy leads to confusion because it is often the lower yield products that have value and can be sourced from many species across different categories. Similarly a classification based on highest current usage of biomass products can quickly become anachronistic. For these reasons we first consider the main food waste resources individually, examining their constitution, availability and current uses. This makes it easier to explore the resources which could be used to develop new markets in hydrophobic polymers.

This survey of the food waste resource indicates the raw materials that are potentially available, *inter alia*, for the production of biopolymers. Where the total amount of waste is indicated, this is calculated from the total worldwide production which is not the same as the industrial food waste.[66] It is the industrial waste that is collectable as agricultural, postharvest, processing and distribution wastes and is sufficiently uncontaminated that it can be used in secondary processes such as polymer production. Some authors[47] use the term 'food losses' to describe pre-consumer waste thus reserving the term 'waste' with its attendant value-judgement for domestic or consumer waste. The proportions of industrial and consumer waste vary with food type.[47] For example 16% of initial production of cereals is pre-consumer loss and a further 12% is lost by the consumer on average. These proportions vary geographically, the more affluent nations tending to have higher consumer loss and lower pre-consumer losses. For roots and tubers, on the other hand, the pre-consumer loss is 40% of initial production and consumer loss only 6% on average. For oilseeds and tubers pre-consumer losses again dominate at 20% while the consumer loses only 2% on the initial production. In can generally be assumed that consumer wastes are too contaminated for secondary processes other than gasification.

1.5.1 Potato waste

Potato (*Solanum tuberosum L.)* is particularly popular in Europe[67]: the UK *per capita* consumption was 102 kg in 2005. Approximately 25% of the input to a potato processing plant emerges as waste, consisting of a portion of the peel and whole or cut potatoes discarded due to size, blemishes, or failure to meet quality standards.

China is now the biggest potato producer at 72 Tg per year (Table 7) and almost a third of all potatoes are harvested in China and Russia. Starch is the main resource at 68 % based on dry weight (Table 5) and uses for starch in polymers and as a precursor to furan derivatives are described in the starch and sugars sections (1.5.1.1 and 1.5.1.7).

Table 7**.** Production of potato (data for 2007)[67]

Country	**Production /Tg**
China	72
Russian Federation	37
India	26
USA	20
Ukraine	19
Poland	12
Germany	12
Belarus	9
Netherlands	7
France	6
World	325

Potato waste is also a source of polyphenols which are found mainly in the subsurface. The structures of polyphenols and chlorogenic acid isomers found in the potato tuber are shown in Table 8. Chlorogenic acid constitutes 90% of the total phenolic content. The possible polymerisation of these minor constituents is discussed below.

Table 8**.** Structures of potato polyphenols and chlorogenic acid isomers.[68]

Structure		**Trade name**	**Synonym**	**IUPAC nomenclature**
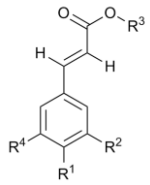	R^1=R^2=R^3=R^4=H	cinnamic acid	-------	(E)-3-phenylprop-2-enoic acid
	R^1=OH, R^2=R^3=R^4=H	p-coumaric acid	4-hydroxycinnamic acid	(*E*)-3-(4-hydroxyphenyl)prop-2-enoic acid
	R^1=R^2=OH, R^3=R^4=H	caffeic acid	3,4-dihydroxy-trans-cinnamic acid	(*E*)-3-(3,4-dihydroxyphenyl)prop-2-enoic acid
	R^1=OH, R^2=OCH_3, R^3=R^4=H	ferulic acid	4-hydroxy-3-methoxycinnamic acid	(*E*)-3-(4-hydroxy-3-methoxyphenyl)prop-2-enoic acid
	R^1=R^2=OH, R^3=quinic acid R^4=H	chlorogenic acid	3*R*-[[3-(3,4-dihydroxyphenyl)-1-oxo-2-propenyl]oxy]-1*S*,4*R*,5*R*-trihydroxy-cyclohexanecarboxylic acid	(1*R*,3*R*,4*S*,5*R*)-3-[(*E*)-3-(3,4-dihydroxyphenyl)prop-2-enoyl]oxy-1,4,5-trihydroxy-cyclohexane-1-carboxylic acid
	R^1=OH, R^2=R^4=OCH_3, R^3=H	sinapic acid	4-Hydroxy-3,5-dimethoxycinnamic acid	(*E*)-3-(4-hydroxy-3,5-dimethoxyphenyl)prop-2-enoic acid

Large amounts of potato waste are left in open fields to decompose and some used to feed cattle which can consume up to 12% of their body weight of fresh potatoes daily: potato delivers four times the energy value of cereal grain for beef cattle.[49] Several novel projects have addressed the opportunities provided by the extensive availability of potato waste. In one example, potato waste, digested in four stages - hydrolysis, acidification, acetogenesis and methanogenesis, enabled a biogas plant to provide electricity to the public grid and to preheat industrial dryers.[69] This technology

has also been applied in the UK.[70] Another application is the use of potato waste as a new medium for the fermentation of xanthan[71], a thickening agent used in food products and currently obtained expensively from sugar. Polylactic acid (PLA) has also been produced from potato waste which can be used as a non-petroleum based polymer.[72]

1.5.2 Corn stover

Corn, also known as maize, has been a dietary staple in the Americas since prehistoric times. According to the Food and Agriculture Organization of the United Nations (FAO)[59], in 2009, 819 Tg of corn were harvested and the USA produced 333 Tg per year, 40% of the world's total production. Ten countries who contribute 70% of worldwide production are listed in Table 9.

Table 9**.** World's corn production 2009.[59]

Country	Production /Tg
USA	333
China	164.1
Brazil	51.2
Mexico	20.1
Indonesia	17.6
India	16.7
France	15.3
Argentina	13.1
South Africa	12.1
Ukraine	10.5
World	818.8

Corn waste (or corn stover) compromises five parts: nodes, leaves, shell, core and sheath: the morphological structure is shown in Figure 5. At harvest, the grain represents only 15% of the weight: the rest is treated as food waste. This means that around 696 Tg of total corn waste is produced each year.

The components of corn stover are shown in Table 10. This is the most abundant ligno-cellulose renewable resource in the world due to its chemical composition and the enormous quantity produced annually worldwide. As seen in Table 10, 70% of the total corn stover is composed of ligno-cellulose corresponding to 487 Tg.

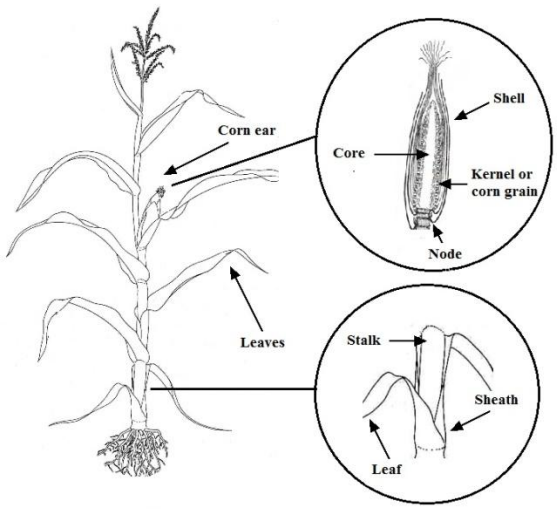

Figure 5**.** Corn stover structure.[73]

The main application for corn stovers is as fertilizer but new opportunities for its use are emerging, among them research on enzymatic hydrolysis and solid state fermentation[62], as a renewable source for ethanol production[74], using *Pichia stipitis*[75], a cellulolytic extremophile[76] and with biocatalysts.[77] Another application is in the production of biopolymers. Polyhydroxyalkanoates (PHA) can be produced from corn grains but there are attempts to produce it in combination with corn stover.[78]

Table 10**.** Chemical composition of corn stover.[62]

Part	**Weight ratio (%)**	**Cellulose (%)**	**Hemicellulose (%)**	**Lignin (%)**	**Ash (%)**	**Acid insolvable ash (%)**
Leaf	32.0	26.2 ± 2.3	33.9 ±1.9	9.3 ± 1.4	11.6 ± 1.5	1.6 ± 0.6
Shell	9.4	36.7 ± 3.2	27.5 ± 2.2	14.2 ± 1.0	4.6 ± 0.2	0.5 ± 0.2
Core	15.4	33.3 ± 4.9	32.2 ± 3.2	10.1 ± 1.8	4.9 ± 1.1	0.5 ±0.2
Node	22.9	28.9 ± 3.9	32.2 ± 2.4	12.5 ± 1.5	5.4 ±1.3	0.5 ± 0.1
Whole	100	27.8 ± 2.8	32.0 ± 2.6	11.0 ± 1.8	7.8 ±1.6	0.9 ± 0.3

Another approach is the chemical liquefaction of the lignocellulosic materials in the corn stover, which is about 71% (Table 10) of its total composition, using ethylene carbonate and/or ethylene glycol as solvent and sulphuric acid as catalyst for the preparation of polyols. The lignocellulosic material is partially degraded into polyols, providing OH groups which can be used for the production of polymers without further separation, modification or purification. Biodegradable polyesters can be obtained by cross-linking the polyols with multi-functional carboxyl acids and/or cyclic acid anhydrides.[79] Furthermore, the polyols obtained can be used directly for the preparation of polyurethane foams by a one-shot method using dibutyltin dilaurate as co-catalyst,

silicone as surfactant and water as blowing agent. The mechanical strength of the obtained polyurethane foams can be controlled and improved by using polymethylene polyphenylisocyanate (PAPI) as co-monomer which varies the [NCO]/[OH] ratio in the structure of the foam.[80]

1.5.3 Mango seed

Mango (*Mangifera indica*) is a native tropical fruit from southern Asia which is now cultivated in most frost-free tropical and warmer subtropical climates. Seven countries are responsible for almost 74% of the entire world production of mango (2008 data).[59] India is the largest producer with 13.6 Tg equivalent to 39% of world production (Table 11). During the processing of mango, peel and almond are generated as waste materials and they represent around 40-50% of the total fruit weight so that the total world production yields approximately 15.7 Tg of mango waste per annum.

Table 11. World production of Mango (2008 data).[59]

Country	Production /Tg
India	13.6
China	4.0
Thailand	2.4
Indonesia	2.0
Mexico	1.9
Pakistan	1.8
Brazil	1.2
Bangladesh	0.8
World	34.9

The mango almond contains high quantities of carbohydrates (such as starch), fat and fibre (Table 12). Through microbial fermentation it is possible to obtain pectins, comestible fibres, vinegar and citric acid.[81]

Table 12. Chemical composition of mango almond.[51]

Constituent	Amount %
Moisture	40.5
Protein	1.43
Fatty acids	4.92
Fibre	3.96
Carbohydrates	48.19
Ash	0.83

The almond contains around 5% of fat, 95% composed of neutral lipids and the reminder of polar lipids. The oil obtained consists of 44-48% saturated fatty acids and 52-56% unsaturated.[51] Oleic acid is the primary component at 40.8% and protein content varies from 5.5 to 9.5% which represents 31-35% of total essential amino acids (Table 13). Other acids are found: palmitic, stearic, linoleic, linolenic, arachidic, lignoceric and behenic. The oil obtained from the seed is used for confectionery, chocolate elaboration, cosmetics and soap production. It is principally used as a substitute for cocoa butter.[81]

Table 13**.** Profile of fatty acids in mango almond.[81]

Fatty acid			**%**
Systematic name	**Traditional name**	**Abbreviation**	
Hexadecanoic	Palmitic	16:0	9.3
Octadecanoic	Stearic	18:0	39.1
cis-9-Octadecenoic acid	Oleic	18:1 *cis*-9	40.8
cis-9,12-Octadecadienoic acid	Linoleic	18:2 *cis*-9,12	6.1
cis-9,12,15-Octadecatrienoic acid	Linolenic	18:3 *cis*-9,12,15	0.6
Eicosanoic	Arachidic	20:0	2.5
Docosanoic	Behenic	22:0	0.6
Tetracosanoic	Lignoceric	24:0	0.5
-	Not identified	-	0.5

The kernel obtained after decortication of the mango seed is used in India and Indonesia for the production of flour or as a supplement to wheat flour. It is also used as cattle food and fertilizer. Polysaccharide based biopolymer films have been produced using the starch (carbohydrate) from mango seed waste and pectin from tree tomato.[82]

1.5.4 Citrus' fruit waste

Citrus waste provides interesting potential precursors for materials manufacture. The world citrus production is divided into four categories; orange (*Citrus sinensis*), mandarins/tangarines (*Citrus nobilis*), grapefruit (*Citrus paradise*) and lemon (*Citrus limon*)/lime (*Citrus aurantifolia*). The total production of citrus in 2009-2010 according to the United States Department of Agriculture (USDA)[59] was 82 Tg where 60.7% of production corresponds to oranges, 25.3% to mandarins, 6.7% to grapefruit and 7.3% to lemons/limes.

Table 14 gives the world orange production which is mostly attributed to five countries who contribute 71% of all world production, Brazil being the largest producer (33%). For mandarin/tangerine production, 64% is produced by China. Grapefruit and lemon/lime have a lower worldwide production. Even though Brazil only produces

orange, the quantity of 16.2 Tg makes it the second biggest producer of citrus (20%). The third producer is the EU-27 which includes almost all European countries (12.8%), followed by Mexico (7.2%) and Turkey (3.9%). These five countries produce 71.4% of the total citrus world production.

Table 14. World citrus production in 2009-2010.[59]

Orange		Mandarin/tangerines		Grapefruit		Lemon and lime	
Country	**/Tg**	**Country**	**/Tg**	**Country**	**/Tg**	**Country**	**/Tg**
Brazil	16.24	China	13.30	China	2.90	Argentina	1.00
China	6.35	EU-27	3.07	Israel	0.25	EU-27	1.16
Egypt	3.57	Japan	1.10	Mexico	0.41	Mexico	2.04
EU-27	6.20	Korea, South	0.70	South Africa	0.35	Turkey	0.68
Mexico	3.45	Turkey	0.75	United States	1.11	Unites States	0.78
World	49.78	World	20.71	World	5.47	World	5.99

The citrus peel represents about 15% of the total fruit weight meaning that the worldwide production of total waste from citrus crops is potentially of the order 12.3 Tg per year. From this quantity 7.4 Tg is attributed to orange production, 3.1 to mandarins, 0.8 to grapefruit and 0.9 to lemons/limes. According to USDA[59], China produces 3.4 Tg of citrus waste, while Brazil produces 2.4 Tg followed by EU-27 with 1.6 Tg, Mexico with 0.9 Tg and Turkey with 0.5 Tg.

The approximate composition of different citrus peel is presented in Table 15. All provide essential oils and so have been used since ancient times for perfumes and as aromatic substances. Table 16 presents the main compounds: monoterpenes, aldehydes, alcohols and esters of the oils.

Table 15**.** Chemical composition of citrus' peel.

Constituent (%)	**Grapefruit** [53]	**Lemon**[54]	**Lime**[53]	**Orange**[55]	**Mandarin**[55]
Dry matter	91.8	89.4	89.9	-	-
Ash	4.2	5.2	5.1	2.6 ± 0.1	5.1 ± 0.2
Crude protein	4.9	9.3	9.7	9.1 ± 0.4	7.5 ± 0.2
Crude Fibre	11.9	14.9	14.4	-	-
Sugars	-	-	-	9.6 ± 0.2	10.1 ± 0.5
Fatty acids[c]	1.06[a]	1.51 ± 0.11[b]	1.24[a]	4.0 ± 0.2	1.6 ± 0.1
Pectin	-	-	-	23.0 ± 2.1	16.0 ± 1.2
Flavonoid	-	-	-	4.5 ± 0.2	5.1 ± 0.1
Lignin	-	-	-	7.5 ± 0.6	8.6 ± 0.8
Cellulose	-	-	-	37.1 ± 3.1	22.6 ± 2.2
Hemicellulose	-	-	-	11.0 ± 1.1	6.0 ± 0.6
Ether extract	1.1	2.8	2.9	-	-
Nitrogen free extract	69.6	67.8	67.9	-	-

[a] These % compositions were extracted from ref. 83

[b] This information comes from source ref. 84

[c] Includes terpenes and volatile species

Different studies show variations in the percentage concentration of oil in the peel as it is influenced by the country of origin, the species, the harvesting season, meteorological and environmental factors. The results can also be affected by the analytical method used for the extraction[83] but on average, the percentage of oil in the grapefruit, lemon, lime, orange and mandarin are 1.0, 1.5, 1.2, 4.0 and 1.6 % respectively.

Table 16**.** Percentages of constituent in citrus peel oils.[85]

Constituent	Orange	Mandarin	Grapefruit	Lemon	Lime
			% of oil		
Monoterpenes	**89-91**	**98**	**88**	**81-85**	**69**
D-limonene	83-90	65-68	88-90	72-80[b]	64
α-Pinene	0.5	0.8	1.6	2	1.2
β-Pinene	1	-	-	7.13	1.2
Myrcene	2	2	1.9	2	-
γ-Terpinene	0.1	-	0.5	10	22
ρ-cymene	-	2.8	0.4	-	1.9
Aldehydes	**1.8**	**-**	**1.2-1.8**	**-**	**-**
Heptanal	3[a]	-	4[a]	1	-
Octanal	39[a]	-	16-35[a]	4[a]	-
Nonanal	5[a]	-	7[a]	6[a]	-
Decanal	42[a]	5	43-54[a]	3[a]	-
Citral	0.05-0.2	-	0.06	1.9-2.6	3.1-5.3
Alcohols	**0.9**	**-**	**0.3-1.3**	**-**	**-**
Octanol	2.8	-	-	1	-
Decanol	-	-	-	-	-
Linalool	5.3	2	0-3[b]	-	-
Ester	**2.9**	**-**	**3-4**	**-**	**-**

[a] % of total aldehydes, [b] % of total terpene fraction

Most citrus peel wastes are used for cattle feed and the rest is disposed, creating a large quantity of natural residue waste.[54] For these reasons in the last few years there have been various initiatives to explore alternative uses. Citrus peels can be used as natural sources of customized functional fibres.[55] Specifically, for orange peel there are initiatives to use them as fermentation substrates for fungal multienzyme production[86] and as a source of Xanthophyll pigment for the improvement of egg yolk colour.[87] Researchers from Spain have been working on the generation of bioethanol from pretreated mandarin peel wastes, with steam explosion, due to the high content of carbohydrates.[88] They are also employed as a renewable source for pectin production which is used in the food and pharmacological industry.[89]

1.5.5 Grape waste

The total world production of grapes (*Vitis vinifera*) is around 15 Tg per year and the main producers are listed in Table 17. According to Organisation Internationale de la Vigne et du Vin (OIV) (2007)[90], 65% is used for wine and juice (9.8 Tg), 23% as fresh fruit (3.5 Tg) and 12% as dried fruit (1.8 Tg).

Table 17. Main grape producers (2009-2010).[90]

Country	Production /Tg
Brazil	1.30
Chile	1.03
China	5.62
EU-27	2.00
Turkey	2.00
World	15.08

The main wine producers (2010 data)[91] are France, Italy and Spain sometimes known as the "Big Three" of wine. Approximately 30 kg of waste is produced in the production of 100 L of wine and each litre of wine needs on average 1.3 kg of grapes so that 23% of the grapes used become available waste.[92] The quantity of grapes used in wine production varies with the year and the vineyard. Regarding the production of champagne, according to INAO's (Institut National des Appellations d'Origine) regulations, the obligatory proportion has to be 160 kg/100 L and 150 kg/100 L for sparkling wines. From the available information, during 2009, 2.6 Tg of wine residue, also known as marc or pomace was produced for which a range of uses have been proposed.[93]

Grape solid wastes comprise mainly skins, pulp, pip, seeds, stems, yeast and juice that are left after each part of the wine process. A standard process for white wine is presented in Figure 6 showing the different types of residues produced in each stage of the process. The first grape pressing yields marketable wine and avoids over-pressing of the raw material. Winemakers send the alcohol produced from the remaining pomace to other industries, a part of the process known as "prestation d'alcool vinique". The last pressings can be discarded or used for vinegar or brandy. In brandy production, the grape marc must be fermented separately from the juice.

Over-pressing of the grapes gives an astringent liquid and an acid juice which are undrinkable making them undesirable products. For this reason continuous pressing is proscribed. The maximum limit to which the pomace is pressed is until oil is obtained.

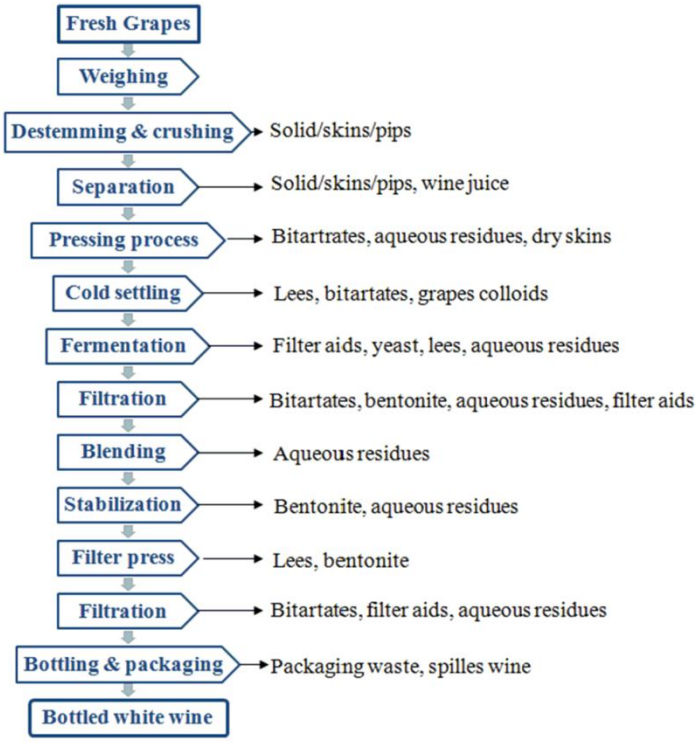

Figure 6. Scheme for conventional white wine production.[94]

Grape seed oil contains about 10-20% of oil which is rich in unsaturated fatty acids such as linoleic acid (69-78%, w/w) which contributes to the production of biodiesel (Table 18). The biodiesel quality depends on the fatty acid composition of the oil: unsaturated fatty acids help improve its low-temperature properties.[95]

Table 18. Fatty acids founded in grape seed oil.[93]

Fatty acid			%
Systematic name	**Trade name**	**Abbreviation**	
Hexadecanoic acid	Palmitic	16:0	5-11
cis-9-Hexadecenoic acid	Palmitoleic	16:1 *cis*-9	0.5-0.7
Octadecanoic acid	Stearic	18:0	3-6
cis-9-Octadecenoic acid	Oleic	18:1*cis*-9	15-20
cis-9,12-Octadecadienoic acid	Linoleic	18:2 *cis*-9,12	69-78
cis-9,12,15-Octadecatrienoic acid	Linolenic	18:3 *cis*-9,12,15	0.3-1

Grape seeds also contain substances with antioxidant properties such as tocopherols in a range from 240-410 ppm, polyphenols and oligomeric proanthocyanidins (OPC) which have medical and cosmetic applications. Polyphenolic compounds with antioxidant properties are present in the skin of red grapes (Table 19) but the quantity varies according to the grapevine, cultivar, season and environmental factors. The most abundant compounds are: 3-acetylglycosides , 3-glycosides, 3-p-coumaroylglycosides of malvidin (Mv), peonidin (Pn), delphinidin (Dp), petunidin (Pt), cyanidin (Cy) and

tartaric esters of hydroxycinnamic acids, monomeric and dimeric flavanols, flavonols and stilbenes. The other principal use of red wine waste is the solid-liquid extraction of anthocyanin pigments which are used in cosmetics, food and the pharmaceutical industry.[96]

Table 19**.** Phenolic substances in grape seeds.[93]

Antioxidants	**g L^{-1}**	**g per 100 g dry matter**
Total phenols (GAE)	2.86 ± 0.01	8.58 ± 0.03
Total flavanoids (CE)	2.79 ± 0.01	8.36 ± 0.04
Proanthocyanidins (CyE)	1.38 ± 0.06	5.95 ± 0.17

(GAE: gallic acid equivalent; CE: catechin equivalent; CyE: cyanidin equivalent)

In contrast to many food wastes, a wide range of industries already benefit from grape waste including composting, dietary supplements, gas production for heating purposes, pharmaceutical additives and animal feedstuffs. It can therefore be argued that with this extensive waste utilization programme already underway, grape waste does not provide a strong and unique opportunity for obtaining chemical precursors for other uses.

1.5.6 Pumpkin seed

Also known as "pepitas" in most spanish speaking countries, pumpkin seeds are cooked and eaten. The seed represents approximately 20% of the total weight of the pumpkin, and according to Table 20, which lists the main suppliers the annual production of seeds is 4.2 Tg. The main consumers of pumpkin seeds are countries from Latin America, notably Mexico and Central America and Asian countries due to their type of cuisine, traditions and diet.

Table 20. Word production of pumpkins in 2009.[59]

Country	**Production /Tg**
China	6.5
Russian Federation	1.23
United States of America	0.75
Egypt	0.7
Ukraine	0.56
World	21.2

Pumpkin seeds are also a source for natural oils which are very rich in unsaturated fatty acids (up to 78%) (Table 21). Expected therefore to be vulnerable to oxidative degradation, it is found experimentally to be a vegetable oil with high oxidative stability partly because of the low 18:3 and high 18:1 contents, partly the high δ-tocopherol content which absorbs free radicals and partly the low fraction of sterols in the oil. Sterols are fatty acid esters that can be hydrolyzed producing free fatty acids promoting the autoxidation sequence.

Table 21**.** Fatty acids in pumpkin seed oil.[97]

Fatty acid			**%**
Systematic name	**Traditional name**	**Abbreviation**	
Hexadecanoic acid	Palmitic	16:0	6.2
Octadecanoic acid	Stearic	18:0	1.9
cis-9-Octadecenoic acid	Oleic	18:1 *cis*-9	32.6
cis-11-Octadecenoic acid	cis-Vaccenic	18:1 *cis*-11	0.6
cis-9,12-Octadecadienoic acid	Linoleic	18:2 *cis*-9,12	58.2
***cis*-9,12,15-Octadecatrienoic acid**	Linolenic	18:3 *cis*-9,12,15	0.2
Eicosanoic acid	Arachidic	20:0	0.1
cis-11-Eicosenoic acid	Gondoic	22:1 *cis*-11	0.1

1.5.7 Sugar bagasse

Sugar cane (*Saccharum L.*) is mainly cultivated for sugar and ethanol production and world production in 2010-2011 was 130 Tg, with Brazil and India being the main producers with 50% of total production (Table 22).

Table 22**.** World production of sugar cane during 2010/2011.[59]

Country	**Production /Tg**
Brazil	39.40
China	11.72
India	25.70
Mexico	5.45
Thailand	6.87
World	130.43

The processing of sugar cane is divided in two stages; milling and refinery. Milling involves extraction of the raw sugar by crushing the canes between rollers to obtain a white juice with 15% sugar. Through different methods, mainly evaporation and centrifugation, the juice is purified into a raw sugar containing 60% sucrose after which the refining process purifies and concentrates the sugar to 99% sucrose by boiling in a vacuum pan.[98] The industrial waste from milling is the sugar cane remaining, known as

sugar bagasse, and represents 28% of the dry weight of the original. The main constituents of the sugar bagasse are glucan (39 %), lignin (25 %) and xylan (22%) (Table 23). Annual production of bagasse is thus approximately 36.5 Tg and much is currently used in distillery plants as a source of energy, for pulp and the paper industry, for the production of: particle board, fibre board, cardboard, furfural, microcrystalline cellulose, hydrolysed bagasse, pre-digested pith, molasses - urea - pith, furfural cement and compost.[99]

Table 23**.** Chemical composition of sugar cane bagasse.[52]

Constituent	**%**
Glucan	39
Xylan	21.8
Galactan	0.8
Arabinan	1.8
Acetyl	3.3
Lignin	24.8
Ash	3.9
Protein	0.5
Sucrose	0.7
Water extractives	2.7
Ethanol extractives	1.9

As seen in Table 23, sugar cane is a lignocellulosic material and hence an attractive feedstock for ethanol fuel production. From this perspective, it can be indicated that it is mainly composed of lignin (20-30%), cellulose (40-45%) and hemicelluloses (30-35%).[100] The limiting step is the degradation of cellulose and hemicelluloses into sugars for ethanol production which is complex, energy-consuming and has a high cost. Clearly, the main source for bioethanol is the primary sugars but this prompts competition over land use between food and the biofuel production.[99] The production of ethanol from sugar cane bagasse is more complex involving five processes; biomass pre-treatment, cellulose hydrolysis, fermentation of hexoses and pentoses, separation and effluent treatment (Figure 7).[100] The biomass pretreatment is based on the solubilization and separation of the components needed (polysaccharides and carbohydrates) for their further treatment. Subsequent hydrolysis breaks the hydrogen bonds of the major molecules into their sugar components, which are then fermented into ethanol.[101]

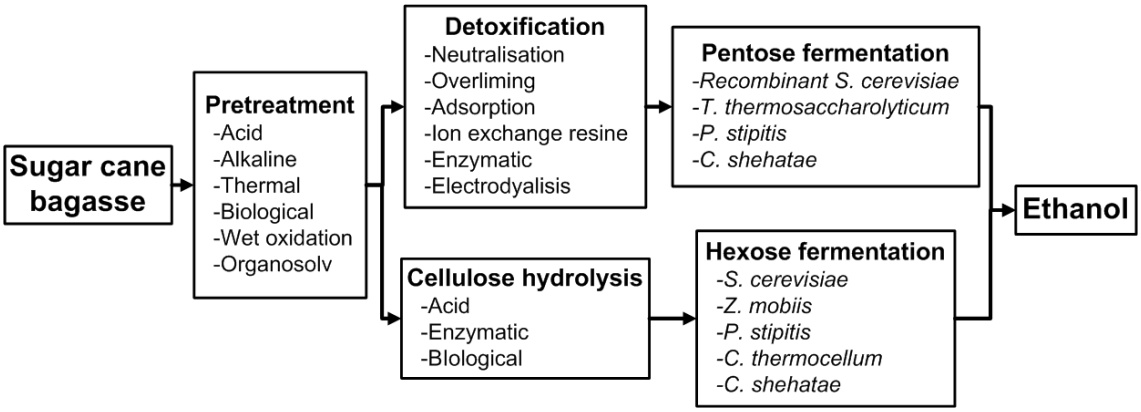

Figure 7**.** Industrial process for fuel ethanol production from sugarcane bagasse. Possibilities for reaction integration are shown inside the shaded boxes: CF, co-fermentation; SSF, simultaneous saccharification and fermentation; SSCF, simultaneous saccharification and co-fermentation.[100]

The importance of the ethanol route is that ethanol can undergo an acid catalyzed dehydration to ethene, which can enter directly into conventional chemical process plant. It can be converted into polyethylene and used in the synthesis of vinyl chloride and for the production of styrene and hence to their polymers.

1.5.8 Coffee waste

World coffee (*Coffea sp*.) production exceeds 8.4 Tg and there are two main varieties, *Coffea arabica* and *Coffea robusta*. Brazil and Vietnam are the main producers controlling 53% of world total production (Table 24).[59]

Table 24. Coffee world production, 2010/2011.[59]

Country	Production /Tg
Guatemala	0.24
Mexico	0.28
Brazil	3.32
Colombia	0.54
Peru	0.24
India	0.28
Indonesia	0.58
Vietnam	1.12
Ethiopia	0.25
Uganda	0.19
World	8.38

The industrial process to obtain isolate coffee powder consists of removing the shell and mucilaginous part of the cherries[102] by either a wet or dry process, each producing wastes with different compositions. Endocarp, mesocarp and exocarp from the dried

fruit represent 60% of total weight, i.e. 5 Tg of coffee waste are produced each year where 55% comes from Latin America where there are as yet no industrial uses for it.

Coffee husk and pulp chemical compositions are shown in Table 25 although clearly, these vary with plant, cultivation conditions and crop. The residues still have a significant percentage of caffeine which restricts their subsequent use while tannins inhibit its use as cattle feed because of counter-nutritional effects. Solution treatments and ensilage diminish the amount of anti nutritional substances like polyphenols, tannins and caffeine.[103]

Through biotechnology processes, coffee wastes are used to produce enzymes such as pectinase, tannase and caffeinase, flavour and aroma compounds used in the food industry. It is also used in the cultivation of mushrooms, for biogas production by anaerobic digestion and for composting.[58] Applications involving a bioconversion process generally need detoxification of tannins and caffeine in the coffee residues as a prerequisite. The latest applications include the use as fibres for the production of particleboard[104] and as a source for the synthesis of SiO_2 nanoparticles.[105]

Table 25**.** Chemical composition of coffee waste.[58] (% dry weight basis)

Constituents	[a] **Coffee pulp** [b] %		**Coffee husk** %
Carbohydrates	50	44	57.8
Proteins	10	12	9.2
Fibres	18	21	-
Fat	2.5	-	2
Caffeine	1.3	1.3	1.3
Tannins	1.8-8.6	-	4.5
Polyphenols	-	1	-
Pectins	-	-	12.4

[a, b] information from different sources.

1.5.9 Banana waste

Banana (*Musa sapientum*) is one of the most well known and popular tropical fruits in the world and it is available throughout the year. The peel represents 40% of the banana fruit[106] generating annually around 22 Tg of peels much of which is domestic waste. The four main producers are India, Brazil, Ecuador and China (Table 26) who generate 27 Tg of bananas per year, being practically 50% of the worldwide output and thus produce 10.9 Tg of potential banana wastes.

Table 26**.** World production of bananas in 2000.[106]

Country	Production /Tg
India	11
Brazil	6.3
Ecuador	5
China	4.8
Philippines	3.6
Indonesia	3.2
World	55.2

The chemical composition of peel varies with the stage of maturation. Increasing soluble sugar, protein and lipid content and decreasing hemicellulose and starch take place over time. The degradation of starch and hemicelluloses by enzymes explains the late stage increase of sugar.[107] The general chemical composition of banana peel is shown in Table 27. The high content of protein (7.9%) and carbohydrates (59.5%), make it suitable for fungus cultivation and the high fraction of fatty acids (11.6%) indicates it can be used as an alternative source of energy and potentially for biopolymers. The ash has high levels of phosphorus, potassium, sodium and magnesium and low levels of calcium and iron.

Table 27**.** (a) Constitution of banana peel and (b) mineral content of banana peel.[61]

Constituent	Dry Matter %
Dry matter	14.1
Crude protein	7.9
Crude fat	11.6
Crude fibre	7.7
Total ash	13.4
Carbohydrate	59.5
Moisture	78.4

(a)

Constituent	mg/100 g
Ca	7
Na	34
P	40
K	44
Fe	0.9
Mg	26
S	12
Ascorbic	18

(b)

Banana peel is a source of pectins and dietary fibre.[108] It can be used for mycological research as a medium and as a substrate for microfungal biomass production.[61] From the biomethanation of banana peel, it is also possible to obtain methane by fermentation[109] using flocculating yeast to provide continuous ethanol production[110], and it is used for the treatment of wastewater plants as an adsorbent for impurities like heavy metals.[111] It is also used as cattle feed, as fertilizer due to the high content of ash and for the extraction of banana oil, pentyl ethanoate (amyl acetate).

1.5.10 Avocado seed

Avocado (*Persea Americana*) is the fruit of a native Mexican tree and it is mainly cultivated in tropical climates. According to FAO[59] the world production is around 3.9 Tg per year where 76% of the total production is controlled by 10 countries (Table 28). As it originated from Mexico, this country is the biggest producer with 32% of world output.

Table 28. World production of avocado 2009.[59]

Country	Production / Tg
Mexico	1.23
Chile	0.33
USA	0.27
Indonesia	0.26
Dominican Republic	0.18
Colombia	0.17
Peru	0.16
Brazil	0.14
China	0.10
Guatemala	0.09
World	3.85

The avocado fruit comprises a dark green peel, green oily pulp and a large seed which represents 10-22% of the total weight depending on the species[112], meaning that it contributes potentially 0.85 Tg of waste. The seed is mainly composed of moisture and carbohydrates, while the remaining 10% is lipids, proteins, ashes and fibre (Table 29).

Table 29. Aproximate composition of the avocado seed.[113]

Constituents	%
Moisture	56.0 ± 2.6
Lipids	1.9 ± 0.3
Protein	2.0 ± 0.2
Ash	1.9 ± 0.2
Fibre	5.1 ± 1.1
Carbohydrates	33.2 ± 2.7

The fatty acid composition of the avocado seed is shown in Table 30. It contains 27 fatty acids where 17 are saturated (32% of total fatty acids), 7 are monounsaturated (21%) and 3 are polyunsaturated fatty acids (47%).

Table 30. Fatty acids found in the avocado seed.[113]

Fatty acid			%
Systematic name	**Common name**	**Abbreviation**	**of the total fatty acid**
Saturated fatty acids			32.50
Hexanoic acid	Caproic	6:0	0.80 ± 0.05
Heptanoic acid	Enanthic	7:0	0.29 ± 0.10
Octanoic acid	Caprylic	8:0	0.28 ± 0.05
Nonanoic acid	Pelargonic	9:0	0.22 ± 0.01
Decanoic acid	Capric	10:0	Traces (<0.06%)
Undecanoic acid	Undecylic	11:0	Traces (<0.06%)
Dodecanoic acid	Lauric	12:0	0.28 ± 0.05
Tridecanoic acid	Tridecylic	13:0	0.17 ± 0.01
Tetradecanoic acid	Myristic	14:0	0.54 ± 0.05
Pentadecanoic acid	Pentadecylic	15:0	2.33 ± 0.11
Hexadecanoic acid	Palmitic	16:0	20.85 ± 0.84
Heptadecanoic acid	Margaric	17:0	1.73 ± 0.02
Octadecanoic acid	Stearic	18:0	1.19 ± 0.01
Nonadecanoic acid	Nonadecylic	19:0	0.61 ± 0.34
Eicosanoic acid	Arachidic	20:0	0.04 ± 0.02
Docosanoic acid	Behenic	22:0	1.11 ± 0.02
Tetracosanoic acid	Lignoceric	24:0	1.69 ± 0.05
Monounsaturated fatty acids			20.71
cis-9-Tetradecenoic acid	Myristoleic	14:1 *cis*-9	0.25 ± 0.002
cis-10-Pentadecenoic acid		15:1 *cis*-10	0.32 ± 0.16
cis-9-Hexadecenoic acid	Palmitoleic	16:1 *cis*-9	1.79 ± 0.33
cis-10-Heptadecanoic acid		17:1 *cis*-10	0.37 ± 0.08
cis-9-Octadecenoic acid	Oleic	18:1 *cis*-9	17.41 ± 0.06
cis-11-Eicosenoic acid	Gondoic	20:1 *cis*-11	0.45 ± 0.28
cis-13-Docosenoic acid	Erucic	22:1 *cis*-13	0.12 ± 0.04
Polyunsaturated fatty acids			46.73
cis-9,12-Octadecadienoic acid	Linoleic	18:2 *cis*-9,12	38.89 ± 0.59
cis-9,12,15-Octadecatrienoic acid	Linolenic	18:3 *cis*-11	6.58 ± 0.03
cis-11,14,17-Eicosatrienoic acid		20:3 *cis*-11	1.26 ± 0.03

Research on avocado seed extract has focused mainly on medical and cosmetic applications. There includes studies on the antimicrobial potential[114], skin and hair aerosol uses[115], for hepatic collagen solubility[116], skin collagen-metabolism[117] and effects on liver disease.[118] Clearly wider applications for fatty acids from avocado seed extract may exist including their deployment in polymerization.

1.5.11 Carrot waste

The carrot (*Daucus carota*) is globally the second most popular vegetable after the potato. World production is 33.6 Tg[59], China being the main producer at 36% (Table 31).

Carrot food waste is made up of peel, the pomace left after juice production and leaves from harvesting. Approximately 40-30% of carrot pulp is produced after the extraction of juice, leaving a high potential total world production of by-product. The

leaf has the major quantity of crude protein and carbohydrates, while the pomace contains more than 60% of fibre. Lipids and ash are present in similar amounts in each of the carrot by-products (Table 32). The by-products are being studied as raw materials for the production of antioxidants. The carotenoids concentrations of α-carotene, β–carotene and lutein in the carrots pomace are 51, 6 and 36 ppm, respectively.[119]

Table 31**.** World production of carrot 2009.[59]

Country	Production /Tg
China	12.09
USA	1.45
Russia	1.35
Poland	0.94
Uzbekistan	0.82
United Kingdom	0.75
Japan	0.67
Turkey	0.64
Ukraine	0.60
Italy	0.57
World	33.58

As with all the other food wastes, carrot leaf is mainly used to complement cattle food. Pomace and peel are used as alternative RACOD (Rapidly Acidifying Chemical Oxygen Demand) source[120] of organic-acids from microbal-production[121], as a source of soluble-fibre hydrolyzate from enzymatic production[122] and for the removal of chromium from aqueous solutions.[123] The carbohydrate can be used for the production of PLA (section 1.3.2.5).[124]

Table 32**.** Chemical composition and natural antioxidants of carrot by-products

Constituent (%)	Pomace[63]	Peel[64]	Leaf [65]
Moisture	--	--	7.2 ± 0.1
Crude protein	8.4 ± 0.2	9.7 ± 0.3	15.1 ± 0.5
Crude lipid	1.1 ± 0.1	1.5 ± 0.1	--
Fibre	63.5 ± 1.5	45.5 ± 0.4	12.0 ± 0.3
Ash	7.7 ± 0.01	10.3 ± 0.3	10.5 ± 0.3
Carbohydrate	19.3	33.0 ± 0.8	52.7 ± 0.7
Others	--	--	2.5 ± 0.1
Antioxidants			
β -carotene (mg/100g dry weight)	--	20.5 ± 0.5	8.7 ±0.3
Total phenolic (mg GAE/100g dry weight)	--	1371 ± 14	--
Total antioxidant activity (% of high dietary fibre powder)	--	96.7 ± 1.2	--
Vitamin C (mg/100g dry weight)	--	--	203.0 ± 3.8

1.5.12 Peanut husk

Peanut (*Arachis hypogaea L.)* is widely harvested and used in most cultures. The worldwide production of peanut in 2011 reached 34 Tg.[59] The grain constitutes about 30%, indicating that 10 Tg of total residues are produced in the form of husks. The five main producing countries are China (14.6 Tg) India (6 Tg), USA (1.8 Tg) and Nigeria (1.6 Tg). The literature differs on the chemical composition of peanut husk[48,125-127] but the most complete version is presented in Table 33.

Table 33. Peanut husk composition.[127]

Constituent	Weight %
Lignin	34.8
Glucan	21.1
Extractives	14.2
Protein	11.1
Xylan	7.9
Ash	3.4
Arabinan	0.7
Galactan	0.2
Mannan	0.1
Others (e.g. free carbohydrates)	6.5

The incineration of peanut husks has given way to various recycling schemes. The high lignin and low nitrogen contents mean that degradation is difficult to achieve which limits their use as fertilizers so the main uses are as feed for cattle, pigs and birds, as a culture medium for fungi and for protection of plants.

According to the US Department of Agriculture Chemist, National Peanut Research Laboratory[128] one third (33%) is used as cattle feed, another third (33%) as a base for litter and bedding, 30% functions as a chemical absorbent because when combined with activated carbon it helps remove offensive tastes, odours, colours, chlorine and organics substances and the remaining 3% is mainly a source of hydrogen for fuel cells. In some countries, notably China, the shells are used as a biomass fuel in stoves and boilers as a replacement for coal. It is claimed that peanut shell provides higher energy efficiency than traditional coal boilers as well as being cheaper to operate.[129] A catalytic pyrolysis process for the production of renewable hydrogen from peanut shells is available.[130] In another application, the fibrous skeleton that supports the cellulosic layer of the peanut husk can be used in the form of nonwoven biodegradable fabrics to control soil erosion until vegetation is matured.[131] Peanut shells are also employed for the absorption of toxic metal ions including cadmium copper, nickel, lead and zinc from solution[132] and

in the treatment of industrial wastewaters.[133] In comparison with pine sawdust, a common copper remover in industry, peanut husk removes 98% of copper ions from wastewaters while pine sawdust removes only 44%.[134] Peanut shell waste is mainly composed of fibre and is used as such in the form of reinforcement in polymer composites while the oil obtained from the seed can be polymerized.

1.5.13 Cereals straw

According to FAO in 2011 the worldwide production of cereals was of 2.6 Pg. This category includes the production of: wheat, rice paddy, barley, maize, popcorn, rye, oats, millets, sorghum, buckwheat, quinoa, fonio, triticale, canary seed, mixed grains (mixture of cereal species that are sown and harvested together) and cereals nes (cereal crops that are not identified separately because of their minor relevance at the international level).[59] The top producer countries are shown in Table 34. China is the main producer with 20 % of the world production, followed by USA and India with 15% and 11%, respectively. These three countries produce 42% of worldwide production.

Table 34. Cereals production in 2011.[59]

Country	Production /Tg
China	520.9
USA	386.8
India	285.5
Russia	91.8
Indonesia	83.4
Brazil	77.6
France	65.7
Ukraine	56.3
Bangladesh	52.6
Argentina	50.9
World	2587

The cereal crop residues after harvesting comprises 50-75% of the total production.[135] This indicates that at least 2.6 Pg of residues are produced after harvesting the crops. In Table 35 is presented the composition of wheat straw as an example of the straws obtained from cereals. It can be seen that these residues mainly contain fibre, cellulose and hemicelluloses.

Table 35. Chemical composition of wheat straw.[60,135]

Constituent	Weight % Dry matter
Protein	7.8 ± 2.2
Fibre	54.6 ± 0.61
Lignin	4.2 ±1.3
Cellulose	28.0 ± 0.59
Hemicellulose	22.3 ± 0.76
Straw: grain ratio	1.7:1

Some of this residue is left on the soil in order to reduce its erosion and as fertilizer as it reincorporates organic matter in the soil.[135] It is also used for the production of waxes by CO_2 extraction[136] for their use in cosmetics, polishes or the coating industry, and as a biofuel in energy plants where it is burned in order to produce high pressure steam which is used to drive a turbine to generate electricity[137], the use of the ligno-cellulosic material to produce strawboards[138], as fire-retardant of wood,[139] and their use in the construction industry.[140] They are also used as reinforcements for different materials, especially for polymers, this is further explained in section 1.7.

1.5.14 Animal waste

Article 3 of Regulation (EC) 1069/2009 of the European Parliament and the Council of the European Union restricts the use and controls the disposal of animal by-products. Such wastes include catering waste, used cooking oil, former foodstuffs, butcher and slaughterhouse waste, blood, feathers, wool, hides, shells and skins, fallen stock among others. These wastes are given three categories for disposal of which Category 3, low risk materials, includes the remains of animals, which are approved for human consumption, after passing through slaughterhouses. These parts are not eaten (bones, feathers, blood, skin, hair, shells) or are discarded for commercial reasons and include the waste from food factories and retail premises.[141] Figure 8 shows the by-products from the meat industry.

Some inedible by-products are treated for animal feed, fertilizer or protein based adhesives. Some tissues are used to produce composite bone-cum-protein meals or individual products like bone-meal, meat-meal and blood-meal. The total amount of waste is 10-15% of the live weight killed (LWK) animal.[142] In 2011, the worldwide meat production, according to USDA, reached 244 Tg where 42 % corresponds to pork, 35 % to poultry and 23% to beef.[143] Approximately 25 Tg of category 3 meat waste is produced annually in the world.

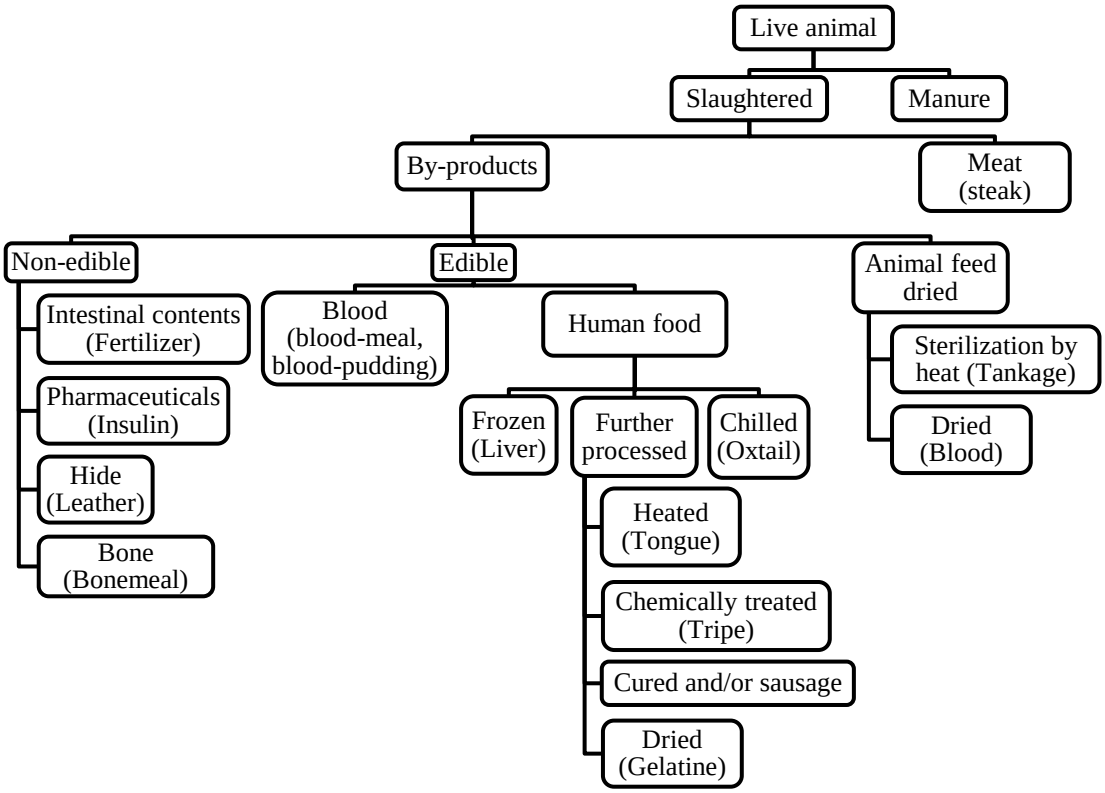

Figure 8. Schematic pathways for industrial meat and by-products.[141]

One application is the use of fat and oils for the production of biofuels. Triacylglycerols comprised of three long-chain fatty acids can be hydrolysed or transesterified to acids or esters and one glycerol. The esters can be used as biodiesel once the glycerol is removed.[144] Other waste which is studied for its exploitation is the feathers which can be used for the production of biodegradable thermoplastic films though graft polymerization with methyl acrylate.[145]

In the case of seafood, the shellfish catch consists approximately of 30% crustaceans and 70% molluscs. Crustacean processing waste compromises 40% exoskeletons (shell) while the mollusc processing waste consists of 65% shells.[146] In 2010, 20.8 Tg of mollusc and 11.8 Tg of crustaceans were caught, producing 18.2 Tg of shell waste.[59] This waste contains approximately 10% of chitin on dry weight.[147]

1.6 Strategies for production of biopolymers from food waste

This section explores how this huge resource might be exploited by making use of some of its constituents for the production of polymers with an emphasis on hydrophobic polymers, routes to hydrophilic polymers having been well explored and reviewed in other works.[19,24] Figure 9 shows the main pathways (direct and indirect) from the food waste resource, in some cases passing through hydrophilic polymer precursors, to the monomer which can be converted to hydrophobic polymers. The main goal is to reach, at the end of the process, a polymer which can act as a competitive replacement for the mineral oil-derived equivalent.

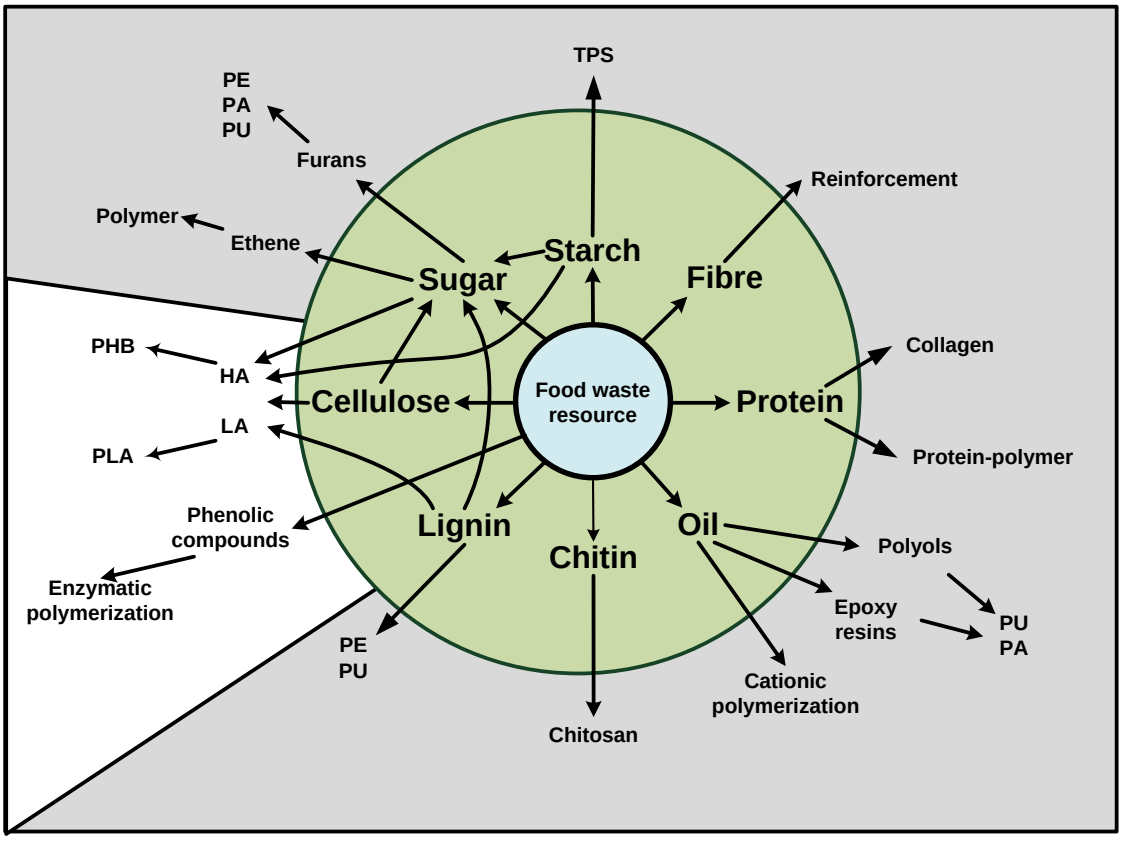

Figure 9. A schematic chart of the categories of biomass-sourced polymers showing the direct and indirect paths to hydrophobicity. Sugar has to be first converted into ethanol in order to obtain the ethene monomer. PE = polyester, PU = polyurethane, PA = polyamide, TPS = thermoplastic starch, HA = hydroxyalkanoates, LA = lactic acid, PHB = polyhydroxyalkanoate, PLA = poly lactic acid.

There are three basic strategies for the production of polymers which are designed to finish their useful life in composting, incineration or biodegradation.[148] The lifecycles for such materials are illustrated in Figure 10. The traditional strategy is the direct use

of biomass (wood, straw, cork) or biomass components (fibres, natural rubber, starch, cellulose, sugar, oils) in a finished product via physical changes such as mixing or chemical changes such as crosslinking. Much current interest is focused on a higher level of human intervention in the conversion of biomass resources by isolating monomers or oligomers to generate new compounds by industrial biotechnology involving chemical methods or fermentation (white biotechnology). Looking to the future, the strategy that seems likely to become more important especially to achieve enhanced yields, is the development of transgenic plants for production of biopolymers or polymer building blocks.

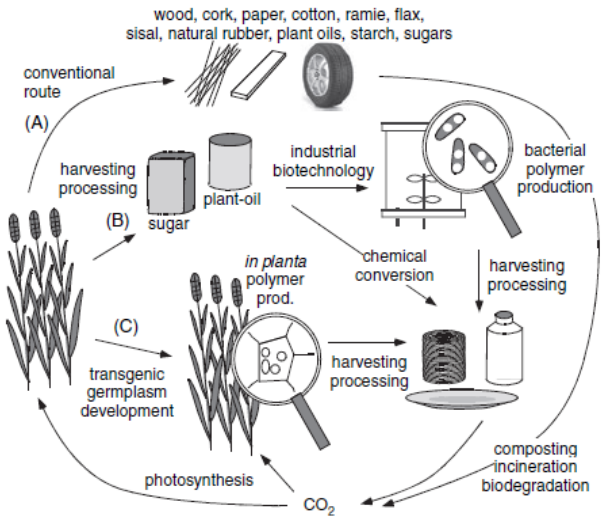

Figure 10. A pictorial representation production cycles for biodegradable polymers from reference.[148]

1.6.1 Biomass-sourced polymers

The first three classes of raw material are starches, celluloses and chitin which fall under the general heading of polysaccharides, carbohydrates formed by the condensation of monosaccharide residues through hemi-acetal or hemi-ketal linkages. They can also be found as short oligosaccharide sequences or polymeric repeat units linked to other biopolymers. They are biopolymers which are extracted directly as raw materials from plants and animals. Organisms use polysaccharides for energy storage and structural components.[149] The major representative macromolecules on this sector are cellulose fibre, chitin film and starch granules, and together they make-up around 22 to 37% of food waste resources as shown in Tables 5 and 6.

Although they are known as the unmodified polymers, they generally need to have a bulk or surface chemical modification, mainly on the hydroxyl groups of their

backbone structure for their use as biopolymers. The bulk modification relates to the formation of derivatives, of which chitosan is an example, while surface modification involves compatibility and minimization of hydrophilicity of natural fibres through covalent bonds between the fibres surface and the matrix.

The modification of natural polysaccharides has mainly focused on reducing hydrophilicity (hydrophobization) by lowering the surface energy or by creating an adequate surface morphology to obtain a water contact angle higher than 90°.[150,151]

1.6.1.1 Starch

Starch is produced from agricultural plants, mainly from potatoes, rice, maize and wheat in the form of hydrophilic crystallites with dimensions ranging from 1 to 100 μm. It appears as a food waste however mainly in potato and to a lesser extent mango seed. It is a hydrocolloid biopolymer comprised of two types of α-glucan: amylose (poly-α-1,4-D-glucopyranoside) a linear polymer and amylopectine (poly-α-1,4-D-glucopyranoside and α-1,6-D-glucopyranoside) as shown in Figure 11.[152,153] Depending on the botanical source, the percentage of each polymer varies, as well as the morphology, molecular structure and composition, affecting the properties of the extracted starch. The most well known source of starch is the potato which according to Table 5 contains around 67 wt.% starch.

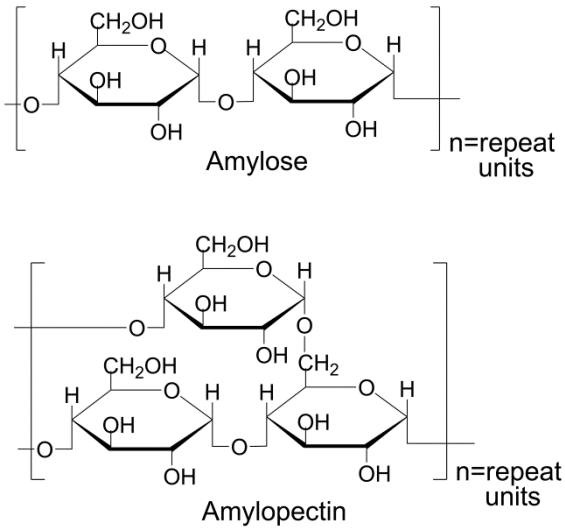

Figure 11. Structure of starch

Starch rich in amylose is preferred in different processes because its linearity guarantees better flow properties and an increase in elongation and strength.[154,155] Starch stability is broken when: (i) it is heated at 150 °C where the glucoside links start to break, (ii) at 250 °C due to the collapse of structure and (iii) at low temperatures when the retrogradation of starch takes place (amylase and amylopectin reorganize themselves causing gelatization of starch).[156]

Starch can be used in its natural form, mixed or as a filler for, *inter alia*, the formulation of tablets and capsules, for medical prosthesis or to enhance paper performance. For use in its natural form it should be modified to overcome the poor thermal, shear and acid stability as well as high rates and extents of retrogradation. It has two available functional groups for modification; the nucleophilic hydroxyl groups and ether bonds. Starch can be chemically modified, e.g. partial acid hydrolysis on the amorphous regions of the starch granules generate starch nanocrystals[157], or physically modified by hydrothermal treatment, where the starch structure and properties are changed without destroying its granular structure.[158] In the case of starch-filled polymer systems, starch should also be modified to develop compatibility between the starch and the synthetic polymers.[159]

To be used as a thermoplastic matrix, the granular structure of starch has to be destroyed through chemical methods, heat treatments, water absorption or thermomechanical treatment, such as extrusion, to form a homogeneous amorphous phase. Thermoplastic starch (TPS), can also be prepared in the presence of plasticizers like polyols, glycerol, fructose, xylitol, sorbitol, maltitol, ethanolamine, formamide and urea which promote starch granule destruction by breaking the hydrogen bonds in the crystallites.[24] TPS has enormous advantages as it is cheap, abundant and biodegradable but it has two major disadvantages, the poor mechanical strength properties and high moisture sensitivity.[160] There are some solutions for this: TPS can be mixed with appropriate fillers like nanoparticles, the surface can be chemically modified or it can be blended with a hydrophobic polymer[156]; such as polyvinyl alcohol[161], poly(ethylene-co-vinyl alcohol), PLA, polycaprolactone (PCL), poly (butylene succinate) (PBS), polyhydroxybutyrate (PHB) and poly(3-hydroxybutyrate-co-3-hydroxyvalerate) (PHBV). [151]

Starch biodegradation is accomplished by enzymatic hydrolysis of the acetal linkage. The α-1,4 link is attacked by amylases while the α-1,6 is cleaved by amylo-glucosidases, breaking down the starch structure into sugars (Scheme 1). When α-amylose is used a combination of maltotriose, maltose and dextrins are obtained as it

attacks the starch structure randomly, while β-amylase works at the end of the polymer hydrolyzing the second α-1,4 glycosidic bond producing two-glucose sugar maltose and γ-amylase attacks the α-1,4 glycosidic bond at the end of the amylase producing glucose.[162] The sugars obtained can be subsequently dehydrated to furfural derivatives for the production of furans, which is explained below in the sugar section.

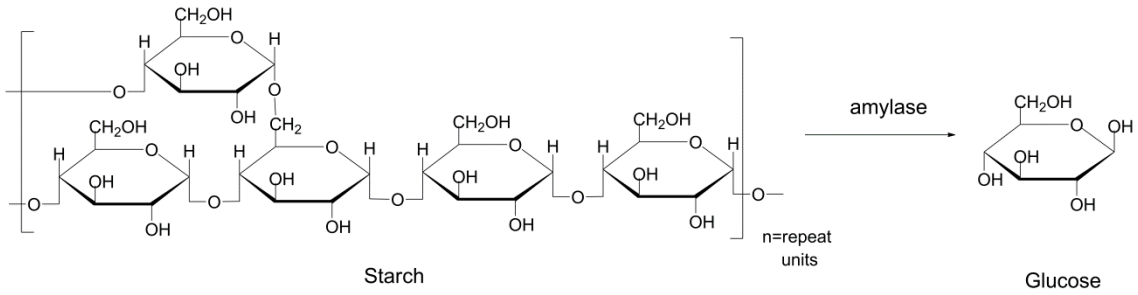

Scheme 1. Hydrolysis of starch into sugars

The release of hydrolysis products varies according to the botanical origin, chemical or physical previous modification, granule integrity, crystallinity, porosity, amylase and amylopectin rate, structural inhomogeneities, phosphates, protein and lipids content.[163]

1.6.1.2 Cellulose

Cellulose is a linear polymer with repeating units of anhydro-D-glucopyranose (cellobiose) where each monomer contains three hydroxyl groups (Figure 12). It is a highly crystalline and high molecular weight biopolymer. Cellulose is characterized by its poor solubility due to the strong intra- and inter- molecular hydrogen bonds within and among the individual chains. The reactivity of cellulose is affected by the morphology and degree of crystallinity, which vary according to the origin and pretreatment of the material.[164] As summarized in Tables 5 and 6, food wastes which contain cellulose in high concentrations are peanut husks, citrus peels, straw and corn stover.

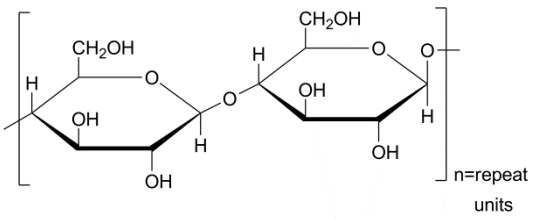

Figure 12. Structure of Cellulose

The macroscopic morphology of cellulose is always in the shape of fibres. Cellulose fibres are used as reinforcements, replacing glass fibre in composite materials with thermoplastics or thermosetting polymer matrices. They offer the advantages of reduction in density and cost, lower fibre abrasion on processing machinery, the ubiquitous availability of lignocellulosic fibres, recycling opportunities or combustion for energy recovery; procedures which cannot be applied to glass fibre.[151]

Surface chemical modification is used to improve adhesion between the polar OH groups of the cellulose fibre and non-polar polymer matrices; the ideal solution is to create covalent bonds between the fibre surface and the matrix. Chemical modification reduces hydrophilicity and hence moisture absorption of cellulose fibre.[151] The most common derivatives from the modification of one or more hydroxyl groups in the cellulose structure are ethers, esters and acetals; such modified materials being already commercially available.[156]

There is extensive research on both chemical and physical modification. Examples of chemical modification for the papermaking industry are cellulose ester elaboration, transesterification reactions, esterification of cellulose nanofibres and cellulose silylation. Physical modifications include surface treatment with cold-plasma, grafting of reactive natural products, coating cellulose with different polymers without covalent attachments or with titanium dioxide followed by an alkyl-chain silica layer produced by sol-gel chemistry.[150]

Native cellulose does not have thermoplastic properties but through mechanical treatment it is possible to obtain plastic properties in cellulose fibres, useful for the manufacture of films based on cellulose. On the other hand, chemical modification such as esterification of hydroxyl groups with acids on the cellulose structure confers new properties of flow, resistance and durability comparable to those of a synthetic plastic. Also more resistant materials with improved durability can be achieved by the chemical grafting of biopolymers. The formation of covalent links between the chains from the hydrophilic functions diminishes the hydration possibilities and flow properties while increasing cohesion.[24] As explained previously in section 1.5.1.2 cellulose can be turned into polyols by liquefaction processes for the production of polyurethane[71] foams and polyesters.[79]

Cellulose degradation can be achieved by enzymes secreted from fungi, bacteria and protozoans which catalyze the oxidation reactions of cellulose, or lower molecular weight oligomers produced from the enzymatic hydrolysis of cellulose.

The hydrolysis by cellulose enzymes decomposes the cellulose structure into glucose (Scheme 2). Some examples of such enzymes are the endo-1,4-β-glucanase which attacks the internal bonds and the exo-1,4-β-glucanase which attacks the end of the cellulose structure and separates the cellobiose into two glucose moieties.[162]

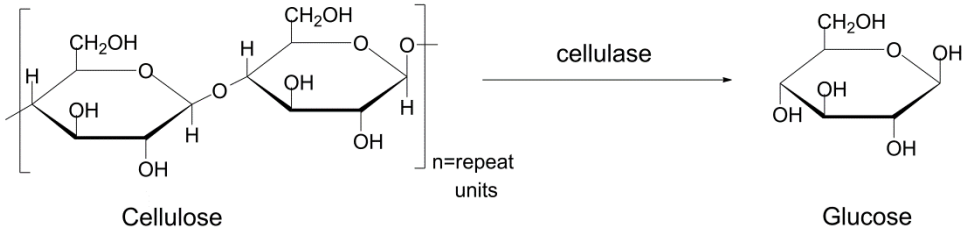

Scheme 2. Hydrolysis of cellulose into glucose

Other examples are the peroxidases which provide hydrogen peroxide for the free radical attack on the C2-C3 positions of cellulose to form aldehydes followed by their hydrolysis to form lower molecular weight fragments. Bacteria produce endo- and exoenzymes which form complexes that degrade cellulose into carbohydrates which are used by microorganisms as nutrients. The final products from aerobic biodegradation are carbon dioxide and water while anaerobic degradation produces carbon dioxide, hydrogen, methane, hydrogen sulphide and ammonia.[43,165] Methane emissions resulting from this degradation promote climate change particularly in the case of disposal to landfill. When it is composted it decreases the need for peat extraction and restricts such gas emissions. As with many biodegradable polymers, the environmental effect may vary depending on the disposal method applied.[166]

1.6.1.3 Chitin

Chitin is a polymer found in crustacean and insect exoskeleton, and can also be found in mushrooms and yeasts. As mentioned in section 1.4.14, the main source is from sea food processing waste which produces around 18 Tg of shell waste.

It is a linear cationic heteropolymer of (1-4)-linked *N*-acetyl-β-D-glucosamine (Scheme 3). Because chitin has an intractable character and very poor solubility, its direct uses as a macromolecular material are limited. However it can be chemically modified by partial alkaline *N*-deacetylation at high temperatures which generates the corresponding primary amino function. The percentage conversion of acetyl glucosamine to glucosamine is described as the degree of deacetylation. This influences the physical, chemical and biological properties.[167]

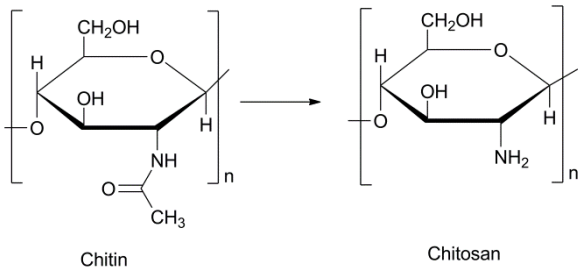

Scheme 3. Chitin and chitosan chemical structure

Chitosan, the *N*-deacetylated product of chitin, is only accepted when the degree of deacetylation permits its solubility in acidic media. With 40% level of acetylation, the polysaccharide chains become moderately soluble, forming stable aggregates in which the *N*-acetyl groups are unevenly distributed. When it is higher than 60% it becomes insoluble and acquires structural flexibility.[168]

The derivative chitosan is somewhat the opposite of chitin; due to its rigid crystalline structure, strong hydrogen bonding and free protonable amino groups it is soluble in mildly acidic aqueous solutions and insoluble in water and alkaline media.[169] It can be chemically modified at either or both the amino and hydroxyl functions for further applications while chitin only has two hydroxyl groups to be modified (Scheme 3). The modifications of chitin and chitosan do not change the original physicochemical and biochemical properties.

There are several reviews on the chemical modification of chitin and chitosan.[170-172] Some examples are: modification through graft copolymerization with polymers like polyurethanes, poly(2-alkyl-oxazolines), poly(ethylene-glycol)s, block polyethers, poly(ethylene-imine)s, poly(2-hydroxyalkanoate)s, poly(dimethylsiloxane)s and dendrimer-like hyperbranched polymers.[170] It can also be chemically phosphorylated[171], acylated and alkylated, a Schiffs base formed and then reduced, carboxylated, phthaloylation, silylated, tosylated and the, quaternary salt formated, sulfated and thiolated.[172]

Chitosan can be moulded as fibres[169], films[173] or precipitated in different micromorphologies from its acidic aqueous solutions. Both substrates, chitin and chitosan, are also being used as antibacterial agents, cell-stimulating materials in animals and plants, hydrogels, blood anti-coagulants, food additives, haemostatic materials, anti-thrombogenic materials, textile material, cosmetic ingredient, for drug delivery, tissue engineering, biocatalyst immobilization, waste water treatment, molecular imprinting and in metal nanocomposites, etc. [174-179]

The enzyme chitinase is responsible for the degradation of chitin while chitosanase and lysozymes degrade chitosan. They can be depolymerized chemically, enzymatically or by physical methods. The chemical process is based on an acid hydrolysis with hydrogen chloride or an oxidative reaction with nitrous acid and hydrogen peroxide. In enzymatic processes, chitosan can be depolymerized by enzymes such as chitinase, chitosanase, gluconase, some proteases, lysozyme, cellulase, lipase, amylase and pectinase. Physical degradation can be achieved by radiation, ultrasound, microwave and thermal treatments.[177]

The *in*-vivo biodegradation of chitin and chitosan produces non-toxic oligosaccharides of different lengths which are later incorporated to metabolic pathways to give glycosaminoglycans and glycoproteins or are excreted. The biodegradation rate depends on the degree of acetylation, distribution of acetyl groups and length of the chain.[176] In the case of medical applications it is important to avoid fast rates of degradation as this can lead to the accumulation of amino sugars which provoke an inflammatory response.[180]

1.6.1.4 Lignin

Lignin is a three-dimensional network formed by the monomers: *p*-coumaryl, coniferyl and sinapyl alcohols, Figure 13.[181] Lignin is a complex highly branched structure and irregular macromolecule in which basic blocks can be defined as "C9" units, however the structure varies according to the vegetable source. In lignocellulosic materials, lignin is the matrix that surrounds cellulosic fibres.

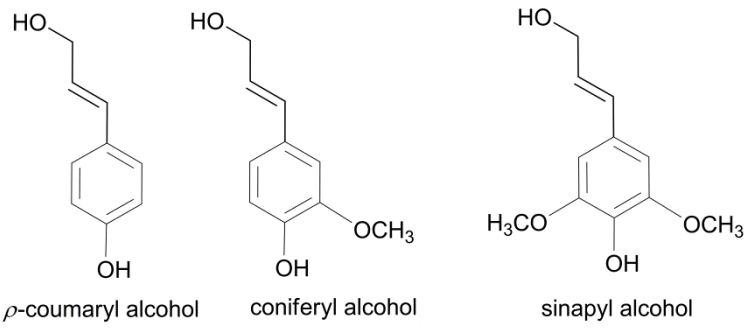

Figure 13. Monomers which form lignin complex structure

Lignin is viewed as a waste material, available in large quantities from peanut husks, citrus peels, sugar bagasse and corn stover (Tables 5 and 6) and is also derived from wood pulp. Commercially, lignins are available as co-products whose main

derivatives are lignosulfates and kraft lignins.[182] Their main structure is based on lamellar macromolecular complexes which link through non-covalent interactions.[24] The lignin structure can undergo chemical modification to allow the synthesis of polymers. It can be modified on both the phenolic and aliphatic hydroxyl groups, to prepare polyesters and polyurethanes though liquefaction processes, as previously explained in section 1.4.2, which used the lignocellulosic material found in the corn stover as feedstock.[79,80] It can also be fragmented into monoaromatic monomers to produce polyether-polyol polymers. Polyols can be obtained through oxypropylation. In general, the polymers obtained from these monomers possess advantageous thermal and mechanical properties due to the present aromatic character, some examples are shown in Scheme 4.[183]

Lignin biological degradation can be achieved by enzymes and mediated by extracellular lignolytic enzymes such as lignin peroxidases, manganese peroxidases and laccases (Scheme 5).[184] These enzymes oxidize the phenolic compounds and the aryl-ether position of the molecule. The by-products of biodegradation are aromatic lignin monomers such as hydrocinnamic acid and vanillic acid. The size, nonhydrolyzability, heterogeneity and molecular complexity of lignin are the variables responsible for non specific biodegradation.[185]

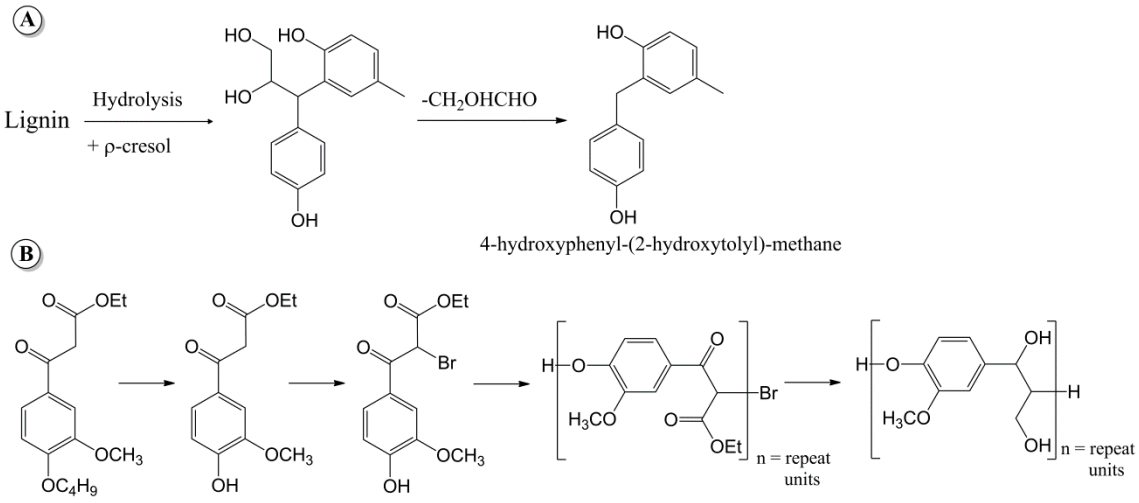

Scheme 4. A) monomer for the synthesis of polyesters and polyethers.[186] B) linear polyetherification of monoaromatic monomer from lignin.[187]

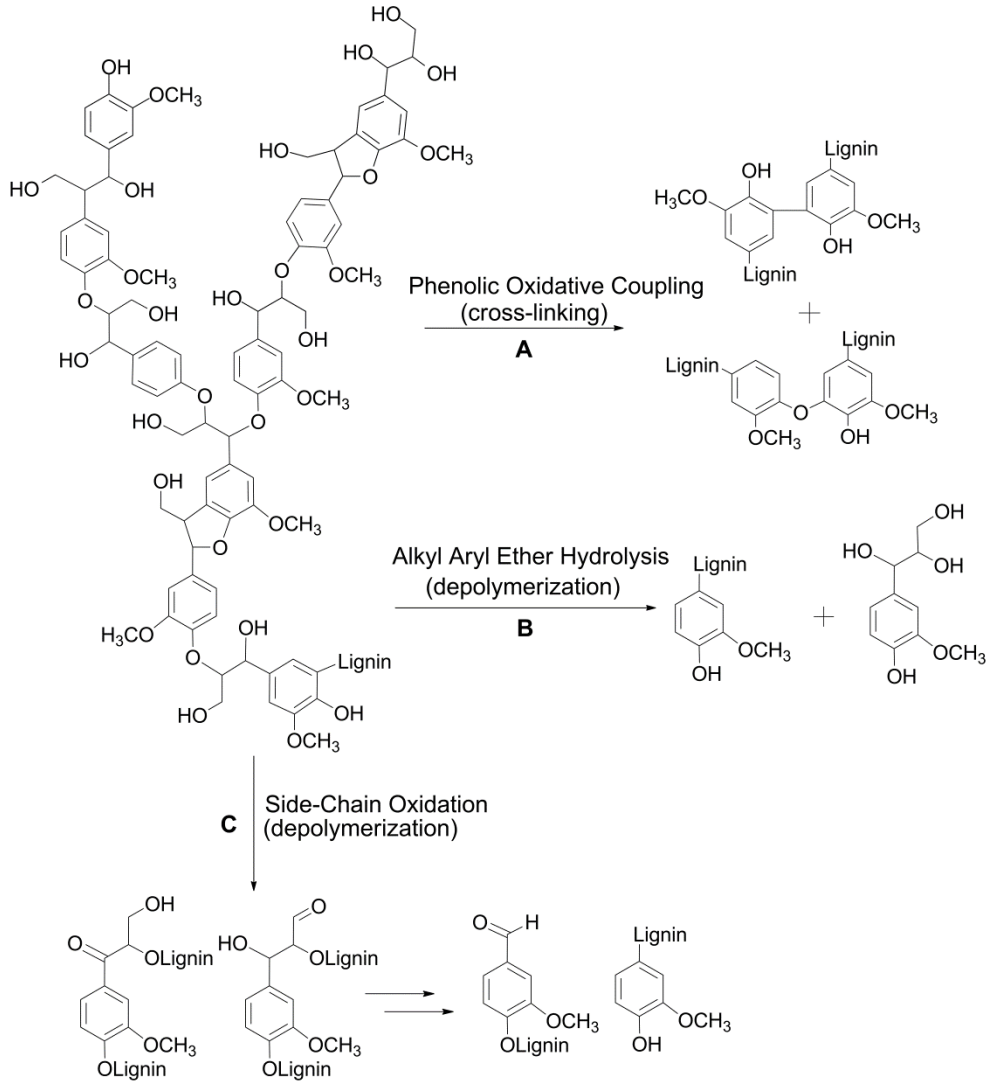

Scheme 5. Oxidative pathways for lignin biodegradation.[188]

1.6.1.5 Proteins

Proteins are heteropolymers formed essentially from 20 amino acid monomers ordered in different sequences, to give various polymers with a wide range of chain lengths, from 50 monomer units, e.g. insulin, to over 100 000 monomer units, e.g. wheat gluten. Their complex structure can be partially destroyed or modified by temperature, pressure or chemical modification.[24]

The most widely used proteins are from grains (soybean, sunflower), cereal co-products (wheat gluten, maize zein) and animal tissue structures (collagen, keratine, gelatine). Grain proteins are usually blended to improve their water resistance and their applications are as films in food packaging, preservation and thermopressed objects such as automobile body parts.[189] They can be processed through compression moulding, injection moulding and extrusion.[190] Cereal proteins are obtained after

extraction of the grain starch and are comprised by glutenins (polymeric proteins that provide viscous character) and gliadines (monomeric proteins which confer elastic properties). They are used as film-forming agents.[24,156]

Proteins from animal sources include collagen which is composed of different peptides, mainly glycine, proline, hydroxyproline and lysine. They are enzymatically degradable[156] and can be obtained from animal waste such as bones and skin (section 1.4.14). Gelatine is a semicrystalline protein produced from the splitting and depolymerization of collagen molecules. It is a high molecular weight polypeptide and commonly it is cross-linked to other substances to improve the thermal and mechanical properties. Due to its water affinity, it is suitable for injection moulding and it is used for film production.[191]

Proteins are considered to be ideal templates for biomaterials as temporary replacement implants due to their ease of processability, adhesion to various substrates and surface active properties. Their main application is in the biomedical area, food packaging[190] and for moulded products or edible films.[192] They are biodegraded via amide hydrolysis reactions by enzymes such as proteases.[43,193]

1.6.1.6 Plant oils

Fatty acids and terpenes perhaps provide the most familiar routes to polymers derived from biomass. Henry Ford said of waste products from farming "Now we've got all this useless waste, let's see if we can do something with it." and in 1932-33, the Ford Motor Company spent over a million dollars on soybean research, equivalent to 16.5 million dollars today using consumer price index.[194]

Triglycerides are triesters of glycerol with long-chain fatty acids with variations in the fatty acid compositions (Figure 14). They can be obtained from several food wastes such as peanut husks, potato waste, mango seed, citrus peels, coffee waste, pumpkin seed and banana peel (Tables 5 and 6). The difference in structure depends on plant, crop, season and growing conditions of the plant. The stereochemistry of the double bonds of the fatty acid chains, the degree of unsaturation and the length of fatty acids are the parameters that affect the physical and chemical properties.[195]

Fatty acids are classified depending on their iodine value.[196] Values higher than 130 corresponds to drying oils, between 90 and 130 are semi-drying oils and values lower than 90 are for non-drying oils. Drying oils are mainly used in industry for their high capability for autoxidation, peroxide formation and subsequent radical polymerization.[190]

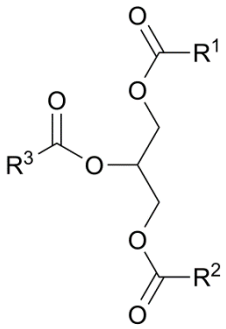

Figure 14. Basic structure of natural triglycerides, where R^1,R^2 and R^3 are fatty acids aliphatic chains.

Two sites in the triglyceride structure are suitable for a chemical modification; (i) ester moieties which can be hydrolyzed or transesterified and then subjected to further modification, (ii) reactive functions along the aliphatic chains, most frequently at the C=C unsaturated site and OH groups. These are mainly converted into hydroxyl groups, which can be directly transformed into other reactive moieties, such as polymerizable acrylics or styrenic functions.[151]

Epoxidized plant oils and fatty acids have been used widely for the production of epoxy resins, as plasticizers, stabilizers for PVC, components in painting and coating formulations and for the production of thermosetting biomaterials. On an industrial scale, the unsaturated fatty compounds are converted into epoxidized plant oils by the *in situ* performic acid procedure.[190] Their incorporation into biopolymers increases flexibility, lowers the melting point and increases hydrophobicity. Their use for the preparation of several biopolymers, as polyols for polyurethanes production, has been already reviewed.[26,197,198] General synthetic routes for the production of biopolymers from oils are explained in Figure 15.

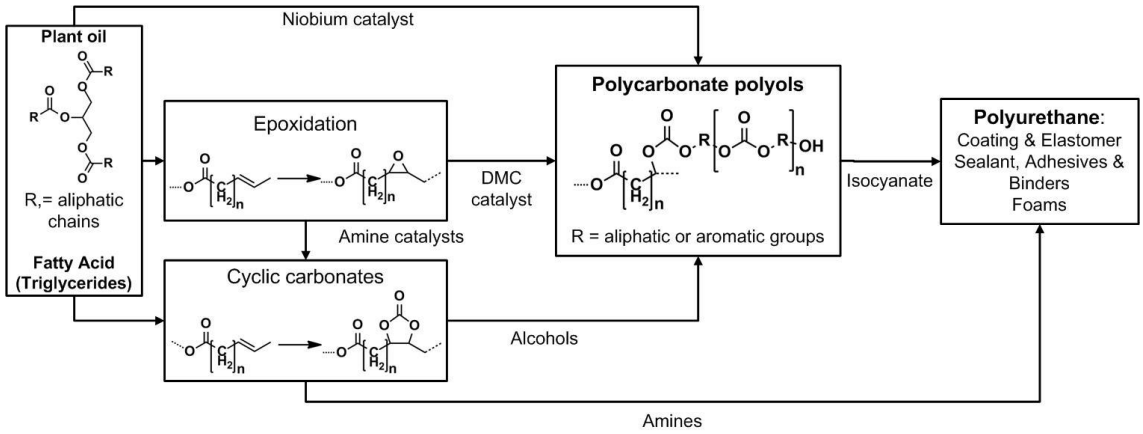

Figure 15**.** Synthetic routes for biopolymer production from plant oils.[198]

One major example is limonene which is the main component of citrus peel oil. Limonene can be dehydrogenated by a palladium catalyst reaction in order to produce α,ρ-dimethylstyrene which has a similar structure to styrene. This subject is explained more detailed in section 1.8.

1.6.1.7 Sugars

As explained previously, starch and lignin can be decomposed into sugars which can be further utilized for the production of furfural derivatives which are used for the production of furans.

The most common furfural derivatives are, in order of importance, 5-hydroxy-methylfurfural (5-HMF); 2,5-furan-dicarboxylic acid (2,5-FDCA); 2,5-dimethylfuran (2,5-DMF); 2,5-diformylfuran (2,5-DFF) and 2,5-bis(hydroxymethyl)-furan (2,5-BHF). They are mainly produced from the acid catalyzed dehydration of hexoses such as glucose and fructose and polysaccharides such as xylan, sucrose, starch, cellulose and lignocelluloses, as mentioned in sections 1.5.1.1 and 1.5.1.2. Under acidic conditions the pentosan is initially converted to a pentose, followed by its dehydration and cyclization to furfural (Scheme 6).

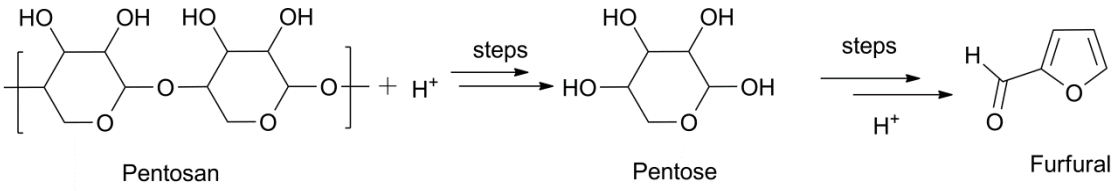

Scheme 6. Synthesis of furfural.[199]

The synthesis of 2,5-diformylfuran, 2,5-furandicarboxyl acid and 2,5-bis(hydroxymethyl)-furan come from the further catalytic transformation of the 5-hydroxymethylfurfural (Figure 16 and Figure 17). Several authors have reviewed the the possible chemical modification that can be applied to 5-HMF.[200-202]

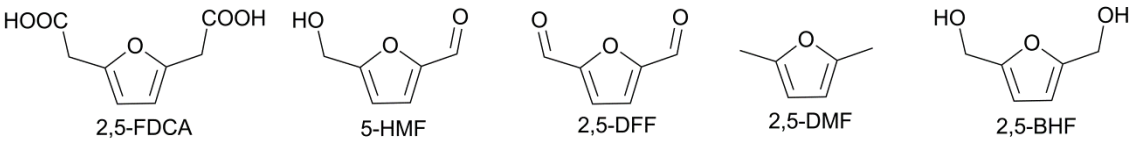

Figure 16. Main structures of furfural derivatives.[201]

These furfurals and their derivatives can be used as monomers for the production of polymeric materials such as polyesters, polyamides and polyurethanes. It is also possible to obtain biopolymers such as Kevlar-like polyamides, furan-based polyconjugated polymers and they are used as replacements for terephthalic acid.[201]

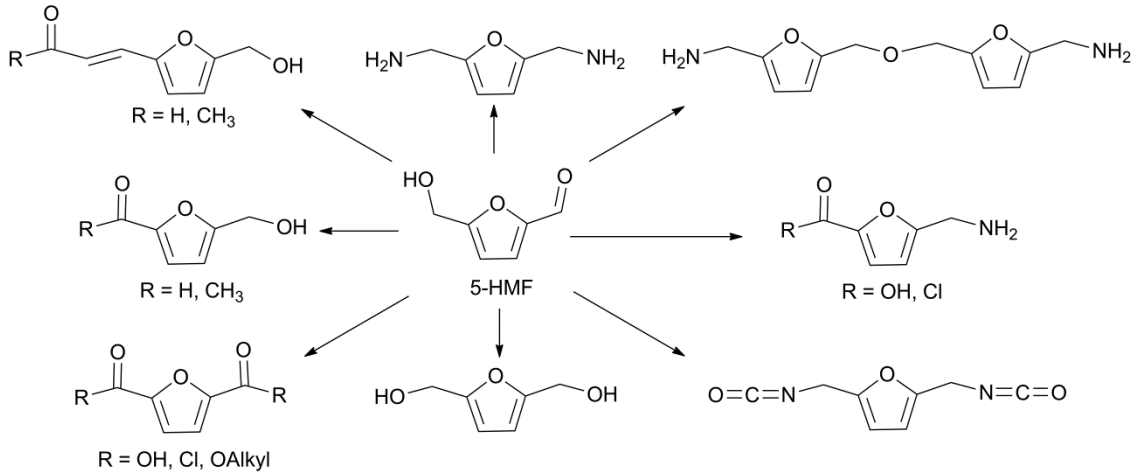

Figure 17. Monomers derived from 5-Hydroxymethylfurfuran.[202]

1.6.2 Industrial biotechnology (White biotechnology)

White biotechnology is a term used for the conversion of renewable resources into new compounds by combined fermentation and enzymatic processes. Applied in the area of polymers, it includes polymers that can be produced in fermentation process or by chemical polymerization using substrates generated by a fermentation process. The most well-known examples are the aliphatic polyesters PHA and PLA.

Aliphatic polyesters are divided in two main groups according to their bonding mode of the constituent monomers (Figure 18). One group is the poly(alkylene dicarboxylate)s which are synthesized by polycondensation reactions of diols (HO-R-OH) and dicarboxylic acids (HOOC-R-COOH). The second group contains the polyhydroxyalkanoates which are formed by repeating units of hydroxy acids (HO-R-COOH). The polyhydroxyalkanoates are divided into α, β and ω-hydroxyacids according to the position of the OH group with respect to the COOH end group.

Aliphatic polyesters are categorized as biodegradable substances because of their potentially hydrolysable ester bonds but being biodegradable does not necessarily imply that they are bio-based polymers. Only poly(α-hydroxy acid) and poly(β-hydroxy acid)s are derived from agro-resources while the rest are petroleum-based.[203]

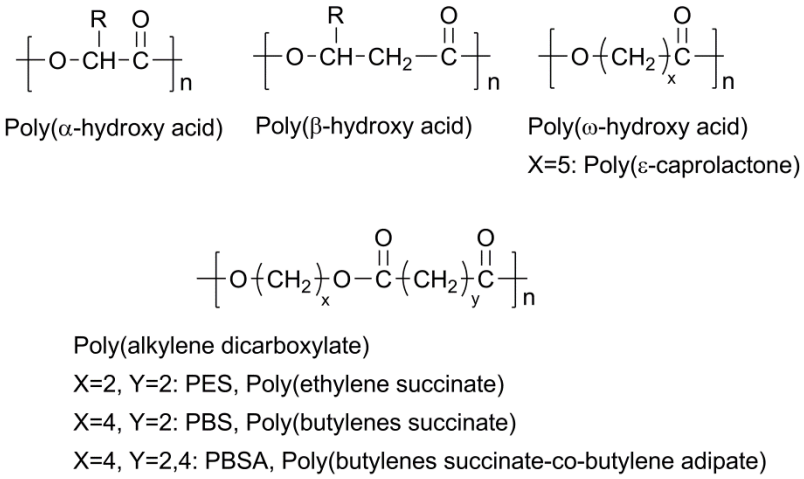

Figure 18**.** Structures of Aliphatic Polyesteres. n = polymer degree

PLA is produced by the chemical condensation of lactic acid obtained by fermentation while PHA comes from bacterial processes. Both biopolymers use carbohydrate feedstocks for their production. These can be obtained from the food wastes studied in section 1.4, notably peanut husk, coffee waste, banana peel, avocado seed, carrot waste and oat husks. For this reason only these biopolymers are discussed here.

1.6.2.1 Poly(β-hydroxyalkanoate)s - PHAs

Poly(β-hydroxyalkanoate)s (PHAs) are aliphatic polyesters synthesized by different types of bacterial fermentation: microbes such as *Bacillus megaterium, Alcaligens eutrophus, Alcaligens eutrophus* and natural isolates of *Actinobacillus, Azotobacter, Agrobacterium, Rhodobacter*, and *Sphaerotilius* accumulate them as osmotically inert carbon and energy storage compounds in the form of granules.[204] The properties of PHA depend on their structure (Table 36). The simplest PHA is a relatively hard and brittle material with a melting point slightly below the thermal decomposition temperature.[205] With pendent groups C_6 and longer (e.g. Nodax^{TM} produced by Procter & Gamble) they are much easier to process than the shorter chain PHA and are similar to propylene properties.[206] Higher molecular weight monomers are typically rubber-like materials with an amorphous soft/sticky consistency.[207] The choice of polymerase, host, feedstock and conditions produces different PHA ranges during the bacterial fermentation with diverse physical properties. PHA copolymer properties vary according to the co-monomer unit structure, content and distribution on the polymer chains.

The biodegradation of these polymers into water-soluble oligomers and monomers occurs by lipases or by extracellular PHA depolymerase excreted from a variety of microorganisms found in the environment which make use of the resulting products as nutrients.[208] As they are biodegradable, their applications have tended to be focused on medical applications, disposable items and, because of their impermeability to water and air, they are considered for the production of bottles, films and fibres.[209]

Table 36. PHA structures

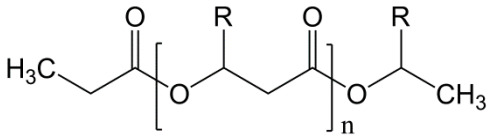

PHB	R = CH_3
PHBV	R = $CH_3ORCH_2CH_3$
mclPHA	R = $(CH_2)_{n= 0-12}\ CH_3$

1.6.2.2 Poly(β-hydroxybutyrate), PHB

Poly(β-hydroxybutyrate) (PHB) in its pure form is a brittle thermoplastic polymer[210] with narrow processability windows.[205] Commercially, it is mixed with other hydroxyalkanoate units to improve the properties, such as the poly(3-hydroxybutyrate-co-3-hydroxyvalerate) (PHBV) produced by Monsanto, known industrially as Biopol™, and Nodax™ PHA copolymers by Procter and Gamble.

1.6.2.3 Poly(hydroxybutyrate-co-hydroxyvalerate), PHBV

PHBV is produced by a microbial fermentation process of glucose and propionic acid. The synthetic pathway for poly(hydroxybutyrate-co-hydroxyvalerate) [P(HB-co-HV)] is achieved by coupling the PHB biosynthesis with the pathway generating 3-propionyl-CoA via threonine deaminase and pyruvate decarboxylase. The synthesis is shown in Scheme 7.

PHBV is a crystalline polymer with thermal properties similar to polypropylene. The disadvantages are (i) the thermal degradation which occurs almost at the melting temperature, (ii) low impact resistance at room temperature, (iii) high crystallinity due to the stereo-regularity of the isotactic chain configuration and (iv) high glass transition

temperature.[211] The high crystallinity results in a hard and brittle material, which combined with other disadvantages limits the range of applications.

By regulating the content of 3HV (hydroxyvalerate) units added to the feedstock, the impact strength, flexural modulus, melting point and extent of crystallization can be controlled. The addition of 3HV decreases the crystallinity and reduces the melting point of the original PHB. Unfortunately the use of 3HV units is limited in efficacy because they can be easily included in the crystal lattice of 3-hydroxybutyrate (3HB).[206]

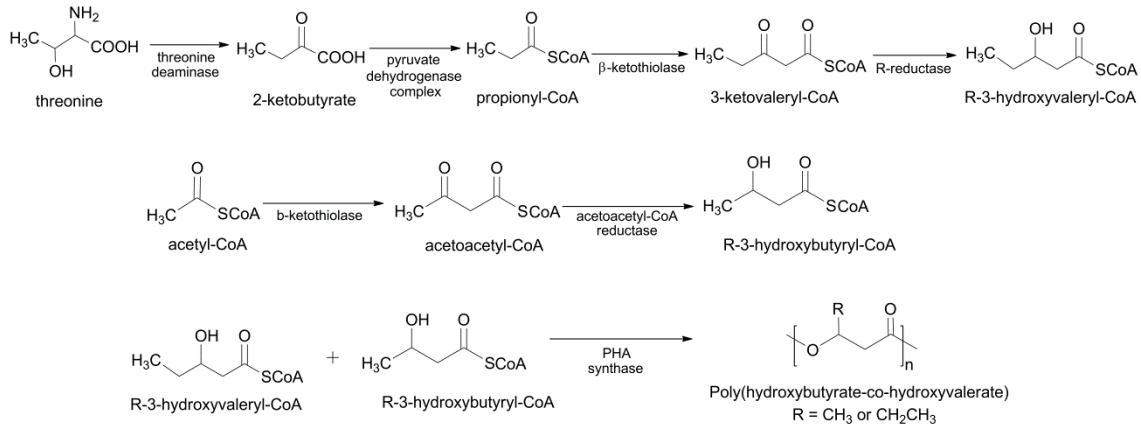

Scheme 7. PHBV pathway synthesis.[148]

1.6.2.4 Poly(β-hydroxyalkanoate) copolymers

This is a copolymer composed of 3HB units and a medium chain length 3-hydroxyalkanoate (mcl-3HA) unit. The chain length of the co-monomer should be larger than the 3HV used in the PHBV so that the copolymer can have side groups with 3 or more carbon units. The copolymer grade depends on the (mcl-3HA) unit selected, its molecular weight, the fraction in the copolymer structure and the side group chain length. Some examples of 3-hydroxyalkanoate are: 3HHX (3-hydroxyhexanoate), 3HO (3-hydroxyoctanoate) and 3HD (3-hydroxydecanoate). The addition of mcl-3HA regulates the melting temperature and crystallinity, resulting in high toughness and ductility. As long as the side group has more than three carbons, the improvements to the physical properties are independent of the mcl-3HA size.[206] Biodegradation can take place under aerobic conditions to produce carbon dioxide but under anaerobic environments there is a danger that methane might be liberated.[212]

The copolymer biosynthesis route is explained in Scheme 8. It involves parallel enzymatic reactions for the production of each co-monomer, and both reactions start with a fatty acid biosynthesis followed by its acid oxidation. These reactions use

microorganisms whose partial genomic DNA sequence showed putative PHA synthase genes (open reading frames, ORFs)[213]; in Scheme 8 they are mentioned as pha genes.

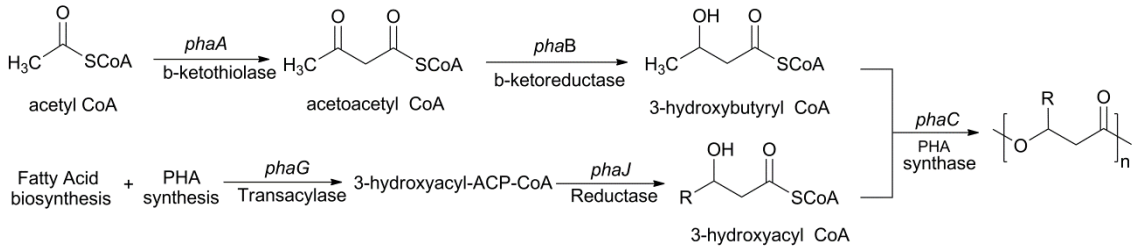

Scheme 8. Biosynthesis of PHA copolymers.[206]

1.6.2.5 Polylactic acid - PLA (Poly(α-hydroxy acid))

PLA is an aliphatic polyester synthesized by the condensation polymerization or ring opening polymerization of the D- or L-lactic acid as the monomer (2-hydroxy propionic acid). Lactic acid chains are produced by the microbial fermentation of starch from renewable sources including food wastes.[214]

The most commonly used carbon sources for PLA production are sugar–containing materials, cassava starch, lignocellulose/hemicellulose hydrolysates, cotton seed hulls, Jerusalem artichokes, corn cobs, corn stalks, beet molasses, wheat bran, rye flour, sweet sorghum, sugarcane press mud, cassava, barley starch, cellulose, carrot processing waste, molasses spent wash, corn fibre hydrolysates and potato starch. The choice of the feedstock depends on the purity, availability and price.[215] It is produced industrially by the bacterial fermentation of carbohydrates at pHs of 5.4 to 6.4 in the temperature range 38-42°C, at low oxygen concentration and in the presence of microorganisms through solvent-free polymerization.[216] The microbal fermentation can be carried out by bacterial species such as *Lactobacillus, Streptococcus, Leuconostoc* and *Enterococcus* or fungal strains such as *Mucor, Monilina and Rhizopus* (Table 37).[215] There are three ways to produce lactic acid polymerization: (i) direct condensation polymerization based on monomer esterification, (ii) direct polycondensation in an azeotropic solution using a catalyst and (iii) polymerization through lactide formation without the use of solvent. The main advantage of this biopolymer is the minimum emission of CO_2 during production.[216]

Table 37. Renewable sources and Microorganisms used for PLA production.[217]

Substrate	Microorganism	Lactic acid yield
Wheat and rice bran	*Lactobacillus sp.*	129 g/l
Corn cob	*Rhizopus sp.MK-96–1196*	90 g/l
Pretreated wood	*Lactobacillus delbrueckii*	48–62 g/l
Cellulose	*Lactobacillus coryniformis ssp. Torquens*	0.89 g/g
Barley	*Lactobacillus caseiNRRLB-441*	0.87–0.98 g/g
Cassava bagasse	*L. delbrueckii NCIM 2025* *L casei*	0.9–0.98 g/g
Wheat starch	*Lactococcus lactis ssp. lactis ATCC 19435*	0.77–1 g/g
Whole wheat	*Lactococcus lactis* *Lactobacillus delbrueckii*	0.93–0.95 g/g
Potato starch	*Rhizopus oryzae* *R. arrhizuso*	0.87–0.97 g/g
Corn, rice, wheat starches	*Lactobacillus amylovorous ATCC 33620*	<0.70 g/g
Corn starch	*L. amylovorous NRRL B-4542*	0.935 g/g

The most common polymerization method is the ring-opening polymerization of lactide (the cyclic lactic acid dimer). A low molecular weight PLA (M_W 1000-5000) is formed and then depolymerized through an internal transesterification to the cyclic dimers that can have three different stereoforms (Scheme 9). Catalytic ring opening polymerization is then performed to give a high molecular weight PLA or PDLA (when a mixture of L-lactic and D-lactic acid is used).

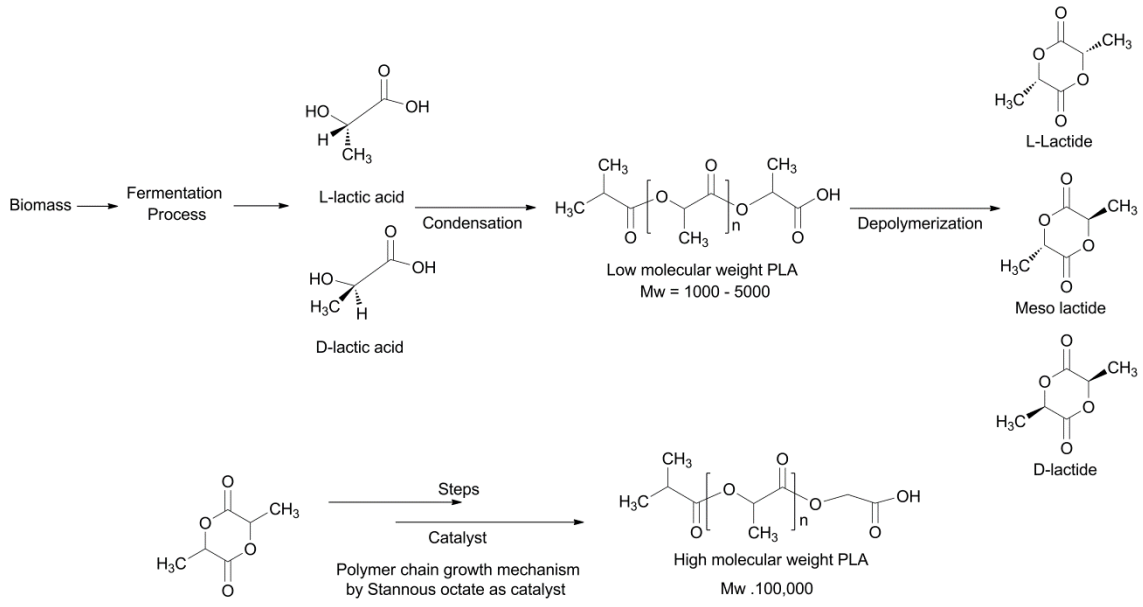

Scheme 9. PLA polymerization.[216]

PLA is a hydrophobic polymer, and a biocompatible thermoplastic with a relatively high melting point (170 °C). It is a completely biodegradable biopolymer with high tensile strength (70 MPa) which can be recycled from 7 to 10 times.[218] PLA is a crystalline polymer while PDLA is an amorphous polymer, but the degree of

crystallinity can be controlled by the ratio of D to L enantiomers used. Table 38 indicates the general properties of PLA: the physical properties and biodegradability can be regulated by racemisation of the monomer or using a co-monomer component of hydroxyl acids.[211]

PLA is classified as a hydro-biodegradable polymer because it has to pass though a high temperature chemical hydrolysis for its degradation. Moisture splits the macromolecules into smaller units which are consumed by microbes and converted to carbon dioxide and water. It can also be degraded by depolymerisation in alkaline conditions to the cyclic dimer.

From a chemical point of view, the polymer degradation occurs when an electrophilic attack to the hydroxyl end-group on the second carbonyl group provokes a ring formation and the polymer is shortened by the hydrolysis of the ester link from the resulting lactide. Subsequently the hydrolysis of the ester group from the free lactide releases two molecules of lactic acid.[217]

Table 38. PLA characteristic properties.[45,217]

Physical properties	
Melt flow rate (g/10 min)	4.3–2.4
Density /kg m^{-3}	1250
Haze	2.2
Yellowness index	20–60
Mechanical properties	
Tensile strength at yield /MPa	70
Tensile module /GPa	3
Melt flow rate (g/10min)	3
Impact strength index /kJ/m^2	2.6
Elongation at yield (%)	10–100
Flexural modulus /MPa	350–450
Thermal properties	
Heat Distortion Temperature /°C	40–45
VICAT Softening point /°C	135
Melting point /°C	150-170

1.6.2.6 Enzymatic polymerization

There are two types of enzymatic polymerization:

- *In vivo.* It uses very complex enzymes and produces especially well-defined and pure materials. Some examples of this polymerization are the production of DNA, proteins, spider-silk and poly(4-hydroxybutyrate).
- *In vitro.* Isolated enzymes from living organisms are applied in organic media or water to catalyse some specific reactions without the use of the complete organism.

In nature enzymes are divided in six different types (Table 39), but only three of them are able to produce *in vitro* polymerization: hydrolases, tranferases and oxido-reductase enzymes. The product polymers are obtained under mild reaction conditions without using toxic reagents.

Table 39. Enzymes founded on nature, their specific reactions and the polymers they can produce.[219]

Enzyme	Specific reaction	Typical polymers
Oxido-reductases	Catalyze redox-reactions by electron transfer.	polyphenols, polyanilines, vinyl polymers.
Transferases	Catalyze the transfer of a functional group, for example a methyl group or a glycosyl group, from one compound (donor) to another compound (acceptor).	Polysaccharides, cyclic oligosaccharides, polyesters.
Hydrolases	Catalyze the hydrolysis of various bonds in order to transfer functional groups to water.	Polysaccharides, polyesters, polycarbonates, poly(amino acid)s
Lyases	Catalyze the cleavage of C-C, C-O, C-N and other bonds by otherwise than by hydrolysis or oxidation.	-
Isomerases	Catalyze either racemization or epimerization of chiral centres; isomerases are subdivided according to their substrates.	-
Ligases	Catalyze the coupling of two molecules with concomitant hydrolysis of the diphosphate-bond in ATP or a similar triphosphate.	-

The hydrolase enzymes catalyse hydrolysis reactions and their respective reverse reactions. The most known hydrolase enzymes are:

- Glycosidase: Synthesize polysaccharides
- Protease: Peptide bond formation
- Lipase: Hydrolysis of fatty esters, polycondensation, polytransesterification, ring-opening polymerization and polymer modification reactions.

Transferases catalyse group transfer reactions (transfer a group of atoms from one molecule to another). They mainly synthesize oligomers with minimum lengths of four glucosyl-residues.

The oxido-reductase enzymes catalyse the decomposition of hydrogen peroxide at the expense of aromatic proton donors letting the polymerization take place. They contain low-valent metals as catalytic centre like:

- Iron (III) - (HRP – horse radish peroxidase)
- Copper (I) - (Laccase)
- Manganese (II) - (Manganese peroxidase)

When polymerization takes place with oxido-reductase enzymes, it is known as enzymatic oxidative polymerization. The most common enzyme used for this polymerization processes is the HRP. This particular enzyme contains porphyrin-type structure which takes hydrogen peroxide as oxidant. The polymerization reaction takes place at room temperature in aqueous solutions producing oligomeric compounds which usually have low solubility toward the solvent causing polymers of low molecular weight. The catalyst reaction is shown in Figure 19.

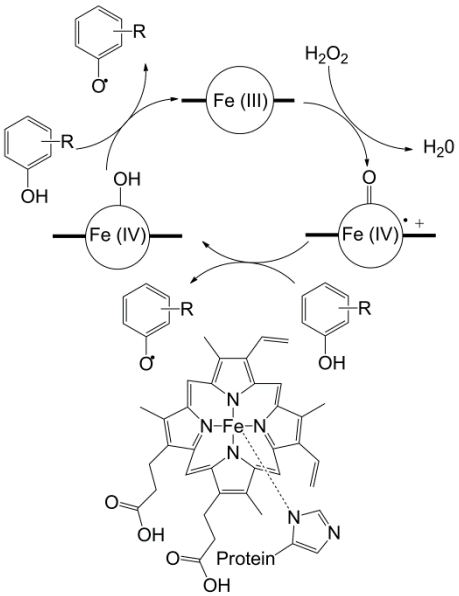

Figure 19. HRP catalytic reaction.[220]

1.6.3 Transgenic Plants

The scope for genetic modification to food crops in order to increase yield, resist predators or confer resistance to arid conditions, extends also to plants intended to yield raw materials that replace those derived from mineral oil. Of particular interest is the potential to exploit land which is presently unusable and to resist desertification driven by climate change.[221-223] More specifically, this technology may facilitate and extend the synthesis of polymers in agricultural crops. Modification by using genetic engineering techniques to introduce microbial genes which encode the biosynthetic conversion of specific substances in the plant, followed by polymer recovery through extraction with organic solvents is one route. The goal is to obtain engineered crops that would obtain biomass-derived polymers with better properties and potentially on large scale production compared to those obtained from mineral oil sources.[224-226] Due to the

natural decomposition of organic tissues such as those present in plants, it is a priority also to consider the time between the harvesting season and the extraction of the polymer. Because of this, the production of the polymer in seeds, which usually can be stored for a long time without changing their biochemical characteristics, is a potentially interesting solution.

The development of this technology has three major disadvantages, the current high cost of industrial production, the greenhouse gas emission from the overall production process[227] and the lack of public acceptance for genetically modified plants. The overall cost of discovery, research and development, breeding, production, admission and regulatory clearance for each country can, under present circumstances be prohibitive.[228] Currently sugar beet, sugar cane, certain potato varieties and fibre crops are being used for the in industrial production of crops.[148]

1.7 Fibres and other reinforcements

The mechanical properties of such polymers can be improved by fibre reinforcement to produce polymer matrix composites[229,230] and short staple fibres for this purpose can also be derived from biomass and potentially from food wastes. Already hemp, jute, ramie and flax fibres are appearing in fibre reinforced polymers[231,232] and have even been used in the bodywork of sports cars: the Lotus Eco Elise has body panels and trim made of hemp, eco wool and sisal.[233] In another example, rice-hull is being used as a filler material for polymer composites.[234] Rice hulls were identified as a source of silicon carbide in 1975 and so contribute to the production of ceramic materials as well as polymer composites.[235] They have been used to generate materials with polyvinyl chloride (PVC)[236], PLA[237], polypropylene (PP)[238], polyethylene (PE)[239] and high density polyethylene (HDPE).[240] Other examples are pineapple and coconut husk used as natural reinforcing fibres.[241-243] Fibres generated from straw waste are also used as reinforcement as well as having many other uses.[244] A general classification of natural fibres and examples of applications is shown in Figure 20.

Fibres such as sugarcane bagasse, oat hulls, corn husks, rice, and wheat straw can be used for the production of furfural resins. The furanic monomers are obtained directly from the hemicelluloses found in these agricultural residues by an acid-catalyzed hydrolysis of pentosans followed by the dehydration and cyclization of the pentoses. Its industrial utilization started in 1960 when the Quaker Oats Company (USA) introduced furan resins as binders in the foundry industry and since then it has

been used in combination with formaldehyde, urea, phenol, and casein, for decades.[245] Further discussion of furans and their derivatives is given in section 1.6.1.7.

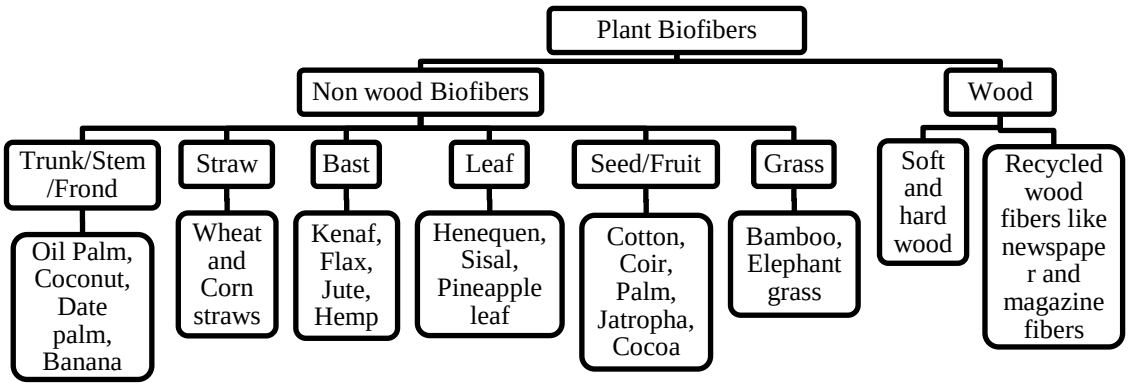

Figure 20**.** Classification of natural fibres.[232]

Moving outside the area of food wastes but keeping the theme of zero embodied fossil carbon materials, another source of reinforcement is the use of smectite clays to produce polymer-clay nanocomposites. These were first used by Toyota Motor Corporation[246] and interest has expanded considerably since[247,248] An advantage of the use of short fibre or smectite clay reinforcement is that it does not restrict the fabrication routes for thermoplastic biomass polymers so that extrusion and injection moulding, for example can still be used but it enhances elastic modulus and may help to ameliorate seasonal or annually variations in products due to prevailing growth conditions.

1.8 Biodegradation of polymers from food waste

Biodegradation of polymers can be defined as the macromolecular degradation of a solid polymeric material into by-products such as water, carbon dioxide, minerals, oligomers, monomers or intermediate compounds in a natural environment resulting in the loss of the mechanical, structural and chemical integrity of the original bulk polymer (based on ref. 249). The biodegradability of a polymer and hence its final product composition depends on the chemical structure of the bulk material. It tends to be less dependent on the raw materials used for the production of the polymer. The pathways by which biodegradation of natural and synthetic polymeric substances can be achieved are: (i) the use of microorganisms which are divided into two groups: fungal digestion under aerobic conditions and bacterial digestion which can be aerobic or anaerobic; (ii) enzymatic degradation and (iii) non-enzymatic degradation. Comparison of the last two techniques is shown in Table 40.

Table 40**.** Differences between enzymatic and non-enzymatic degradation.[208]

Enzymatic degradation	**Non-enzymatic**
Based on biological oxidation and biological hydrolysis.	Based in chemical hydrolysis and diffusion of reagents into the polymer.
Surface degradation	Bulk degradation
Enzymes cannot penetrate polymer systems.	Depth degradation by water penetrating the complete polymer structure.
Enzymes first degrade amorphous and less ordered regions and subsequently crystalline regions.	Crystallinity, crosslinking and morphological properties of the polymer affect the diffusion.
Major molecular weight changes do not occur.	Random scission in the hydrolytic chain produce a reduction in the molecular weight causing decline of mechanical properties.
The polymer on the surface is degraded by enzymes and the low molecular weight degradation products are removed by solubilization in the aqueous medium.	Morphological fragmentation of the polymer only occurs at the last stage of the degradation.
It can be endo-type degradation (at random points in the chain) or exo-type degradation (at the ends of the chain)	----

Hydrolytic degradation realized by enzymes and chemical hydrolysis is shown by the example in Scheme 10.[43] The first reaction (8a) is a biological oxidation, generally performed by enzyme degradation processes. There are three different enzymes that perform this reaction; (i) hydroxylase enzymes which directly incorporate oxygen in the substrate, (ii) oxygenase enzymes that insert the whole oxygen molecule and (iii) oxidase enzymes that use the oxygen molecule as a hydrogen acceptor producing H_2O and a H_2O_2. The second reaction (8b) is the hydrolysis of the peptide bond followed by the hydrolysis of the ester bond (8c). The hydrolytic degradation process can progress via a surface or bulk degradation pathway according to the diffusion-reaction of the degradation process, Figure 21.

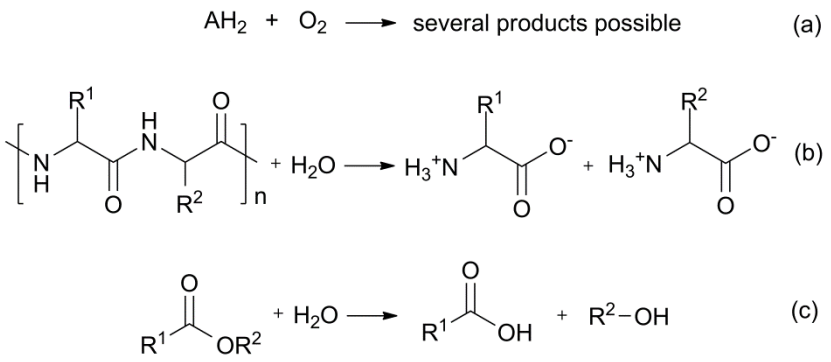

Scheme 10 . General biological hydrolytic degradation by enzymes.[43]

Surface degradation, known as erosion degradation, involves the hydrolytic reaction taking place on the surface of the polymer. In this process the production of oligomers and monomers is faster than the rate of water intrusion into the polymer bulk, provoking a thinning of the polymer without affecting the molecular weight of the polymer bulk. This process follows shrinking unreacted core kinetics[250] so that progress of degradation is predictable making such polymers suitable for use as vehicles for drug delivery.

On the other hand, bulk degradation is caused when the hydrolysis is achieved by the penetration of water into the bulk polymer producing a reduction in the molecular weight of the polymer. Typically, equilibrium exists between the water introduced into the bulk material and the outward diffusion of monomer or oligomer. If this equilibrium is disturbed, an internal autocatalytic degradation process (in the case of aliphatic polyesters made via the carboxyl and hydroxyl end group by-products) may occur. This autocatalysis accelerates the internal degradation compared to that on the surface and can produce a hollowed out structure with a bimodal molecular weight distribution, i.e. with an outer layer with high molecular weight and an internal layer of lower molecular weight. [249]

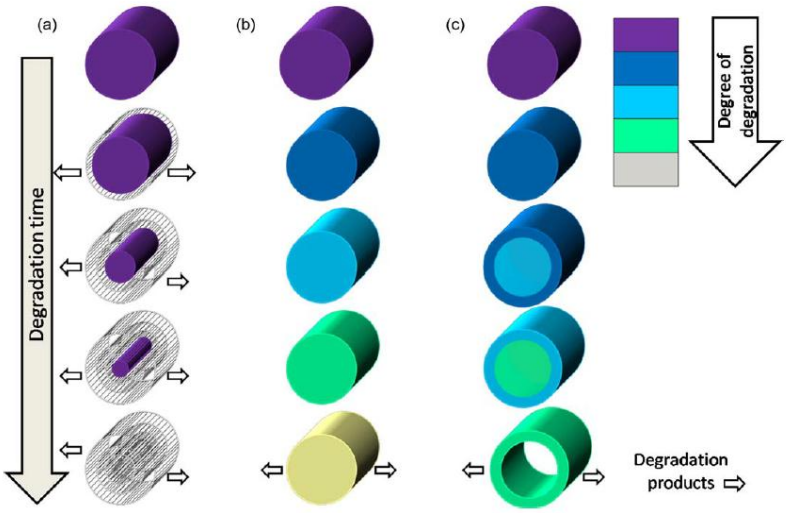

Figure 21. Degradation pathways.

a) Surface erosion, b) bulk degradation, c) bulk degradation with autocatalysis.[249]

Now that a general background from the natural resources from food waste, their amount and constitution had been made and that the different strategies for the production of biopolymers derived from them had been studied. A more detailed study was made from the food wastes chosen for this project: D-Limonene from citrus peel oil and chlorogenic acid obtained from potato waste.

1.9 D-limonene

1.9.1 Description, synthesis, extraction and applications.

Limonene (Figure 22) is the major chemical compound found in citrus peel oil, which is obtained from this substantial food waste (Table 16). It is an optically active monocyclic hydrocarbon terpene, made up of two isoprene units (isoprene rule, Wallach 1887). It is a non-conjugated diolefin with internal and external double bonds.

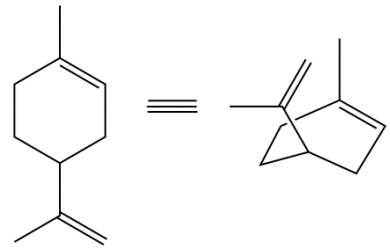

Figure 22. D-limonene chemical structure. $C_{10}H_{16}$
1-methyl-4-(1-methylethenyl)-cyclohexene

The biosynthesis of limonene is carried out by an enzymatic cyclization process catalysed by cyclases (soluble enzymes). These enzymes transform geranyl diphosphate to a cyclic product by a process that involves a preliminary isomerization step that does not require intermediates. The reaction is achieved by a divalent metal ion that promotes the ionization steps. The mechanism is show in Scheme 11.[251]

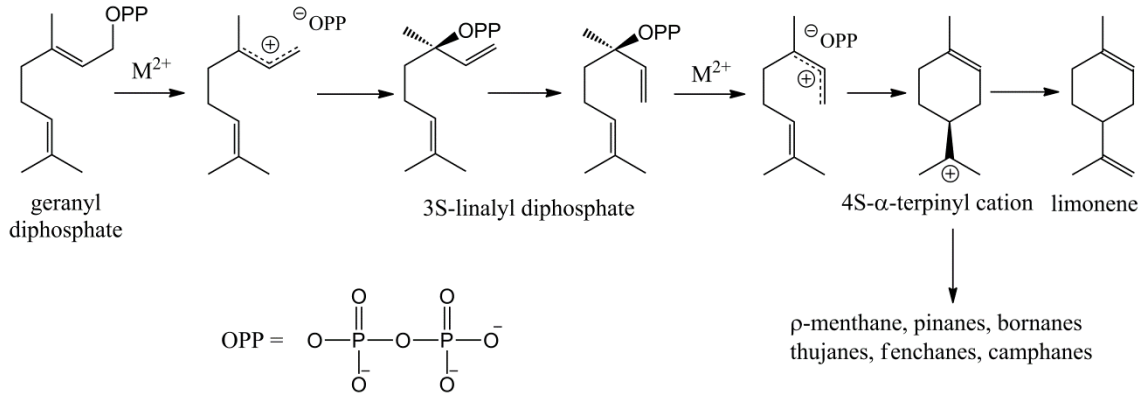

Scheme 11. Mechanism of cyclization of geranyl diphosphate to limonene.[251]

During the citrus juice process it is possible to obtain two grades of D-limonene; food and technical grade. First, citrus fruits are pressed to obtain the juice and oil comes out of the rind. Afterwards oil and juice are separated and the oil is distilled to recover

fragrance and flavour compounds. In this part of the process food grade D-limonene is obtained. After the pressing process for juicing, peels are lead to a steam extractor to remove the oil. When the steam is condensed into water, the oil stays in the upper layer and it is separated. In this step the technical grade D-limonene is obtained. The process is explained in Figure 23.

Limonene is mainly used for fragrances, cooling fluid, cleaning products, straight solvent, water dispersable, medical and pharmaceutical research. Due to the fact that D-limonene is not water soluble it can replace different solvents like methyl ethyl ketone, acetone, toluene, glycol ethers and, of course, fluorinated and chlorinated organic solvents. Also it has a KB (Kari-Butanol) value of 67, a reason why it is used as a wipe cleaner. When it is mixed with a surfactant package, with around 5-15 % concentration, a water based cleaner is obtained than can work as spray or direct wipe cleaner for house work. Furthermore, it also works as a good cooling fluid because it is an effective low temperature heat transfer fluid and it has excellent thermo physical properties with a range operating temperatures from -100 to 72 F (-73 to 22 °C). It has a closed-cup flash point around 50 °C, while it provides a freeze point below -96.7 °C. In Appendix 1 are presented the physicochemical characteristics of D-limonene.

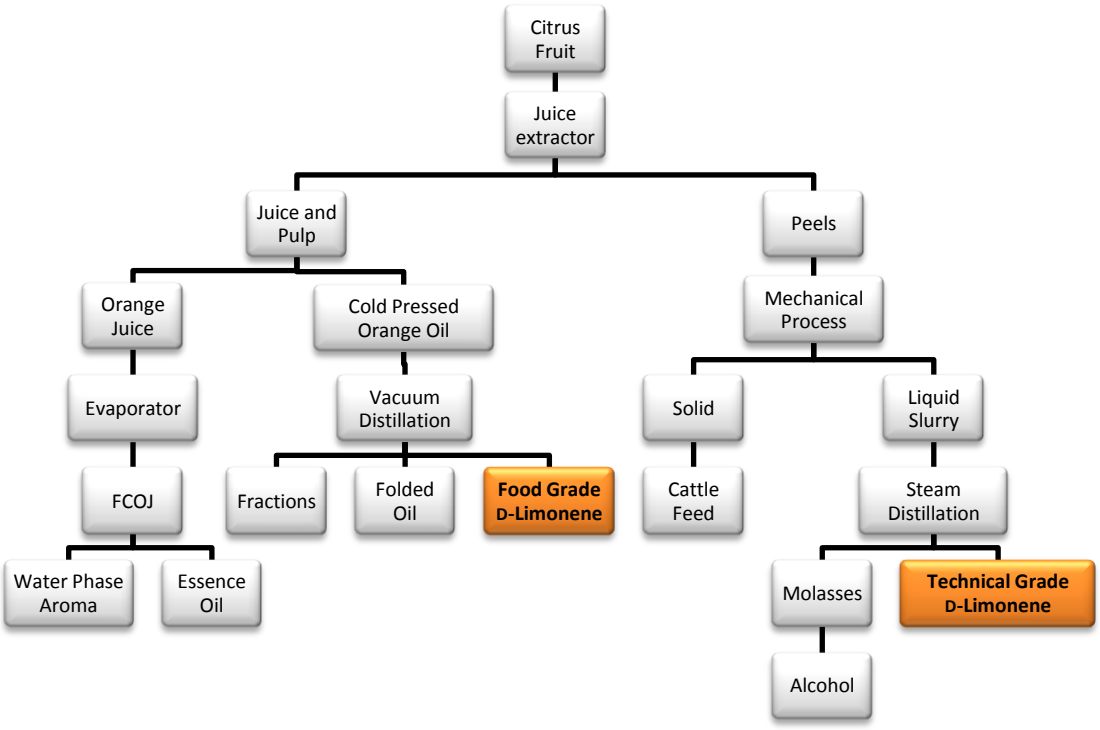

Figure 23. Citrus oil manufacturing process.[252]
FCOJ = Frozen concentrated orange juice

1.9.2 Catalytic reaction over palladium

The catalytic reaction of the endo-extracyclic diene, D-limonene, over palladium catalyst generates terpinolene, γ-terpinene, α-terpinene, carvone, ρ-cymene, dimethylstyrene, ρ-menthene and ρ-menthane. The reaction mechanism of terpenes like D-limonene with solid acids catalysts initiates with an isomerisation on the acid sites followed by the dehydrogenation of the resultant intermediates. The use of a noble metal as catalyst enhances the dehydrogenation activity of the reaction.[253]

The direct hydrogenation of limonene produces ρ-menthene and ρ-menthane. The further appearance of terpinolene, α-terpinene and γ-terpinene indicates that an isomerisation process precedes hydrogenation, while simultaneously a dehydrogenation takes place generating ρ-cymene and dimethylstyrene. Limonene and terpinolene are coupled by a fast isomerisation reaction forming ρ-menthene, α-terpinene and γ-terpinene, while ρ-cymene is formed from γ-terpinene via dehydrogenation process and stabilized by π-electron delocalization through resonance. The further hydrogenation of ρ-menthene forms ρ-menthane while the dehydrogenation of ρ-cymene forms dimethylstyrene (Scheme 12).[253,254]

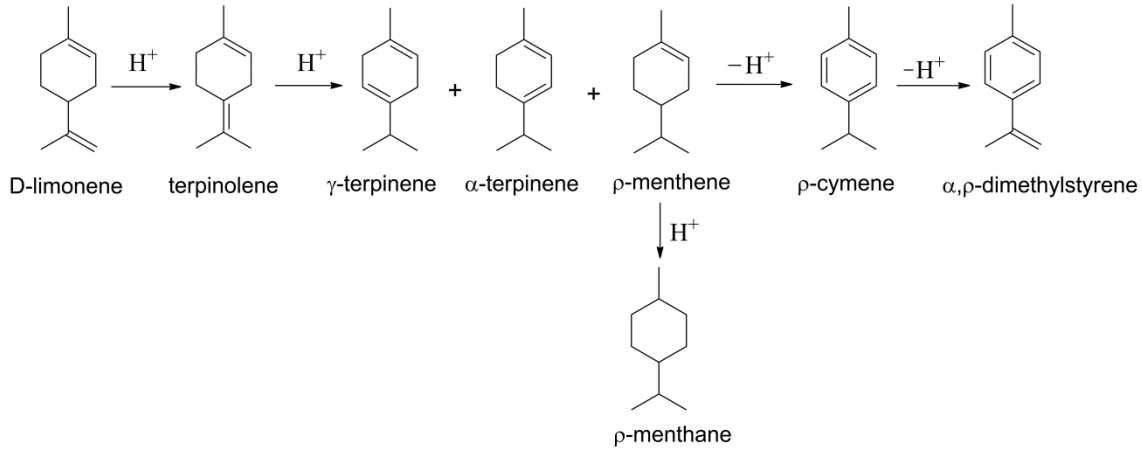

Scheme 12 . Hydrogenation, isomerisation and dehydrogenation of D-limonene over Pd catalyst.

The hydrogenation and isomerisation process are promoted through -allyl-adsorbed species. The formation of endocyclic adsorbed species are limited because the adsorption of the exocyclic double bond has lower steric hindrance than the endocylic double bond. The adsorption of the extracyclic double bond of D-limonene takes place on the acid sites forming a primary carbonium ion which stabilizes in a tertiary carbonium ion by a displacement of the proton forming terpinolenes and terpinenes.[254]

Most researches are focused on the conversion of D-limonene into the intermediate ρ-cymene[255-258] (detailed Section 1.8.3) as it can be used for the production of fragrances, herbicides, pharmaceuticals and heat transfer media. But the further dehydrogenation produces dimethylstyrene which has a similar structure to styrene and hence can be polymerized[259,260] or copolymerized.[261-263]

1.9.3 Production of ρ-cymene from D-limonene

When the reaction takes place in a liquid-phase environment with hydrogen[253] the conjugated cyclic diene intermediates, like α-terpinene, are not produced. They are adsorbed much more strongly than non-conjugated dienes which avoids their desorption before reacting further. When the Pd is supported over alumina[253] the mechanism is explained though Lewis acid sites provided by the alumina. In this case, the limonene isomerizes over alumina via π-allylic route while terpinene and terpinolene do so via a carbonium ion mechanism (Scheme 13). Instead when Pd is supported over zeolite[254] the acidity plays an important role. If low acidic zeolites are used, the reaction does not dehydrogenate, generating only isomerized $C_{10}H_{16}$ terpenes, but as acidity is increased, so do the dehydrogenation properties. The palladium-sites promote dehydroisomerization while acid sites promote ring-opening and cracking to selective products. To increase the acidity, Ce is used to promote ion exchange with the Pd enhancing its dispersion and accessibility into the zeolite generating Brønsted acidity.

Dehydrogenation of D-limonene can also be achieved in solvent free conditions supported over mesoporous silica-alumina and heated by microwave irradiation. In this conditions only α-terpinene, γ-terpinene, terpinolene and ρ-cymene are produced. The selectivity and conversion towards ρ-cymene is proportional to the irradiation time and silica content and it can be explained by the rapid aromatisation of the intermediates over the acid centres of the alumina. The advantage of this reaction is that 100% conversion with selectivity higher than 90% can be achieved over 10 min of irradiation compared to the 40% selectivity obtained after 3h with the conventional heating.[255]

Aromatization of D-limonene can be accomplished by using heteropoly compounds as liquid-phase electron-transfer oxidation catalysts. In this reaction, isomerisation takes place thorough reversible electron transfer between the heteropoly compound and the substrate while the aromatization is preceded by a double-bond isomerisation to an endocyclic position. The dehydrogenation occurs when reduced heteropoly is formed by two electron transfers and proton abstractions from the endocyclic diene to the

heteropoly acid. Afterwards the reduced heteropoly acid is reoxidized by dioxygen forming water.[256]

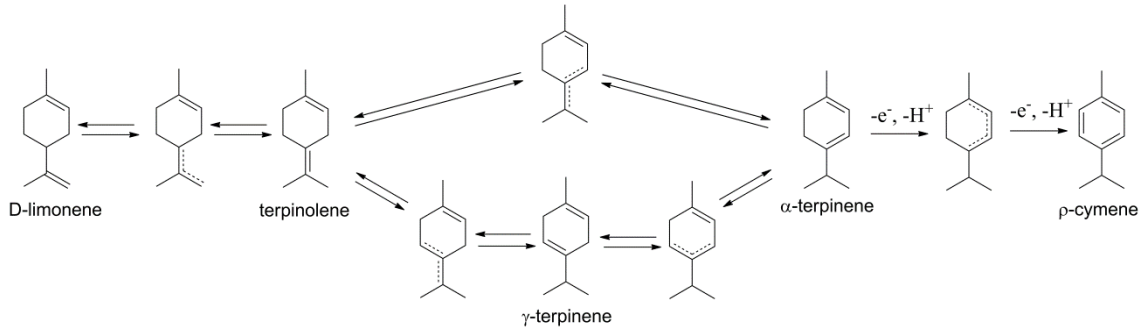

Scheme 13 . Reaction of D-limonene dehydrogenation through electron-transfer oxidation.[256]

As acid activated catalysts, bentonite clays[257] can be used because the iron in the octahedral sheet of the clay lets the dehydrogenation of D-limonene take place, as well as ρ-benzoquinone under acetic acid solutions with the presence of $Cu(OAc)_2$ as co-catalyst.[258]

1.9.4 Polymerization and copolymerization reactions

D-limonene has been polymerized or copolymerized, without the ρ-cymene or dimethylstyrene intermediates, by the methods explained below.

1. Polymerization with Ziegler-type catalysts aluminium alkyl-metal halide in a 1:1 molar ratio giving conversions up to 68 %. The catalyst works through a cationic mechanism producing a low molecular weight polymer. The reaction mechanism is shown in Scheme 14.[264]

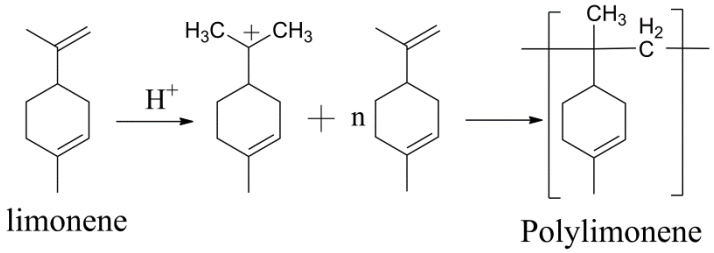

Scheme 14 . Polymerization of limonene.[264]

2. Emulsion polymerization for the production of polyalkylene sulphides with branching in the chain from the nonconjugated diolefin, D-limonene. The structure of the final product is assumed from the free radical non-Markownikoff addition of thiolacetic acid to the double bond of the D-limonene, as seen on Scheme 15. The polymer obtained is a viscous sticky material due to its low molecular weight, it presents rubber-like properties and an inherent viscosity in chloroform solution of 0.3 - 0.4[1].[265]

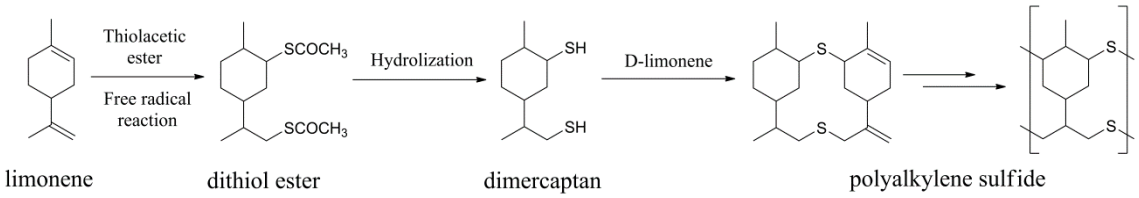

Scheme 15. Mechanism for the polyalkylene sulphide made of D-limonene.

3. Copolymerization with acrylonitrile though the terminal methylene group of limonene. The reaction is initiated by benzoyl peroxide (BPO) while the limonene acts as a chain-transfer agent (Scheme 16). The reaction activation energy is 26 kJ/mol and takes place in DMF at 70°C for 3 h under a nitrogen atmosphere.[266]

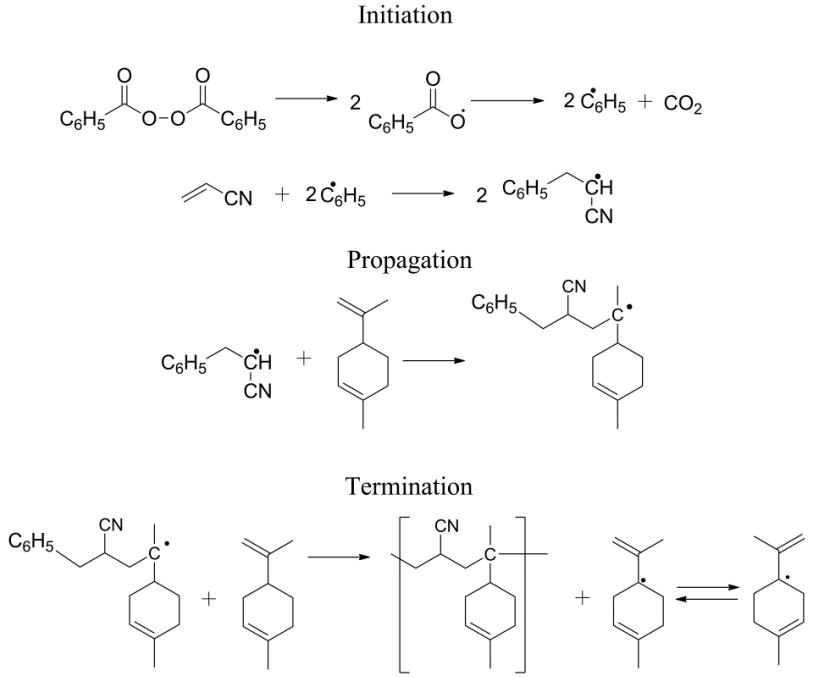

Scheme 16 . Mechanism for the copolymerization of limonene with acrylonitrile.[266]

[1] The inherent viscosity, which is the ratio of logarithm of relative viscosity to the mass concentration of the polymer, should have units of volume/mass. But this precise paper does not indicate the units obtained in this measurement.

4. Copolymerization with methyl methacrylate. The reaction is initiated by benzoyl peroxide (BPO) giving an unsaturated copolymer (Scheme 17). The reaction activation energy is 49 kJ/mol and takes place in xylene at 80°C for 1 h under a nitrogen atmosphere.[267]

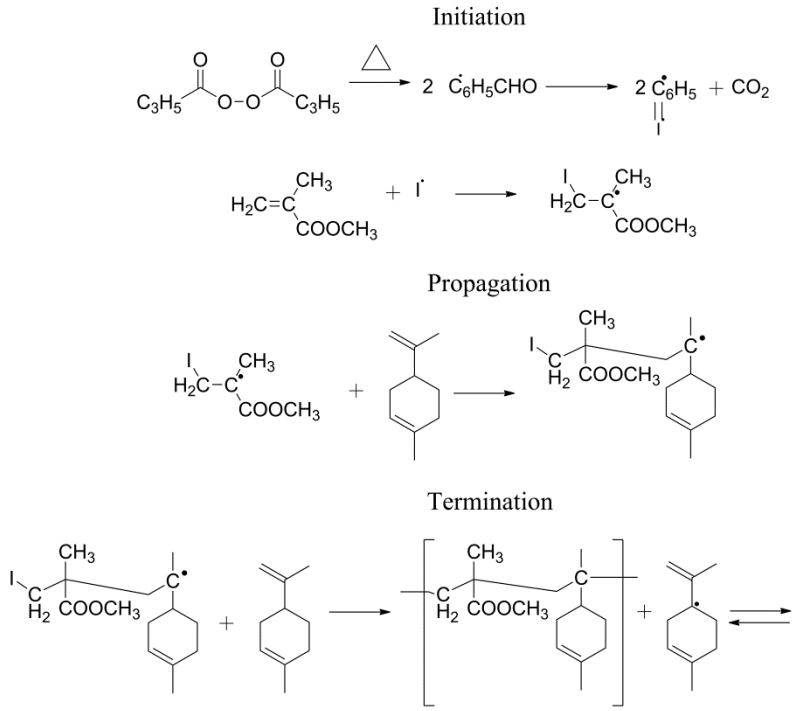

Scheme 17. Mechanism for the copolymerization of limonene with methyl methacrylate.[267]

5. Cyclocopolymerization with maleic anhydride initiated by α,α'-azobisisobutyronitrile (AIBN) in tetrahydrofuran (THF) at 40°C under a nitrogen atmosphere producing a 1:2 alternating non-cross-linked copolymer via a charge-transfer complex as shown on Scheme 18.[268]

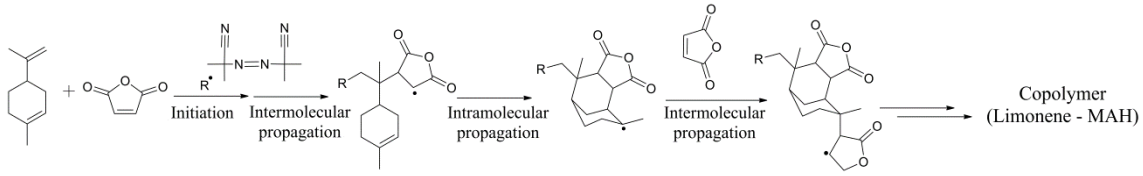

Scheme 18. Mechanism for the 1:2 copolymerization.[268]

6. Copolymerization with maleimide. This reaction uses α,α'-azobisisobutyronitrile (AIBN) as radical initiator and reversible-addition fragmentation transfer (RAFT) agents, such as n-butyl cumyl trithiocarbonate (CBTC) or n-butyl 2-cyano-2propyl trithiocarbonate (CPBTC). It can be achieved with DMF, cumyl alcohol [$PhC(CH_3)_2OH$], and fluorinated cumyl alcohol [$PhC(CF_3)_2OH$] as

solvents. It gives a chiral copolymer with a 1:2 regulated sequence (AAB). It presents high glass transition temperature (220-250 °C) due to the specific rigid cyclic structure of the monomer in the backbone structure of the copolymer as seen in Scheme 19.[269]

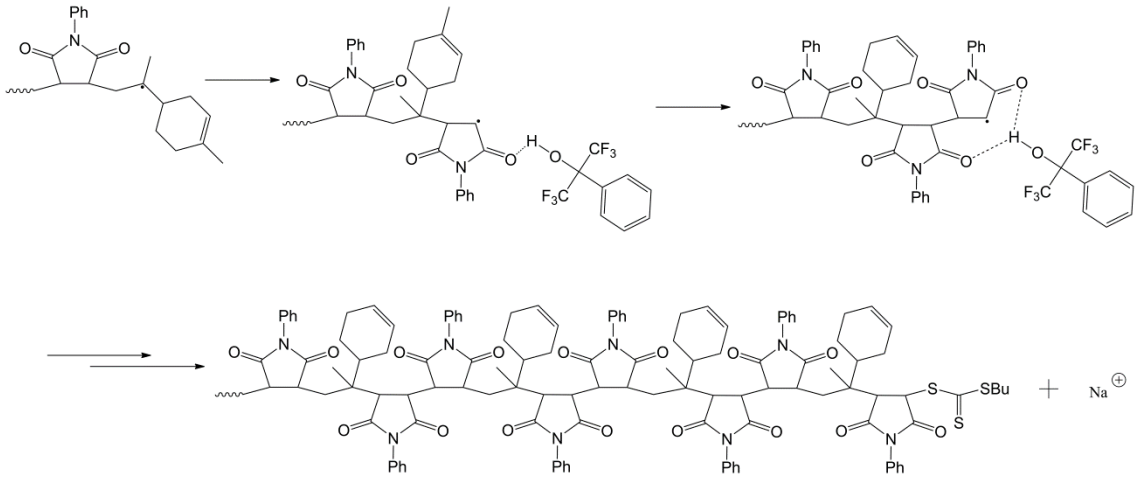

Scheme 19 . Mechanism for the copolymerization of limonene with maleimides.

7. Copolymerization of limonene oxide and carbon dioxide for the production of high molecular weight polycarbonate copolymer (Mn = 25 kg/mol). This reaction uses 0.4 mol % of β-diiminate zinc acetate complexes as catalysts and takes place at 50°C at 670 kPa of CO_2 for 24 h (Scheme 20).[270] For the production of limonene oxide see Appendix 2.

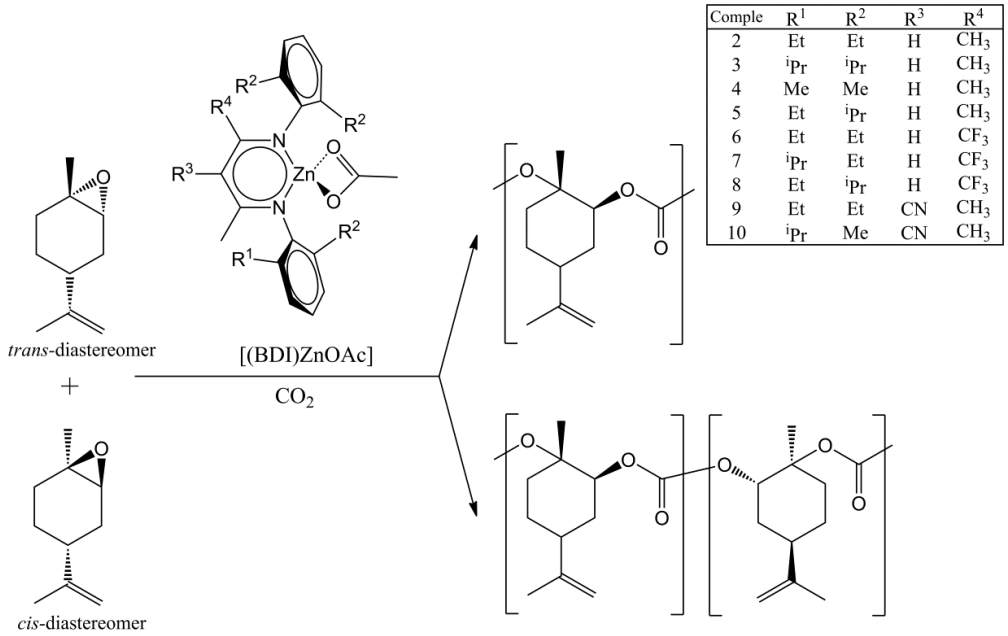

Comple	R^1	R^2	R^3	R^4
2	Et	Et	H	CH_3
3	^{i}Pr	^{i}Pr	H	CH_3
4	Me	Me	H	CH_3
5	Et	^{i}Pr	H	CH_3
6	Et	Et	H	CF_3
7	^{i}Pr	Et	H	CF_3
8	Et	^{i}Pr	H	CF_3
9	Et	Et	CN	CH_3
10	^{i}Pr	Me	CN	CH_3

Scheme 20. Copolymerization of *trans*- and *cis*- limonene oxide and CO_2 using β-diiminate zinc acetate complexes.[270]

1.9.5 Other uses of D-limonene in polymerization processes

D-limonene is not always used as a monomer, it is also used as a tool to adjust the morphology, mechanical and thermal properties of poly(L-lactide) films. It helps to produce ductile films with an elongation at break up to 200%. Its addition decreases the transition temperatures; it reduces by 30 °C the T_g, 45°C the T_c and 15°C the T_m. It also helps to diminish crystallinity by 14%.[271]

Another example is its use in the polymerization of dicyclopentadiene as a chain transfer during the ring-opening metathesis polymerization process (ROMP). In this specific procedure, D-limonene reacts with the metathesis ruthenium initiator in order to introduce a molecule with high degree of branching, to provide chemical functionalities and to control the molecular weight, finally producing homogeneous and soluble polymer (Scheme 21).[272]

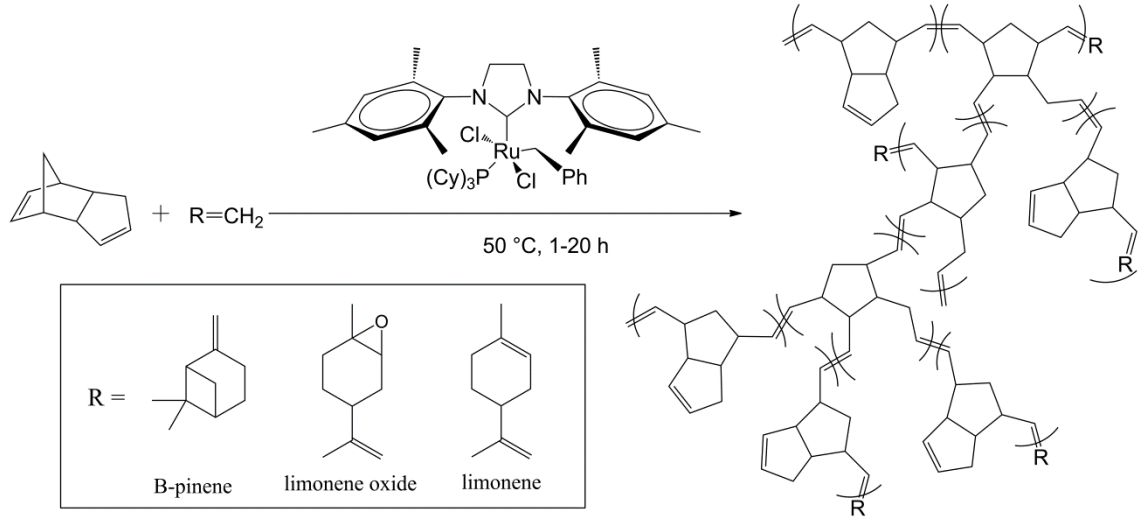

Scheme 21 . Mechanism for the polymerization of dicyclopentadiene with monoterpenes using a ruthenium initiator. [272]

1.10 Chlorogenic acid

1.10.1 Description, synthesis and applications

Chlorogenic acid is a nonflavonoid catecholic ester formed by the combination of quinic acid and caffeic acid (Scheme 22). This reaction can form different isomers but the most abundant is 5-*O*-caffeoylquinic acid, known as neochlorogenic acid.

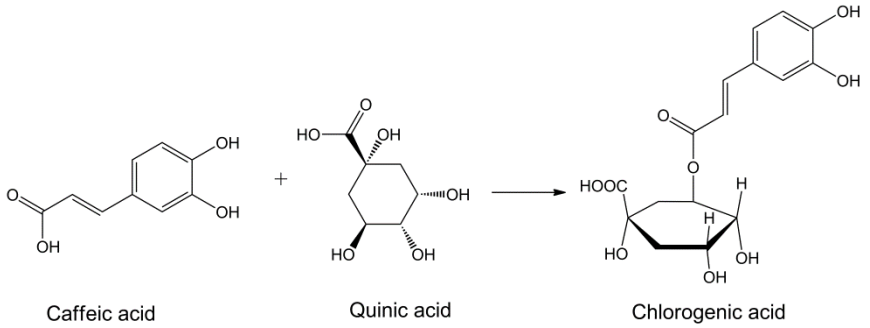

Scheme 22 . Chlorogenic acid chemical structure. (1*R*,3*R*,4*S*,5*R*)-3-[(*E*)-3-(3,4-dihydroxyphenyl)prop-2-enoyl]oxy-1,4,5-trihydroxy-cyclohexane-1-carboxylic acid

Chlorogenic acid is derived from phenylalanine, which is generated from phosphoenol pyruvate and erythrose 4-phosphate via the shikimate pathway, summarised in Scheme 23. The biosynthesis of chlorogenic acid can be achieved by three different pathways, as shown in Scheme 24. The first route is the one identified in potatoes while the second and third occur in other plants such as tomatoes.

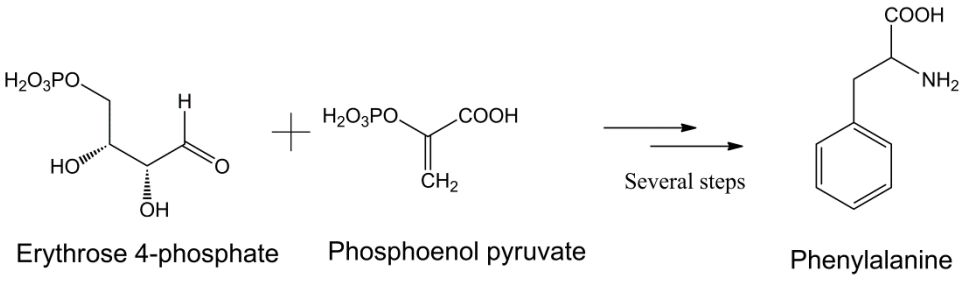

Scheme 23. Chemical formation of chlorogenic acid precursor

The first route uses caffeoyl *D*-glucose as an intermediate while the second route involves the combination of caffeoyl-CoA and quinic acid by means of quinate transferase (HQT) and the third route is generated by the synthesis of *ρ*-coumaroyl-CoA by HCT transferase followed by its hydroxylation caused by *ρ*-coumarate-3'-hydroxylase (C3'H) to form chlorogenic acid.

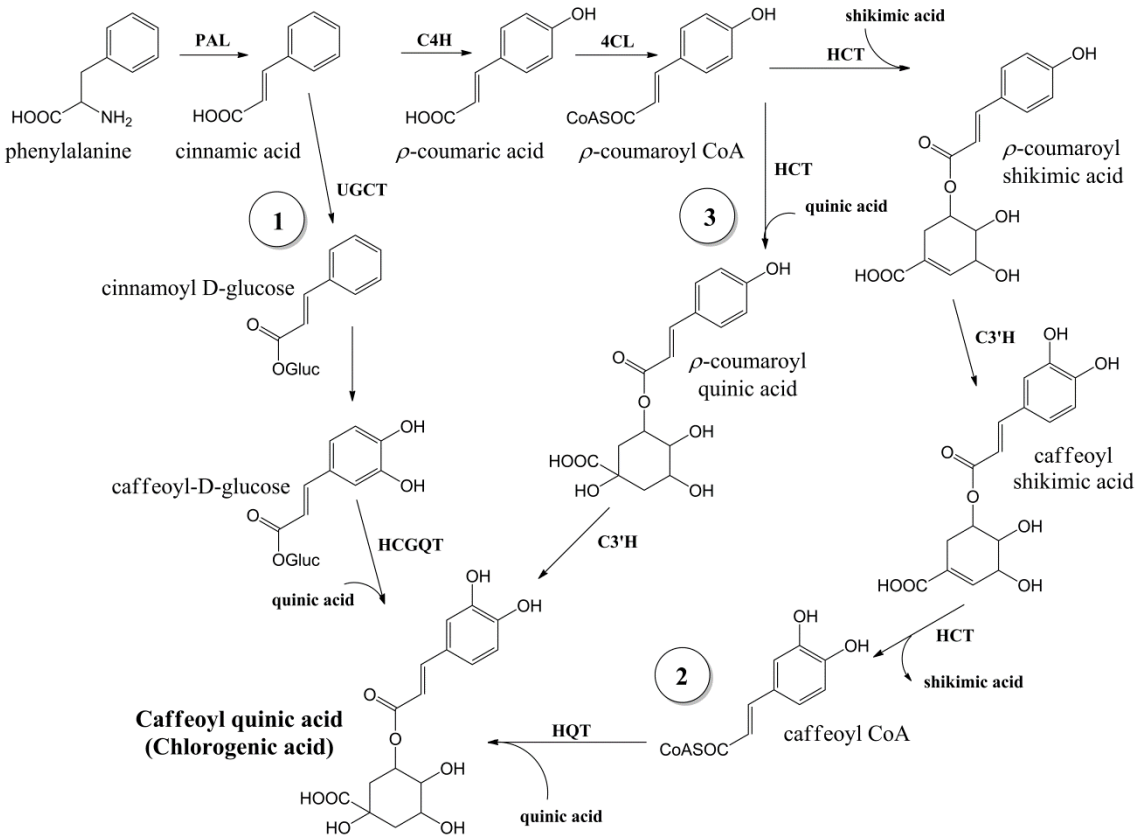

Scheme 24 . Pathways for the biosynthesis of chlorogenic acid.[273]

The enzymes involved in Scheme 24 are:

- PAL = phenylalanine ammonia lyase
- C4H = cinnamate-4-hydroxylase
- 4CL = 4-hydroxycinnamoyl CoA ligase
- HCT = hydroxycinnamoyl CoA shikimate/quinate hydroxycinnamoyl transferase
- C3H = *ρ*-coumarate 3'-hydroxylase
- HQT = hydroxycinnamoyl CoA quinate hydroxycinnamoyl transferase
- UGCT = UDP glucose: cinnamate glucosyl transferase
- HCGQT = hydroxycinnamoyl D-glucose: quinate hydroxycinnamoyl transferase

Due to the antibacterial, antiviral and antioxidant properties of chlorogenic acid it is a highly valuable compound for medicine and the food industry. It is used for food production and conservation, in drug molecules, cosmetics, beverage and beauty products. Since it is a nonflavonoid catecholic it is believed to have anti-inflammatory, antimutagenic and anticarcinogenic properties.

1.10.2 Presence in potato waste and its extraction

As mentioned before (section 1.4.1) chlorogenic acid constitutes around 90% of the phenolic compounds of potato waste. Products from phenolic compound oxidation protect the potato against invading pathogens like viruses, fungi and bacteria. Their oxidative polymerization is also used to heal injuries on the potato surface from insect and fungal predators. These phenolic compounds can be found mainly in the peel and the cortex of the potato. Around 50% of them are situated in the skin and the adjoining tissues, while the rest are distributed from the outside to the centre of the tuber.[50,274,275]

Karim et al[50] reported the chemical composition of aerial and subterranean potato tuber of two different types; the Desiree (red skin) and Epicure (white skin) (Table 41). Chlorogenic acid is higher in aerial tubers compared to subterranean ones since the exposure of the tuber to the light stimulates the production of secondary metabolite synthesis.

Table 41. Chlorogenic acid present in aerial and subterranean tubers of two potato genotypes (mg per 100 g of dry weight)

	Subterranean tubers	**Aerial tubers**
Cv Desiree	86.5	237.7
Cv Epicure	112.4	272.3

Using UV spectroscopy, Friedman[276] measured the distribution of chlorogenic acid in processed potatoes. According to his results, microwaved potatoes contain 55 % and boiled potatoes only 35 % of the total original amount while oven-baked potatoes, French fries and mashed potatoes flakes contain none (Table 42).

Table 42 . Distribution of chlorogenic acid in potato (milligrams per 100g of fresh weight).[276]

Processed potato	**chlorogenic acid / mg**
Fresh	0.800 ± 0.05
Baked	0.000
Boiled	0.319 ± 0.01
Microwaved	0.434 ± 0.02

The conventional methods used to extract chlorogenic acid from the potato are based on solid-liquid extraction methods using organic solvents such as methanol, ethanol and acetone.[277-280] Siwawej and Jaisaard[281] also published an extraction method using water, methanol, ethanolbutylated hydroxyanisole and hydroxytoluene as solvents and supercritical CO_2[282] and water in reflux[283] have been also used.

With time these methods have been improved. One of the latest technologies uses microwave energy to heat the waste and allow the extraction of the compound from the sample into the solvent; this method is known as microwave-assisted extraction (MAE). The advantages of this method are the shorter extraction time, higher selectivity of the specific extracted compound and lower solvent consumption.[284] The best experimental parameters for chlorogenic acid were methanol solvent at 100% v/v, with a microwave power level of 10% for 5 minutes.

Another new method for the extraction of chlorogenic acid is subcritical water extraction (SCW) which takes place in a batch reactor and uses water at high temperatures (about 100 – 374 °C) at elevated pressure (around 6 - 22 MPa respectively). Best results obtained were at 160 °C at 6 MPa for 60 minutes. The advantages of this method are that uses only 1/3 of the time and 40% of solvent volume compared to conventional methods and removes higher amounts.[285]

The characterization and separation of chlorogenic acid from its isomers and other components is through the use of high performance liquid chromatography (HPLC)[286] or the Maslak separation procedure.[287]

1.10.3 Enzymatic oxidative polymerization

The initial step in the enzymatic oxidative polymerization of chlorogenic acid is the formation of an o-quinone by enzymatic oxidation (explained in section 1.5.2.6). The subsequent steps rely on non-enzymatic reactions; as the second step is the conversion of half of the quinone into hydroxyquinone and regeneration of chlorogenic acid. At the end, polymerization of the hydroxyquinone takes place (Figure 24).[288]

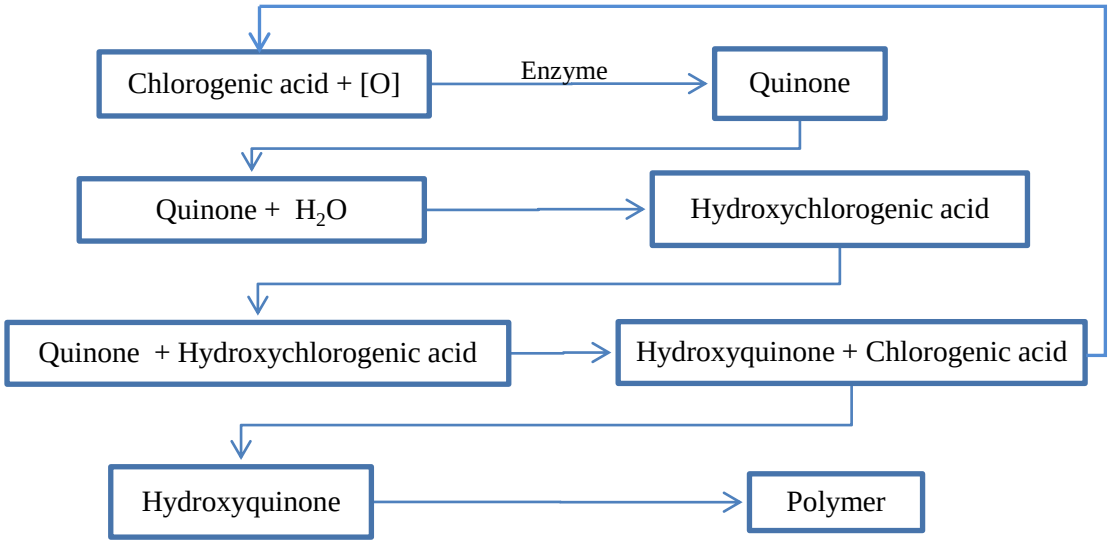

Figure 24. Diagram of the enzymatic oxidative polymerization of chlorogenic acid.

There are some enzymes that catalyse the polymerisation while some chemical species inhibit steps. These enzymes interfere with polyphenol oxidation by inhibiting the enzyme and by combining with the quinine product.[289] The enzymes and inhibitors for this reaction are shown below.

Enzymes:

- o-diphenol oxidase (mushrooms)
- tobacco-leaf
- Polyphenol oxidase (apple)
- Oxidoreductases

Enzyme inhibitors:

- Ascorbate
- Potassium ethyl xanthate
- Diethyldithiocarbamate
- Cysteine
- 2-Mercaptobenzothiazole
- Polyvinylpyrrolidone
- Thioglycollate: just reduces reaction
- NaF

2. Experimental Procedure

2.1 Materials

Details of reagents and materials used for experiments on the polymerization of derivatives of D-limonene are given in Table 43, those for experiments with chlorogenic acid in Table 44 and those for experiments with oleic acid from mango seed butter in Table 45. For these experiments most reagents were used as supplied, except 2,6-lutidine which was dried with 4A molecular sieves overnight. Particular care was taken with D-limonene disposal as it is toxic to aquatic organisms and has persistent effects.

Table 43. Details of reagents and materials used for experiments on the polymerization of derivatives of D-limonene.

Experiment 1 (D-Limonene polymerization)		
Substance (supplied within UK)	**Supplier**	**Purity %**
D-limonene	Sigma Aldrich	90
4-methylstyrene	Sigma Aldrich	96
α-methylstyrene (stab with 4-*tert*-butylcatechol)	Alfa Aesar	99
Dimethylstyrene	Sigma Aldrich	98
Styrene (stab with 4-*tert*-butylcatechol)	Sigma Aldrich	≥ 99
Polystyrene M_w = 192000	Sigma Aldrich	-
Palladium (II) trifluoroacetate	Acros Organics	97
Palladium (II) acetate	Sigma Aldrich	98
Palladium (II) chloride	Alfa Aesar	47 of Pd
Copper (II) chloride	Alfa Aesar	98
Dimethylformamide	Acros Organics	99.8
Dimethyl Sulfoxide	Sigma Aldrich	99.6
Acetonitrile	Sigma Aldrich	99.9
Toluene	Fisher Chemical	99.9
Tetrahydrofuran	Sigma Aldrich	99.9
2-methyl tetrahydrofuran	Sigma Aldrich	99.9
Cyclopentyl methyl esther	Sigma Aldrich	99.9
2,6-di-tert-butylpyridine	Sigma Aldrich	≥ 97
2,6-lutidine	Sigma Aldrich	99+
2,2,6,6,-tetramethylpiperidine	Sigma Aldrich	≥99
N,N-Diisopropylethylamine	Sigma Aldrich	≥99
Diisopropylamine	Sigma Aldrich	≥99
2,4,6-collidine	Sigma Aldrich	99
Boron trifluoride -diethyl ether complex	Merck Millipore	-
L-lysine monohydrochloride	Alfa Aesar	+ 99
Silica gel. Part.size 0.2-0.05mm. Pore size 40 Å	Fisher Chemical	-
4A Molecular Sieves	Sigma Aldrich	-

Table 44. Details of reagents and materials used for experiments on the polymerization of chlorogenic acid and analogues.

Experiment 2 (Chlorogenic acid polymerization)		
Substance (supplied within UK)	**Supplier**	**Purity %**
Phenol	Research Chemicals Ltd.	99
Caffeic acid	Sigma Aldrich	95
Chlorogenic acid	Carbosynth	98
Horseradish peroxidase (140 u/mg)	Sigma Aldrich	-
Hydrogen peroxide	Sigma Aldrich	35
Phosphate buffer pH 7	Sigma Aldrich	-
Methanol	Sigma Aldrich	99.5
Poly(ethylene glycol) Mn = $1.5x10^3$	Prolabo	-
2,3 Dihydroxybenzoic acid	Alfa Aesar	98
2,4 Dihydroxybenzoic acid	Sigma Aldrich	97
3,5 Dihydroxybenzoic acid	Sigma Aldrich	97
1,2 Dihydroxybenzene (catechol)	Fisher Scientific	$\geq$ 99

Table 45. Details of reagents and materials used for experiments on the polymerization of oleic acid from mango seed butter.

Experiment 3 (Oleic acid polymerization)		
Substance (supplied within UK)	**Supplier**	**Purity %**
Mango seed butter ultra refined (USA)	Biochemica International	-
Oleic acid	Sigma Aldrich	90
4-(Dimethylamino) pyridine	Sigma Aldrich	$\geq$ 99
N,N'-dicyclohexylcarbodiimide	Sigma Aldrich	$\geq$ 99
Diethylenetriamine	Sigma Aldrich	99
ρ-phenylenediamine	Sigma Aldrich	$\geq$ 99
Triethylamine	Merck KGaA	$\geq$ 99
Hydrogen peroxide	Merck KGaA	30
Formic acid	VWR International	$\geq$ 85
1,3-propanediol	Alfa Aesar	99
cis-1,2-cyclohexanedicarboxylic anhydride	Alfa Aesar	98
Toluene	Fisher Chemical	99.9
Dichloromethane	Fisher Chemical	99.9

The clay used was a natural montmorillonite with the commercial name of Nanofil1®116 while the organoclay used is known as Cloisite 10A which is also a montmorillonite clay but modified with a 2MBHT (dimethyl-benzyl-hydrogenated tallow, quaternary ammonium), where the hydrogenated tallow is a mixture of ~ 65% of C18, ~ 30% of C16 and ~ 5% of C14 with chloride as anion. Both clays were obtained from Southern Clay Products, a subsidiary of Rockwood Additives LTD, UK.

2.2 Equipment

Description of the techniques deployed in this research can be found in Appendix 6.

2.2.1 Gas chromatography (GC)

Gas chromatography was used in experiments that involved dimethylstyrene synthesis from D-limonene extracted from citrus food waste to provide information on the number of components in the mixture, as well as their quantity. This method made it possible to analyse the by-products from the D-limonene reaction and to know the amount of DMS formed every time the reaction was modified.

GC analysis was carried out in a Hewlett Packard HP4890-A GC with a High Performance Capillary Column HP-5 (Crosslinked 5% PH ME Siloxane) with film thickness of 0.25 µm, phase ratio of 320, length of 30 m and column ID of 0.32 mm produced by Hewlett Packard in USA, CA. The carrier gas was helium with a column flow rate of 2 ml min^{-1}. The injector was operated at 250 °C in split mode with a split ratio of 1:20. The oven was heated at 50 °C and then 1 °C min^{-1} to 80 °C.

2.2.2 Fourier Transformation-Infrared (FT-IR) spectroscopy

The IR spectra were used to observe changes to monomer structure after polymerization and to identify where the changes in the monomer structure took place. This technique complements the NMR spectrum for the complete identification of the polymer structure. IR measurements were carried out on a Perkin Elmer Spectrum 100 Series with a ZnSe crystal with a scan rate of 16 and a wavelength range from 4000 to 600 cm^{-1}.

2.2.3 Nuclear Magnetic Resonance (NMR) spectroscopy

This technique was used to characterize the polymerization of potato waste derivatives in order to determine the structures of the polymers obtained: different structures can be obtained during these procedures. ^{1}H NMR analyses were recorded on a 300MHz Bruker AMX300 (Billerica, MA, USA) spectrometer while ^{13}C NMR were obtained on a Bruker AVANCE500. Both instruments present an accuracy of ± 5%. Samples from citrus and potato derivatives were carried out with DMSO-d_6 solvent which can be seen at the peak 2.5 ppm in the spectra, while experiments from mango butter were in chloroform-d_6 which can be seen at 7.2 ppm.

2.2.4 X-ray Diffraction (XRD)

X-ray diffraction was used to characterize the clay, particularly to measure the basal plane spacing (d_{001}) and hence to detect changes indicative of monomer intercalation between the clay layers. The measurements were made on a Siemens D500 instrument from 2-25 degrees of 2 θ in 0.05 steps and at 4 sec/step.

2.2.5 Viscometer and temperature stabilisation

A reverse flow Cannon-Fenske viscometer (type Reverse Flow) size 100 from Rheotek^{TM} was used, supplied with a United Kingdom Accreditation Service (UKAS) certificate of calibration issued by Primary Standards Laboratory (PSL) on the 3rd of August 2010 as certificate No. 31294.

All measurements were made in a water tank at 25 ± 0.05 °C. Temperature was measured with a mercury-in-glass thermometer with a range from -5 °C to +105 °C by 0.1 °C with an uncertainty correction of ± 0.05 °C, calibration was issued by the British Standards Institution (BSI) Testing – Metrology Section on 26th of January 1989 by certificate No. 153283/1. The tank was heated with an analogue control thermoregulator Te-10A provided by Techne- UK with a temperature range of -20°C to +95°C and cooled with an immersed copper cooling coil which passed cold water.

2.2.6 Ultrasonic probe

This instrument was used during the study of the interaction of the monomers with the montmorillonite clay. Ultrasonic vibrations were used to facilitate the dispersion of the substance into the clay galleries. Ultrasonic homogenizer sonicator model U200S-Control from IKA Labortechnik Staufen, Germany was used at duty cycle 0.5 with constant amplitude of 60%.

2.2.7 Thermal analysis

A DigiMelt-MPA160 apparatus produced by Stanford Research Systems, USA was employed for the melting point measurements. Differential Scanning Calorimetry (DSC) analyses were made in order to verify the stability and formation of complex between PEG-monomer. The analyses were performed on a STA 449 C instrument produced by NETZSCH-Gerätebau GmbH. DSC measurements were made at 5 °C/min heating rate under a helium flow rate of 30 ml/min with a temperature range of 20-250 °C.

2.3 Polymerization of citrus waste derivatives

The monomer synthesis procedure was based on the liquid phase palladium-catalyzed dehydrogenation described in the work of Horrillo-Martinez[290] followed by a polymerization method. Subsequently, a study of the interaction between the monomer obtained and montmorillonite clay was made. The general sequence is explored in Figure 25.

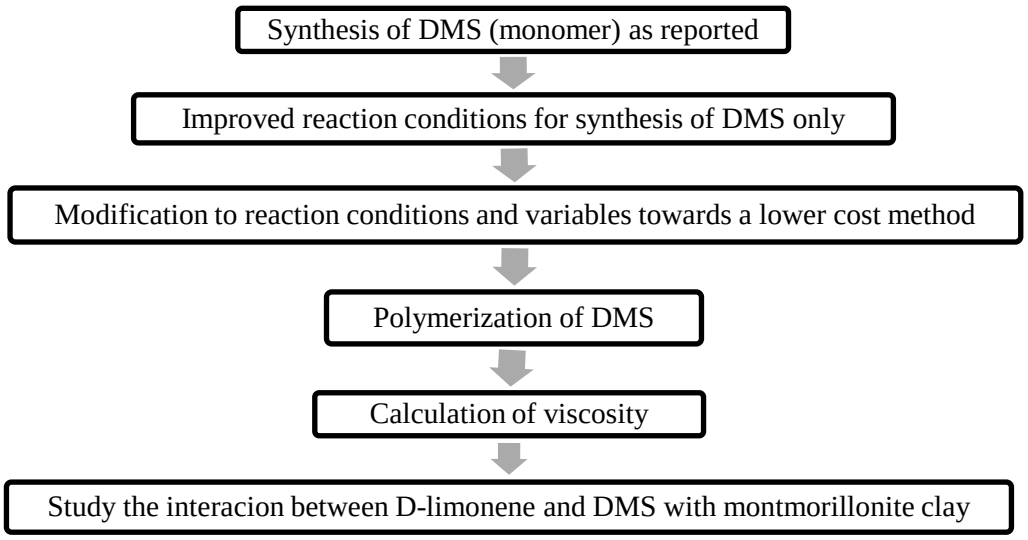

Figure 25. Method for the polymerization of citrus waste and the formation of nanocomposites.

2.3.1 Synthesis of monomer

D-limonene (1 equivalent) was added to a prepared solution of PdX_2 (catalyst, 5 %mol), $CuCl_2$ (oxidant, 2 equivalents) and base (3 equivalents) in dry solvent and heated at 80°C for 40 h under an argon atmosphere in the presence of molecular sieves. At the end of reaction, filtration was made through silica with THF followed by a GC analysis (Section 2.2.1).

Initially, calibration of the gas chromatography instrument was done by running 'standards' consisting of each expected reaction product in different concentrations in order to calculate the relation between the peak area and amount of substance. These calibration graphs are shown below in Figure 27. In each calibration the retention time was recorded in order to identify each substance. The recorded retention times for α-terpinene, ρ-cymene, D-limonene, γ–terpinene, terpinolene and DMS were 14.2, 14.8, 16.9, 20.2, 22.7 and 24 minutes respectively, as shown in Figure 26.

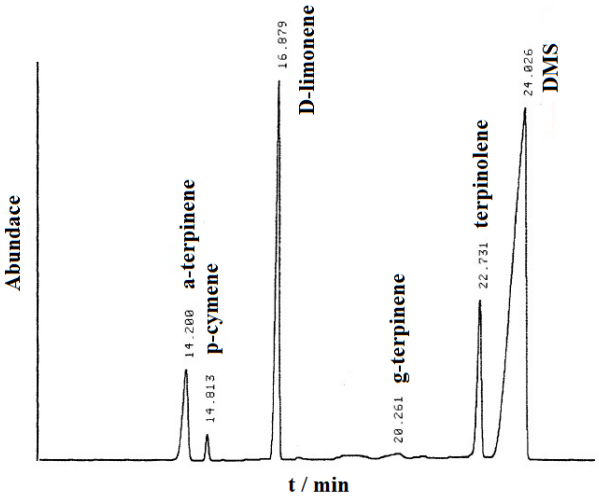

Figure 26. GC analysis from reaction using anhydrous DMF, anhydrous 2,6-tBu_2Py, 5 % mol of $Pd(OTFA)_2$, $CuCl_2$ and 4A molecular sieves at 80°C under argon atmosphere for 40 h. (Table 46, exp 4)

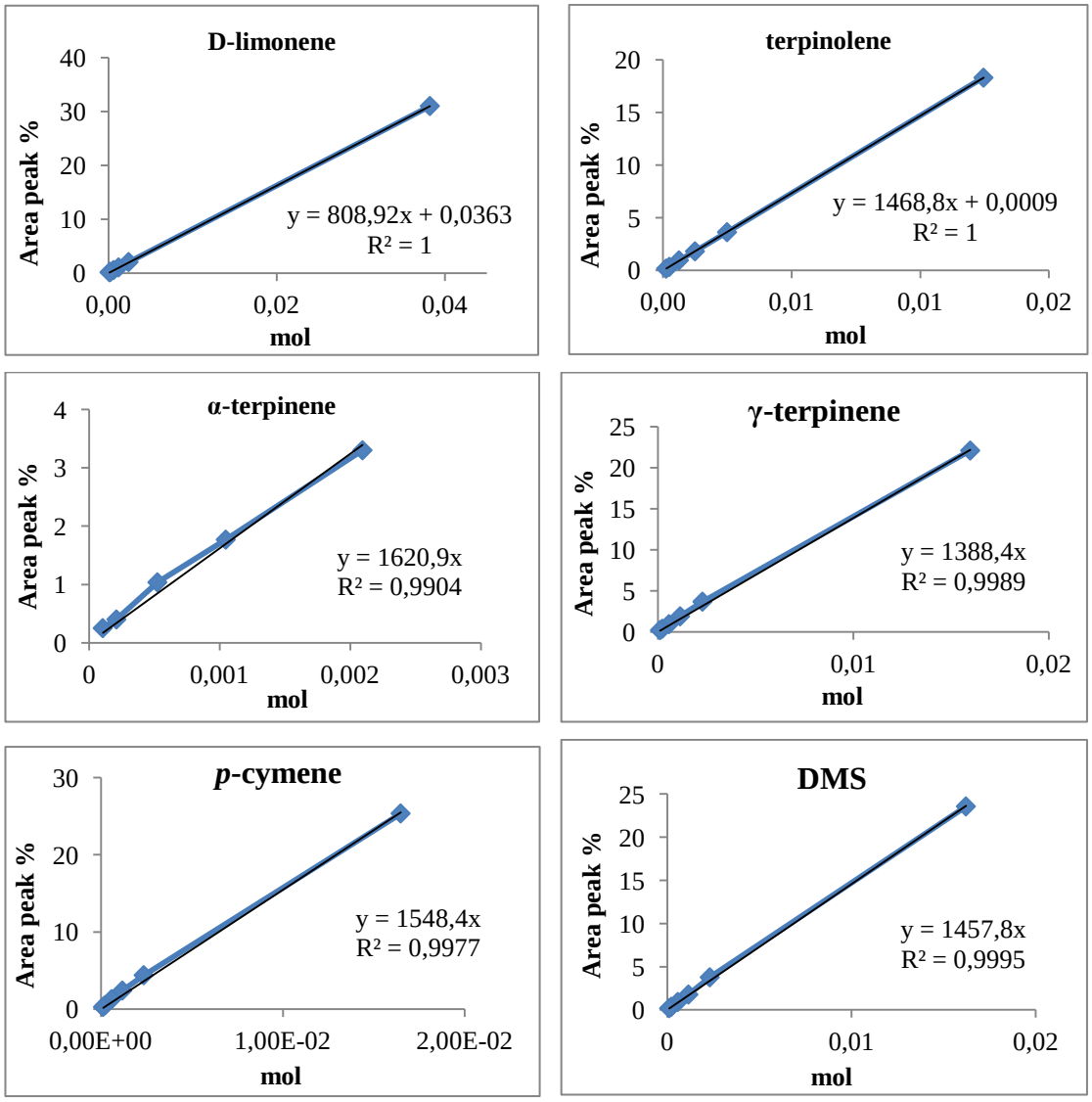

Figure 27. Calibration graphs for the gas chromatography technique.

For replication of the Horrillo-Martinez method[290] DMF was used as solvent, $Pd(OTFA)_2$ as catalyst and 2,6-t-Bu_2Py as base. Subsequently, with the intention of reducing the cost of reactants and in order to limit the number and quantity of by-products, the procedure was repeated by changing the base while leaving the DMF as solvent and $Pd(OTFA)_2$ as catalyst. The alternative bases used were 2,6-lutidine, 2,2,6,6-tetramethylpiperidine, N,N-diisopropylethylamine, diisopropylamine and 2,4,6-collidine.

To improve the reaction further, an increase of temperature from 80 °C to 120 °C was made in the original reaction as well as in the reaction with the base with the intention of providing higher DMS conversion. To further understand the reaction, the procedure was repeated firstly with double the amount of $Pd(OTFA)_2$ (10 %mol), secondly with the addition of 6 equivalents of base and finally in the absence of copper (II) chloride.

Consequently, the procedures that yielded the highest DMS conversion from the previous experiments were repeated by substituting different solvents, namely dimethyl sulfoxide, heptanes, acetonitrile, 2-methyl tetrahydrofuran and cyclopentyl methyl ether.

Finally, again with the intention to improve the cost of the reaction and thus make it more attractive commercially, other palladium catalysts were tested. These were $Pd(OAc)_2$ and $PdCl_2$. Temperature and quantity of reactants were also changed in order to obtain the highest possible DMS yield.

Once the reaction was chemically improved, the kinetics of the reaction were studied in order to comprehend the conversion development during a 40 h period and thus to try to enhance the reaction time.

2.3.2 Polymerization of DMS

The monomer was obtained using the procedure in section 2.3.1 and its purification was made through a vacuum distillation. For the polymerization, a solution of 20 parts of α,ρ-dimethylstyrene (DMS) and 80 parts of toluene was made up and placed in a three neck flask with continuous stirring under N_2 atmosphere and immersed in a dry ice-acetone cooling bath at -78°C (195 K). Subsequently 0.3 parts of catalyst, boron trifluoride etherate, was slowly added making sure that temperature did not increase above -78°C as this addition produced an exothermic reaction. Afterwards the reaction was left for one hour under the same conditions. Once the reaction subsided, pre-cooled methanol was added in order to quench the reaction and to precipitate the polymer. The precipitate was separated and washed with methanol to remove the catalyst and monomers and then dried under vacuum.

2.3.3 Measurement of viscosity

The procedure followed the recommendations from "Methods for determination of the viscosity of liquids" published by the British Standard Insitution as BS188.[291] The viscometer was carefully cleaned and dried before each measurement. To introduce the sample, the viscometer was inverted and the narrower tube was immersed in the liquid sample. By applying suction through the other tube, the viscometer was charged with liquid. Once filled with the necessary amount, it was inverted and inserted in a vertical position in the temperature bath at 25 ± 0.05° C with use of a holder. The viscometer was left in the bath for 15 minutes so the sample reached the temperature of the bath. The flow time was measured between both graduations with use of a timer. The measurements were repeated until four results were closely obtained in order to have good repeatability as specified in BS188.

Despite the fact that the viscometer used was professionally calibrated, an initial calibration of the instrument was performed in the laboratory using distilled water. The density[292] of water at 25 °C is 997.04 kg/m^3 and the dynamic viscosity[292] is 0.8902 mPas. Therefore the theoretical kinematic viscosity (obtained by dividing the kinematic viscosity by the density, equation 7 in section 3.2) is 0.8928 mm^2/s. By using the glass viscometer the experimental dynamic viscosity obtained was 0.8978 mm^2/s, giving an experimental error of 0.6%. Subsequently the viscosity of toluene and 5 different concentrations of: (1) poly-DMS, (ii) A-MS and (iii) a polystyrene of known Mw were measured.

2.4 Polymerization of potato waste derivatives

For the polymerization of monomers derived from potato waste, two different methods of enzymatic polymerization were attempted: solution polymerization and template polymerization.[293] Furthermore, different conditions were used for the solution polymerization, one originating from the enzymatic phenol polymerization conditions described in Oguchi's work[294] and the second from the caffeic acid polymerization described by Xu and co-workers.[295] The methods reported for the polymerization of waste derivatives are summarised in Figure 28.

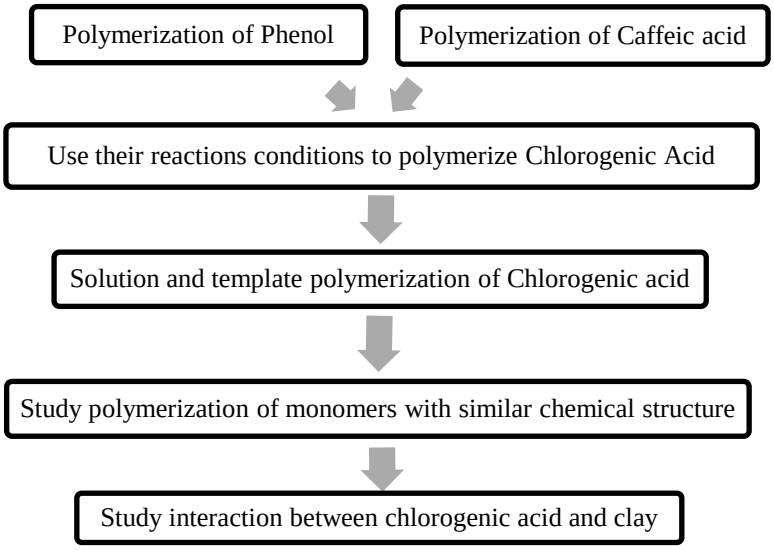

Figure 28. Method for the polymerization of potato waste and the formation of nanocomposites

2.4.1 Enzymatic polymerization in pH 7 phosphate solution with methanol

The monomer (10.6 mmol) and HRP (220 U[2]) were dissolved in MeOH and phosphate buffer pH 7 (1:1 by volume, 20 ml). To the solution hydrogen peroxide (3.6 ml of 10%, 10.6 mmol) was added dropwise over 5 h with constant stirring. A uniform addition of hydrogen peroxide was obtained by using an electromagnetic ink-jet printer valve (Lee Valves, Chalfont St. Peter, UK) driven by two NE555 timers arranged as monostables switching a Darlington transistor so that the valve on-time and off-time could be independently set (Diagram in Appendix 3). This simple use of an inkjet valve makes it possible to add reagents at very low controlled rates and deserves to be more widely used. After the addition of the hydrogen peroxide, the reaction was stirred for an additional 1 hour. Afterwards, the precipitate was separated from the solution and washed with methanol, followed by drying under vacuum.

The first monomer to be used was phenol, to replicate previously reported work.[294] Subsequently, the method was repeated by changing the monomer for caffeic acid and chlorogenic acid, using same ratios and quantities, for their enzymatic polymerization. In addition, a control reaction using phenol as monomer was executed without the enzyme with the intention to corroborate the catalytic effect of the enzyme during the polymerization.

[2] A unit of enzyme activity is the amount of enzyme which will catalyse the transformation of 1 micromole of the substrate per minute under standard conditions.

To further understand the polymerization reaction, monomers with similar chemical structures (Figure 44) were used: 1,2-dihydroxybenzene, 2,3-dihydroxybenzoic acid, 2,4-dihydroxybenzoic acid and 3,5-dihydroxybenzoic acid.

For those monomers which were not soluble in the equivolume mixture of MeOH/Phosphate buffer (pH 7) the temperature was raised from 25 °C to 50 °C in order to increase their solubility. Methanol as a solvent was also replaced with ethanol due to the higher solubility of the monomer in this solvent.

2.4.2 Enzymatic polymerization in aqueous solution with methanol

A stock solution of 2000 U of HRP/ml of phosphate buffer was prepared. The monomer (1 mmol) was added to 10 ml of an equivolume solution of methanol and water. Afterwards, 200 μl of the stock solution was added. To this solution, a stoichiometric amount of hydrogen peroxide was added (1 mmol) during the course of 1 h using the ink-jet printing dispenser. After the addition of the hydrogen peroxide, the reaction was stirred for 2 h. At the end of the reaction, the precipitate was separated from the solution by centrifugation, washed with water and dried in a vacuum.

The monomers used for this method were: phenol, caffeic acid, chlorogenic acid, catechol, 2,3-dihydroxybenzoic acid, 2,4-dihydroxybenzoic acid and 3,5-dihydroxybenzoic acid. As in the previous method, a control reaction of phenol without enzyme was also carried out.

2.4.3 Enzymatic template polymerization in water-soluble polymer.

The monomer (0.47 g) and PEG (0.47 g) were dissolved in 20 ml of phosphate buffer (pH 7). A solution HRP (440 U in 5 ml of phosphate buffer) was added to the first solution. To this solution hydrogen peroxide (5.6 mmol, 3.4 ml of 5 %) was added dropwise over 2 h with constant stirring. After the addition of hydrogen peroxide, the reaction was left stirred for 1 h. Afterwards, the precipitate was separated by centrifugation, washed to remove unreacted water soluble PEG and dried in a vacuum.

As in the previous experiments, the first monomer to be tested was phenol, followed by caffeic acid and chlorogenic acid. Additionally, reactions using the same monomers but without PEG were made in order to assess the effect of PEG addition on the process.

2.5 Polymerization of oleic acid from mango seed butter

Oleic acid was first purified from commercial mango butter; subsequently an esterification between two oleic acid molecules was done in order to create di-esters. Afterwards, epoxidation of the double bonds was made for the polymerization to take place. Two different curing agents, anhydride and amine, were used for the polymerization process. Subsequently, the potential of oleic acid-clay intercalation was tested. The general sequence is explored in Figure 29.

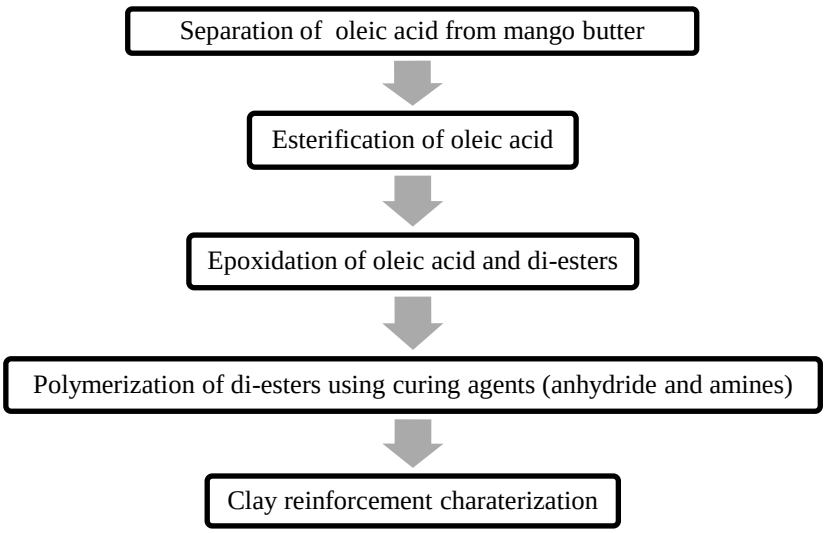

Figure 29. Method for the polymerization of oleic acid from mango seed butter.

2.5.1 Separation of oleic acid

As indicated in the specification sheet (appendix 4), mango butter contains around 40-50% of oleic acid. Its purification from the rest of the fatty acids, mainly stearic acid which is 40-45%, was made by crystallization of stearic and palmitic acids from aqueous acetone solution at -25°C.[296,297] Reduced pressure distillation was used for the removal of residual acetone from the purified oleic acid. FT-IR analyses of the oleic and stearic acids obtained were used to quantify the separation process.

2.5.2 Esterification of oleic acid

Di-esters were synthesized by esterification of oleic acid.[298] 1,3-propanediol, orcinol and resorcinol were used to create the ester linkages.

First, oleic acid and a diol were dissolved in dichloromethane (DCM) in a molar ratio of 2:1 at 0°C by use of an ice bath, followed by first the slow addition of 4-

(dimethylamino)pyridine (DMAP) and then N,N'-dicyclohexylcarbodiimide (DCC) in a molar ratio of 0.03 and 0.24 respectively, based on 1 mol of monomer. The ice bath was removed when a homogeneous solution was obtained. Subsequently, the mixture was stirred for 24 h at room temperature and atmospheric pressure. At the end of reaction, the solid was removed by filtration and di-ester was purified by evaporation under reduced pressure. FTIR was used for characterization of the di-ester.

2.5.3 Epoxidation of oleic acid and di-esters.

Epoxidation was carried out by using hydrogen peroxide and formic acid for reaction with double bonds in a molar ratio of 20:2:1, respectively. Toluene was used as solvent in order to minimize ring opening. Initially, oleic acid or di-ester was dissolved in toluene and formic acid was added at room temperature. Subsequently, the hydrogen peroxide was added dropwise for 1 hour; afterwards the temperature was slowly increased to 80°C (taking 1 hour to reach the final temperature). Once reaction was finished, the epoxide (the organic layer) was separated by a liquid-liquid extraction using distilled water to remove residual H_2O_2.[299,300]

2.5.4 Polymerization of di-esters using curing agents.

The curing process of the epoxidized monomers, obtained from the previous step (Section 2.5.3), in order to obtain a polymer was studied by using two different types of curing agents.

1. Anhydride agents. The epoxidized monomer, *cis*-1,2-cyclohexanedicarboxylic anhydride (curing agent) and triethylamine (initiator) were mixed in a molar ratio of 0.5/0.5/0.0085, respectively. Two different conditions of curing time and temperature were attempted, one originating from Nicolau's work[301] which uses 165 °C for 3 hours and the second from Rosch's work[302] using 200 °C during 1 hour. The final products were stored in a vacuum desiccator at room temperature.
2. Amine agents. Diethylenetriamine (DET) and ρ-phenylenediamine (PPD) were tested as agents. The epoxidized monomer and the amine curing agents were mixed in a ratio of 1:1 at room temperature until a homogeneous mixture was obtained, e.g. for PPD it took 24 h. Subsequently the mixture was left to react over time for 4 days. FT-IR analysis was used to monitor polymerization reaction.

FT-IR and ^{1}H NMR techniques were performed for chemical structure characterization of all samples.

2. 6 Interaction of monomers with clay.

Tests were made with the purpose of determining if the monomers intercalate between the clays layers and if exfoliation takes place, in order to create a polymer nano-composite. Samples of (i) clay, (ii) clay + solvent, (iii) clay + monomer and (iv) clay + monomer + solvent were made using 1 g of monomer, 1g of clay and/or 10 ml of solvent, respectively. All the samples were exposed for 10 min under the ultrasonic sonicator at cycle 0.5 with constant amplitude of 60% with the exception of organoclay which was just minimum hand mixed and left to interact. The samples with solvent provide controls for the effect of solvent retention on the basal plane spacing of the clay. All samples were dried at 60°C overnight.

2.6.1 Modification of clay

The clay used was the natural montmorillonite Nanofil1®116. This clay is characterized as having a cation exchange capacity of 116 meq/100 g clay. With this property it is possible to calculate the amount of L-lysine monohydrochloride needed for its modification by using the following expression.

$$\text{grams of clay}\left(\frac{116\ \text{meq}}{100\ \text{g clay}}\right)\left(\frac{1\ \text{eq}}{1000\ \text{meq}}\right)\left(\frac{1\ \text{mol}}{1\ \text{eq}}\right)\left(\frac{182.65\ \text{g}}{1\ \text{mol}}\right)=\text{grams of L-lysine}$$

Thus for 20 g of clay 4.2 g of L-lysine monohydrocloride should be used. Therefore, for the chemical modification, 4.2 g of L-lysine monohydrochloride was dissolved in distilled water and added to 20 g of montmorillonite under continuous stirring over 1 hour until a brown homogeneous mixture was formed. Afterwards, the mixture was centrifuged to sediment the clay. The clay was washed several times with water to eliminate unattached L-lysine and any sodium chloride formed during the reaction. Subsequently the clay was dried at 60 °C overnight.

3. Results and Discussion of Citrus Waste Experiments.

This chapter describes experiments on the dehydrogenation of D-limonene, an inexpensive industrial feed-stock from a renewable resource, in order to produce 1-methyl-4-(2-propenyl)benzene (dimethylstyrene, DMS) monomer which was subsequently polymerized. The viscosity and molecular weight of the soluble part of the new polymer were calculated. In addition, an interaction study between the monomer obtained (DMS) and the precursor (D-limonene) with montmorillonite clay was made. An interaction between the polymer matrix and the natural clay reinforcement should improve the natural polymer properties.

3.1 Synthesis of DMS monomer by liquid phase palladium-catalyzed dehydrogenation

As introduced in section 1.8.3, dimethylstyrene can be obtained in the 2 steps dehydrogenation process of D-limonene using solid acid catalysts. However, Horrillo-Martinez's[290] have reported a direct selective dehydrogenation route from D-limonene to dimethylstyrene based on a Wacker-type process. (this process is detailed in appendix 5). The reaction was described to be heterogeneously catalyzed by palladium (II) trifluoroacetate ($Pd(OTFA)_2$) using anhydrous copper chloride ($CuCl_2$) as oxidant in the presence of 2,6-di-*tert*-butylpyridine (2,6-*t*Bu_2Py) a sterically hindered base. From this reaction monoterpenes were also obtained as by-products, (Scheme 25). According to Horrillo-Martinez's work, a 65% yield was obtained with a selectivity of DMS to *ρ*-cymene and terpinolene of 14.3:1.

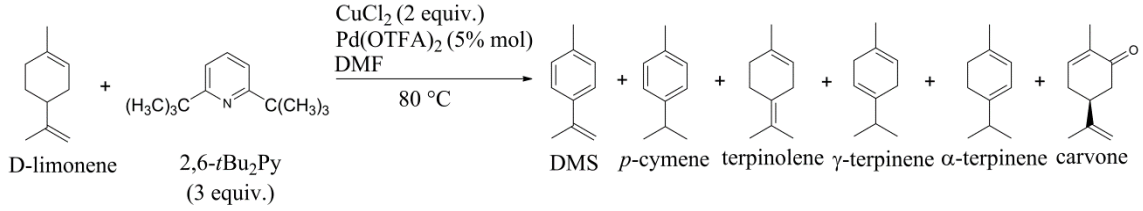

Scheme 25. D-limonene liquid phase palladium catalyzed dehydrogenation from Horrillo-Martinez's work.[290]

The endocyclic allylic C-H bond of D-limonene is believed to be activated by the palladium species, forming an π-allyl complex intermediate which suffers a β-hydride elimination, forming 1,3-cyclohexadiene and a palladium hydride. A second β-hydride elimination of the intermediate 1,3-cyclohexadiene forms the monomer dimethylstyrene.

Reductive elimination of the HPdX species produces HX and palladium (0), which is reoxidized to palladium (II) chloride by the oxidant copper chloride. The palladium (II) chloride then reacts with HX, as seen on Scheme 26.

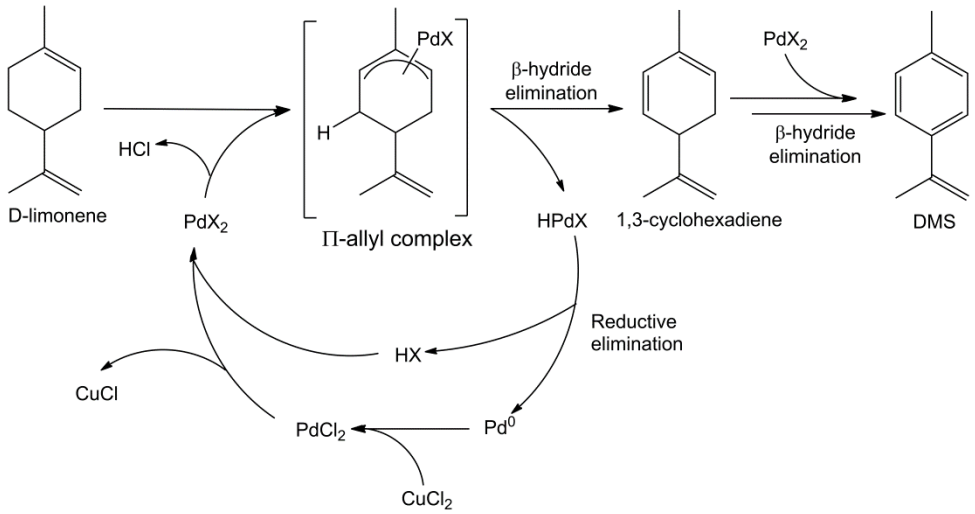

Scheme 26. Reaction of liquid-phase palladium catalyzed dehydrogenation of D-limonene into DMS

The use of a hindered base, referred to as an "additive" in the article, was to quench the palladium hydride species during the reaction in order to improve the selectivity toward DMS, however it can also react with the HCl formed at the end of the catalytic cycle forming a salt (Scheme 27).[290]

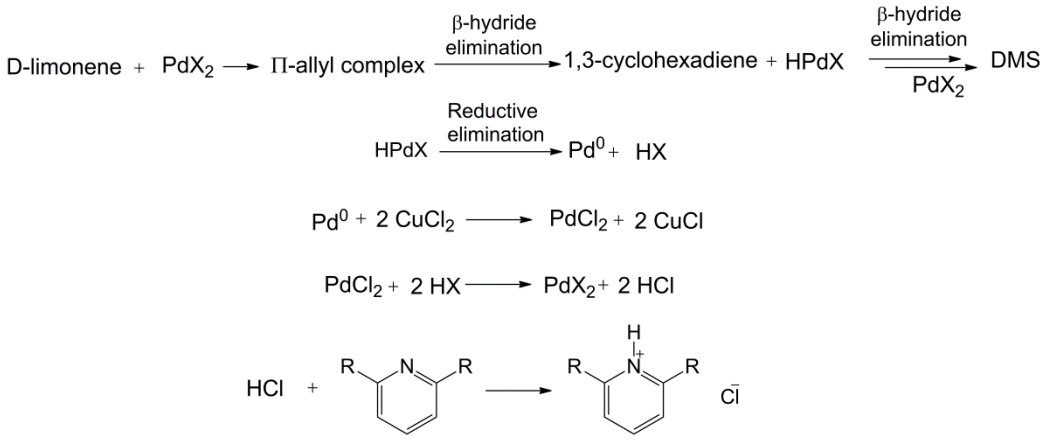

Scheme 27. Reactions involved in the liquid-phase palladium catalyzed dehydrogenation of D-limonene into DMS

3.1.1 Initial conditions

Initial studies investigated the procedure reported by Horrillo-Martinez's[290] to confirm the method reported therein; however, here different results were observed and only a 3% DMS conversion was obtained (Table 46, exp 1). Nevertheless, there were three procedural differences that could account for the disparity: (i) in Horrillo's work, limonene was dried over CaH_2, purified by vacuum transfer and stored under argon (although no final purity was specified). The limonene used here in these initial experiments was stated as 97% pure and was not further purified; (ii) there was a difference in the scale of the reactions which may have affected the experiment. Thus, while Horrillo's experiments used only 81 µl of limonene, here 0.5 ml of limonene was used routinely in each experiment. Errors may have occurred in the assay which could have adversely affected the yield when the quantity used was only 81 µl. Finally (iii) the yield and conversion calculations in the original article importantly do not specify if they are only for DMS or for the three main by-products (limonene, *p*-cymene and terpinolene). By comparison, in this work the total conversion of limonene to all by-products as well as only for DMS was calculated.

3.1.2 Effect of water

In order to obtain greater consistency with the prior work and in the belief that water may be decreasing the selectivity towards DMS conversion, modifications were made to the procedure and further precautions were taken to exclude water. First, the reaction was repeated using 4 Å molecular sieves and it was carried out under an argon atmosphere (Table 46, exp 2), as a result the dimethylstyrene yield increased from 3 to 20%. Then the experiment was performed under an argon atmosphere and with anhydrous solvent and anhydrous base, without using molecular sieves (because the liquids were already anhydrous) (Table 46, exp 3). However the DMS yield decreased by 50% (from 20% to 10%). Therefore the experiment was conducted using: dry reagents, dry solvent, 4 Å molecular sieves and under an argon atmosphere (Table 46, exp 4) and comparable results to those of Horrillo's work, indicated in section 3.1, were then obtained.

These precautions do not distinguish between the effects of excluding water and of oxygen. In order to test the hypothesis that water was limiting the reaction, the procedure was repeated using 5 drops of water as a base and no conversion was obtained, confirming that the presence of water affected the palladium-catalyzed

dehydrogenation of D-limonene (Table 46, exp 5). Finally in order to demonstrate that the base quenched potential palladium hydride species formed during the reaction, a control experiment was executed without the base (Table 46, exp 6). This showed that the total conversion was unchanged within experimental error but the dimethylstyrene conversion was only 11% without a base compared with 57% when it was used.

According to Horrillo-Martinez's work when the reaction takes place without the use of a base a 46% yield was obtained, but when tetrafluoroborate sterically hindered base was used the yield increased to 67%. Furthermore, when he used water as a base, the yield decreased to 40% indicating that water affects the palladium efficiency. When these results are compared to those obtained here (Table 46), it can be seen that both indicated that water inhibits the dehydrogenation of limonene. It has been reported that the effect of water on the Pd catalyst depends on the nature of the complex and the conditions reaction, e.g. when used in the reaction of styrene with iodobenzene[303] it promotes the catalyst activity while for the reduction of NOx by methane it deactivates the catalyst by promoting Pd-agglomeration.[304]

As previously described in Horrillo-Martinez's work (Scheme 25) another 4 monoterpenes were obtained as by-products. The calibration of the gas chromatograph (section 2.3.1) made it possible to identify these resulting from each experiment. In these experiments no carvone was generated as a by-product from the dehydrogenation of D-limonene with water present and it is unclear why this is the case.

Table 46. Effect of water on conversion and selectivity.[a]

Exp	Solvent	Base	Mol. Sieves	Ar	Total Conversion	DMS	*p*-cymene	*γ*-terpinene	*α*-terpinene	terpinolene
					%					
H[b]	DMF hydrous	2,6-tBu_2Py	No	No	74.8	65[c]	Not specified			
1	DMF hydrous	2,6-tBu_2Py	No	No	43.2	3	35	0.2	1	4
2	DMF hydrous	2,6-tBu_2Py	Yes	Yes	55	20	0	17	18	0
3	DMF anhydrous	2,6-tBu_2Py anhydrous	No	Yes	70	10	17	14	21	8
4	DMF anhydrous	2,6-tBu_2Py anhydrous	Yes	Yes	72	57	1	0.6	5	8
5	DMF anhydrous	Water	No	Yes	0	0	0	0	0	0
6	DMF anhydrous	None	Yes	Yes	39	11	0	0	2	26

[a] Reaction at 80 °C for 40 h using 5 mol.% of $Pd(OTFA)_2$ and $CuCl_2$
[b] Results from reference 290
[c] The author states that this figure is yield % but it is not clear if this includes other products.

3.1.3 Effect of base

In order to make the reaction (Table 46, exp 4) more economically viable from an industrial perspective and hence promote it as a useful industrial process, alternative bases were tested (Table 47) especially low cost hindered bases with similar chemical structures (Figure 30).

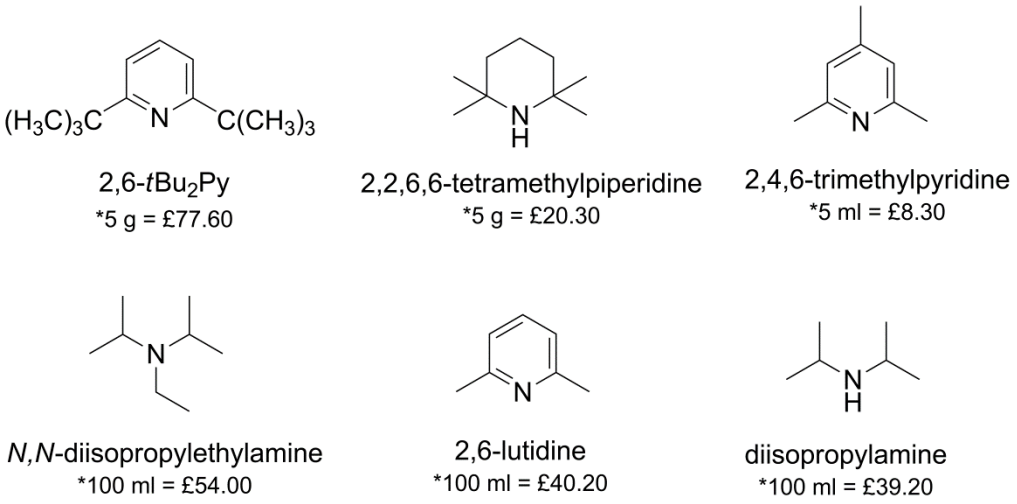

Figure 30. Other bases for the D-limonene palladium-catalyzed dehydrogenation.
*Prices based in Sigma-Aldrich UK on 14/01/14

The use of anhydrous 2,6-lutidine and 2,4,6-trimethylpyridine allowed the conversion of D-limonene to DMS but in low yield, and inhibited the production of other monoterpenes by-products (Table 47, exp 7 and 16). In subsequent experiments 2,6-lutidine was selected over 2,4,6-trimethylpyridine because of its lower cost and higher conversion to DMS during the reaction.

Table 47. Effect of base on conversion and selectivity.[a]

Exp	Base	Conversion %	DMS %	Selectivity
4[b]	2,6-*t*Bu$_2$Py anhydrous	72	57	Table 46
7	2,6-lutidine hydrous	0	0	0
8	2,6-lutidine anhydrous	1.4	1.4	just DMS
9	2,2,6,6-tetramethylpiperidine hydrous	0	0	0
10	2,2,6,6-tetramethylpiperidine anhydrous	0	0	0
11	*N',N'*-diisopropylethylamine hydrous	0	0	0
12	*N',N'*-diisopropylethylamine anhydrous	0	0	0
13	diisopropylamine hydrous	0	0	0
14	diisopropylamine anhydrous	0	0	0
15	2,4,6-trimethylpyridine hydrous	0	0	0
16	2,4,6-collidine anhydrous	1	1	just DMS

[a] Reaction under Argon at 80 °C for 40 h, using anhydrous DMF, 4A molecular sieves and 5 mol.% of Pd(OTFA)$_2$ and CuCl$_2$. [b] Reference experiment for comparison

3.1.4 Effect of temperature

In order to increase the conversion of D-limonene to DMS, the experiments which presented the highest conversions (Table 47, exp 4 and 8), were repeated at a temperature of 120 °C (Table 48). The experiment with 2,6-*t*Bu_2Py at 120 °C (Table 48, exp 17) produced an increase in the total conversion to 98% but with a dimethylstyrene selectivity of 0.01 compared to *p*-cymene and terpinolene having, as a result, a final DMS conversion of only 1%. In contrast the experiment with 2,6-lutidine at 120 °C increased the dimethylstyrene conversion from 1.4 to 18% (Table 48, exp 18), and in the absence of molecular sieves up to 22% (Table 48, exp 19). In this case, therefore the use of molecular sieves was not essential.

Table 48. Effect of temperature on conversion and selectivity.[a]

Exp	Base (anhydrous)	Temp /°C	Mol. Sieves	Total Conversion %	DMS	*p*-cymene	γ-terpinene	α-terpinene	terpinolene
4[a,b]	2,6-*t*Bu_2Py	80	Yes	72	57	1	0.6	5	8
17	2,6-*t*Bu_2Py	120	Yes	98	1	36	2	25	34
8[a,b]	2,6-lutidine	80	Yes	1.4	1.4	just DMS			
18	2,6-lutidine	120	Yes	18	18	just DMS			
19	2,6-lutidine	120	No	22	22	just DMS			

[a] Reaction under Argon for 40 h, using anhydrous DMF and 5 mol.% of $Pd(OTFA)_2$ and $CuCl_2$.
[b] Reference experiment for comparison

3.1.5 Effect of reactant quantities

The procedure using 2,6-lutidine as base (Table 49, exp 8) was then repeated three times using different amounts of reactants each time. In the first experiment the amount of catalyst was increased to 10 mol.% which completely inhibited the reaction (Table 49, entry 20), consistent with Horrillo-Martinez work. In the second attempt, twice the amount of 2,6-lutidine (6 equivalents) significantly reduced the DMS conversion (Table 49, exp 21). Finally the experiment was repeated in the absence of copper(II) chloride at 120 °C which had the same effect as the increase in the amount of catalyst (Table 49, exp 22). In order to ensure that the inhibition of DMS formation was due to the lack of oxidant and not the change of base, the reaction was repeated using the original base suggested in the source article (2,6-*t*Bu_2Py) and again no DMS was formed (Table 49, entry 23).

Table 49. Effect in the amount of reactants.[a]

Exp	Oxidant	Catalyst $Pd(OTFA)_2$ mol. %	Base (anhydrous)	T /°C	Conversion %	DMS %	Selectivity
8[a,b]	$CuCl_2$	5	2,6-lutidine	80	1.4	1.4	just DMS
20	$CuCl_2$	10	2,6-lutidine	80	0	0	0
21	$CuCl_2$	5	2,6-lutidine (double)	80	~ 0	traces	just DMS
22	No	5	2,6-lutidine	120	0	0	0
23	No	5	2,6-*t*Bu_2Py	120	0	0	0

[a] Reaction under Argon for 40 h, using anhydrous DMF and 4A molecules sieves.
[b] Reference experiment for comparison

3.1.6 Effect of solvent

The original solvent (DMF) is known to present health hazards and to be a potential water pollutant as indicated by the World Health Organization.[305] This could be seen as an impediment to commercialisation of the process, this solvent was replaced by solvents which improve laboratory safety, reduce impact on human health and eliminate contamination of the environment but importantly improve the industrial viability of this process.

The GlaxoSmithKline (GSK) solvent selection guide and assessment information, ranks solvents according to their toxicity, health and safety issues. In order to improve solvent selection by reducing the environmental footprint of the process, the alternative solvents chosen were acetonitrile, dimethylsulfoxide, cyclopentyl methyl ether (CPME), 2-methyltetrahydrofuran and heptane.

When acetonitrile and heptane were used, the reaction was inhibited due to the non-polar nature of heptane which is unable to support the change of ionic strength during the reaction since $CuCl_2$ is reduced to CuCl and chloride. Secondly, the low boiling point of acetonitrile only allowed to work at a maximum temperature of 70 °C and no reaction occurred. As 2-methyl THF also boils at arounds 70 °C and terpenes were obtained at the end of the reaction, it is suggested that acetonitrile also affects the catalytic activity of palladium via complexation.

When CPME was used, only *ρ*-cymene was observed, whereas 2-methyl THF induced the conversion of α-terpinene and dimethylsulfoxide encouraged the conversion into γ-terpinene (Table 50). As seen in Table 48, the absence of molecular sieves increased the conversion of D-limonene, therefore experiments with the less toxic solvents (CPME and 2-methyl THF) were repeated with no molecular sieves. The results showed that the total conversion using CPME improved by 54% while that using 2-methyl THF increased by 33% (Table 50, exp 30 and 32). As the use of different

solvents did not produce higher conversions or improve the production of DMS, further experiments were continued with anhydrous dimethylformamide.

It is worth highlighting that even when DMS was not obtained from the experiments outlined in Table 50, they nevertheless provide useful alternative routes for the individual production of γ-terpinene, *ρ*-cymene and α-terpinene.

Table 50. Effects of solvent.[a]

Exp	Solvent	T /°C	Mol. Sieves	Conversion %	Selectivity
18[a,b]	DMF anhydrous	120	Yes	18	just DMS
24	MeCN hydrous	70	Yes	0	0
25	MeCN anhydrous	70	Yes	0	0
26	DMSO hydrous	120	Yes	3	just γ-terpinene
27	DMSO anhydrous	120	Yes	2	just γ-terpinene
28	Heptane anhydrous	90	Yes	0	0
29	Cyclopentyl methyl ether	90	Yes	34	just *ρ*-cymene
30	Cyclopentyl methyl ether	90	No	30	just *ρ*-cymene
31	2-methyl THF anhydrous	70	Yes	3	α-terpinene 2.4% terpinolene 0.6%
32	2-methyl THF anhydrous	70	No	55	α-terpinene 30% *ρ*-cymene 25%

[a] Reaction under Argon for 40 h, using 5 mol. % of $Pd(OTFA)_2$, $CuCl_2$ and 2,6-lutidine.
[b] Reference experiment for comparison

3.1.7 Effect of different palladium complexes

Other palladium complexes were then explored with the intention of making the process more commercially viable (Table 51). The use of $PdCl_2$ inhibited the reaction while palladium acetate showed a conversion of 2% into DMS. In order to increase the conversion to DMS, palladium acetate was used in the reaction at 120 °C and in the absence of molecular sieves, as previous experiments had shown that these conditions encourage the conversion and selectivity of converting D-limonene into DMS. The DMS conversion increased from 2% to 19%. The amount of catalyst was also altered. Reducing it from 5 mol% to 2 mol% decreased the conversion from 19% to 5% and produced γ-terpinene as a by-product. On the other hand, an increase from 5 mol% to 10 mol% of catalyst inhibited the reaction (Table 51, exp 36 and 35). Finally, since increasing the temperature from 80 °C to 120 °C had previously increased the conversion to DMS (Table 48) the reaction with 5 mol% palladium(II) acetate (Table 51, exp 35), was repeated at 150 °C but the conversion was decreased from 19% to 15%.

Table 51. Effect of catalyst.[a]

Exp	Catalyst	T /°C	Mol. Sieves	Conversion %	DMS %	Selectivity (DMS: cymene + terpinolene)
18[a,b]	5 mol. % - $Pd(OTFA)_2$	120	Yes	18	18	just DMS
33	5 mol. % - $PdCl_2$	80	Yes	0	0	0
34	5 mol. % - $Pd(OAc)_2$	80	Yes	2	2	just DMS
35	5 mol. % - $Pd(OAc)_2$	120	No	19	19	just DMS
36	10 mol. % - $Pd(OAc)_2$	120	No	0	0	0
37	2 mol. % - $Pd(OAc)_2$	120	No	6	5	DMS / γ-terpinene
38	5 mol. % - $Pd(OAc)_2$	150	No	15	15	just DMS

[a] Reaction under Argon for 40 h, using anhydrous DMF, $CuCl_2$ and 2,6-lutidine
[b] Reference experiment for comparison

In summary, the improved reaction for the synthesis of DMS from D-limonene was obtained using 5 mol% palladium(II) acetate as catalyst, 2 equivalents of $CuCl_2$ as oxidant, 1 equivalent of D-limonene, 3 equivalents of 2,6-lutidine as base and anhydrous DMF as solvent under an argon atmosphere and at a temperature of 120 °C (Table 51, exp 35).

3.1.8 Study of reaction profile

The progression of the reaction was studied over a 40 hours period. Samples were taken every hour in order to monitor the conversion by gas chromatography (Table 51, exp 35) (triplicate reactions). The average data for the triplicate experiments are shown in Figure 31, which indicated that the reaction stopped after 4 h giving an average conversion of 19%.

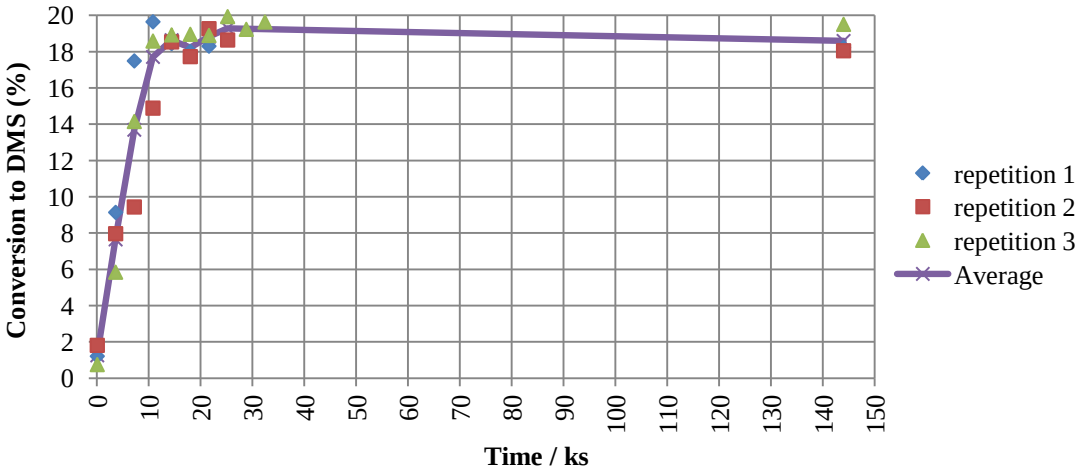

Figure 31. Reaction profile of the conversion of DMS from D-limonene.

The reaction may have stopped due to consumption of one of the reactants. To clarify this, after the 4 h, 3 more equivalents of oxidant $CuCl_2$ were added. As seen from

the results in Figure 32, the addition of oxidant did not improve the conversion to DMS (green line) and the reaction remained at a 20 % conversion level for the next 4 hours. After the total of 8 hours, 1 ml (3 equivalents) of base were added (red line) and immediately the conversion increased from 20 to 28%.

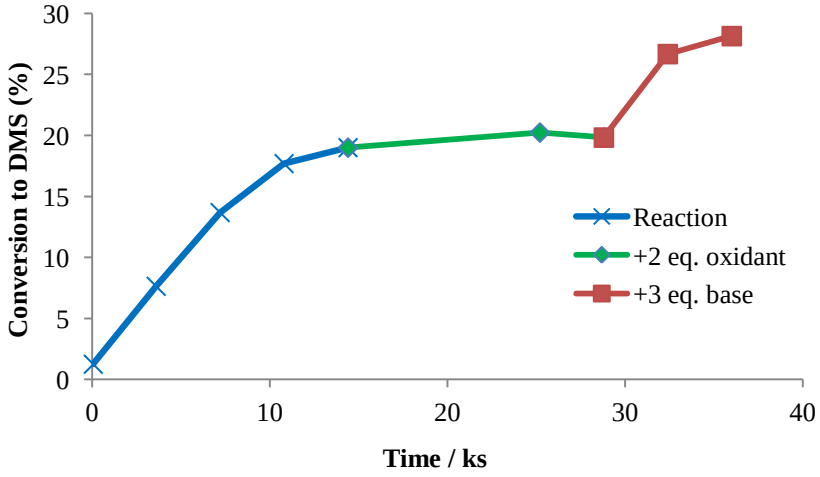

Figure 32. Reaction profile using double the amount of oxidant and base

Since the experiment and results illustrated in Figure 32 showed that the base was consumed after 4 h, the next reaction was conducted with excess base. Therefore 3 ml of 2,6-lutidine (9 equivalents) was added at the start of the reaction. After 2 hours the reaction had reached 24% conversion into DMS and then progressed no further on the next 2 hours (Figure 33, blue line). This implied that reactant was consumed and so, more catalyst was added (5 mol%) but no change in the conversion was observed (Figure 33, green line). In a further attempt to improve the conversion, 2 more equivalents of $CuCl_2$ were added and the conversion increased to 38 % (Figure 33, red line).

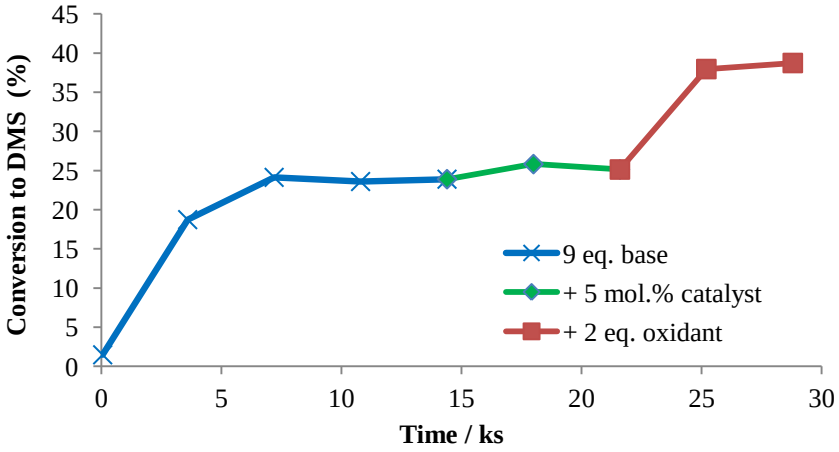

Figure 33. Reaction profile using triple amount of base and double the amount of catalyst and oxidant.

The addition of extra catalyst did not improve the DMS conversion, indicating it was not a limiting reactant but clearly the oxidant had some effect (Figure 33). Therfore, the experiment was repeated using 9 equivalents of 2,6-lutidine, 5 mol% of $Pd(OAc)_2$ and 4 equivalents of $CuCl_2$. The DMS conversion reached 40% after 5 hours (Figure 34, blue line). In an attempt to improve this result further, the reaction was repeated but using double the amount of catalyst (Figure 34, red line). The reaction reached almost the same percentage conversion (38%) but more rapidly. In the belief that oxidant was being consumed as occurred in the experiment and results illustrated in Figure 33, the reaction was repeated using triple the amount of oxidant (Figure 34, green line) nevertheless the conversion did not increase (38%) and the only difference was that the reaction time was decreased.

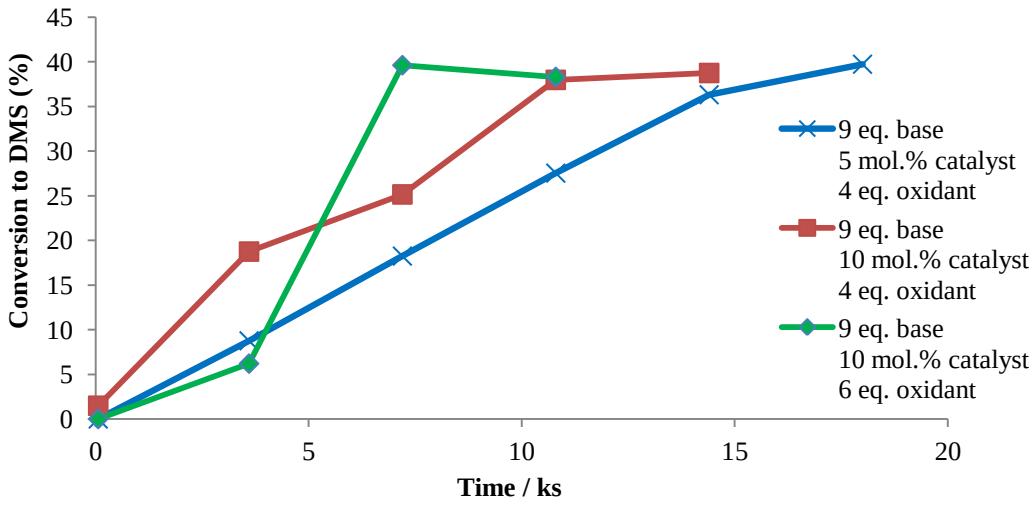

Figure 34. Reaction profile while changing the amounts of base, catalyst and oxidant.

In the previous experiments where the effect of different amounts of reactants was studied (Table 49) it was observed that an increase in catalyst or base inhibited the conversion of D-limonene to any product. However, by studying the reaction progression it was concluded that substances like the catalyst, base and oxidant became exhausted after about four hours and therefore more of the limiting reagent should be added. This may seem to be a contradiction but it should be noted that the reactions conducted to study kinetics and the reactions to determine the amounts needed were made under different conditions.

The first difference is the reaction temperature. In the data in Table 49, reactions were performed at 80 °C while all reaction profile study was performed at 120 °C. The different results can be explained in terms of the activation energy needed for the reaction. As explained in Scheme 25 several reactions take place and at higher

temperatures those with lower activation energies tend to be rate limiting whereas at low temperatures those with higher activation energies tend to be slower and control the rate. This could be corroborated with experiment 38 (Table 51) which was carried out at 150 °C and gave almost the same DMS conversion as the reaction at 120 °C, indicating that 120 °C is necessary for the D-limonene conversion reaction.

The second difference is the reaction time. The reaction profile study was completed after 4 hours while the original article indicated the reaction required 40 hours. It may be that the base or catalyst added was not the limiting reactant and an excess inhibited it by forming a complex with another substance present in the reaction. Another important difference is the presence of molecular sieves in the study of the effects of reactant quantities and its absence in the kinetics study. Molecular sieves were proven to affect the conversion yields given in Table 51, and therefore it can be assumed that they also affected the results given in Table 49. It could be argued that the surface area of the molecular sieves affected the performance of the palladium catalyst[306] or the copper chloride as oxidant. Finally, during the studies, different palladium salts were used as catalysts and it could be possible that the reaction mechanisms or rate limiting steps are not the same or maybe the ligands affect the base or oxidant.

In summary, for the synthesis of DMS from D-limonene the best conditions among those investigated for the reaction were: 1 equivalent of D-limonene, 9 equivalents of 2,6-lutidine, 10 mol% of $Pd(OAc)_2$ and 4 equivalents of $CuCl_2$ in 15 ml of anhydrous DMF under argon at 120 °C for 4 h (Scheme 28).

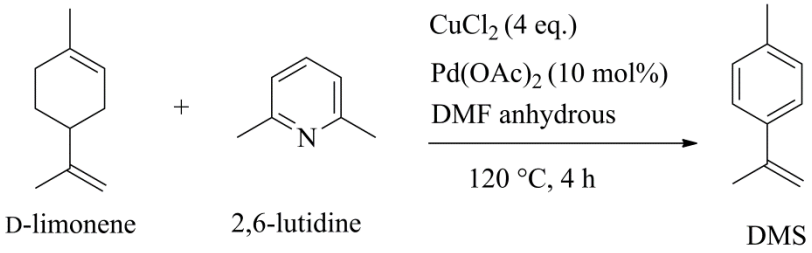

Scheme 28. Improved reaction for D-limonene dehydrogenation

These new conditions encourage the conversion of D-limonene into DMS in the 40% yield. The difference in chemical structure between the original base (2,6-*t*Bu_2Py) and the new base (2,6-lutidine) is the substitution of the two tert-butyl groups for two methyl groups, respectively. It can be suggested that the presence of these two tert-butyl groups produce steric hindrance allowing the formation of several terpenes, moreover

they might cause an effect in the palladium hydride species making the reaction steps slower.

3.2 Poly-dimethylstyrene

The characterization of the viscosity and molecular weight of the soluble part of the polymer obtained from DMS are described in this section.

When dimethylstyrene was purified by vacuum distillation from its synthesis from D-limonene (section 3.1) and polymerized at -78 °C under nitrogen atmosphere using boron trifluoride etherate as catalyst in a toluene medium, a white polymer was obtained and a 99% polymerization conversion was achieved (Scheme 29).[307]

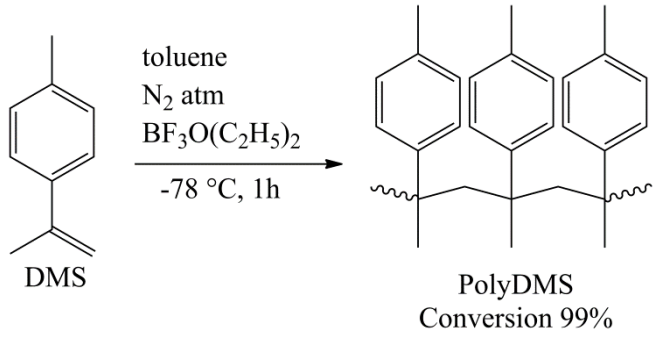

Scheme 29. Polymerization of dimethylstyrene

The viscosity of the poly-dimethylstyrene obtained was measured at five different concentrations in toluene (Section 2.3.2). In addition a commercial polystyrene of known molecular weight (Mn = $1.5x10^3$) and poly-α-methylstyrene synthesised by the same polymerization method were also measured for comparison purposes. The kinematic viscosity (υ) was calculated (equation 1) by multiplying the constant (C) obtained for the calibration certificate by the flow time (*t* in seconds) obtained in the measures.

$$\upsilon = Ct \quad (1)$$

In the case of pure toluene the reported dynamic viscosity[308] (η_{dyn}) at 25 °C is 0.547 mPas and density[309] (ρ) is 862 g/ml. Therefore and according to equation 2 the kinematic viscosity is 0.893 mm^2/s. This result gives an error of 1% which is close to the 0.6% error previously obtained from the calibration with water. (Section 2.3.3)

$$\eta_{dyn} = \upsilon\rho \quad (2)$$

In Figure 35 are presented the kinematic viscosity data obtained for each polymer at different concentrations. As expected, the polystyrene presents a high gradient due to its high molecular weight of 192,000 g/mol. It was observed that the poly-α-methylstyrene presented similar behaviour to the polystyrene, indicating that a polymer was produced with high molecular weight.

During the preparation of the solutions it was observed that styrene and poly-αMS were totally soluble in toluene whereas poly-DMS did not fully dissolve. Only 34% of the poly-DMS from D-limonene and 31% of the polymer obtained from pure DMS were soluble. This can be explained by the crystalline structure produced by the high syndiotactic content in the polymer structure.[260]

A small gradient in the kinematic viscosities on the poly-dimethylstyrene solutions are observed as only the low molecular weight molecules and waxes produced during the polymerization process were able to dissolve in the toluene.

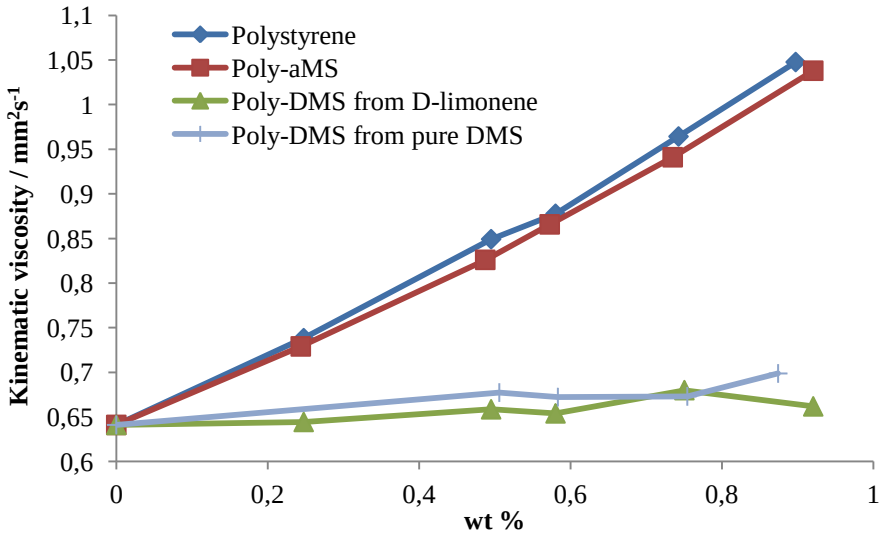

Figure 35. Kinematic viscosity of polymers at different concentrations on toluene solutions

Subsequently, an attempt to calculate the molecular weight of the soluble part of the poly-dimethylstyrene though the measurement of viscosity was made. The Mark-Houwink equation (3) correlates the intrinsic viscosity [η_{int}] of a polymer with the viscosity average molecular weight (Mv) by using constants (K and a) which are dependent on the solvent, polymer and temperature.

$$[\eta_{int}] = K{M_v}^a \quad (3)$$

In order to use this equation the intrinsic viscosity for each polymer was calculated from the measurements made. From the times measured for each concentration the

specific viscosity (η_{sp}) was calculated from equation 4, where t_0 is the time measured from the pure solvent used to dissolve the polymer, in this case toluene, and t the measured time of the samples with the respective polymer.

$$\frac{t-t_0}{t_0} = \eta_{sp} \quad (4)$$

Subsequently the reduced viscosity (η_{red}) was obtained by dividing the specific viscosity (η_{sp}) by the respective concentration (c) of the sample used (equation 5). The units used for these equations were seconds and gml^{-1}.

$$\frac{\eta_{sp}}{c} = \eta_{red} \quad (5)$$

Once the reduced viscosity (η_{red}) was calculated at different concentrations for each polymer, an equation fitting the data points was found. From this equation the constant term, being the intercept with the y axis, was the intrinsic viscosity [η_{int}].

In Table 52 are shown the intrinsic viscosities obtained for each polymer. The polystyrene with known molecular weight was used as a reference polymer and to ensure that the correct constants for the Mark-Houwink equation were being used as it was found that in literature many mistakes in units and decimals for the K constant had been reproduced, giving each reference a different value. The values used for this calculations are K = 0.011 ml/g[310] and a = 0.72.[311] Using these values for the constants the calculated M_v for the known polystyrene of 192,000 g/mol was of 184,949 g/mol giving an error of only 1%.

As expected the poly-α-methylstyrene presents a high molecular weight of 162,070 g/mol while the soluble parts of the poly-DMS obtained from laboratory degree DMS was of 19,700 g/mol and the one produced from D-limonene of 3,800 g/mol.

Table 52. Calculated intrinsic viscosity and molecular weight of the polymers obtained

Polymer	**Intrinsic viscosity [η_{int}] /ml g^{-1}**	**M_v**
Polystyrene	68.2	185000
Poly-α-MS	62.0	162000
Soluble part of Poly-DMS from D-limonene	4.1	3800
Soluble part of Poly-DMS from pure DMS	13.6	19700

3.3 Addition of clay

A study of the monomer‘s natural interaction with the nano phase was conducted as explained in section 2.5. This was made in order to find the proper conditions for the

production of a nano-polymer composite. The results of this study are presented and explained in this chapter.

3.3.1 XRD study of monomer interactions with montmorillonite clay

A preliminary XRD study was made in order to determine if the monomer intercalates within the layers of the montmorillonite clay.

X-ray diffraction traces of pure DMS (monomer) and toluene (solvent) with the clay, are shown in Figure 36. From the trace for the pure clay (blue line) a broad peak at 7.1° was observed from which the basal plane spacing of the clay was calculated to be 12.46 Å (equations explained in Appendix 6). When this result was compared to those with clay with toluene (Figure 36-a) and clay with DMS (Figure 36-b) it was observed that the peak did not shift, indicating they are not able to enter and interact between the layers of the clay and separate them.

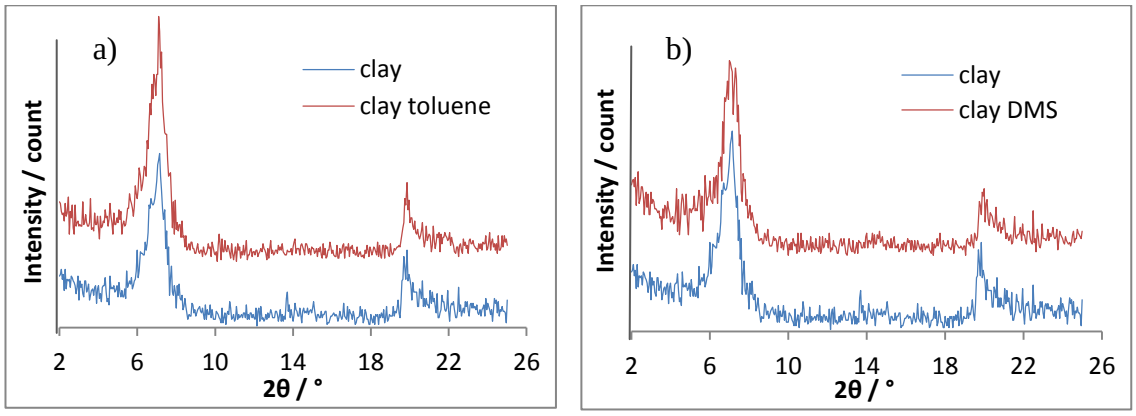

Figure 36. X-ray diffraction of a) clay + toluene and b) clay + dimethylstyrene

Other monomers with similar structure to DMS (Figure 37) but with the methyl groups in different positions, and its precursor D-limonene, were tested with the clay in order to determine that the nature of the molecule and not the structure was the cause for the DMS not to intercalate in the clay.

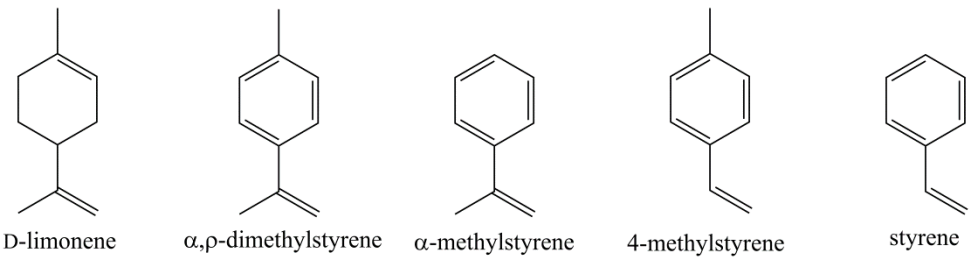

Figure 37. Structures similar to DMS

In Figure 38 are presented the XRD spectra of the interaction of the clay with a) D-limonene, b) α-methystyrene, c) 4-methylstyrene and d) styrene. It was observed that from all the experiments none of the substances was able to intercalate in the clay irrespective of the position of the methyl groups. This indicated that the hydrophobic and non-polar nature of the monomers prevented their intercalation in the clay and therefore it can be deduced that they presented a small thermodynamic potential for their diffusion into the interlamellar spacing of the clay.

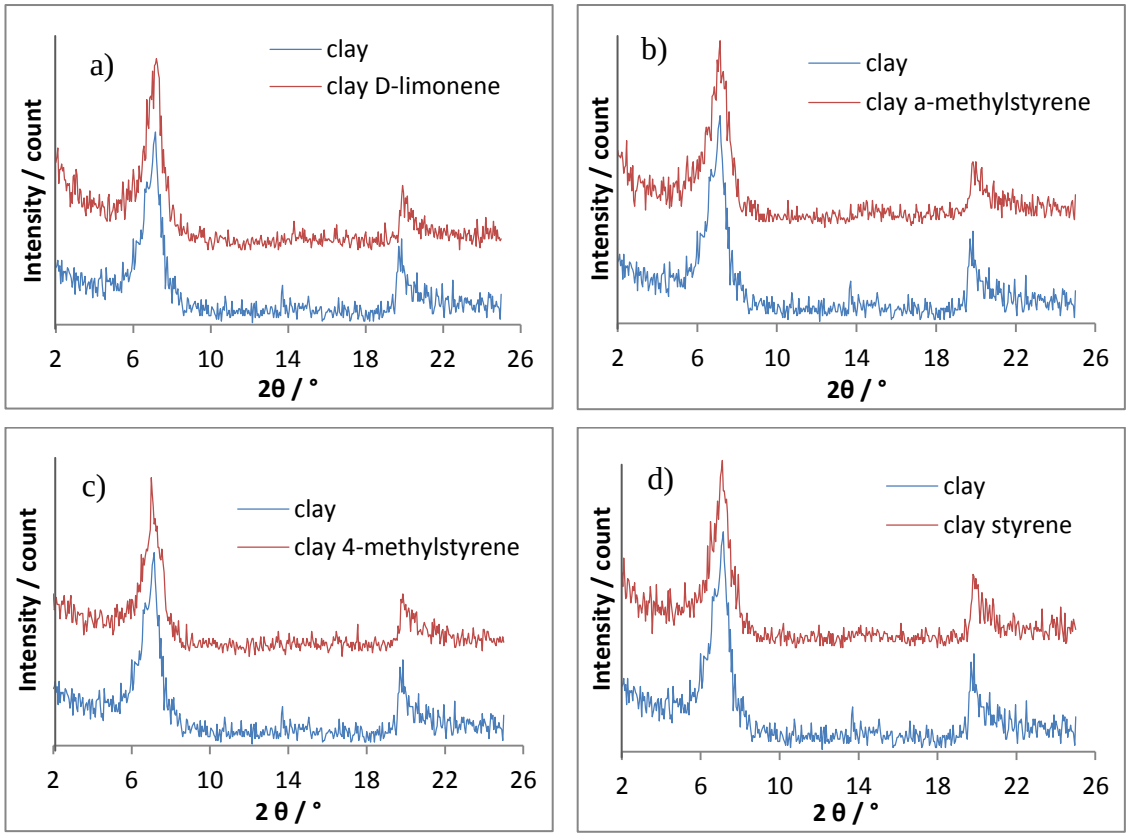

Figure 38. XRD results from the interaction of clay with a) D-limonene, b) α-methylstyrene, c) 4-methylstyrene and d) styrene

3.3.2 XRD study of monomers interaction with modified clay with L-lysine

As α,ρ-dimethylstyrene was not able to intercalate in the montmorollinite clay, the clay was chemical modified with L-lysine in order to increase the interlamellar space and to induce an interaction with the DMS. This chemical modification to the clay had been previously studied by Cuadros[312], Kitadai[313] and Parbhakar[314] confirming a strong bond between the $-NH_3^+$ of the L-lysine and the basal O atoms of the clay, presenting a vertical orientation of the L-lysine over the clay with the side-chain amino group pointing towards the surface (Figure 39).

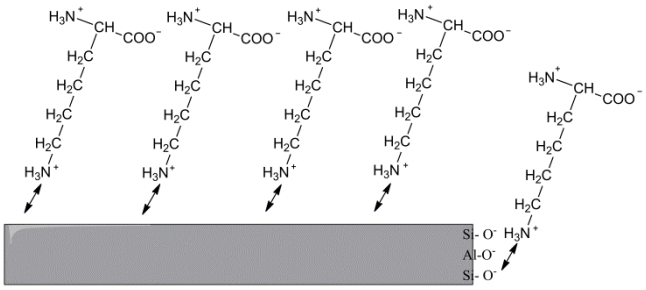

$$Lys_{sol}{}^{\pm} + (Na^{+}, H_2O)_{clay} \rightarrow (Lys^{+}, Na^{+}, OH^{-}) \rightarrow (Lys^{+})_{clay} + Na_{sol}{}^{+} + OH_{sol}{}^{-}$$

Figure 39. Schematic diagram of L-lysine interaction with the clay and the overall exchange reaction.[313,314]

The XRD trace of the L-lysine and clay (Figure 40-a) shows that the interlamellar space between the clay layers increased from 12.46 Å to 13.50 Å, corroborating the entrance of the L-lysine molecules between the clay layers.

Copolymers of poly-lysine and polystyrene had been previously reported[315,316] indicating that an interaction between the amino acid and the monomer can take place. From the results, in Figure 40, it was observed that no interaction between the clay modified with L-lysine and the monomers took place as no shift in the peaks was presented; this difference between the literature and experimental results could be explained by the different methods and difference in conditions in which the L-lysine was interacted with the respective monomers.

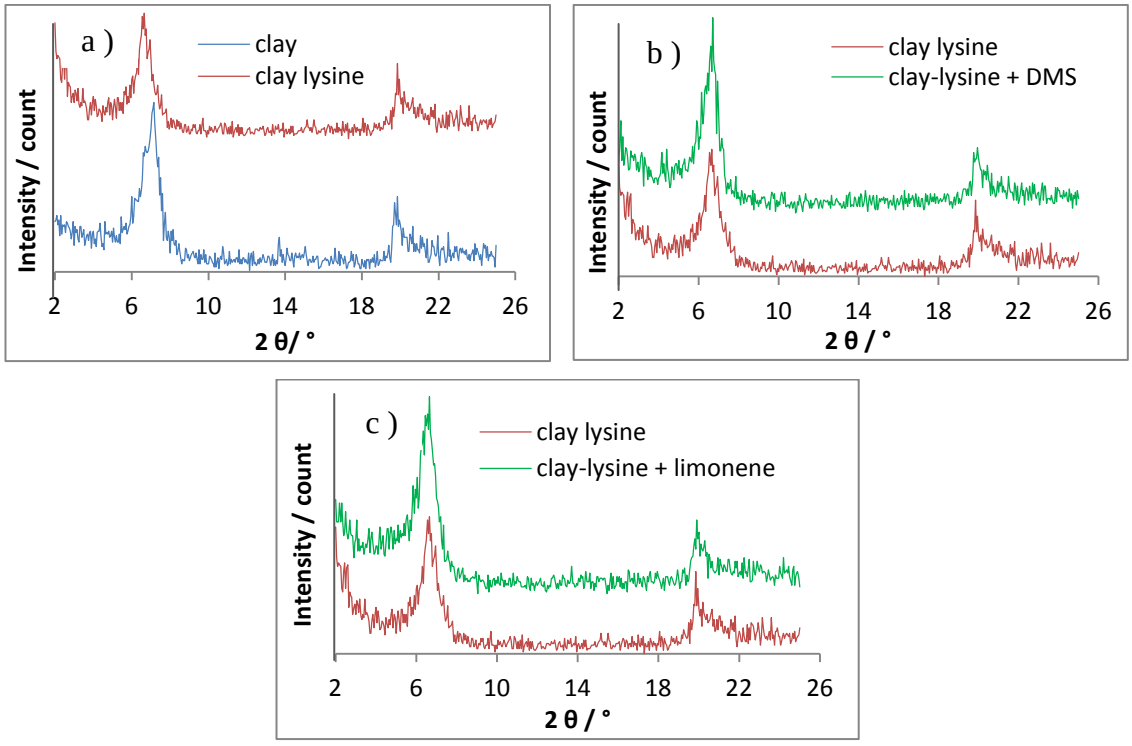

Figure 40. XRD spectrum of a) clay + L-lysine and clay-lysine with b) DMS and c) D-limonene

3.3.3 XRD study of monomer interactions with organoclay (Cloisite 10A)

As a last attempt to interact the clay with the monomers, an organoclay was used. According to the literature several organoclays are compatible with styrene[317-321], which is similar to the DMS structure and should therefore, behave in a similar way. These studies indicate that organoclays modified with a styryl group had the highest compatibility with styrene, forming exfoliated polymer nano-composites. The chosen organoclay is a montmorillonite clay modified with 2MBHT (dimethyl-benzyl-hydrogenated tallow, quaternary ammonium), where the hydrogenated tallow is a mixture of ~ 65% of C18, ~ 30% of C16 and ~ 5% of C14 and chloride as anion, known in the market as Cloisite 10A from Rockwood Additives Ltd, Europe. It has been reported that this organoclay shows the highest compatibility with styrene when compared to other organoclays.[317-319]

In Figure 41-A it can be observed that the organoclay (Cloisite 10A) peak in the XRD trace had shifted from 7.1° of the pure clay to 4.85°, indicating that the basal plane spacing of the organoclay compared to that of the pure clay has separated from 12.46 to 18.22 Å. In Figure 41-B are presented the XRD traces for the interaction between the organoclay and the monomers used in this part of the experimentation. It can be observed that both monomers shifted the main organoclay peak; in case of DMS it shifts from 4.85° to 4.795° which represents a small increase in the basal spacing to 18.43 Å while for D-limonene two peaks can be observed, one at the same place as the organoclay and other at 2.7°. This suggests that part of the organoclay had interacted with the D-limonene separating the clay layers at 32.7 Å while others layers did not interact.

In order to further understand this behaviour, 4 methylstyrene and styrene were mixed with the organoclay and their interaction was analysed. From the results it was observed that 4MS interacted in the same way as D-limonene (Figure 41-C) while styrene had the same behaviour as DMS (Figure 41-D). In the XRD traces of this last comparison (Figure 41-D), a peak at 7.1° can be observed which suggests that some layers of the organoclay had return to the pure clay basal plane spacing of 12.46 Å. This behaviour is also observed in Figure 1 from Timochenco's work[317] but no explanation is given, therefore we suggest that this could indicate that all quaternary ammonium salt which was in the organoclay was used for the interaction between the monomers and clay layers and during the interaction some salt was extracted from a small percentage

of the layers which therefore retracted to the natural basal space of the montmorillonite clay.

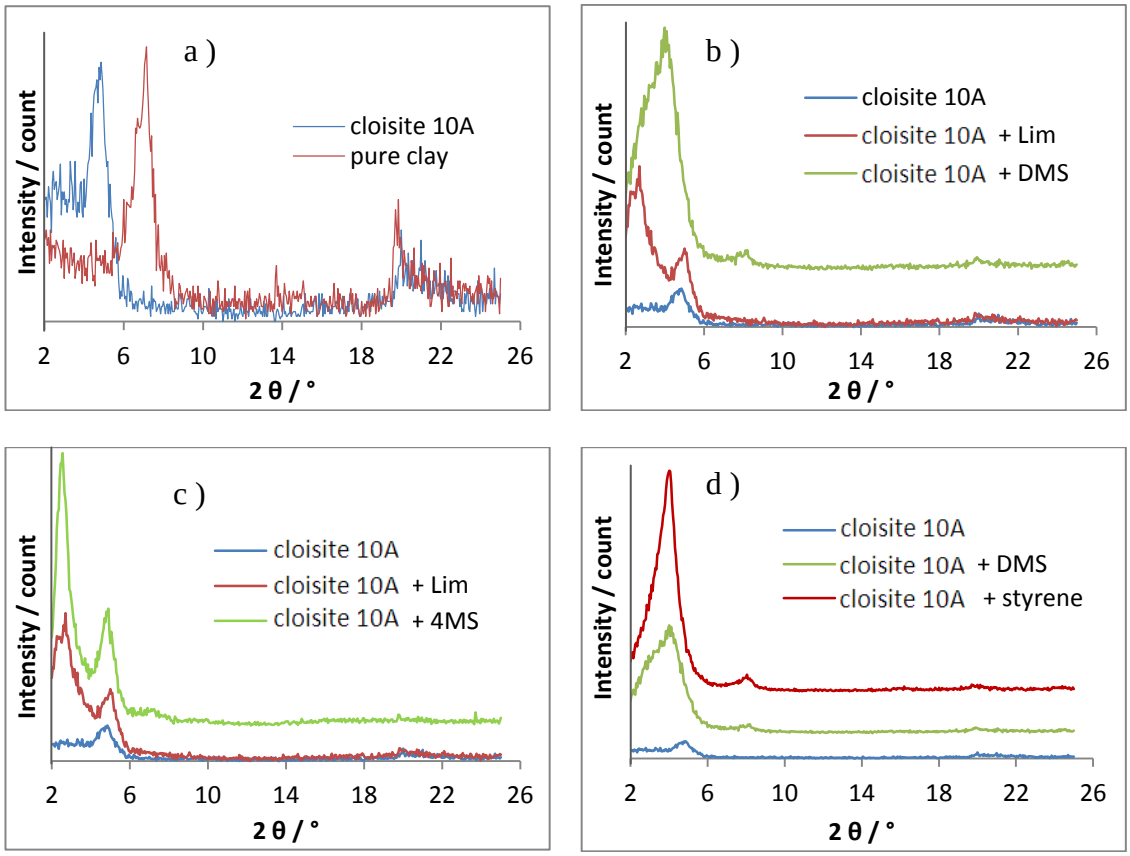

Figure 41. XRD spectrum of organoclay (Cloisite 10A) interaction with monomers. a) organoclay, b) with DMS and D-limonene, c) with D-limonene and 4-methylstyrene and d) with DMS and styrene.

3.4 Summary of results

In the first part of this chapter, the results from the conversion of D-limonene into polydimethylstyrene were presented and discussed in order to understand and to optimize the reaction. As explained, a conversion of almost 40% from D-limonene to the monomer dymethylstyrene (DMS) was accomplished. In Table 53 are presented the most relevant results from each step during the improvement of the synthesis reaction for DMS.

Subsequently the monomer was purified and polymerized at -78 °C giving a polymerization conversion of 99% and producing a white polymer. To this polymer an attempt to measure its viscosity was made. During the procedure it was observed that only 35% of the polymer was soluble which indicated the presence of a crosslinked polymer and that only the low molecular weight fraction and waxes produced during the

polymerization process were dissolved. From the soluble part an intrinsic viscosity [η_{int}] of 4.1 ml g^{-1} was obtained and as expected a low molecular weight of 3800 g/mol was calculated by use of the Mark- Houwink equation.

Finally a study between the interaction of clay, a natural reinforcement, with the monomer and precursor indicated that pure montmorillonite clay was not able to exfoliate and therefore chemical modification to the clay was made. The modification of clay with L-lysine showed a good interaction between them but not with the monomers. As a further attempt the organoclay known in the market as Cloisitie 10A was used. This montmorillonite clay modified with a dimethyl-benzyl-hydrogenated tallow, quaternary ammonium (2MBHT) did interact with the monomers, in case of D-limonene the basal space layers of the organoclay separated from 18.22 Å to 32.7 Å while with DMS to 18.43 Å. These results indicate that this organoclay can be used during the polymerization process to create a well integrated nano-polymer composite which should present improved mechanical properties than the poly-DMS.

Table 53. Summary of results from citrus waste experiments for synthesis of monomer

Purpose	**Base**	**T / °C**	**Catalyst**	**Oxidant**	**Time / h**	**DMS conversion %**
Addition Mol. Sieves and Argon	2,6-tBu_2Py	80	$Pd(OTFA)_2$	$CuCl_2$	40	56.7
Modification of base	2,6 lutidine	80	$Pd(OTFA)_2$	$CuCl_2$	40	1.4
	2,4,6-collidine	80	$Pd(OTFA)_2$	$CuCl_2$	40	1
Modification of temperature	2,6 lutidine	120	$Pd(OTFA)_2$	$CuCl_2$	40	18.2
Modification of catalyst	2,6 lutidine	120	$Pd(OAc)_2$	$CuCl_2$	40	18.6
Modification of reactants and time	2,6 lutidine x3	120	$Pd(OAc)_2$ x 2	$CuCl_2$ x 2	4	38

4. Results and Discussion of Potato Waste Experiments.

In this chapter the results for the polymerization of potato waste derivatives are presented. The polymers generated from potato waste derivatives and analogues were studied using several techniques in order to characterise the structure of the polymers obtained. The polymers obtained were selectively analysed by FT-IR, ^{1}H NMR and DSC analysis. Subsequently, studies on caffeic acid and chlorogenic acid monomers interactions with montmorillonite clays were made with the intention of establishing whether it was possible to exfoliate the clay into the polymer matrix in order to improve the mechanical properties.

4.1 Enzymatic polymerization in pH 7 phosphate solution with methanol.

The solution polymerization of the monomers (phenol, caffeic acid and chlorogenic acid) was based on the enzymatic oxidative polymerization of phenol using horseradish peroxide as catalyst reported on Oguchi's work.[294] He focused on polyphenol solubility, composition and molecular weight and how they were affected by modifying the reaction conditions. During experimentation, the polymerization reaction was started by the addition of hydrogen peroxide causing the formation and precipitation of a fine powder which was collected by centrifugation. Oguchi's results indicated that the polyphenol obtained through enzymatic polymerization consisted of two different unit structures: phenylenene and oxyphenylene (Scheme 30).

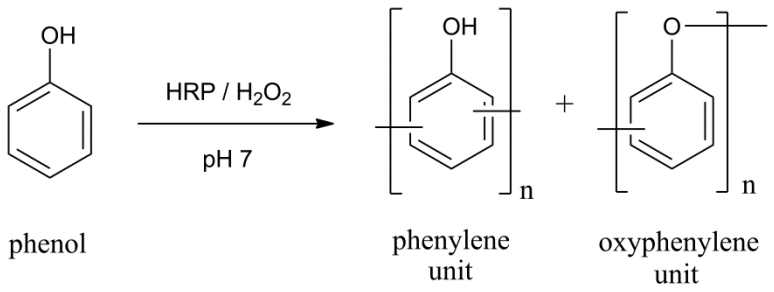

Scheme 30. Polymer structure of polyphenol.
*The polymer structure reported is presented as indicated.[294]

In the reported procedure, the polyphenol was obtained using 10.6 mmol of H_2O_2 and 220 U of enzyme in methanol and phosphate buffer (Pi) (1:1 by volume) after 6h. An 80% conversion was reported with a 48/52 unit ratio of phenylene/oxyphenylene polymers. The polyphenol obtained was analysed by FT-IR, SEC, ^{1}H NMR, TG and DSC analysis.

The results obtained in this work, following the same reaction conditions and analysed by similar techniques, were consistent with these results as outlined below.

4.1.1 Phenol

The reaction using phenol as monomer (methanol and phosphate buffer at pH 7, 1:1 vol) yielded 70% of polyphenol (Table 54, exp 1, p.146). The FT-IR spectra of phenol and the resulting polyphenol are shown in Figure 42. The broad peak at 3220 cm^{-1} is due to vibrations of the O-H linkage of the phenolic group and the peaks at 1590 and 1485 cm^{-1} indicate the aromatic C=C bonds. The peak at 1205 cm^{-1} can be ascribed to the asymmetric vibration of the C-O-C and the C-OH linkages (overlapping) with the peak at 1062 cm^{-1} corresponding to the symmetric vibration of the ether bond. These data indicate that the polyphenol structure obtained by this method is composed of a mixture of phenylene and oxyphenylene units as shown in Scheme 30. The small peak at 1642 cm^{-1} can be attributed to the C=O stretching vibration of a quinone formed by the oxidation of the phenolic hydroxyl groups at the ends of the polymer chain.

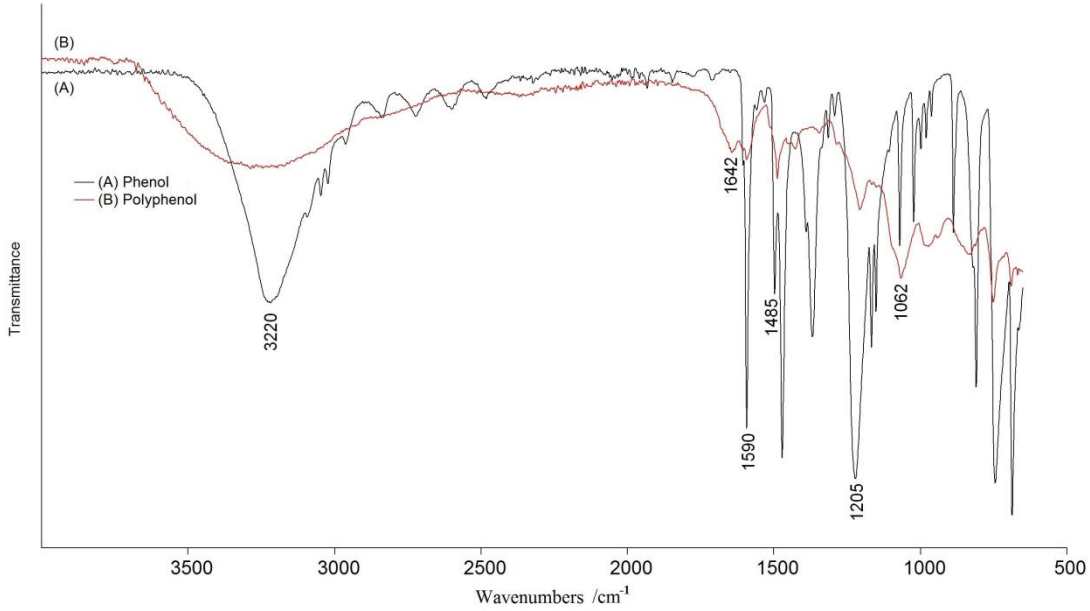

Figure 42. FT-IR spectrum of (A) phenol monomer and (B) polyphenol obtained at pH 7 (methanol: Pi buffer, 1:1).

The ^{1}H NMR spectrum (Figure 43) showed a peak at δ 9.0-10.5 due to the proton of the phenolic hydroxyl group and a peak at δ 6.2-8.0 which was ascribed to aromatic protons. This peak contained two triplets, one at δ 6.7-6.8 and one at δ 7.1-7.2 due to the aromatic protons of the phenol that did not polymerize. From the integrated ratio of the phenolic peak and the aromatic peak, from which the integration of the triplets were subtracted, the ratio of phenylene units and oxyphenylene units was determined. In this case, it indicated a composition ratio of phenylene/oxyphenylene of 70/30. The control reaction, without the enzyme, did not produce the polyphenol, confirming that it was an enzymatic polymerization reaction that took place (Table 54, exp 2, p.146).

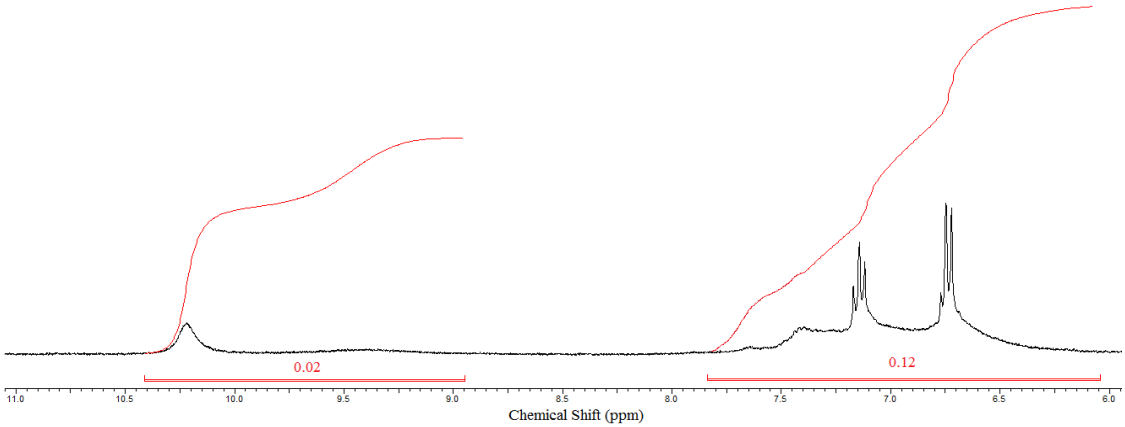

Figure 43. ^{1}H NMR spectrum of polyphenol obtained by solution polymerization at pH 7 (methanol: Pi buffer, 1:1).

4.1.2 Caffeic acid

Caffeic acid was not soluble in the equivolume mixture of methanol and Pi buffer at pH 7 (Table 54, exp 3, p.146), so the temperature was raised from 25 °C to 50 °C to increase its solubility but no increase in solubility was observed as it stayed in solid form (Table 54, exp 9, p.146). According to the literature and MSDS specifications[322], caffeic acid should be soluble in ethanol so the reaction was repeated using an equivolume mixture of ethanol and phosphate buffer at pH 7, but the monomer was still insoluble (Table 54, exp 12, p.146). In order to improve the solubility, the temperature was increased once again; however caffeic acid remained undissolved (Table 54, exp 13, p.146). The difference in solubility could be due to the solvent mixture of ethanol with phosphate buffer which is needed for the reaction to take place. As it was not possible to dissolve the caffeic acid, and therefore not possible to polymerize it by this method, no further efforts were made with this approach but other procedures were attempted and are reported in sections 4.2 and 4.3.

4.1.3 Chlorogenic acid

Chlorogenic acid on the other hand was soluble in the 1:1 solvent mixture of methanol and pH 7 Pi buffer, generating a pale yellow solution. When hydrogen peroxide was added, no reaction took place as no precipitation or colour change was observed (Table 54, exp 4, p.146).

As indicated in the experimental method (Section, 2.4.1) other analogous monomers were selected and tested in order to understand the influence of the chemical structure in this enzymatic polymerization process. The proposed monomers were: 2,3-dihydroxybenzoic acid, 2,4-dihydroxybenzoic acid, 3,5-dihydroxybenzoic acid and 1,2-dihydroxybenzene (catechol) (Figure 44). All monomers were polymerized using the same method previously described (section 2.4.1): with horseradish peroxide enzyme as catalyst in an equivolume mixture of methanol and phosphate buffer at pH 7 and using H_2O_2 as the oxidizing agent.

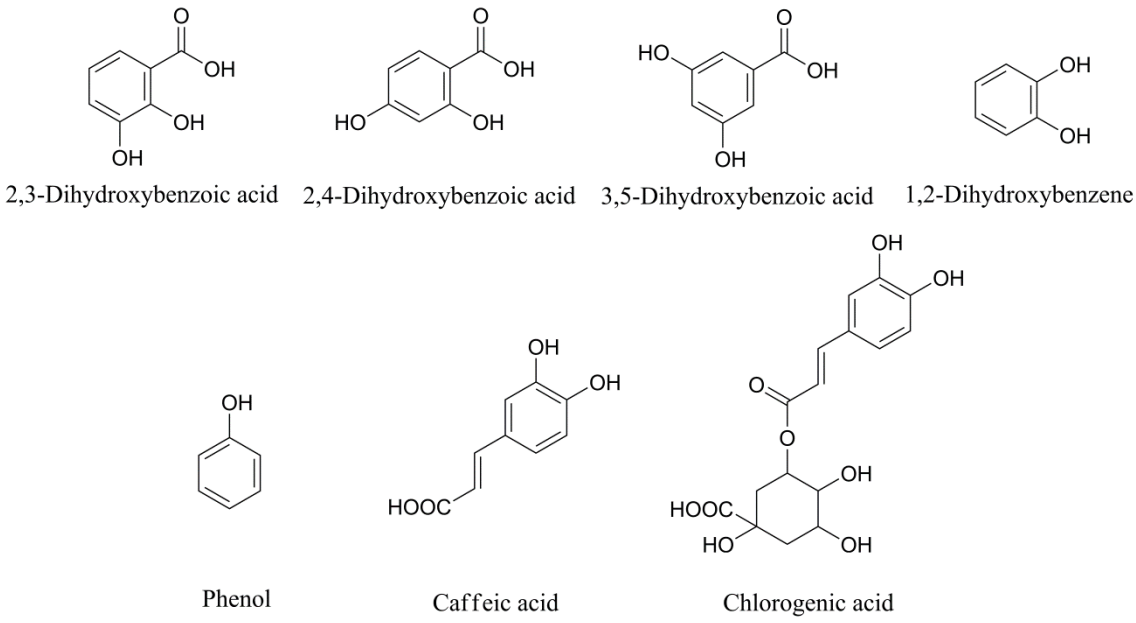

Figure 44. Monomers selected to further understand the polymerization reaction.

4.1.4 2,3-Dihydroxybenzoic acid (2,3-DHBA)

In the reaction with 2,3-dihydroxybenzoic acid, a fine white powder was obtained in 93% yield (Table 54, entry 5, p.146). The infrared spectrum (Figure 45) shows a broad peak at 3075 cm^{-1} due to –OH stretch, a peak at 1665 cm^{-1} for the C=O group vibrations bands, peaks in the range of 1450-1620 cm^{-1} associated with the C=C vibrations of the aromatic ring, a peak at 1320 cm^{-1} attributed to C-C vibrations and a peak at 1170 cm^{-1} for C-O stretch. The changes in the peaks at 1320, 1224 and 1026 cm^{-1} and the

disappearance of the peak at 680 cm^{-1} indicated a change in the monomer structure with new linkages which cannot be precisely predicted just from infra-red spectroscopy.

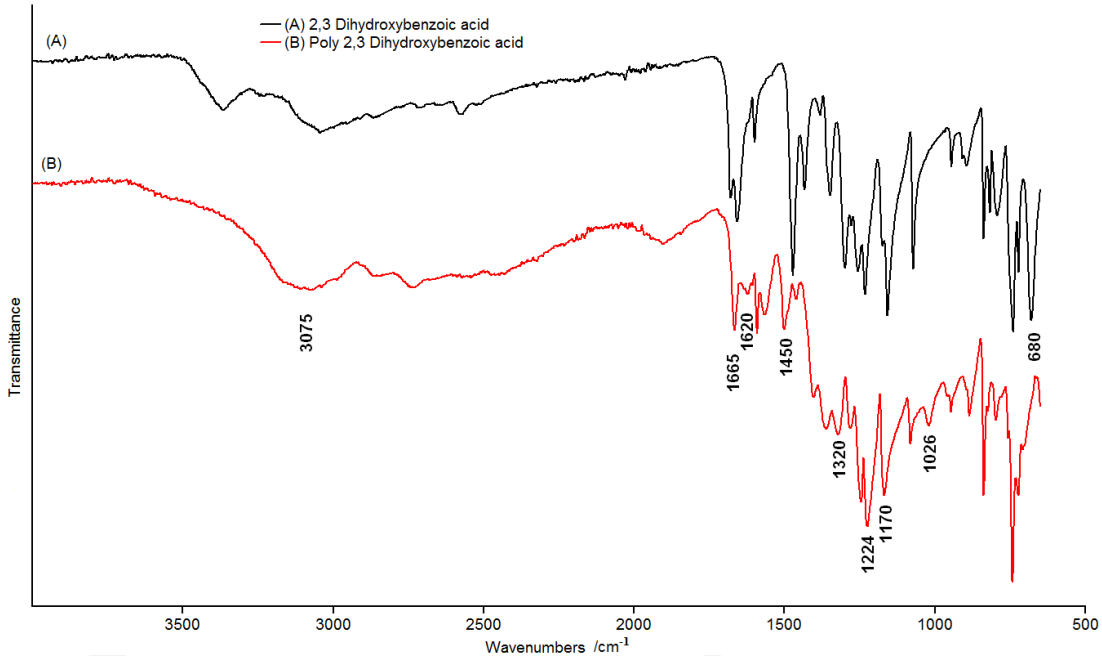

Figure 45. FT-IR of A) 2,3-dihydroxybenzoic acid monomer and B) Poly 2,3- dihydroxybenzoic acid obtained at pH 7 (methanol: Pi buffer, 1:1).

The ^{1}H NMR spectra of the 2,3-dihydroxybenzoic monomer in Figure 46, showed six peaks, three broad singlets and three multiplets in the aromatic region. The three singlets, at δ 13.61, 11.39 and 9.29 ppm corresponded to –OH protons, whereas the three multiplets, one triplet at δ 7.24 and two double doublets at δ 7.21 and 6.97 ppm corresponded to protons H_f, H_g and H_e respectively. For the polymer spectra, the same multiplet peaks indicated that the benzene ring remained but there was a shift in the position of the peaks which can be attributed to a change in linkages outside the aromatic ring. Not enough information of the polymer could be obtained from the ^{1}H NMR spectra so ^{13}C NMR experiments were conducted.

In the ^{13}C NMR spectrum of 2,3-dihydroxybenzoic acid monomer (Figure 47-A) the signal at 172 ppm corresponded to the C=O carbon (C_a) of the carboxylic group, the signals at 150 and 145 ppm to the C-O carbons of C_c and C_d respectively and signals at 120, 119 and 118 and 113 ppm correspondingly to the C_e, C_f, C_g and C_b of the carbons in the benzene ring. In the spectrum of the polymer obtained (Figure 47-B) the signals at 120 ppm shifted upfield by 1.2 ppm and the signal at 113 ppm downfield to 116 ppm indicating a linkage to the carboxylate group.

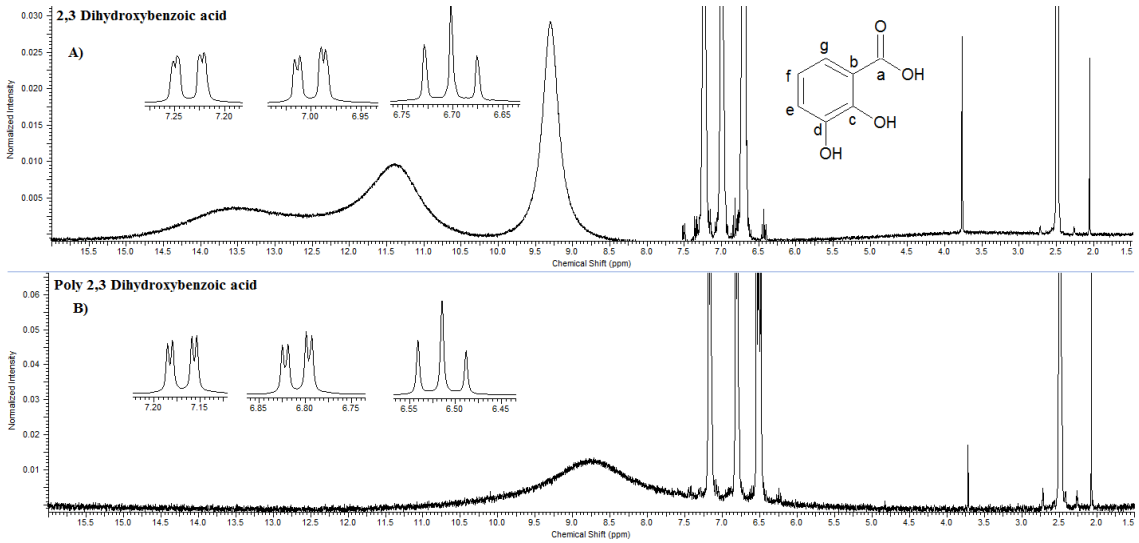

Figure 46. ^{1}H NMR spectrum of A) 2,3-dihydroxybenzoic acid monomer and B) Poly 2,3-dihydroxybenzoic acid obtained at pH 7 (methanol: Pi buffer, 1:1).

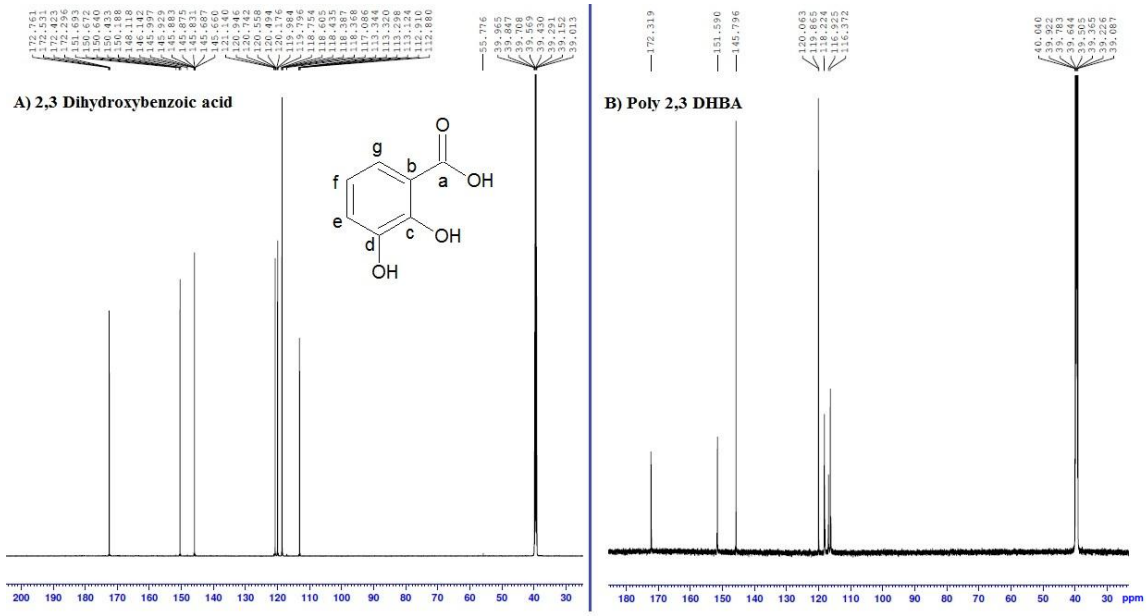

Figure 47. ^{13}C NMR of A) 2,3-dihydroxybenzoic acid and B)) Poly 2,3-dihydroxybenzoic acid obtained at pH 7 (methanol: Pi buffer, 1:1).

Based on the data obtained from these different analyses and the physical appearance of the product, it can be concluded that an enzymatic polymerization took place. Horseradish peroxide enzyme was used as catalyst and by inductive reasoning, since polymerization of the polyphenol did not take place in the absence of the horseradish peroxide enzyme, other factors being the same, the polymerization was enzymatic.

No previous polymerization of 2,3-dihydroxybenzoic acid was found in the literature in order to compare these results and final structure, but polymerization from other types of dihydroxybenzoic acids monomers[323,324], such as the production of

aromatic hyperbranched polyesters synthesized from 3,5-dihydroxybenzoic acid[325,326] and laccase[327-329] and peroxidase catalyzed[330,331] enzymatic oxidative polymerization of catechol were used to support the poly-2,3-dihydroxybenzoic structure.

These previous studies and the results obtained from the analyses in this work indicated that the final structure for the polymer was based on oxyphenylene units, as were those observed in the polyphenol previously obtained. The formation of a hyperbranched polymer was discarded as the structure of 1,3-dihydroxybenzoic acid was not symmetrical. Therefore it was concluded that the final reaction mechanism is as shown in Scheme 31.

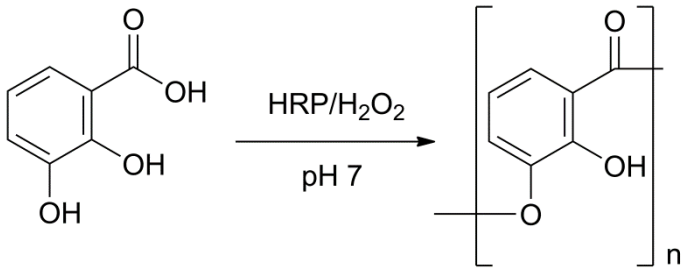

Scheme 31. Polymer structure of poly 2,3-dihydroxybenzoic acid

4.1.5 1,2-Dihydroxybenzene

From the reaction with 1,2-dihydroxybenzene (catechol) a precipitate was obtained, similar to the phenol, but with a lower yield of 23% (Table 54, exp 8, p.146). The FT-IR analysis is shown in Figure 48. In the spectrum of the synthesized polymer, the broad weak peak at 3300 cm^{-1} could be due to the phenolic vibration bands. The peaks in the region of 1465-1655 cm^{-1} can be attributed to the vibrations of the C=C linkage in the benzene ring. The peak at 1490 cm^{-1} can be attributed to the ortho disubstituted benzene ring, the peaks at 1250 and 1100 cm^{-1} correspond to the C-O-C stretching frequency vibrations and the peak at 750 cm^{-1} ascribed to the out-of-plane bending vibrations of =C–H bonds of the aromatic ring. The broad peak at 3300 cm^{-1} and the intense signal at 1250 cm^{-1} suggest that the polymer structure is connected by ether bonds, i.e. formed by oxyphenylene units, with –OH functional groups still in the polycatechol structure.

Finally, by comparing these results with those obtained in laccase[327-329] and peroxidase catalyzed[330,331] enzymatic oxidative polymerization of catechol, it can be concluded that polycatechol obtained in this experiment by an peroxide-catalyzed enzymatic polymerization reaction has the structure shown in Scheme 32.

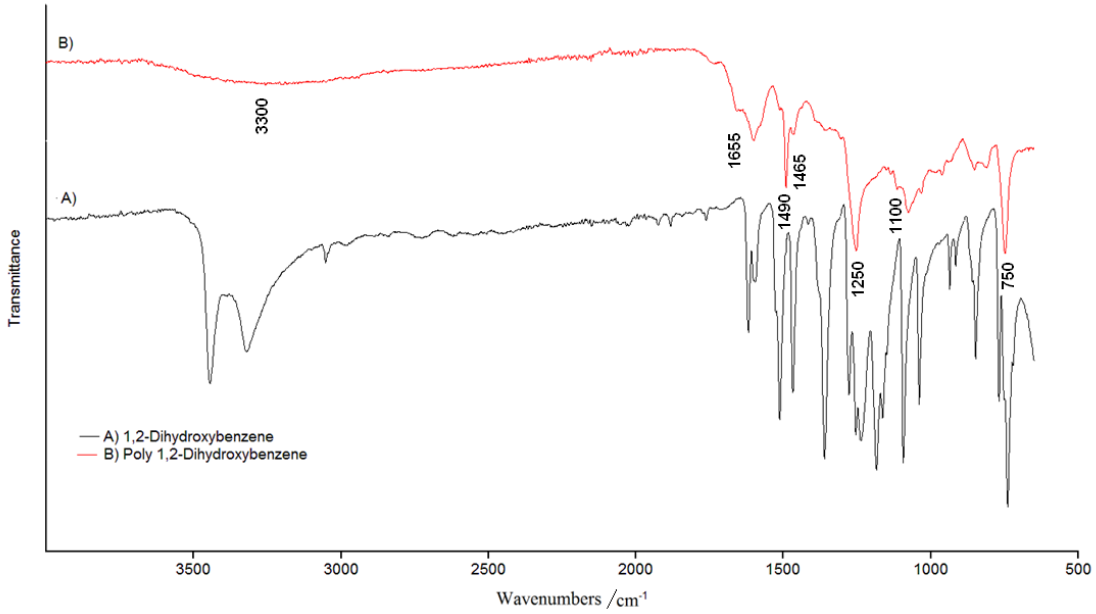

Figure 48. FT-IR of A) 1,2-Dihydroxybenzene B) Poly 1,2-Dihydroxybenzene obtained at pH7 . (methanol: Pi buffer, 1:1).

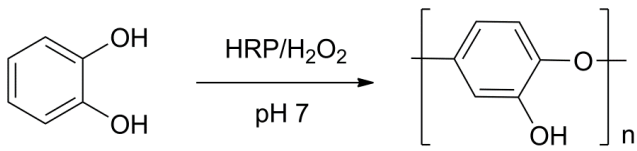

Scheme 32. Polymer structure of poly 1,2-Dihydroxybenzene

On the other hand 2,4-dihydroxybenzoic acid and 3,5-dihydroxybenzoic acid were not soluble in the equivolume mixture of methanol and Pi buffer pH 7 (Table 54, exp 6 and 7, p.146), so the temperature was raised from 25 °C to 50 °C to increase their solubility, as was attempted previously with caffeic acid.

4.1.6 2,4-Dihydroxybenzoic acid (2,4-DHBA)

When the 2,4-dihydroxybenzoic acid was heated in solution, the monomer was mostly soluble in the equivolume mixture of methanol: Pi buffer and so hydrogen peroxide was added (Table 54, exp 10, p.146). At the end of the reaction the solution changed from transparent to dark yellow and the precipitate was collected by centrifugation. A fine yellow powder was dried under vacuum and weighed, indicating a total yield of 58%.

The FT-IR analysis of the monomer and the precipitate were compared to that of the 2,4-dihydroxybenzoic acid monomer (Figure 49). As in the case of the 2,3-dihydroxybenzoic acid monomer; the broad peaks in the regions 3113 and 2784 cm^{-1} can

be assigned to the stretching vibrations of -OH groups and C-H bonds respectively. While peaks in the regions of 1609-1640 cm^{-1}, 1512-1558 cm^{-1}, 1303-1403 cm^{-1} and 1224-1259 cm^{-1} describe C=O group and C=C, C-C and C-O bonds respectively. The broadening of 1094 cm^{-1} peak and the shift of 1259 cm^{-1} peak in the polymer spectra can be attributed to an ester bond.

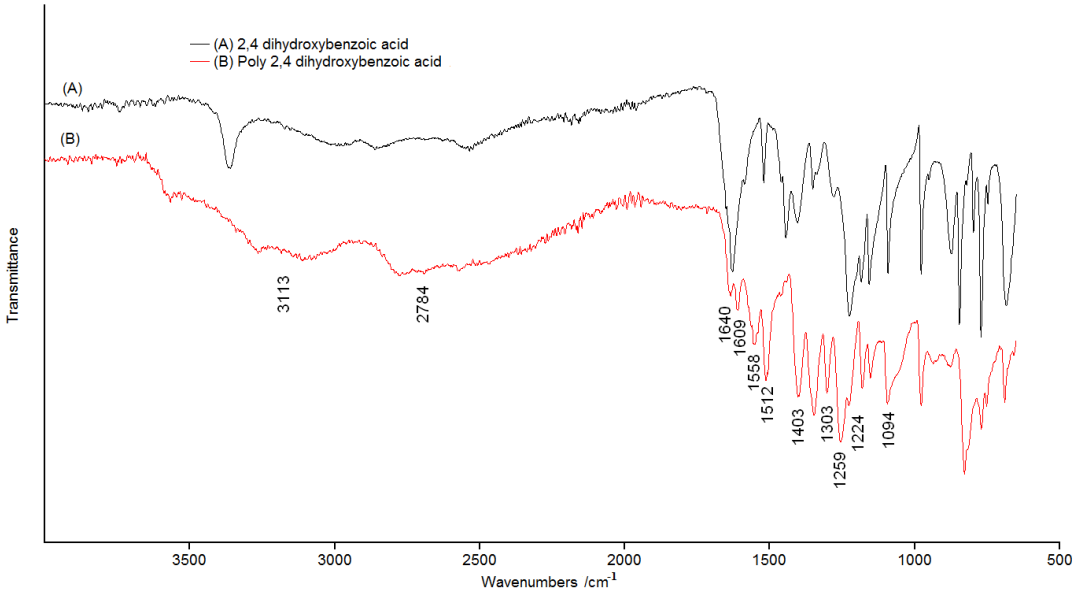

Figure 49. FT-IR of A) 2,4-dihydroxybenzoic acid monomer and B) Poly 2,4-dihydroxybenzoic acid obtained at pH 7 (methanol: Pi buffer, 1:1).

As observed in the 2,3-DHBA ^{1}H NMR spectra, the 2,4-dihydroxybenzoic monomer (Figure 50) also showed six peaks. The three singlets, at δ 13.3, 11.4 and 10.4 ppm correspond to -OH protons and three multiplets were ascribed to an aromatic ring. One double doublet at δ 6.3 ppm describes H_f protons while two doublets at δ 7.6 and 6.2 ppm correspond to protons H_g and H_d, respectively. The shifts observed in these aromatic peaks of around 0.15 ppm suggested a change in the chemical structure without affecting the benzene ring. The disappearance of the –OH peaks and the broadening of the base line can be explained due to the presence of water in the polymer which affects the NMR analysis.

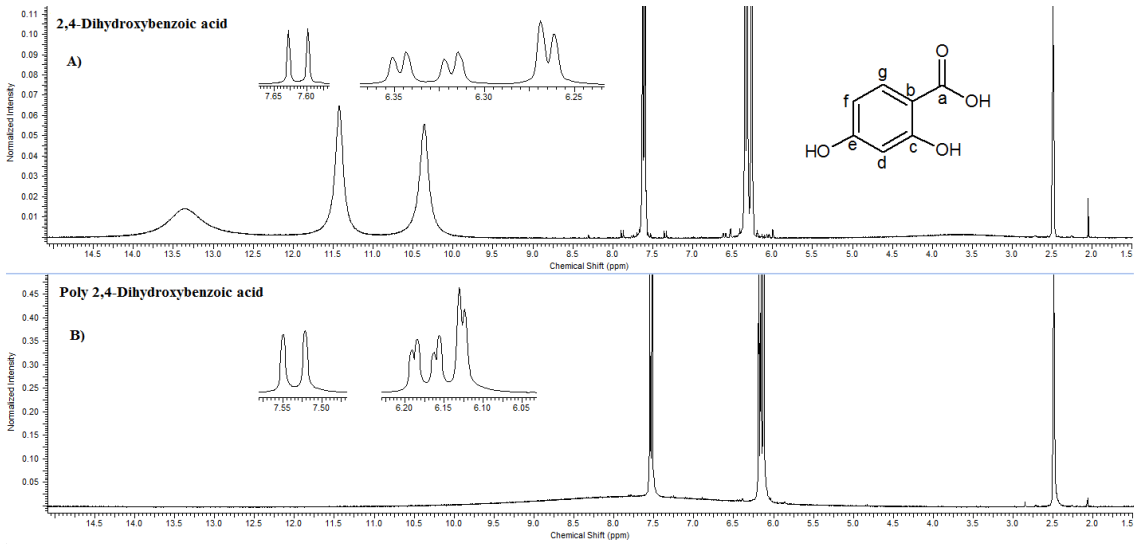

Figure 50. ^{1}H NMR spectrum of A) 2,4-dihydroxybenzoic acid monomer and B) Poly 2,4-dihydroxybenzoic acid obtained at pH 7 (methanol: Pi buffer, 1:1).

The ^{13}C NMR analysis in Figure 51 of the monomer shows a signal at 172 ppm due to the carbon C_a of the carboxylic group and signals at 164, 163, 131, 108, 106, 102 ppm corresponding to the carbons in the benzene ring; C_e, C_c, C_g, C_b, C_f and C_d respectively. In comparison with the polymer spectrum, the signals which correspond to C_b, C_e and C_f have a shift of around 0.5 ppm and the carbonyl peak is found in the region of an ester suggesting there is a new bond between the -OH and -COOH in the molecule, which corroborates the FT-IR interpretation.

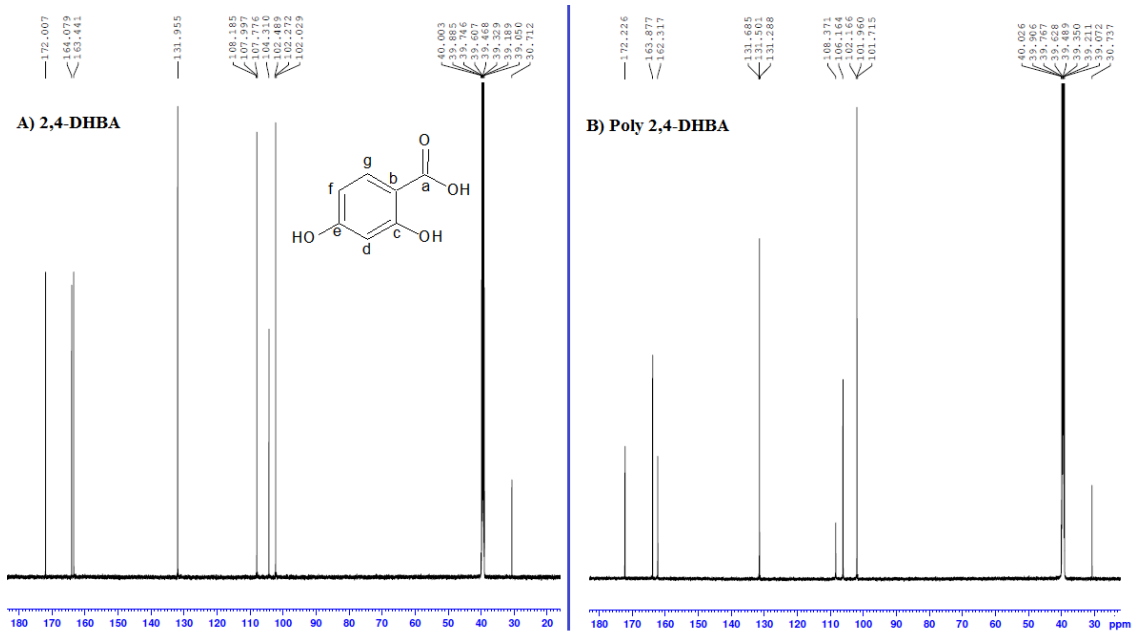

Figure 51. ^{13}C NMR of A) 2,4-dihydroxybenzoic acid and B)) Poly 2,4-dihydroxybenzoic acid obtained at pH 7 (methanol: Pi buffer, 1:1).

According to the results obtained from the analysis, the polymer obtained has the structure shown in the Scheme 33. As for poly-2,3DHBA, this polymer also possesses oxyphenylene units. The product of this reaction did not precipitate from solution and was obtaining in solid form by drying. It appears to be a water-soluble polymer.

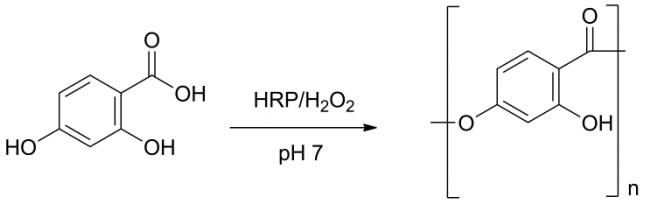

Scheme 33. Polymer structure of poly 2,4-Dihydroxybenzoic acid

4.1.7 3,5-Dihydroxybenzoic acid (3,5-DHBA)

The reaction using 3,5-dihydroxybenzoic acid at 50 °C did produce a precipitate when hydrogen peroxide was added. During the reaction time of 6 h, it yielded 1.4% of a polymer but it was observed that after 24 h more precipitate was formed generating a total yield of 2.3 % (Table 54, exp 11, p.146).

The FT-IR analysis of the monomer and polymer are shown in Figure 52. The polymer spectrum shows a broad peak at 3082 cm^{-1} due to the –OH linkage vibrations, a peak at 1658 cm^{-1} corresponding to C=O stretching vibrations, at 1601 cm^{-1} for the vibrations of the C=C bond in the benzene ring, a peak at 1243 cm^{-1} attributed to C-C bonds and several peaks in the region between 1007 -1162 cm^{-1} corresponding to C-O linkage vibrations.

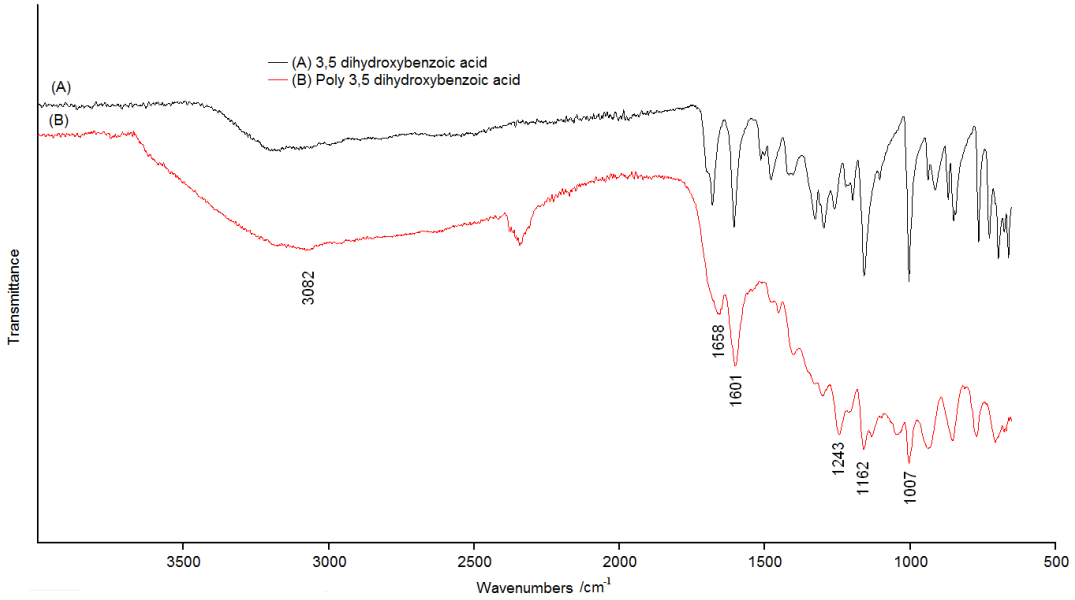

Figure 52. FT-IR of A) 3,5 Dihydroxybenzoic acid monomer and B) Poly-3,5-dihydroxybenzoic acid obtained at pH 7 (methanol: Pi buffer, 1:1).

The ^{1}H NMR spectra of 3,5-dihydroxybenzoic acid (Figure 53) showed two broad singlets and two multiplets in the aromatic region. The singlets at δ 12.65 and 9.55 ppm correspond to –OH protons, while the doublet at δ 6.8 correspond to H_c and H_g protons and the triplet at δ 6.4 to the proton H_e. As in the previous analysis, the shifts in the aromatic region indicated a change in the chemical structure but did not provide enough information to conclusively define the final structure. In addition, the presence of water affected the -OH proton signals making the spectra more difficult to analyse.

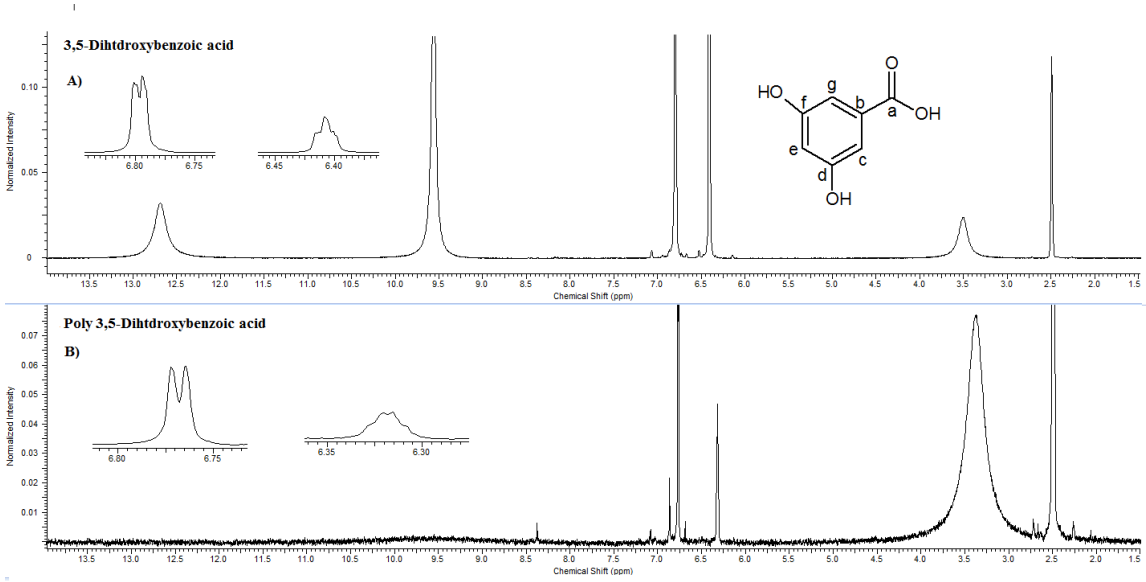

Figure 53. ^{1}H NMR spectrum of A) 3,5-dihydroxybenzoic acid monomer and B) Poly 3,5-dihydroxybenzoic acid obtained at pH 7 (methanol: Pi buffer, 1:1).

The ^{13}C NMR analysis of the 3,5-DHBA monomer (Figure 54-A) shows the carbon of the carboxylic group (C_a) signal at 167 ppm, the C_f and C_d signals overlapping at 158 ppm, C_b signal at 132 ppm, C_g and C_c together at 107 ppm and finally C_e signal at 106 ppm. For a polymer structure, a broadening in the ^{13}C NMR signals is expected as seen in the spectrum obtained (Figure 54-B). Furthermore the disappearance of the C_b signal at 132 ppm suggests a change in the carboxylic group which could be attributed to a new ester linkage. The 1 ppm shifts of the C_e signal from 106 to 105 ppm and C_a from 167 to 168 ppm may also indicate a change in the adjacent OH groups and in the -COOH group respectively, according to Kricheldorf's work.[326]

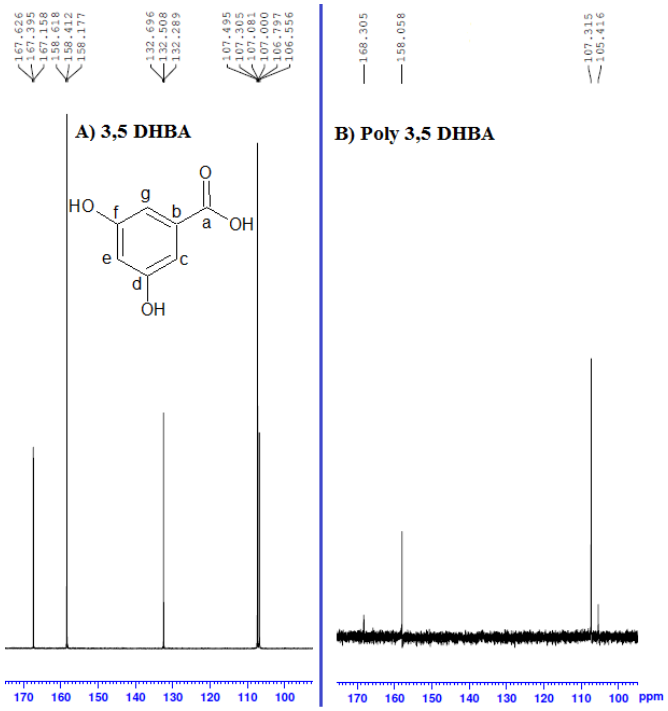

Figure 54. ^{13}C NMR of A) 3,5-dihydroxybenzoic acid and B) Poly 3,5-dihydroxybenzoic acid obtained at pH 7 (methanol: Pi buffer, 1:1).

Furthermore, when these results are compared to those presented in the literature for general hyperbranched and dendrimer polymers[323,332], the differences in FT-IR and NMR spectra from monomers to polymers are similar. With all the information gathered from the analysis and the comparison with literature it can be concluded that an enzymatic HRP-catalyzed polymerization took place obtaining a low yield polymer with the structure shown in Scheme 34.

In contrast with the previous monomers, 3,5-dihydroxybenzoic acid reacts at both OH groups and the low yield observed suggests either low reactivity or the instability of the molecule to form a polymer matrix. This could explain the reason why it has been used in research as a co-monomer or chemically functionalized with other chemical groups[332] in order to improve the original properties.

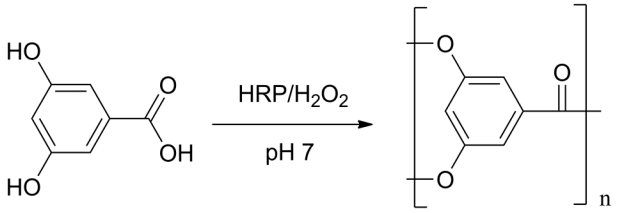

Scheme 34. Polymer structure of poly 3,5-dihydroxybenzoic acid

4.1.8 Summary of results

A summary of the enzymatic polymerization experiments and results using H_2O_2 as oxidizing agent and peroxidise (HRP) enzyme as catalyst at pH 7 (methanol: Pi buffer, 1:1) is show in Table 54. The monomer with highest conversion is 2,3-dihydroxybenzoic acid while the lowest yields was with 3,5-dihydroxybenzoic acid.

Table 54. Results from the enzymatic solution polymerization at pH 7 (methanol: Pi buffer, 1:1).

Exp	Temp /°C	Solvent	Monomer		Yield %	Phe/Oxy
			Name	/g		
1	25	methanol/buffer	Phenol	1	70	70/30
2	25	methanol/buffer	Phenol *No enzyme	1	0	0
3	25	methanol/buffer	Caffeic Acid	1.91	0	0
4	25	methanol/buffer	Chlorogenic Acid	3.75	0	0
5	25	methanol/buffer	2,3 Dihydroxybenzoic acid	1.63	93	0/100
6	25	methanol/buffer	2,4 Dihydroxybenzoic acid	1.63	0	0
7	25	methanol/buffer	3,5 Dihydroxybenzoic acid	1.63	0	0
8	25	methanol/buffer	Catechol	1.17	23	0/100
9	50	methanol/buffer	Caffeic Acid	1.91	0	0
10	50	methanol/buffer	2,4 Dihydroxybenzoic acid	1.63	58	0/100
11*	50	methanol/buffer	3,5 Dihydroxybenzoic acid	1.63	2.3	0/100
12	25	ethanol/buffer	Caffeic Acid	1.91	0	0
13	50	ethanol/buffer	Caffeic Acid	1.91	0	0

* Total reaction time of 24h

As the caffeic acid did not dissolve in the reaction solvents and the chlorogenic acid did not polymerize, to overcome these problems, a new method was applied to all the monomers. From the first stage of the experiment it can be concluded that the position of the hydroxyl group in the monomer structure affects the enzymatic polymerization process. While the 2,3 and 2,4 positions yielded 58% and 93% respectively of polymerized material, the 3,5 position only yielded 2% of polymer.

Further studies were performed in order to support the interpretations of results and conclusions made in this chapter. Enzymatic polymerization using HRP enzyme as the catalyst but instead of using a buffer solution as reaction media an aqueous solution with methanol was used.

4.2 Enzymatic polymerization in aqueous solution with methanol

The enzymatic solution polymerization reactions were also executed according to Xu's work on caffeic acid polymerization.[295] The difference between this method and the previous one used in section 4.1 is the solution in which the polymerization is performed. In this method, it was composed of an equivolume solution of methanol and water. The phosphate buffer at pH 7 was only used for the production of a stock solution for the enzyme. The horseradish peroxide (HRP) enzyme used as catalyst for the polymerization remained the same in both methods. As in the previous method, the reaction started when the hydrogen peroxide was added, forming a precipitate, which was later separated by centrifugation.

Xu's work described the biocatalytic in-situ polymerization of caffeic acid on a functionalized gold surface and its structural comparison with the same polymer obtained by solution enzymatic polymerization. Both reactions were accomplished using horseradish peroxise (HRP) enzyme as catalyst. His results indicated that in solution polymerization, hydrolysis within the caffeic acid benzene ring takes place forming a C-O-C coupling between monomers while in the in-situ surface polymerization, an organized orientation was provided by the reaction conditions forming only C-C ring coupling. The structures are shown in Scheme 35.

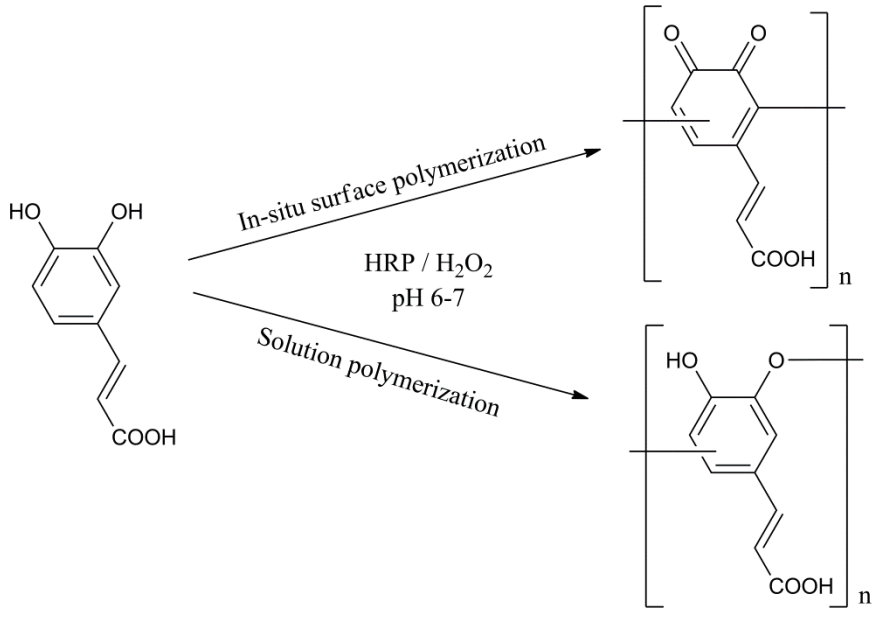

Scheme 35. Xu's work results on caffeic acid polymerization.[295]

4.2.1 Phenol

When this reaction protocol was applied to phenol in an equivolume mixture of methanol and water, 71% of polyphenol was generated (Table 55, exp 1, p.154). The FT-IR spectrum of the resulting polyphenol was compared to the spectrum of the phenol monomer and the polyphenol obtained in the previous method in phosphate buffer and methanol solution (Figure 55).

As explained in the polyphenol FT-IR spectrum of the previous method (section 4.1.1) the peaks at 1588 and 1487 cm^{-1} are due to the aromatic C-C bonds and the peak due to C-O-C and the C-OH linkages are overlapping at 1208 cm^{-1}, both are observed in spectra A and B on Figure 55. These data show that the polymer structure is formed by phenylene and oxyphenylene units. However, the diminution of the broad peak in the aqueous solution (Figure 55-B) at 3220 cm^{-1} due to the O-H bond of the phenolic group can be attributed to the predominance of oxyphenylene units in the polymer structure.

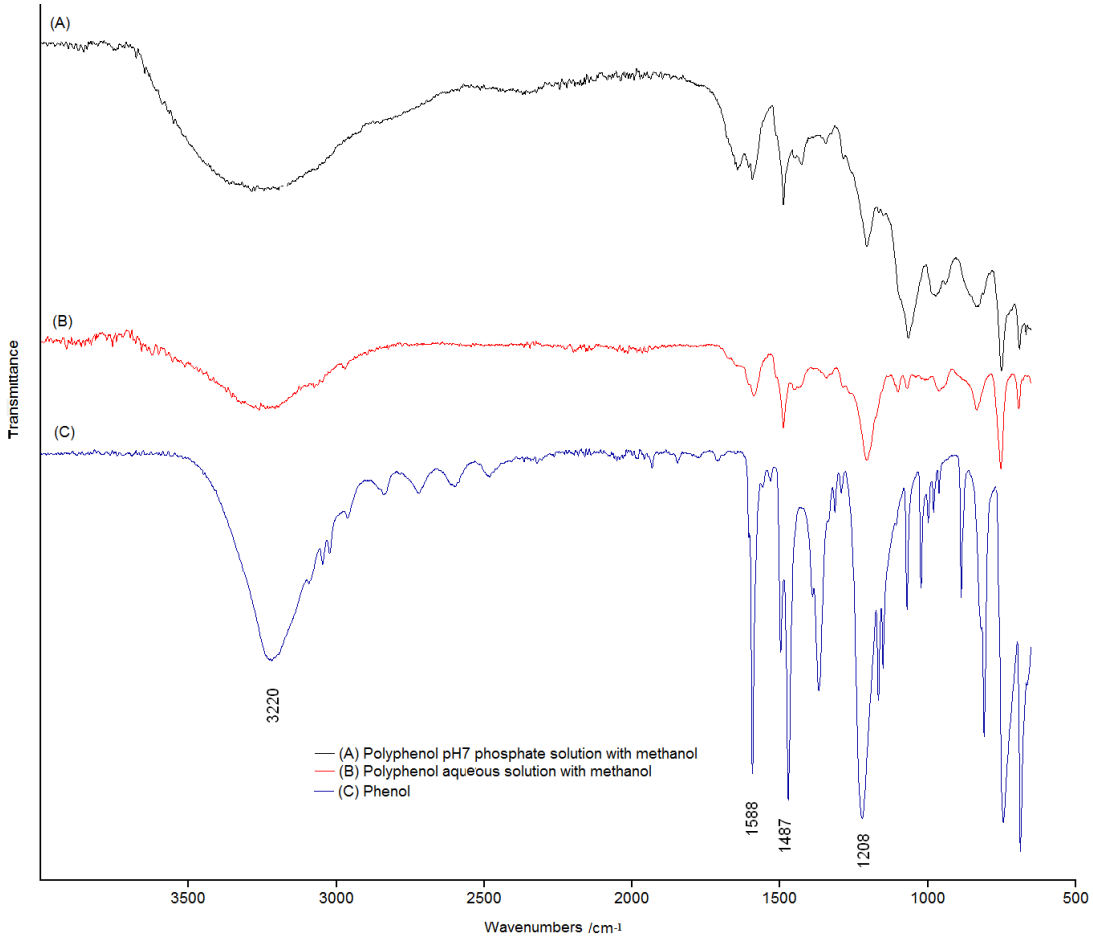

Figure 55. FT-IR spectrum of (A) polyphenol obtained by phosphate buffer with methanol, (B) polyphenol obtained by aqueous solution with methanol and (C) phenol monomer.

When the reaction was repeated without enzyme no precipitate was formed and no change in the colour was observed (Table 55, exp 2, p.154) indicating that the enzyme was needed for the polymerization to take place confirming it is an enzymatic polymerization process.

From the integrated ratio of the ^{1}H NMR peaks shown in Figure 56, the composition ratio of phenylene/oxyphenylene units was found to be 40/60 respectively. If compared to those obtained with the polyphenol obtained in phosphate buffer and methanol (section 4.1.1) which was 70/30, a difference between the structure composition units percentage was observed. This indicated that the absence of phosphate buffer at pH7 has an effect on the polyphenol composition. This might be explained by the accelerated denaturation and reduce thermal stability of the HRP enzyme caused by the presence of phosphate, as previously reported on literature.[333,334] The difference between the structure composition units can be confirmed by the diminution of the 3220 cm^{-1} peak in the FT-IR spectrum of the polyphenol obtained in aqueous solution (Figure 55-B).

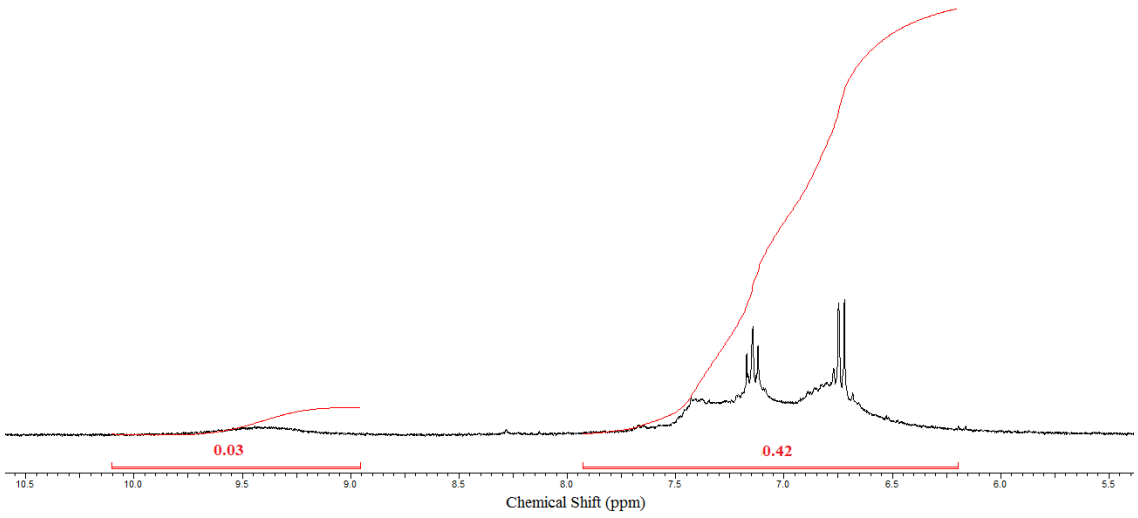

Figure 56.^{1}H NMR spectrum of polyphenol obtained by aqueous solution with methanol.

4.2.2 Caffeic acid

In this case, caffeic acid was soluble in the mixture of methanol and water, which can be attributed to the small amount of phosphate buffer at pH7 in the reaction (Table 55, exp 3, p.154). A yellow precipitate was obtained in 23% yield. The FT-IR spectra of the caffeic acid and the polymer product are shown in Figure 57. For the polymer, the peaks in the region between 1440-1620 cm^{-1} can be attributed to the C=C stretching vibration bands of the benzene ring and the peak at 1670 cm^{-1} to the vibrations of the carboxylic

acid group. The 1213 and 1170 cm^{-1} peaks correspond to the O-H deformation and vibrations bands, respectively. The vibration of C-O-C of a phenyl ester bond can be observed in the peaks at 1276 and 1105 cm^{-1}. The absorption peaks in the benzene ring fingerprint region at 850, 820 and 780 cm^{-1} correspond to out-of-plane deformation vibrations of two isolated hydrogen atoms. All this suggests that the polymer structure is made up of monomers bound to each other through C-O-C aromatic ethers as seen in Scheme 36.

The results are consistent with those observed in Xu's work.[295] His results showed similar peaks for the aromatic ether formation in the region of 1250 to 1000 cm^{-1} and the region under 900 cm^{-1} have similar profiles, which are characteristic for the poly-caffeic acid structure under these conditions. Furthermore, the structure of the polymer obtained was expected as the polyphenol produced by the same enzyme in both methods presents the same C-O-C linkage. Moreover, as caffeic acid has one more hydroxyl group than phenol it can be suggested that one of the –OH groups simulates the phenylene group while the other, which is attached to other benzene ring by ether formation, assimilates the oxyphenylene unit.

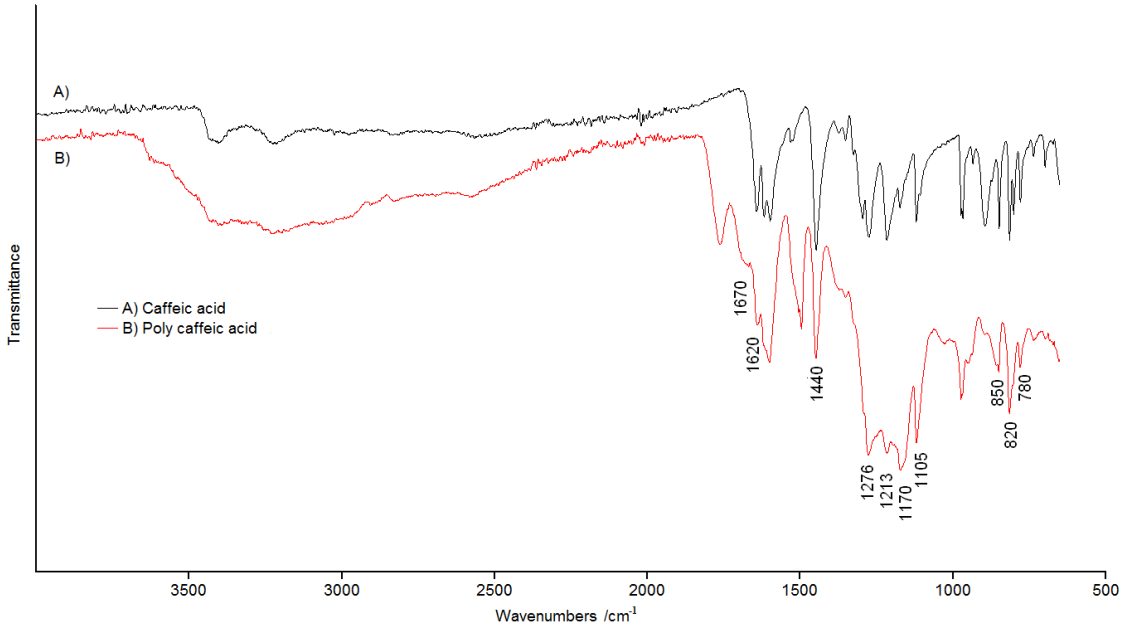

Figure 57. FT-IR spectrum of (A) caffeic acid monomer and (B) polycaffeic acid obtained by aqueous solution with methanol

Additionally, the analyses of the polymer structures obtained from the polymerization of the dihydroxybenzoic acids suggested that most of the time (with the exception of 3,5 -dihydrozybenzoic acid) only one hydroxyl group was involved in the

formation of bonds between the monomers. This can be associated with the structure obtained in the poly(caffeic acid).

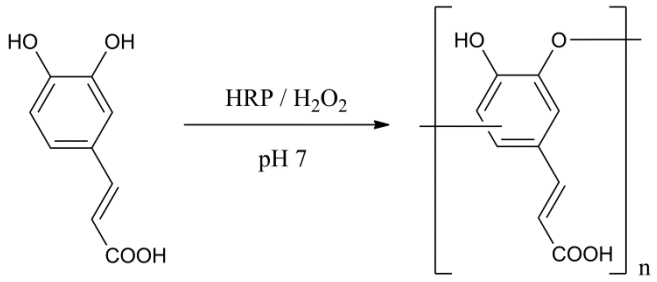

Scheme 36. Polymer structure of poly(caffeic acid)
*The polymer structure reported is represented as indicated.[295]

4.2.3 Chlorogenic acid

For chlorogenic acid as the monomer, a white precipitate was obtained in 2% yield (Table 55, exp 4, p.154). It was analysed by FT-IR and compared with the monomer to observe if there was a chemical change (Figure 58). In the polymer spectrum, the broad peak at 3290 cm^{-1} corresponds to the OH groups in the structure, the peak at 1636 cm^{-1} can be attributed to the overlap of the carboxylic acid stretching vibration and the C=C vibrations of the benzene ring. The benzene ring vibrations can also be observed in the broad peak at 1447 cm^{-1}. As in the spectra of the polycaffeic acid, the presence of a phenyl ether bond as C-O-C can be observed at 1262 and 1120 cm^{-1}. These suggest that the polymer structure is formed by oxyphenylene units. The final structure can be seen in Scheme 37.

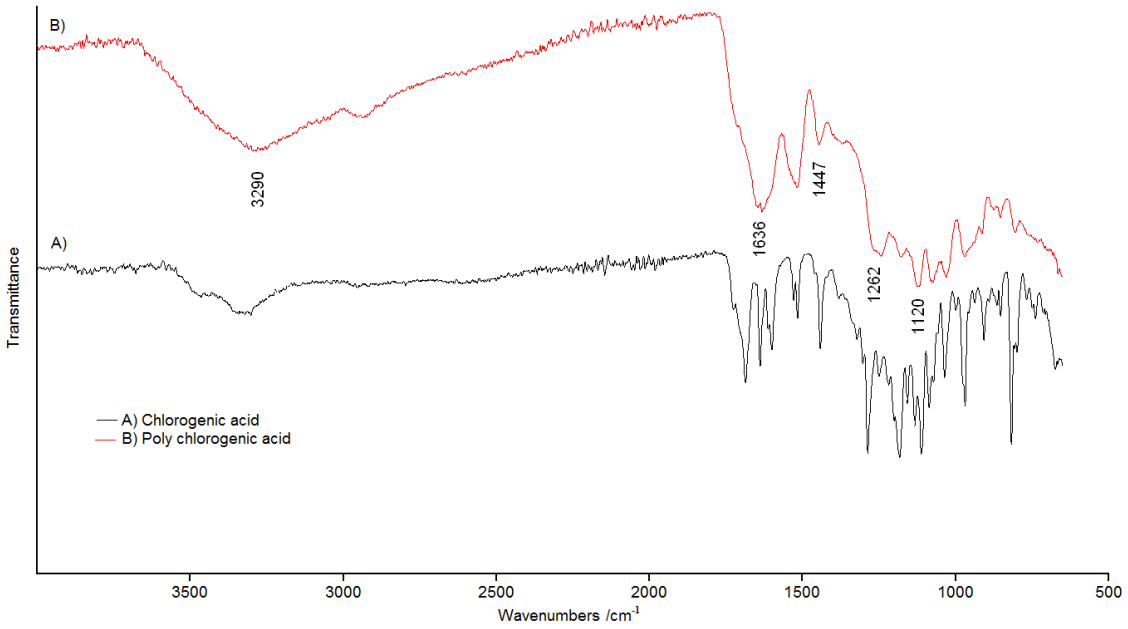

Figure 58. FT-IR spectrum of (A) chlorogenic acid monomer and (B) poly(chlorogenic acid) obtained by aqueous solution with methanol.

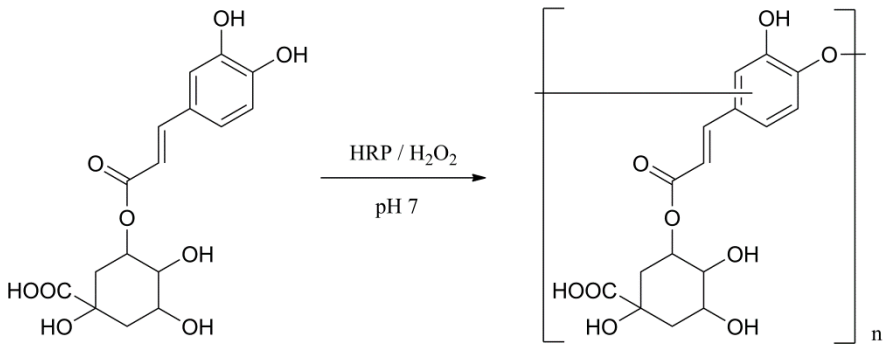

Scheme 37. Polymer structure of poly(chlorogenic acid).
*The polymer structure is represented with a line into the ring following the polyphenol and polycaffeic acid structures.

As in the previous experiment with potato waste derivatives (section 4.1) the procedure was repeated with monomers with similar chemical structure to caffeic and chlorogenic acid as shown in Figure 44.

4.2.4 2,3-Dihydroxybenzoic acid

For the reaction with 2,3-dihydroxybenzoic acid, a fine white powder was obtained at 2% yield (Table 55, entry 5, p.154). The FT-IR spectra of the monomer, polymer obtained by phosphate solution (section 4.1.4) and polymer obtained in this chapter by aqueous solution are shown in Figure 59.

The broad peaks in the region of 3000-3200 cm^{-1} indicate the -OH linkages, peaks at 1650 cm^{-1} are due to the C=O vibrations, peaks from 1430 to 1525 cm^{-1} indicate the double bonds from the aromatic ring, and the peaks at 1380 and 1160 cm^{-1} designate the C-C and C-O linkage vibrations, respectively. The differences between the monomer (Figure 45-C) and the polymer obtained by aqueous solution with methanol (Figure 45-B) are the modifications in 1340, 1278 and 1150 cm^{-1} peaks and the disappearance of peaks in the region of 670-690 cm^{-1} which are also observed in the poly 2,3-dihydroxybenzoic acid spectrum obtained by phosphate buffer with methanol (Figure 45-A). This suggests that the polymer structure formed in methanol/water (1:1) solution is the same as that obtained in the phosphate buffer solution (Scheme 31).

4.2.5 1,2-Dihydroxybenzene

For the reaction involving 1,2-dihydroxybenzene as monomer, the polymer was obtained as a brown precipitate in 4% yield (Table 55, entry 8, p.154). The powder was studied with FT-IR analysis and compared with the spectrum from the polymer obtained using phosphate buffer and methanol as solvents (section 4.1.5). The comparison is shown in Figure 60, and it can be seen that peaks in the spectra are almost identical;

therefore it was concluded that the polycatechol obtained by aqueous solution with methanol had the same structure as that produced in phosphate buffer with methanol.

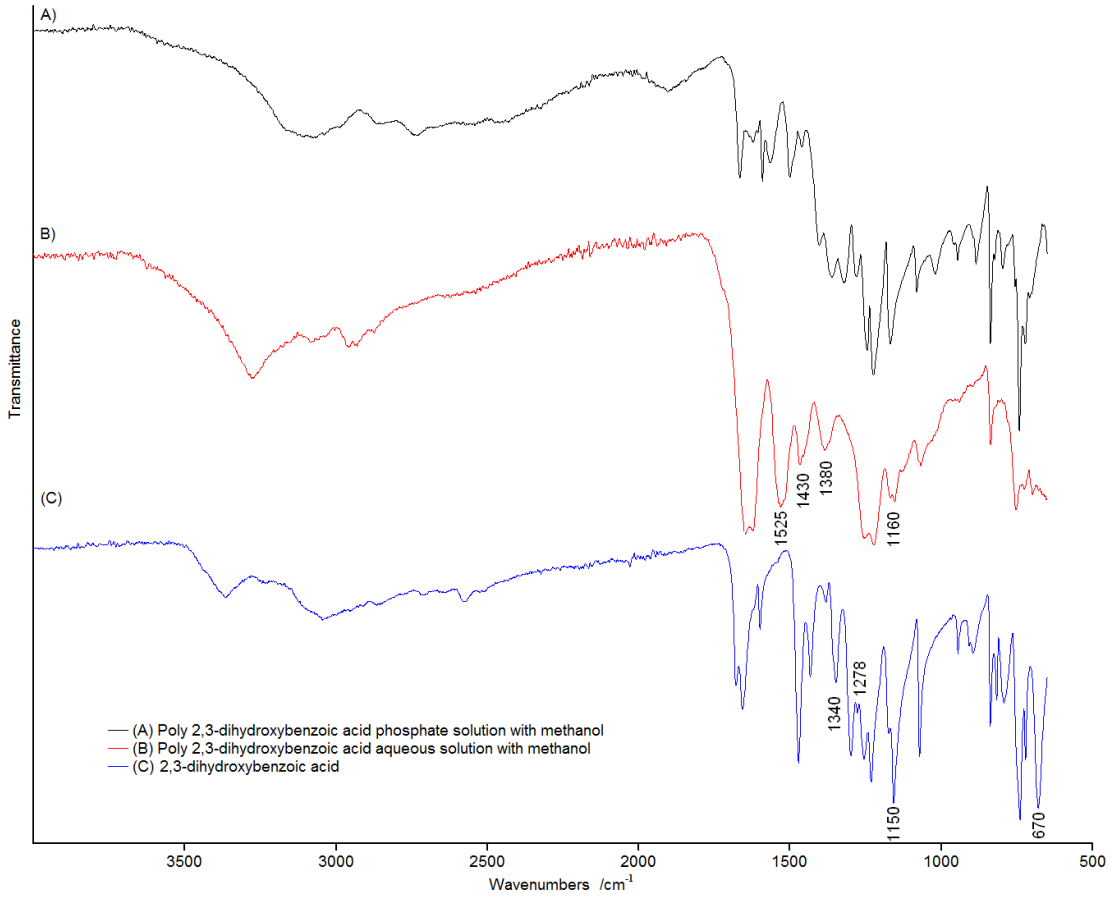

Figure 59. FT-IR spectrum of (A) 2,3 Dihydroxybenzoic acid (B) Poly 2,3-dihydroxybenzoic acid obtained by aqueous solution with methanol.

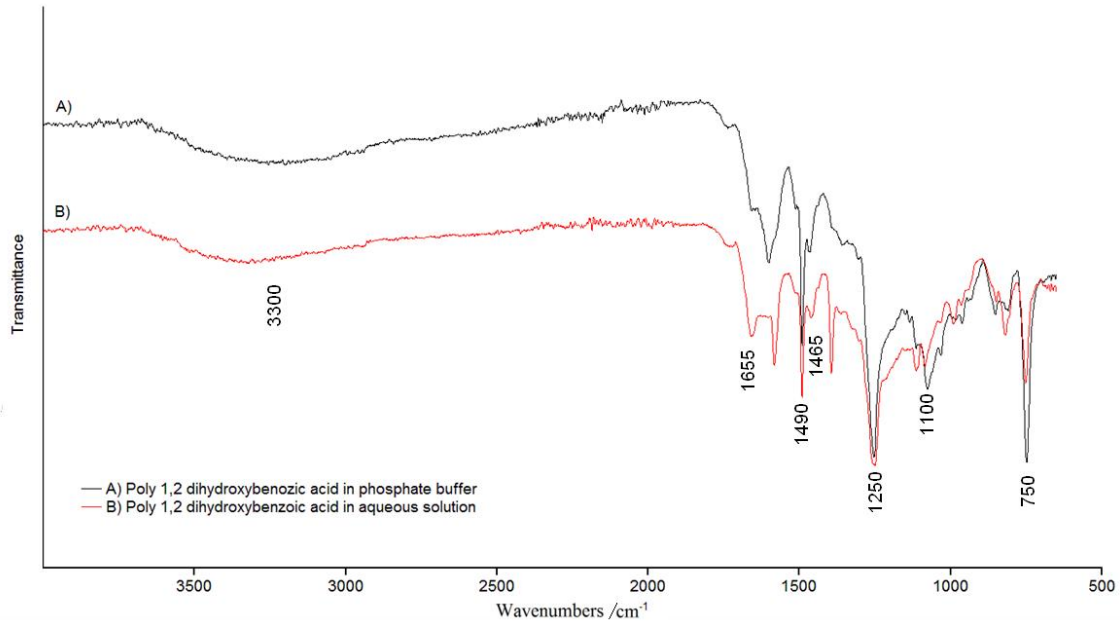

Figure 60. Comparison of FT-IR spectra. A) Poly 1,2-dihydroxybenzoic acid in phosphate buffer, B) poly 1,2-dihydroxybenzoic acid in aqueous solution.

4.2.6 2,4- and 3,5-Dihydroxybenzoic acid

For experiments using 2,4-dihydroxybenzoic acid and 3,5-dihydroxybenzoic acid as monomers the initial transparent solutions changed into opaque solutions after a 3 hour reaction. After centrifugation a small portion of polymer was obtained but once dried under vacuum they formed very thin layers being insufficient for weighing (Table 55, entry 6 and 7, p.154).

4.2.7 Summary of results

In Table 55 a summary of the results obtained in methanol/water (1:1) solution enzymatic polymerizations are shown.

Under these polymerization conditions, caffeic and chlorogenic acid monomers were polymerized in 23% and 1.5% yield, respectively. It can be suggested that the steric interaction slowed the rate polymerization and therefore different yields were observed.

When using the phosphate buffer and methanol solution, all monomers were converted to polymers. Nevertheless, the 2,3-DHBA, 2,4-DHBA and 3,5-DHBA converted in lower yields than those compared to the methanol/Pi buffer (1:1) polymerization. With this, it can be concluded that the nature of the solvent plays an important role in the polymerization process. In order to improve the caffeic and chlorogenic acid polymerization yield, a method using a water soluble template polymer during the procedure was attempted.

Table 55. Results from the enzymatic solution polymerization in aqueous solution with methanol of phenol and derivatives.

Exp	Solvent	Monomer		Yield %	Phe/Oxy
		Name	/ mg		
1	methanol/H_2O	Phenol	94	71	40/60
2	methanol/H_2O	Phenol *No enzyme	94	0	0
3	methanol/H_2O	Caffeic Acid	180	23	0/100
4	methanol/H_2O	Chlorogenic Acid	354	2	0/100
5	methanol/H_2O	2,3 Dihydroxybenzoic acid	154	2	0/100
6	methanol/H_2O	2,4 Dihydroxybenzoic acid	154	traces	0
7	methanol/H_2O	3,5 Dihydroxybenzoic acid	154	traces	0
8	methanol/H_2O	1,2 Dihydroxybenzene	110	4	0/100

4.3 Enzymatic template polymerization in water-soluble polymer.

This third polymerization process for monomers derived from potato waste was executed according to Kim's work[293] on the enzymatic template polymerization of phenol in the presence of water-soluble polymers in an aqueous medium. According to their work, the addition of the water soluble polymer polyethylene glycol during the enzymatic polymerization of phenol using HRP as catalyst produces a miscible complex between the polyphenol and the PEG, yielding a polyphenol conversion of 93%.[293] Furthermore, the polymer regioselectivity was improved giving 88% of phenylene units. They studied the effects of the PEG molecular weight and the unit molar ratio of polyphenol-PEG on the reaction behaviour. Their optimal results were for those using a PEG of Mn=$2x10^3$ and $20x10^3$ in a ratio of 1:1 with the polyphenol.

4.3.1 Phenol

When the experimental procedure reported by Kim[293] was repeated (Table 56, exp 1, p.160), a yield of 53% based on the phenol part in the complex was observed, lower than the 94% reported in the article.[293] Furthermore, when the composition and structure of the polyphenol thus obtained was analysed by ^{1}H NMR spectroscopy, a 60/40 composition ratio of phenylene/oxyphenylene was observed (Figure 61). This experiment was accomplished using PEG of Mn = 1500 in contrast to the PEG of Mn = 2000 used in Kim's work but this is not expected to affect the final polyphenol structure as Kim's work reported the regioselectivity in favour of phenylene units regardless of the molecular weight of the PEG and neither affected the % yield as her report indicated that polyethylene glycols with Mn ranging from 400-20,000 produced between 85 to 93% of the polyphenylene.

When the reaction was repeated under the same conditions but without the use of water soluble polymer (PEG) as template only 6% conversion of polyphenol was obtained (Table 56, exp 2, p.160). This indicated that even in the absence of the PEG the enzymatic polymerization of phenol takes place, due to the presence of the HRP enzyme, but without the formation of a polyphenol-PEG complex the conversion into polyphenol decreased by 47%. When the results of this experiment (Table 56, exp 2, p.160) without the PEG are compared to those when polyphenol was obtained by enzymatic polymerization in a pH7 phosphate solution with methanol (section 4.1.1), it can be observed that the only difference is the presence of methanol in the reaction medium which, according to the results obtained in both experiments, greatly affects the polymer conversion yield. When methanol is introduced in the reaction, a conversion of

70% yield was obtained, while in its absence only 6% is observed. As a result, it can be concluded that the presence of an alcohol in the reaction medium helps the catalytic effect of the horseradish peroxidise enzyme.[335,336] This can be corroborated with works researches on the effect of solvents in the enzymatic polymerization of phenol and derivatives.[335-337]

Due to the similarities in the polymerization processes between this enzymatic template polymerization and the polymerization using phosphate buffer with methanol solution (section 4.1), further analysis on the material was performed.

When the polyphenol obtained without PEG was analysed by ^{1}H NMR (Figure 61), a 55/45 composition ratio of phenylene/oxyphenylene was observed, which was very similar to that seen in the experiment using PEG. This suggests that PEG does not help improve the regioselectivity of the polyphenol products. However when not present, conversion into polyphenol is very low.

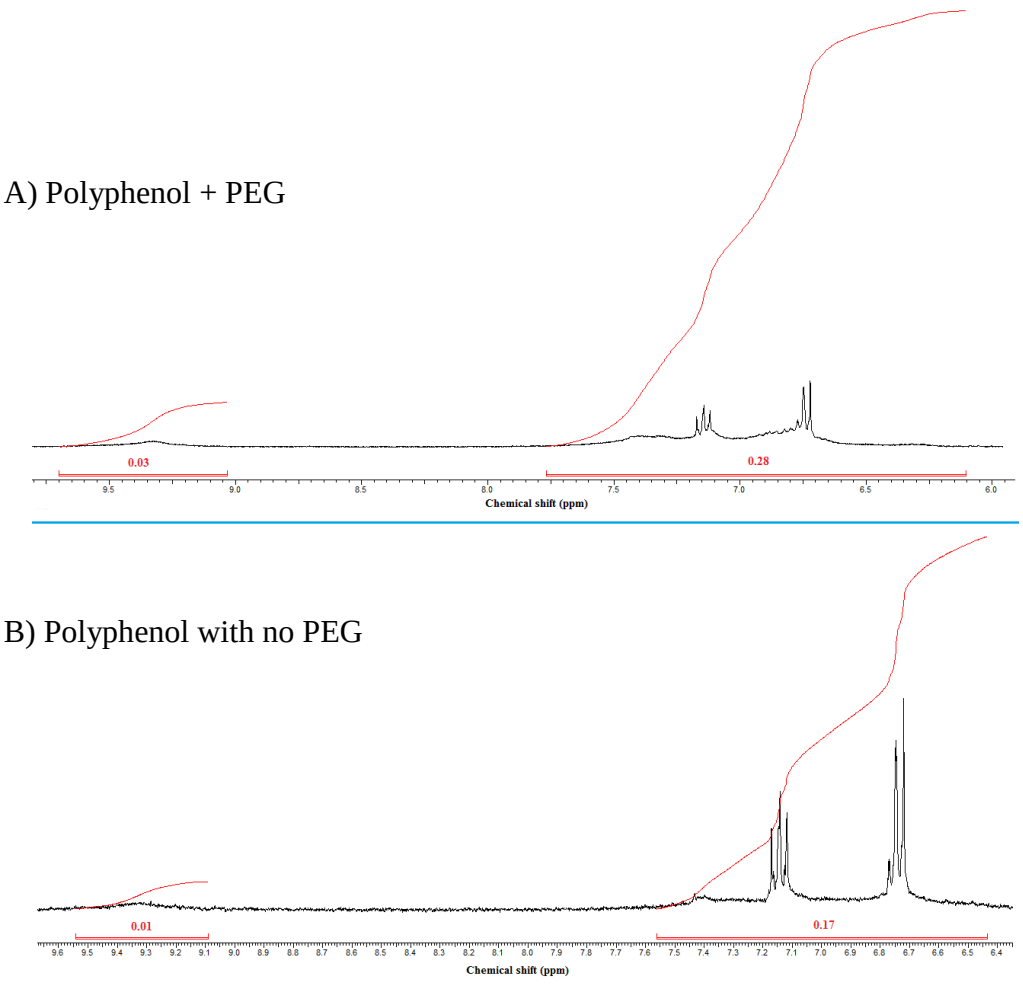

Figure 61. ^{1}H NMR spectra of polyphenols obtained by enzymatic template polymerization A) Polyphenol obtained using PEG as template and B)Polyphenol obtained without PEG

In Figure 62 the FT-IR spectra of polyphenols obtained by different methods are presented. It was observed that the polyphenols obtained in this chapter by enzymatic polymerization with PEG (Figure 62-A) and without it (Figure 62-B) present the same peaks in the region of 1800 cm^{-1} to 500 cm^{-1} as those obtained by enzymatic polymerization in phosphate buffer with methanol solution (Figure 62-C). The peaks are present at the same wavelength varying only in the intensity. In section 4.1.1 and 4.2.1 the study of the polyphenol structure obtained in phosphate buffer with methanol solution was studied corroborating its structure and polymerization, and because of the similarities in the spectra with the polyphenols obtained using PEG it was concluded that a similar polymerization took place.

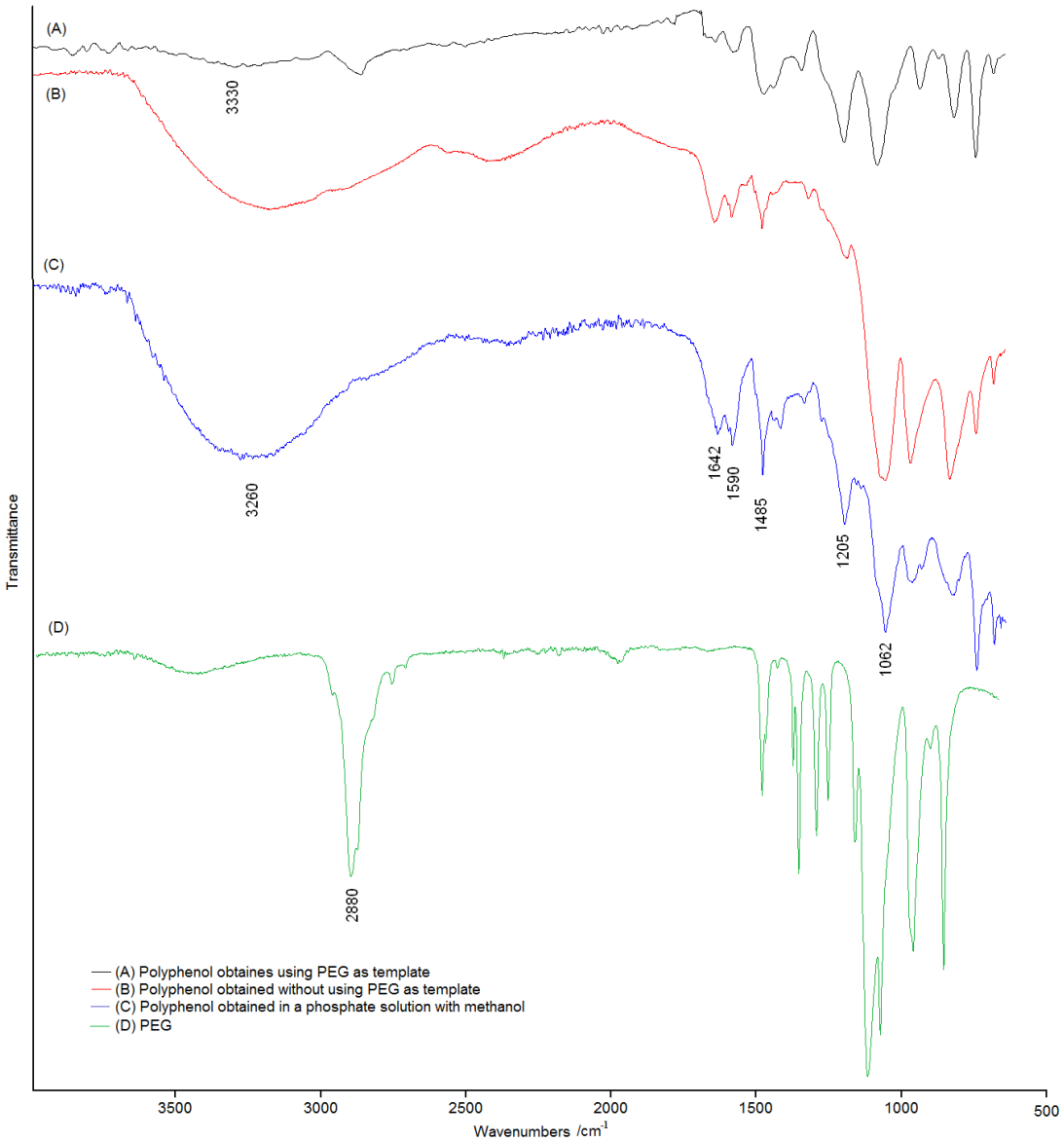

Figure 62. FT-IR spectra of polyphenols obtained by enzymatic polymerization using A) PEG as template, B) without using PEG, C) phosphate solution with methanol and D) PEG

Nonetheless, in the spectrum of polyphenol obtained using PEG, a shift of the peak at 3260 to 3330 cm^{-1} was observed. This shift, which was also observed in Kim's work, could be explained due to the formation of a hydrogen bonding complex between the polyphenol and remaining PEG. The peak found at 2880 cm^{-1} shows the presence of PEG in the polymer (Figure 62 –D).

4.3.2 Caffeic acid

When using caffeic acid as monomer (Table 56, expts 3 and 4, p.160) the temperature had to be raised to 60 °C in order to solubilise the caffeic acid. By using PEG as a template, 11% conversion of the monomer as part of the complex with PEG was obtained while in its absence only 3% conversion was accomplished. These results indicate that the formation of a PEG-complex increases the polymerization of the monomers, as previously identified in Kim's work.[293]

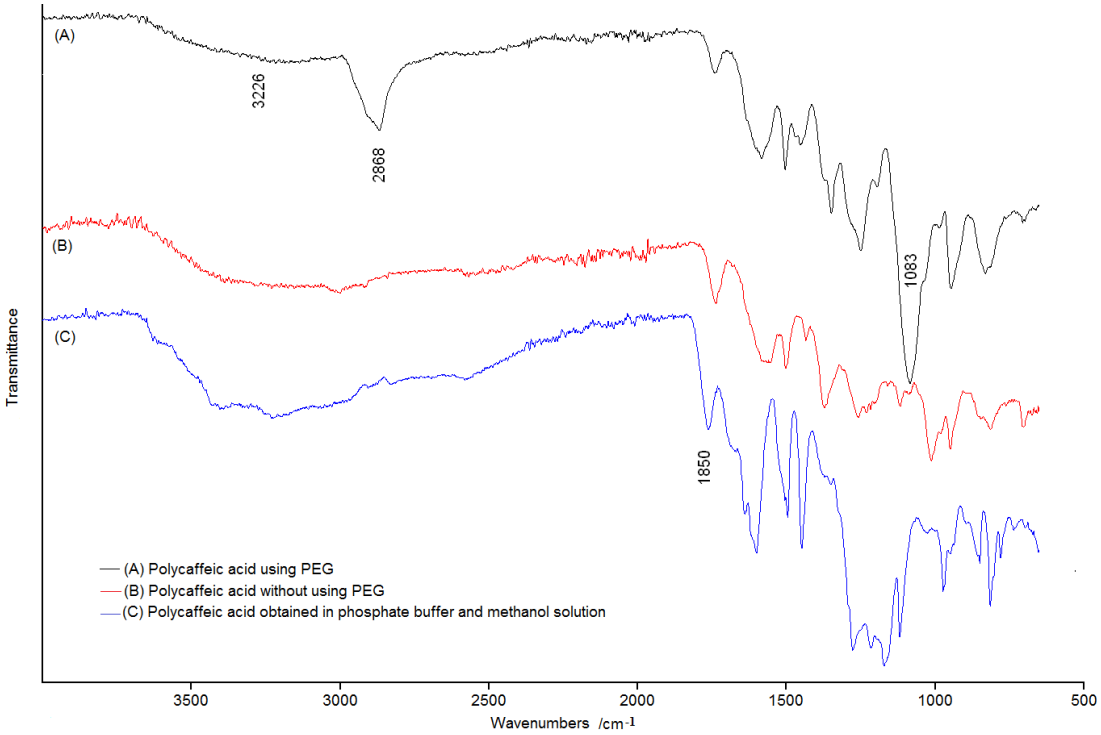

Figure 63. FT-IR spectra of polycaffeic acids obtained by enzymatic polymerization using A) PEG as template, B) without using PEG and C) phosphate solution with methanol

In Figure 63 a comparison of FT-IR spectra between the polycaffeic acid obtained with PEG (Figure 63-A), without PEG (Figure 63-B) and in phosphate buffer and methanol solution (Figure 63-C) are presented. As observed in the previous experiments with phenol, the peaks under 1850 cm^{-1} are very similar in the three processes, the main difference being the presence of the peak at 1083 cm^{-1} in the polymer obtained with

PEG (Figure 63-A) which with the peak at 2868 cm^{-1} indicates the presence of PEG. In this case, no shift of the broad peak at 3226 cm^{-1} was observed but a decrease in the intensity was observed which could suggest a complex was formed between the poly(caffeic acid) and the PEG.

4.3.3 Chlorogenic acid

When chlorogenic was used as a monomer with PEG templating (Table 56, exp 5 and 6, p.160) a 5% conversion yield was obtained, compared to the 1% conversion observed without the use of PEG.

The FT-IR spectra of the polychlorogenic acid obtained by using PEG, without PEG and in phosphate buffer with methanol solution (Figure 64) were compared, it was observed that the peak at 3290 cm^{-1} which was present in the poly(chlorogenic acid) obtained without PEG (Figure 64-B) and in phosphate buffer with methanol solution (Figure 64-C) shifted to 3320 cm^{-1} when PEG was used in the reaction (Figure 64-A). This shift, also observed in the polymerization of phenol and as indicated in Kim's work,[293] suggested the formation of a complex between the polychlorogenic acid and the PEG. The presence of PEG is observed in the peaks at 2887 and 1102 cm^{-1}.

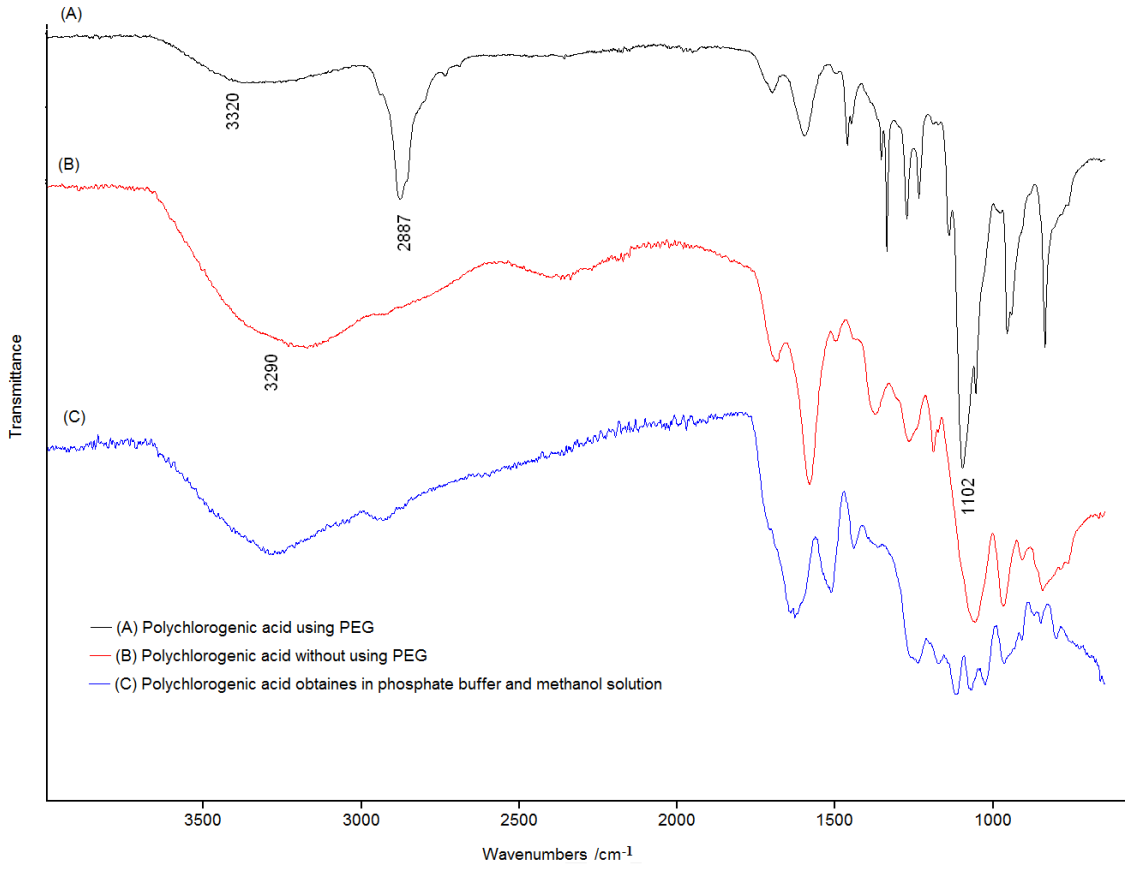

Figure 64. FT-IR spectra of polychlorogenic acids obtained by enzymatic polymerization using A) PEG as template, B) without using PEG and C) phosphate solution with methanol

4.3.3 Summary of results

In Table 56 a summary of the experiments performed using PEG as a water soluble polymer template for the enzymatic polymerization of phenol, caffeic acid and chlorogenic acid is presented. The results indicated that polymerization of the three monomers was accomplished and an improvement of yield conversion was observed when PEG is used in the reaction medium.

Table 56. Results from the enzymatic template polymerization using PEG and HRP of phenol and derivatives

Exp	PEG	Substance		Molar ratio (PEG for monomer)	Yield[a] %	Composition ratio[b] (Polymer:PEG)	(phe/oxy)
	(g)	Name	Quantity (g)				
1	0.47	Phenol	0.47	2.14	53	1:0.78	59/41
2	0	Phenol	0.47	0	6	0	55/45
3	0.47	Caffeic Acid	0.47	4.10	11	1:2	0/100
4	0	Caffeic Acid	0.47	0	3	0	0/100
5	0.47	Chlorogenic Acid	0.47	8.07	5	1: 25.2	0/100
6	0	Chlorogenic Acid	0.47	0	1	0	0/100

[a] Yield of polymer based on the monomer part in the complex product. [b] Molar ratio of monomer unit between polyphenol and PEG of the complex determined by ^{1}H NMR spectroscopy.

4.4 Addition of clay - XRD study of monomers with MMT clay

In this section the results of the XRD analysis from the interaction of clay with the respective monomers are presented.

As described previously in section 2.5 a study of the interaction of monomers with the clay prior to polymerization was undertaken to establish conditions for the formation of a nano-polymer composite by in-situ polymerization. At this stage the intention is to see if the monomer intercalates in the montmorillonite clay layers.

The X-ray diffraction traces of the clay treated with the alcohols used in the three different enzymatic polymerizations (methanol and ethanol) are shown in Figure 65. It was observed that the main peak at 7.1°, which is equal to 12.46 Å, of the pure clay (blue line) is shifted to higher values of 2θ when the clay is mixed with any of these alcohols. This suggests that the alcohols enter the galleries of the clay possibly displacing water and reducing the interplanar spacing. A study of the clay with phosphate buffer was not made as the phosphate buffer is an aqueous solution and it is well known that clay absorbs the water and an exfoliation of the clay layers takes place.

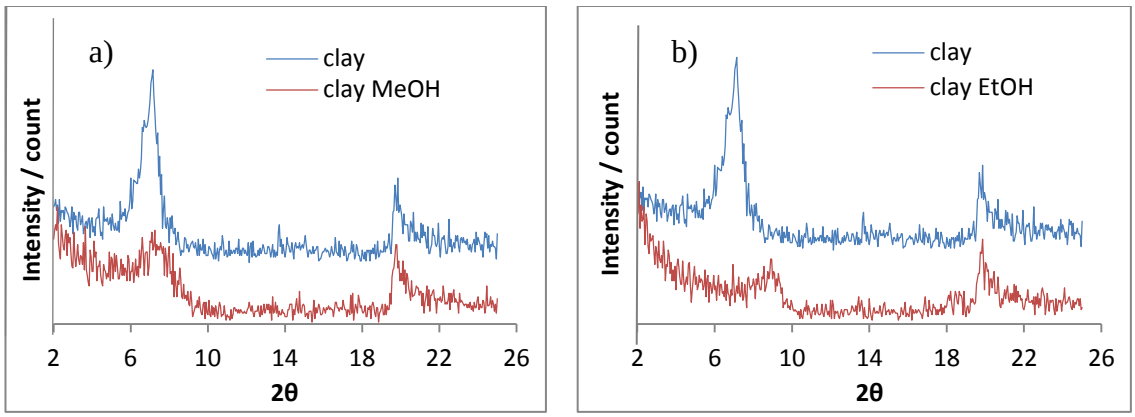

Figure 65. X-ray diffraction spectra of the A) clay with methanol and B) clay with ethanol

When the monomers caffeic acid and chlorogenic acid were mixed with the clay in a methanol solution and put under ultrasound for 10 min, as indicated in section 2.2.6, it was observed from the X-ray diffraction pattern that caffeic acid does not intercalate as the peak at 7.1° from the pure clay does not shift (Figure 66-A). In the case of the chlorogenic acid, the total disappearance of the pure clay peak at 7.1° was observed, indicating that the monomer assists exfoliation of the clay layers thus separating them (Figure 66-B). These results indicate that polymerization of chlorogenic acid with clays as reinforcement additive deserves to be tested.

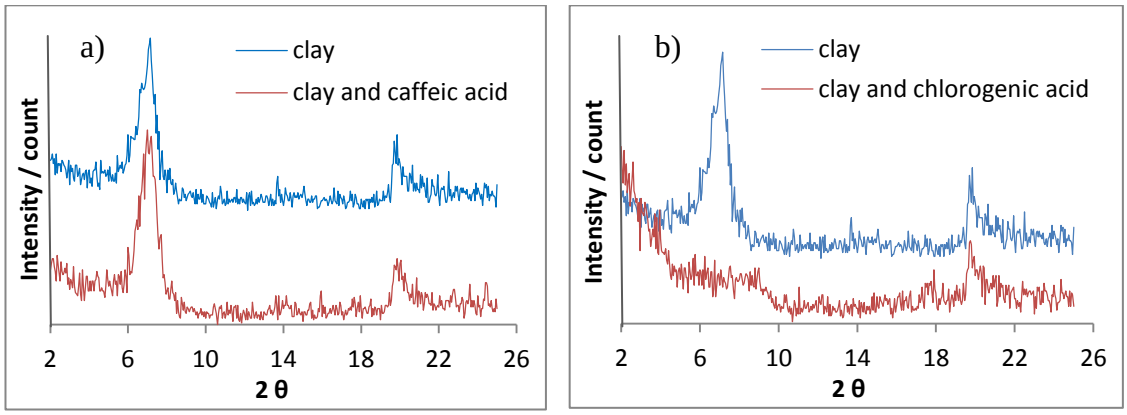

Figure 66. XRD spectra of A) clay with caffeic and B) clay with chlorigenic acid. Both in methanol solutions

4.5 Thermal analysis

In addition to the FT-IR, ^{1}H and C NMR analyses, the melting point and Differential Scanning Calorimetry (DSC) analysis of the polymers obtained were measured and compared to their respective monomer in order to confirm the conversion of the monomer through the polymerization reaction.

4.5.1 Melting points

The melting points obtained are shown in Table 57. For phenol, 1,2-DHBA and 2,3-DHBA it was observed that the polymers obtained presented a higher melting point, indicating strong intermolecular forces and a more thermally stable structure than the monomer. The polyphenols obtained presented low melting points, which could suggest that high molecular weight polymers were not formed. Nevertheless in the DSC thermograms of the polyphenols obtained (Figure 67), endoterm peaks are observed in the same range of temperature which suggests a change in the structure. Moreover when these are compared to the results from other authours who worked in enzymatic polymerization of phenol, comparable peaks are observed at similar temperatures.[294,337,338] However, TGA analyses in different studies suggest that the polyphenols obtained are thermally stable due to the low (10-15) percentage weight loss at high temperatures (350-375 ºC). [294, 336-339]

In case of chlorogenic acid, the polymer obtained without using PEG as a template had a similar melting temperature to the monomer, while the presence of PEG decreased it by 16 °C, indicating the formation of a complex between PEG-chlorogenic acid by strong intermolecular interactions. As for the caffeic acid, same behaviour can be observed where the formation of a complex with the PEG is demonstrated, while the polycaffeic acid obtained in aqueous solution presented a lower melting point. Polymers obtained from 2,4-DHBA and 3,5-DHBA also presented lower melting points than the monomers. The change of melting points indicated the transformation of the monomer into new structures.

Table 57. Melting point of the polymers obtained from potato waste.

	Melting Points / °C				
	Monomer	Polymers obtained in			
		pH7 Pi buffer	aqueous sol	no PEG	PEG
Phenol	42	64	54	50	56
Caffeic acid	209	-	199	217	180
Chlorogenic acid	207	-	NP	208	191
1,2 Dihydroxybenzene	106	121	112	-	-
2,3 Dihydroxybenzoic acid	208	186	186	-	-
2,4 Dihydroxybenzoic acid	218	192	NP	-	-
3,5 Dihydroxybenzoic acid	239	231	231	-	-
PEG	53	-	-	-	-

NP = not possible to read as not enough polymer was obtained

4.5.2 Differential Scanning Calorimetry analysis

DSC analysis of polyphenol is presented in Figure 67. This analysis was also made in Kim work[293], but results from the DSC analysis of the polyphenols obtained in this project cannot be compared to those in the literature as they measured the data in the second heating, while the instrument used here did not have cooling system. The peak at 44 °C is due to the melting of the phenol (Figure 67 – B, black line). The disappearance of the phenol peaks from the polymer charts, indicate that the monomer structure has been modified and new component were formed during the polymerization reaction.

The peak at 54 °C is due to the melting point of PEG (Figure 67 – A, green line), this peak can also be observed in DSC chart of the polyphenol obtained with PEG (Figure 67 – C, blue line), indicting the presence of the PEG-phenol complex in the polymer structure. When the two polymer charts were compared, it was observed the polymer obtained without using PEG (Figure 67 – C, red line) presented several peaks indicating decomposition of the structure with the temperature while the use of PEG during the polymerization created a more thermally stable component as indicated by the continuous line of the polymer chart (Figure 67 – C, blue line).

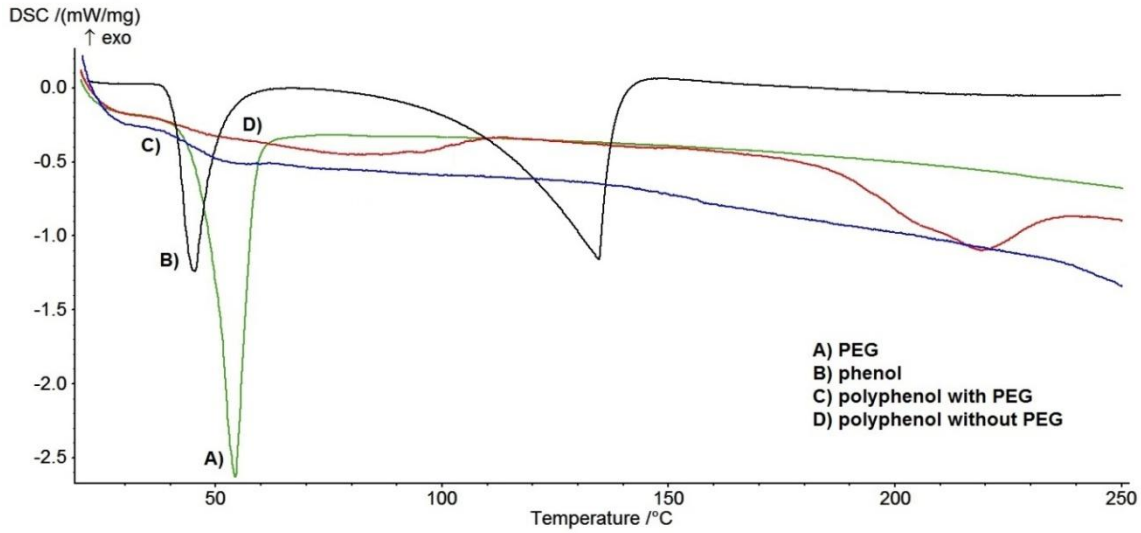

Figure 67. DSC thermograms of A)PEG, B) phenol, C) polyphenol with PEG and D) polyphenol without PEG

The peaks at 220 °C and 228 °C of the caffeic acid (Figure 68 – B, black line) can no longer be observed in the DSC traces for polymers, due to the formation of new structures. The curve observed at 69 °C in the polycaffeic acid obtained with PEG (Figure 68 – C, blue line) can be suggested to be the shift of the peak at 54 °C of the PEG (Figure 68 – A, green line) due to the polymerization between the monomer and the PEG. The presence of two depressions at 187 °C and 214 °C in the polycaffeic acid

obtained without PEG suggest the instability of the structure at high temperatures (Figure 68 – D, red line).

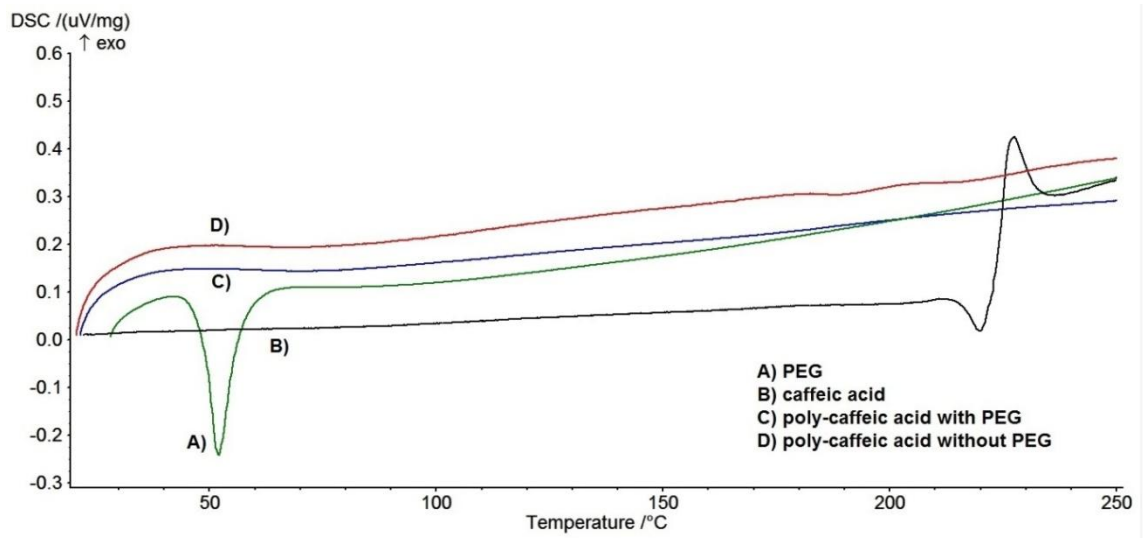

Figure 68. DSC thermograms of A) PEG, B) caffeic acid, C) polycaffeic acid with PEG and D) polycaffeic acid without PEG

As for chlorogenic acid polymer analyses, the peak at 204 °C (Figure 69– B, black line), which indicates the melting temperature of the monomer, is observed in a shifted position in the polymers trace. For the polymer obtained with PEG (Figure 69 – C, blue line) the melting temperature was observed at 191 °C, being lower to the one presented at 196°C from the polymer obtained without PEG (Figure 69– D, red line). This change indicated new intermolecular interactions in the polymer structure compared to the monomer. Conchoidal fracture was observed in the polymers when they were manipulated.

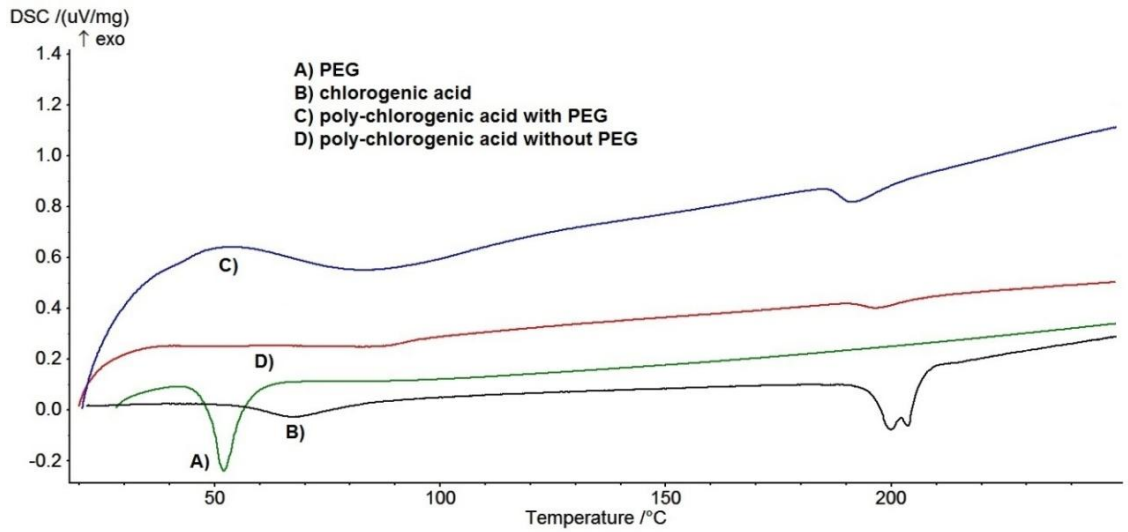

Figure 69. DSC thermograms of A) PEG, B) chlorogenic acid, C) polychlorogenic acid with PEG and D) chlorogenic acid without PEG

5. Results and Discussion of Mango Seed Butter Experiments.

This chapter is based in the creation of a polymer derived from the mango seed, a renewable resource which in many cases is left as waste material or used for the production of butter rich in oleic and stearic acid. The results from the purification of oleic acid from mango seed butter, its esterification and the epoxidation of the double bonds found in the structure of the di-ester obtained, are presented in here. Subsequently the polymerization of the epoxidized monomers by use of anhydride and amine curing agents is discussed. Furthermore, a study of the interaction between the monomers and their respective epoxides with montmorillonite clay was made, with the purpose of exploring the possibility of a nano-composite polymer production.

The experiments of this chapter were prepared, carried out and analysed by Miss Yingxue Hu. The author devised and supervised the project during the development of the experiments and interpreted the results.

5.1 Separation of oleic acid from mango seed butter

As indicated in G. Haraldsson's work,[297] saturated fatty acids (stearic and palmitic acids) have higher melting points than the unsaturated (oleic acid) ones. Therefore during the solvent fraction process, the liquid mixture has to decrease to a temperature at which the majority of saturated fatty acids crystallize while the unsaturated acids remain in solution. This separation principle can be observed in Figure 70.

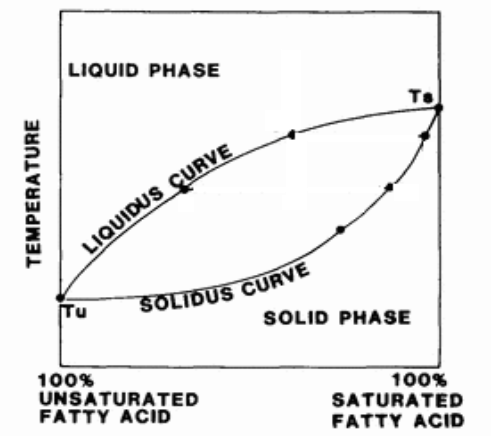

Figure 70. Binary phase diagram for a saturated and an unsaturated fatty acid.[297]

Theoretically, half of the butter is composed of oleic acid; therefore when 3 g of mango butter were dissolved in 30 ml of acetone, 1.5 g should have been obtained. Nevertheless, only 0.5 g of oleic acid was obtained, giving a total yield of 32 %. This could suggest that the presence of the other fatty acids, even when their presence is of 1-4 %, may influence the crystallization mechanism.[297]

The proper separation of oleic acid from the mango seed butter was confirmed by FT-IR and ^{1}H NMR spectra. Figure 71 shows the FT-IR spectrum of the extracted oleic acid. The first two sharp peaks at 2927 and 2856 cm^{-1} indicate the asymmetric and symmetric CH_2 stretch vibrations, respectively. The next sharp peak at 1746 cm^{-1} is attributed to the presence of the C=O stretch and almost overlaps with the small peak observed at 1725 cm^{-1} which corresponds to the C = C stretching vibrations. The peak at 1171 cm^{-1} is due to the C-O bond vibration. The peaks in the regions of 1400 and 700 cm^{-1} are assigned to the OH in-plane and out-of-plane bands, respectively.

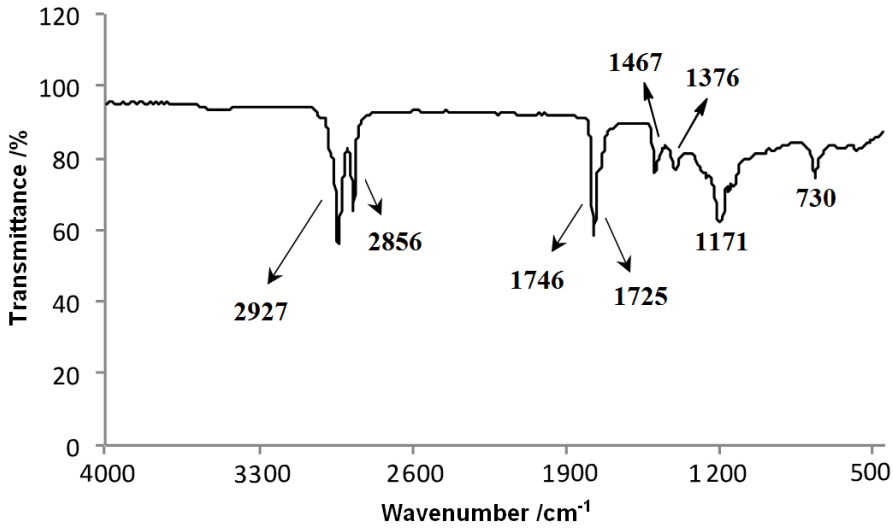

Figure 71. FT-IR spectrum of oleic acid obtained from mango seed butter.

In case of the ^{1}H NMR spectrum (Figure 72), the presence of C=C bond can be seen clearly at 5.33 ppm which indicates the H_A protons on the sp^2 carbons of oleic acid chain. The signals at 2.29, 1.98, 1.58, 1.28, 1.24 and 1.23 ppm correspond to the methylene internal groups of the protons H_B, H_C, H_D, H_E, H_F and H_G, respectively. At 0.86 ppm, the signal for the terminal methyl group proton H_J can be observed.

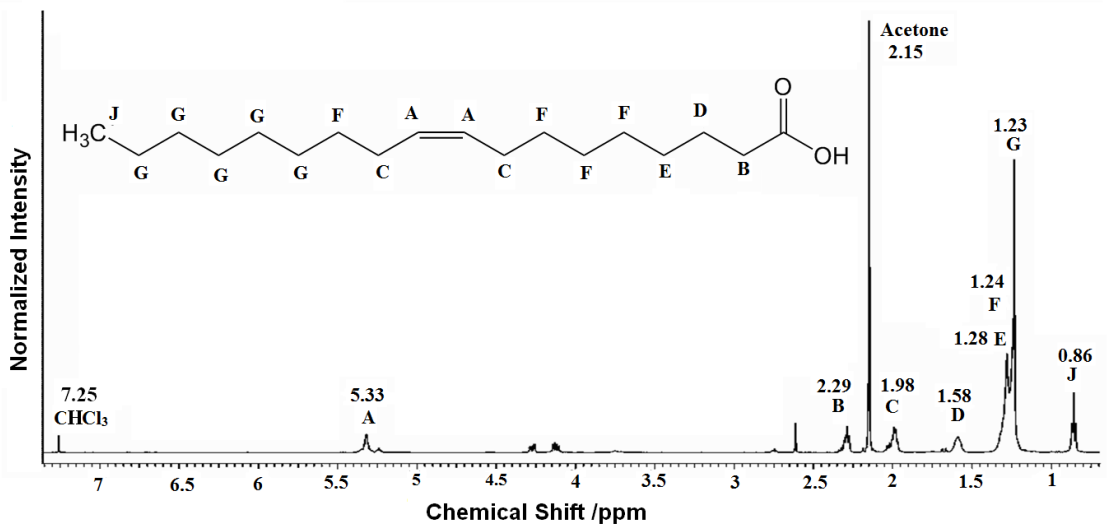

Figure 72. ^{1}H NMR spectrum of oleic acid separated from mango seed butter

5.2 Esterification of oleic acid

Esterification was performed as indicated in Section 2.5.2 using reagent oleic acid bought directly from Sigma Aldrich without further modifications. The chemical structure of the di-esters using different diols was confirmed by FT-IR and ^{1}H NMR analyses.

The comparison of FT-IR spectra of pure oleic acid with the di-esters (Figure 73) shows a peak at 1165 cm^{-1} for 1,3-propanediol and at 1129 cm^{-1} for orcinol and resorcinol which indicates C-O single bond ester stretching vibration.[340] Furthermore, the decrease and almost disappearance of the peak at 1444 cm^{-1} which corresponds to the OH band vibration of the reagent oleic acid, which is used for the ester linkage with the diol, indicates that esterification took place. Nevertheless, FT-IR analysis was not very accurate therefore ^{1}H NMR was also applied to confirm the esterification.

The reaction between oleic acid and 1,3-propanediol was confirmed in the ^{1}H NMR spectrum (Figure 74 – a) by the presence of the peak at 4.12 ppm, which describes the H_A protons of the methylene groups attached to the oxygen in the ester groups. Di-esters formed from orcinol and resorcinol were confirmed by the absence of a multiplet between 3.0–5.0 ppm which would have indicated the presence of -OH protons or an aliphatic hydrogen adjacent to an oxygen (Figure 74 – b, c).[340]

Moreover, the signals at 5.3 ppm corresponding to the H_A proton of a double bond can be seen in each di-ester spectrum, which indicates that during the esterification reaction the double bond of the oleic acid is not affected.

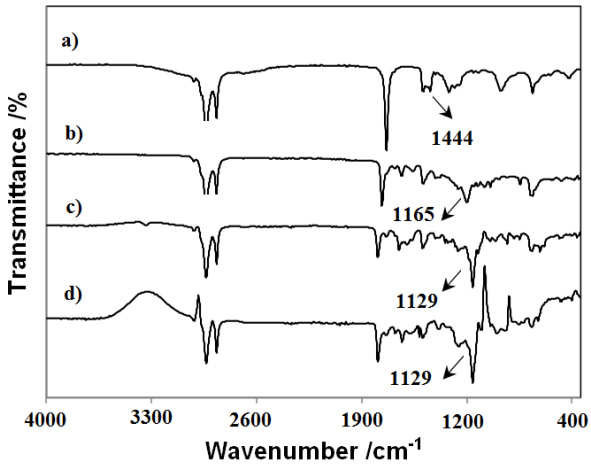

Figure 73. FT-IR spectrum of oleic acid di-ester from a) oleic acid, b)1,3-propanediol, c) orcinol and c) resorcinol

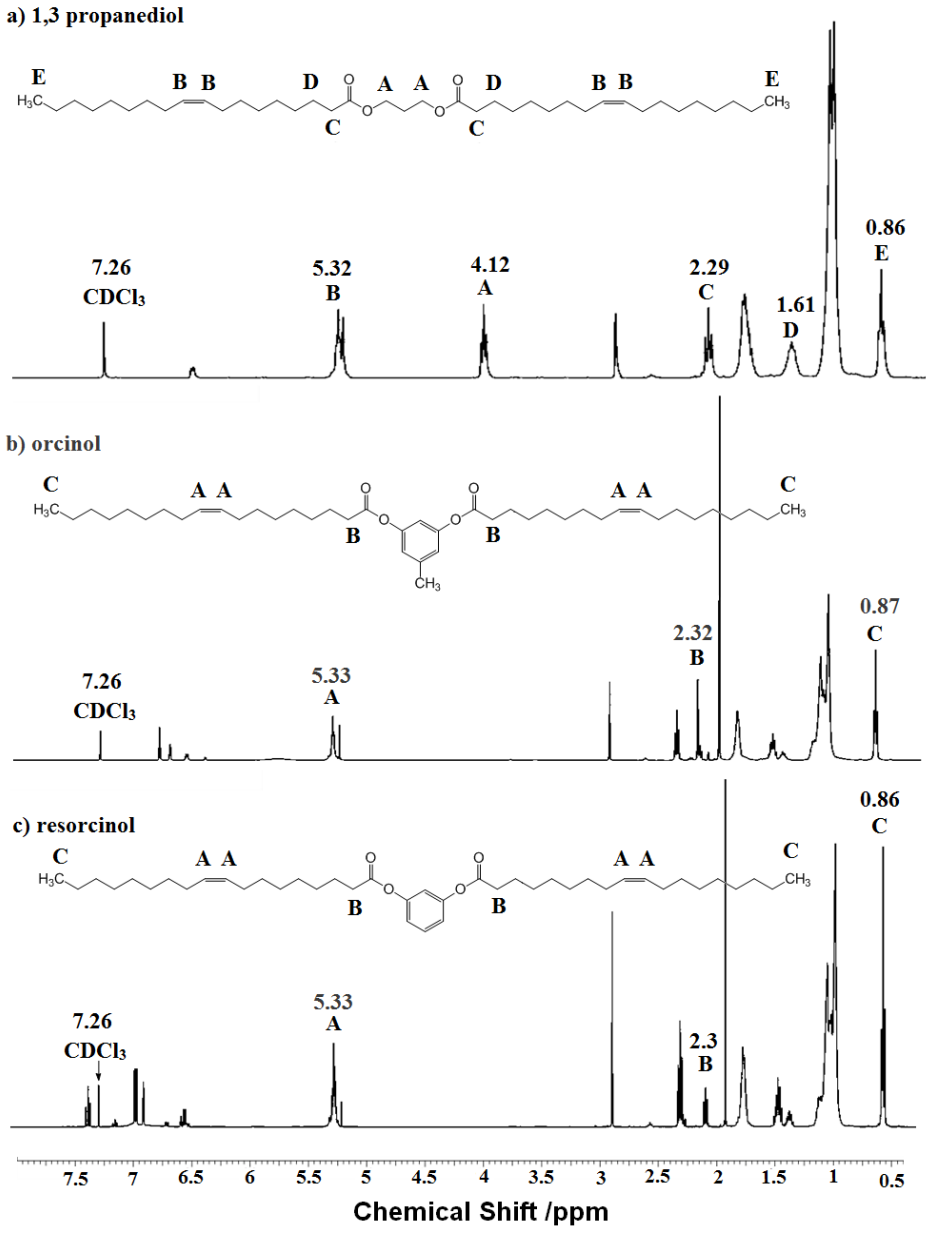

Figure 74. ^{1}H NMR spectrum of oleic acid di-ester from a) 1,3-propanediol, b) orcinol and c) resorcinol

5.3 Epoxidation of oleic acid and di-esters

Epoxidation of the monomers was confirmed by ^{1}H NMR because the characterization of the epoxy group is clearer by this method. A complete epoxidation should be indicated by the total disappearance of the signal at 5.3 ppm which corresponds to the H protons of the double bond (as seen on Figure 74) and the appearance of a peak at 2.9 which describes the H protons of the cyclic ether ring of the epoxy group.

According to the ^{1}H NMR spectra of the epoxidized monomers (Figure 75), the epoxidation of the reagent oleic acid reached 100% conversion as no evidence of a signal at 5.3 was observed (Figure 75-a). However, the spectra of the epoxidized di-esters still have this signal, indicating persistence of vinyl hydrogens, hence a partial epoxidation of the di-esters. From the integrated ratio of the double bond peak and the epoxy group peak, is possible to calculate the ratio of each and consequently the percentage epoxidation. In the case of 1,3-propanediol di-ester it indicated a conversion of 50% (Figure 75-b), while for orcinol di-ester the ratio of double bond to epoxy group was 0.07:1 indicating a 93 % epoxidation yield (Figure 75-c) and finally for resorcinol di-ester the ratio of 0.01:0.02 designated a conversion of 66 % into epoxy groups (Figure 75-d).

It is important to mention that during the epoxidation process in the presence of formic acid, the hydrogen peroxide may also break the ester linkage of the di-ester. In case this would happen, the ^{1}H NMR spectrum would show a signal at 2.7 for the –OH protons of the 1,3-propanediol molecule and signals around 9.1 ppm indicating the –OH protons of separated orcinol or resorcinol molecules. However these do not appear in the ^{1}H NMR spectra, suggesting that there was no ester linkage break down.

A summary for the epoxidation process is shown in Table 58. Even though the same ratio of reactants and the same reaction conditions were used for the three linking agents, the yield efficiency differed.

Table 58. Epoxidation of oleic acid and di-esters summary

Linking agent	**Vinylic hydrogen / epoxide hydrogen ratio**	**Yield %**
-	0	100
1,3-propanediol	1:1	50
Orcinol	7:100	93
Resorcinol	1:2	66

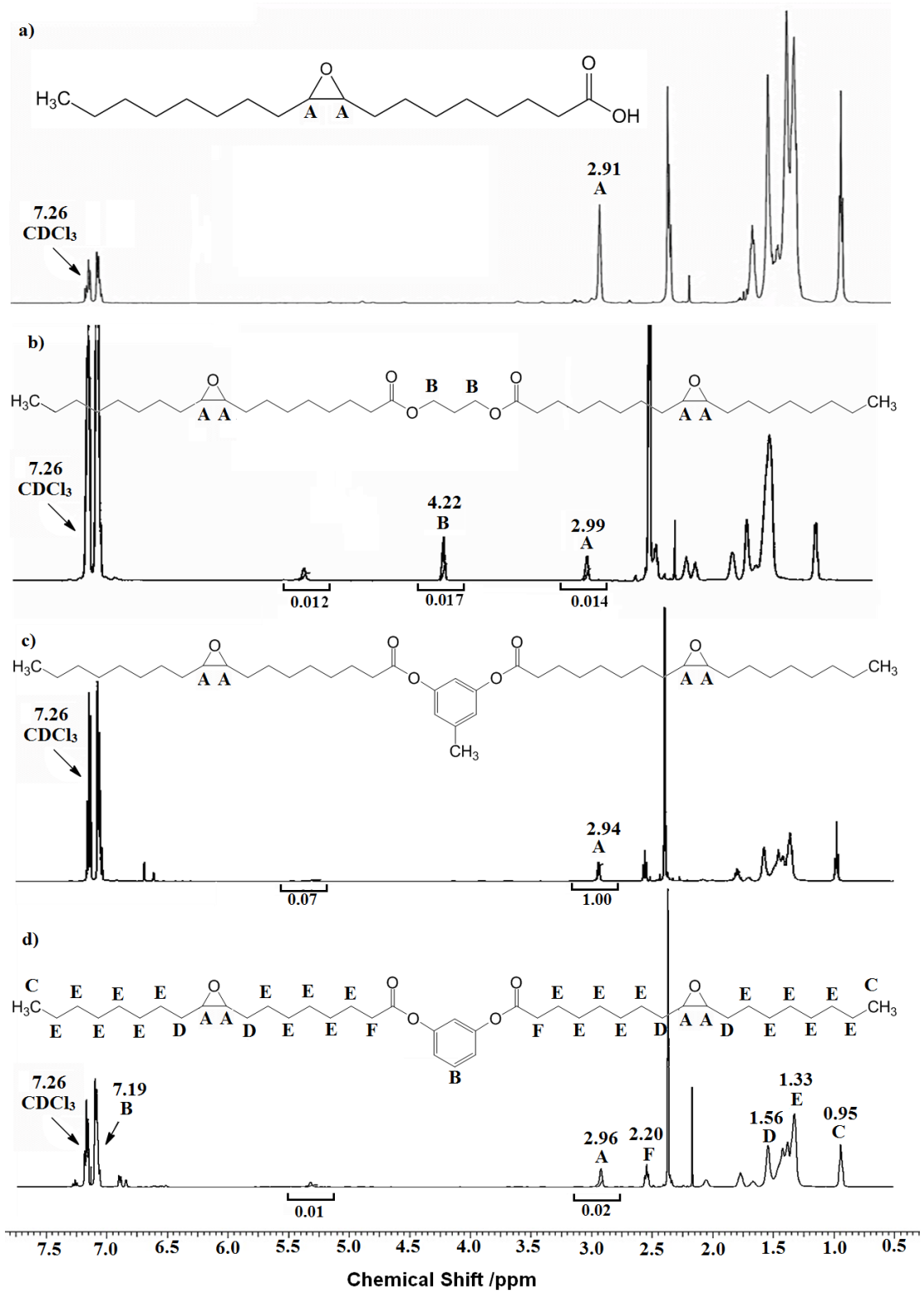

Figure 75. ^{1}H NMR spectrum of epoxide from a)oleic acid, b)1,3-propanediol di-ester, c)orcinol di-ester and d)resorcinol di-ester

In Scheme 38 is presented the esterification reaction of oleic acid, followed by the epoxidation of the di-esters obtained. The chemical structures were confirmed by the FT-IR and ^{1}H NMR analysis as previously discussed.

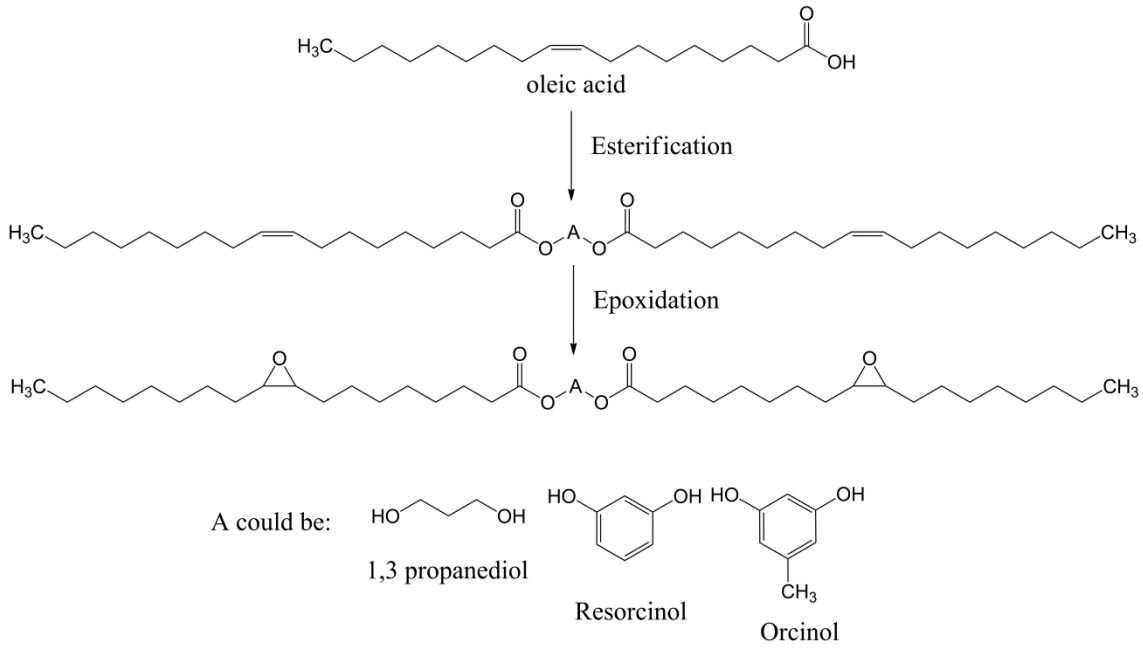

Scheme 38. Reaction for esterification and epoxidation reactions

5.4 Characterization of the products obtained from curing reaction.

The polymerization of the epoxidized monomers was attempted using curing agents for the crosslinking of the chains. In this project, two different crosslinking agents were used: (i) amines and (ii) anhydrides.

According to Tillet et al[341] the curing process of amine and epoxy groups employs stoichiometric ratios and is achieved at room temperature as amines exhibit high nucleophilicity. As for anhydrides, reactions usually use a catalyst to accelerate the curing process.[342]

5.4.1 Anhydride curing agent

It has been previously reported that the polymerization reaction of epoxidized oleic acid using cyclic anhydride as curing agent produces neither crosslinked polymers[301] or rubber-like or highly flexible polymers.[302] Therefore, firstly reagent oleic acid was used to establish these results before using the di-esters for the reaction.

The polymerization of epoxidized oleic acid using cyclic anhydride as curing agent has been previously reported using 165 °C for 3 hours in Nicolau's work[301] and at 200 °C during 1 hour in Rosch's work.[302] The reaction works in the presence of tertiary amine as initiator. The first step is the opening of the oxirane ring from epoxide by tertiary amine to form an alkoxide. Then anhydride is attacked by alkoxide and the

crosslinking between chains takes place in order to create a polymer. The general reaction mechanism can be seen in Scheme 39.

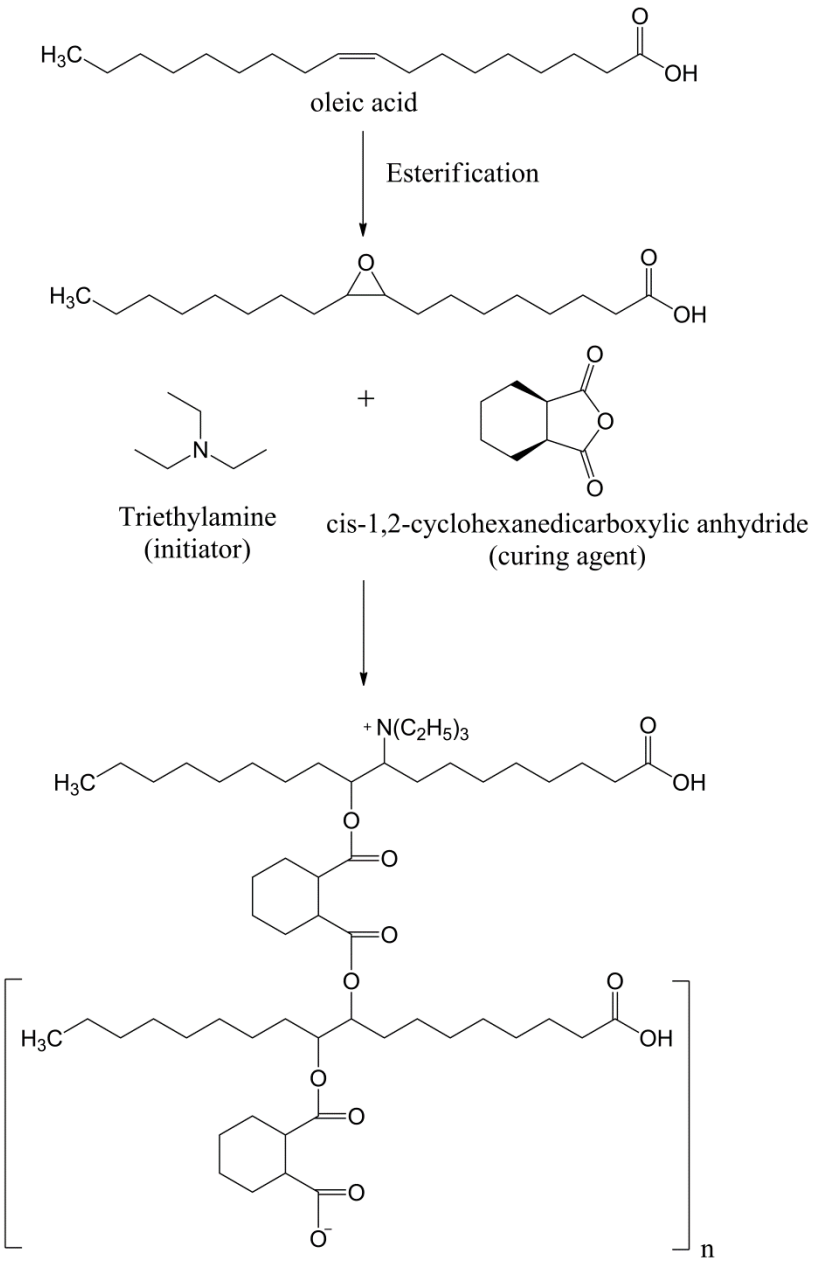

Scheme 39. The mechanism reaction of oleic acid with anhydride. n= polymer degree

The FT-IR spectra of the polymers obtained are shown in Figure 76. The peaks observed in the region of 1735-1729 cm^{-1} are attributed to the stretching vibrations of the C=O of the carboxylic group. The bands at 1250 and 1170 cm^{-1} correspond to the C-O-C bonds of the ester linkages. Peaks around 3000 cm^{-1} represent the CH_2 asymmetric and symmetric stretching vibrations.

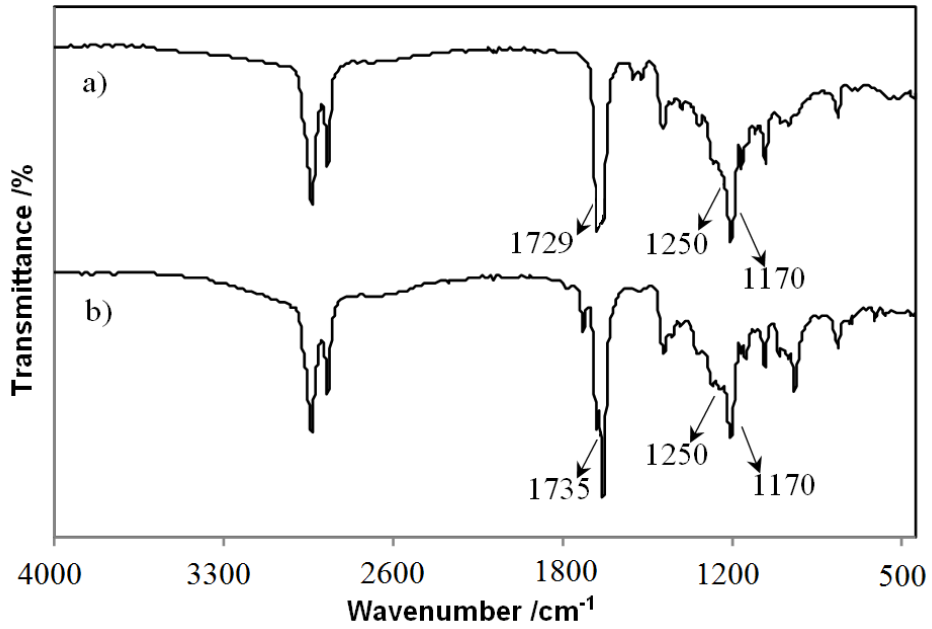

Figure 76. FT-IR spectrum of polymers obtained of epoxidized oleic acid at a) 165 °C for 3h and b) 200 °C for 1h

Figure 77 shows the ^{1}H NMR spectrum of anhydride curing products obtained at 165 °C and 200 °C from epoxidized oleic acid. The singlet at 4.98 ppm is attributed to the H_D protons of the ester linkage formed by the incorporation of the anhydride to the EOA chain while the triplet at 3.07 ppm corresponds to the H protons of the cyclic ether ring of the unreacted epoxy group. The peaks at δ 1.63 and 2.06 ppm correspond to the H_B and H_C protons of the cyclohexane ring of the anhydride and the δ 0.88 ppm to the H_A proton of the terminal methyl group of the oleic acid.

From the integrated ratio of the oxirane ring peak and the ester linkage peak, the reaction efficiency was determined. For the reaction using 165 °C for 3 hours the ratio was 1:3, indicating an efficiency of 67%; while the reaction at 200 °C during 1 hour presented a ratio of 1:2 giving a yield of 50%.

During the ^{1}H NMR analysis it was observed that the polymers obtained were able to dissolve in organic solvents, such as chloroform, DMSO, acetone, toluene and DMF indicating that it was not crosslinked. It can be suggested that dimers were formed instead. According to the literature, the hydrogen bonds in fatty acids dimers produce a weakening in the C=O bonds creating a shift to lower signals of the stretching vibrations in the FT-IR spectra.[343] In monomers of saturated aliphatic acids, the C=O stretching vibration is observed around 1760 cm^{-1}, compared to the 1729 and 1735 cm^{-1} peaks observed in the experimentation. This indicated the presence of the hydrogen bonds and consequently the formation of dimers.

As the polymers obtained with these methods were not crosslinked, according to the characterization previously made by ^{1}H NMR and FT-IR, further experimentation using the di-esters were made using only amine as curing agents. Nevertheless, it is important to mention that future work using aromatic dicarboxylic anhydrides as curing agents for epoxidized di-esters should be studied.

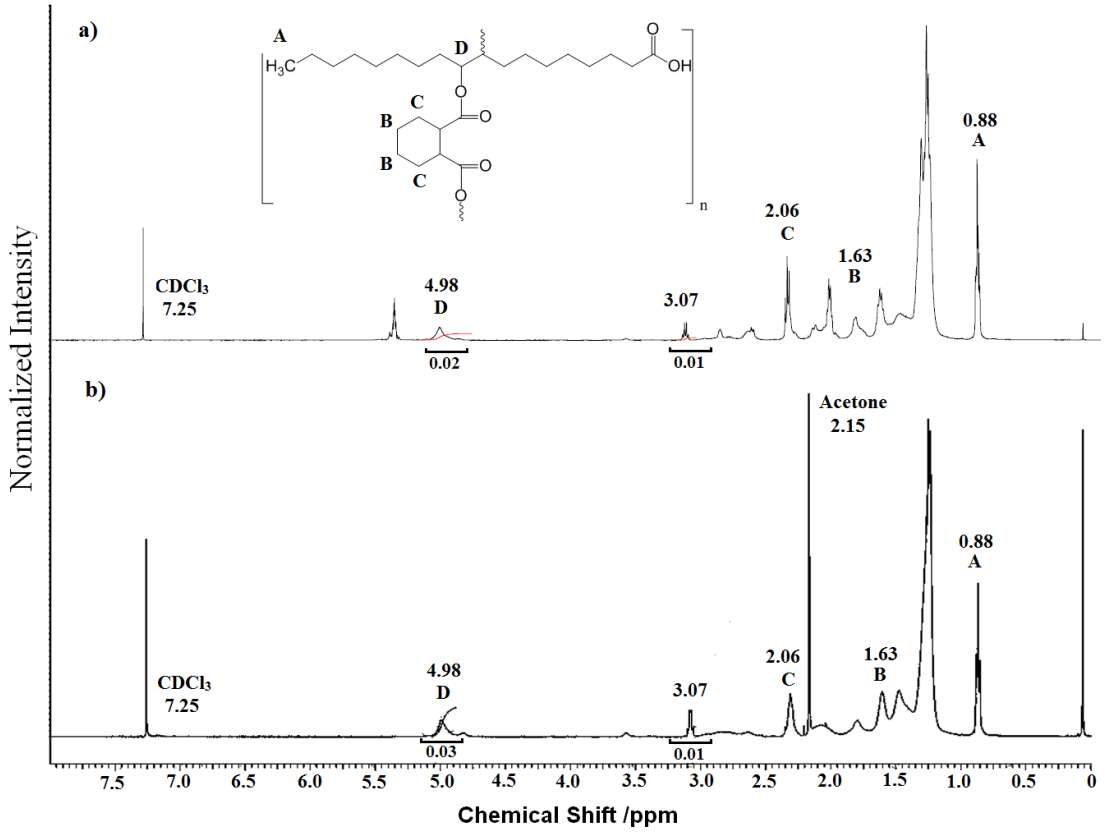

Figure 77. ^{1}H NMR spectrum of polymers obtained of epoxidized oleic acid at a) 200 °C for 1h and b) 165 °C for 3h, where n = degree of polymer

5.4.2 Amine curing agent

For this project diethylenetriamine (DET) and ρ-phenylenediamine (PPD) curing agents were tested with each of the epoxidized oleic acid di-esters previously synthesized with 1,3-propanediol, orcinol and resorcinol in section 5.3. The reactions were accomplished at room temperature in a 1:1 ratio of amine and epoxy group. The potential structures of polymers obtained with DET and PPD as amine curing agents are shown in Figure 78. Theoretically, each reactive hydrogen of the amine groups reacts with one epoxy group. Therefore, one DET molecule should link to five epoxy groups while PPD to four, giving as a result a crosslinked polymer.

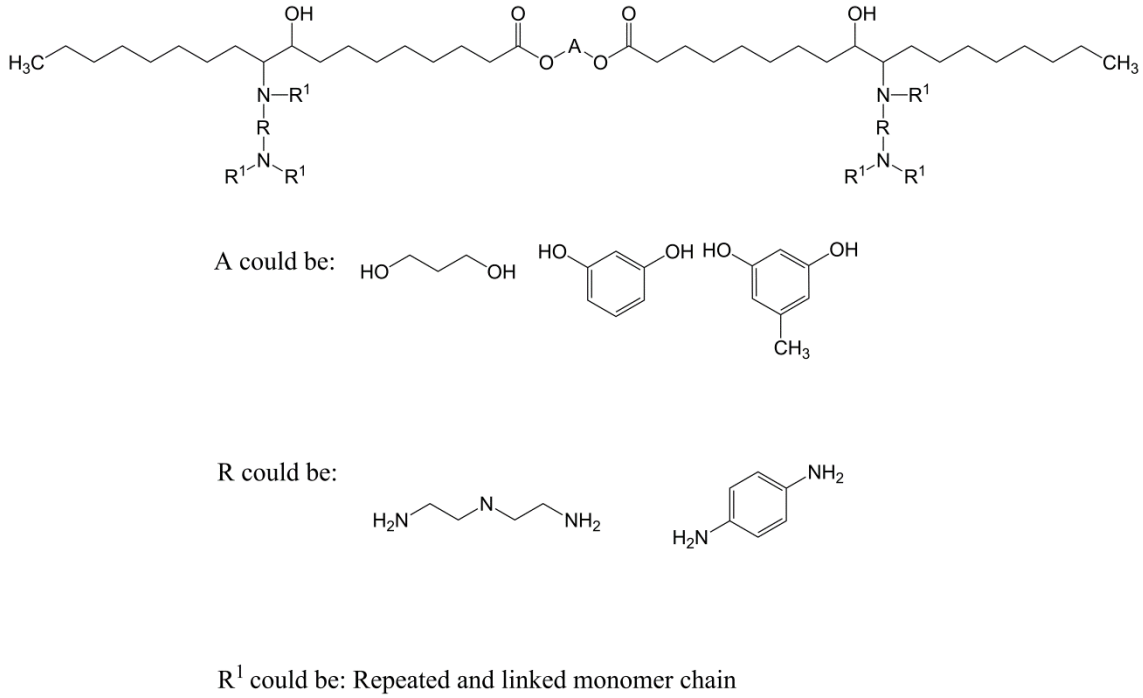

Figure 78. Products obtained from curing reaction with amine crosslink agents.

Figure 79 shows the FT-IR spectra of the products obtained from the curing reactions of epoxides with DET and PPD. As can be observed, all the spectra present similar profiles. The benzene rings can be identified from the C=C linkages vibrations in the region of 1450 – 1600 cm^{-1} and their =C-H bond vibrations which are found in the region of 900-800 cm^{-1}. The peaks in the region of 3350-3400 cm^{-1} can be attributed to the N-H bond vibration of the amine group from the curing agents, indicating that there is residual amine unreacted. Nevertheless, the broadening of the signal in the region of 3200-3570 cm^{-1} could be ascribed to the stretching vibrations of -OH groups from the opening of the oxirane ring needed for the curing reaction and the C-N bonds vibrations which can be observed in the peaks at the region of 1130-1190 cm^{-1}. For further understanding of the reaction ^{1}H NMR spectra was also used for the characterization of cured products.

Firstly ^{1}H NMR analysis of PPD and DET were performed in order to properly analyse the spectra of the cured products obtained (Figure 80). In case the crosslinking reaction was successful, the signals at 3.32 and 0.90 ppm which are ascribed to the H_A protons of the amines in the PPD and DET respectively, should disappear from the spectra of the cured materials.

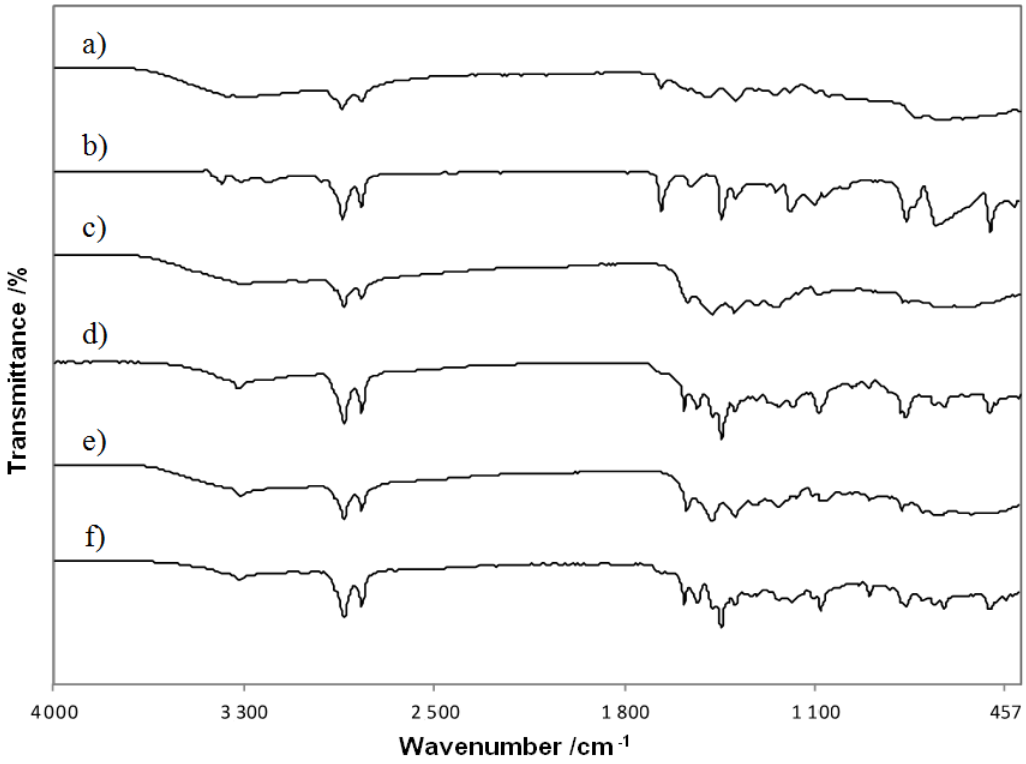

Figure 79. FT-IR spectra of the products from a) 1,3-propanediol di-ester/DET, b) 1,3-propanediol di-ester/PPD, c) Orcinol di-ester/DET, d) Orcinol di-ester/PPD, e) Resorcinol di-ester/DET and f) Resorcinol di-ester/PPD

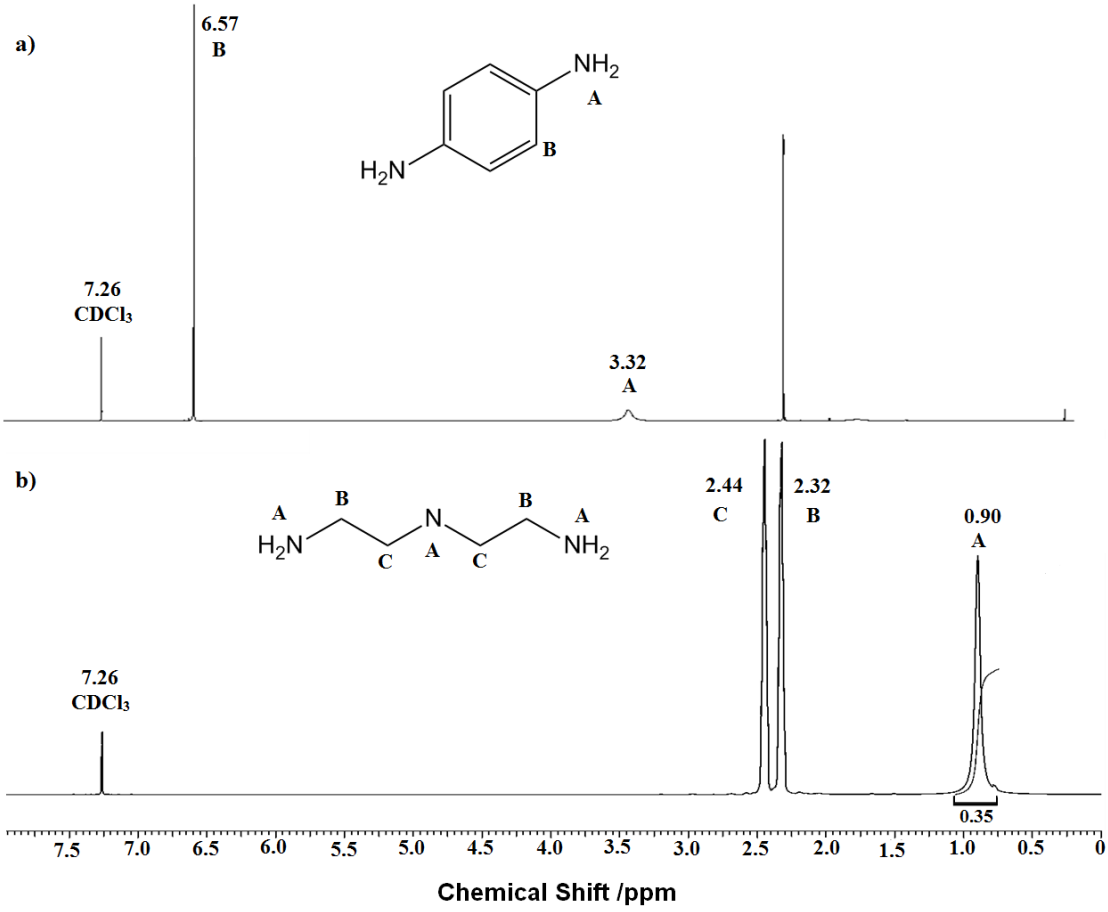

Figure 80. ^{1}H NMR spectra of a) ρ-phenylenediamine (PPD) and b) diethylenetriamine (DET)

The ^{1}H NMR spectra of the cured di-esters are shown in Figure 81. Peaks at 2.7 ppm are ascribed the H protons of C-N bonds formed between the di-ester chain and the curing agent.

In the case of the di-esters formed with 1,3-propanediol, when DET was used, the ^{1}H NMR spectrum (Figure 81 – A) did not present a signal at 3 ppm indicating the absence of epoxy groups, i.e. all oxirane rings were opened and the peak at 2.7 was observed. Nevertheless, there is the presence of a triplet in the region of 0.9 ppm indicating the existence of curing agent unreacted and hence an excess of DET in the reaction. The comparison of the integrated ratio between the C-N bond peak and the amine peak (1: 3.7) indicated that there was an excess of almost four times the amount of DET needed. As for 1,3-propanediol-PPD (Figure 81 – B) ^{1}H NMR spectrum shows peaks in the region of 2.7 ppm and the absence of the peak at 3.32 ppm indicating that all curing agent was used. However the existence of a small peak at 2.9 suggests the presence of oxirane ring, i.e. di-esters unreacted. By comparing the integrated ratio of the terminal methyl groups peak of the di-ester (δ 0.9 ppm**,** Figure 75) and the epoxy group peak, the 2% amount of unreacted di-ester was calculated.

For epoxidized orcinol di-ester the ^{1}H NMR spectrum using DET (Figure 81 – C) no signal at 0.9 ppm was shown and peaks in the region of 2.7 ppm were observed. In addition, the appearance of peaks in the region of 3.3 ppm was ascribed to the -OH protons formed after the opening of the epoxy group during reaction. These indicated that crosslinking between DET and epoxide took place and all curing agent was used. Nonetheless, the peak corresponding to the epoxy group at 2.89 ppm was observed and the 37.5 % of di-ester unreacted was determined from the integrated ratio of the oxirane ring peak and the -OH peak. On the other hand, by using PPD with orcinol di-ester the ^{1}H NMR spectrum (Figure 81 – D) showed an extremely weak signal at 2.7 and presence of a peak at 2.89, indicating that there was almost no evidence of C-N bond and the existence of epoxy groups, respectively. This indicated that reaction was not successful and by comparing the integrated ratio of the terminal methyl groups peak of the di-ester (δ 0.9 ppm**,** Figure 75) and the epoxy group peak it was observed that 70% on the di-ester did not reacted with the curing agent.

Finally the ^{1}H NMR spectrum for epoxidized resorcinol di-ester curing with DET (Figure 81 – E) shows an extremely weak peak at 2.91 indicating minimum presence of epoxy groups unreacted. It can be observed peaks at 3.32 and 2.8 ppm corresponding to the -OH protons and the H proton from the C-N bond, respectively. The 94% efficiency of the curing reaction was calculated by the integration ratio of the -OH protons peak

and the epoxy group peak, in this case the peak at 0.9 ppm was not used as there is an overlapping between the signals of the H protons of the methyl groups and the H protons of the amine in the DET. While for epoxidized resorcinol di-ester using PPD the ^{1}H NMR spectrum (Figure 81 – F) does not present signals showing the existence of amine hydrogen protons (δ 3.32 ppm) but either signals of C-N protons (δ 2.6 ppm) and either of -OH protons (δ 3.3 ppm). Only an extremely weak signal of epoxy group protons (δ 2.91 ppm) was observed. This could suggest that the di-ester crosslinked with the curing agent and only the di-esters unreacted were soluble in the solvent.

As previously observed in section 5.4.1, the cured materials obtained in this procedure were also in the form of waxes and were soluble in chloroform and acetone. It can be suggested that dimers were again formed as the shift into lower wavenumbers of the C=O stretching vibration was also observed, as happened with the epoxy oleic acid with anhydride curing agent.[343]

The purpose of using diethylenetriamine (DET) and ρ-phenylenediamine (PPD) as curing agents was to observe the difference between having a linear or an aromatic ring in the structure, as it is reported that an aromatic ring gives more stiffening to the chain and produces a more rigid polymer.[302] However, polymers obtained were in form of waxes and no difference was observed. Nevertheless, the wax obtained from the epoxidized resorcinol di-ester using PPD was the only one which could suggest the formation of a low molecular weight polyester.

It can be suggested that monomers react with themselves as the epoxides used for this project have long chains with more than 36 carbon atoms in their structure. For this reason, linking agents with aromatic rings were chosen to control the flexibility of the chains and decreases the chance for monomer reacting with itself.

In Table 59 is a summary of the results obtained from the curing reactions between amines and epoxidized di-esters left for 7 days at room temperature.

Table 59. Summary of results from epoxide/amine curing reactions.

Amine	Epoxide	Yield %	Sample	Observation
DET	1,3-propanediol	100	wax	Excess of DET
PPD		98	wax	Unreacted di-ester but no presence of PPD
DET	Orcinol	62.5	wax	Unreacted di-ester but no presence of DET
PPD		30	wax	Minimum indication of C-N bonds
DET	Resorcinol	94	wax	Overlapping of signals
PPD		-	wax	No signal of -OH, C-N or NH_2

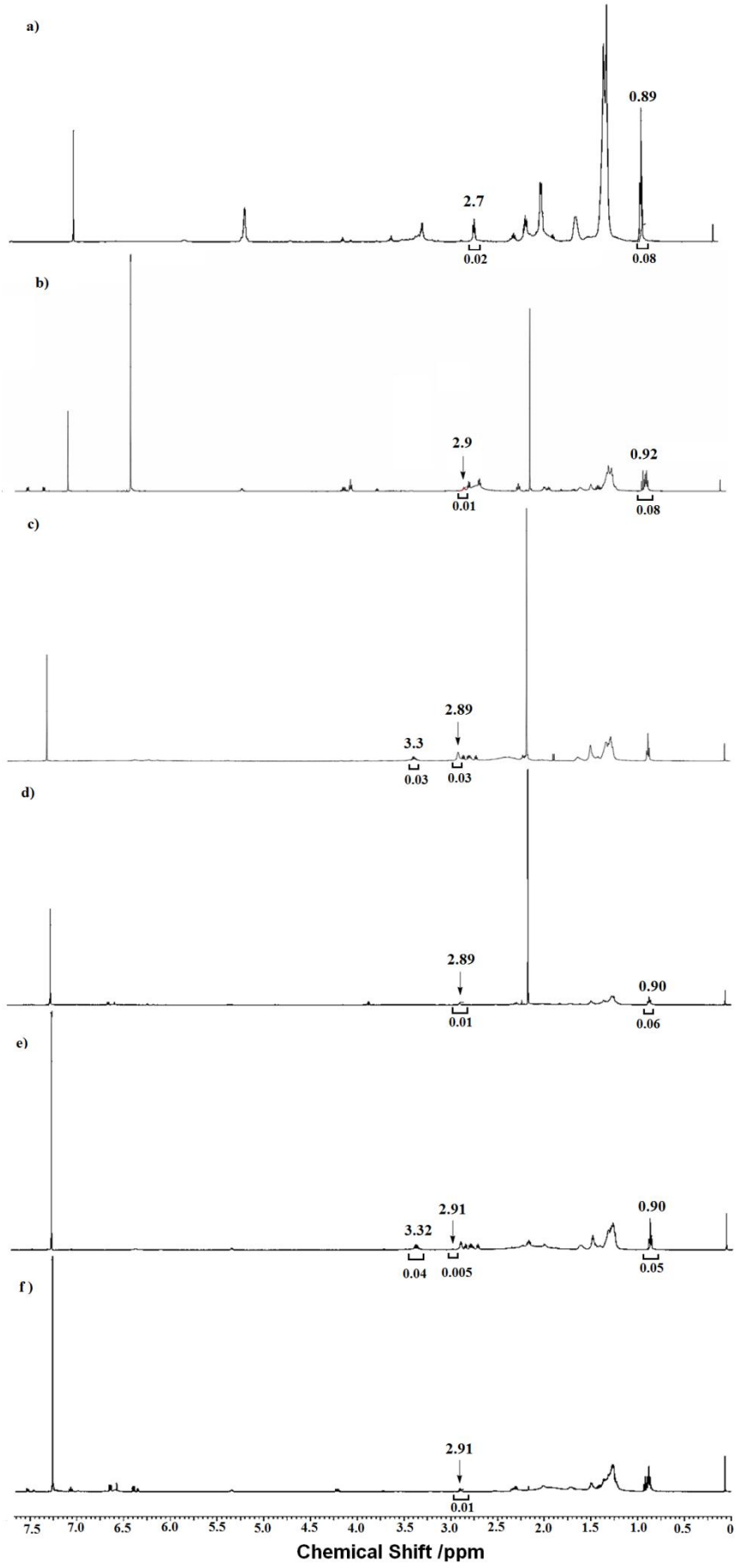

Figure 81. ^{1}H NMR spectra of a) 1,3-propanediol det, b) 1,3-propanediol ppd, c) orcinol det, d) orcinol ppd, e) resorcinol det and f) resorcinol ppd

5.5 Addition of clay

The study of oleic acid and its epoxide interaction with pure and modified montmorillonite clay was studied according to the indications made in section 2.5. This was made to establish the possibility of producing nano-polymer composites.

Six different modifications of the montmorillonite clay were used in this chapter: (i) montmorillonite clay, (ii) Cloisite 10 A, which is the clay modified with a benzyl (hydrogenated tallow alkyl)dimethyl, salt (iii) clay modified with L-lysine, (iv) clay modified with 12-aminolauric acid (ALA), (v) clay modified with diethylenetriamine (DET) and (vi) clay modified with phenylenediamine (PPD). Unmodified montmorillonite clay and Cloisite were purchased from Rockwood Additives and used without further modification, the modification of pure clay with L-lysine is explained in section 2.6.1 and the modification with ALA, DET and PPD were done by M.Sci. student Steve Johnson and the procedure is explained in his work.[344]

5.5.1 XRD study of monomers with pure montmorillonite clay.

The X-ray diffraction traces of the reagent montmorillonite clay and after its interaction with oleic acid or epoxidized oleic acid are shown in Figure 82. From the trace of montmorillonite clay an interlayer distance of 12.20 Å was calculated. When traces of mixtures of clay and oleic acid or epoxidized oleic acid are compared to the reagent one, it can be observed a shift in the peak, to smaller angles, indicating an increase in the interlayer spacing due to intercalation of the monomers. In the case of the clay interaction with oleic acid, two peaks were observed: one indicating an interlayer distance of 28.02 Å, having an increase of 129 % compared to the mmt clay and another at 12.71 Å, which is almost the same distance as the reagent oleic acid, which indicated that not all basal spacing was expanded as monomer intercalated with clay. While for clay-epoxidized oleic acid, three different peaks were observed in the XRD trace indicating interlayer distances of 42.03, 14.48 and 12.80 Å. The maximum interlayer space of 42.03 Å is 245% greater than that obtained with the reagent oleic acid.

The presence of different peaks could suggest that the time in which the clay interacts with the monomer affects the intercalation. For this reason, a sample of oleic acid with clay was left for 2.6 $x10^6$ s (30 days) with the purpose of identifying the effect of time on clay-monomer intercalation. However, the XRD trace did not indicate a bigger space between the clay layers but the opposite, as only one peak corresponding to 13.38 Å was identified which is smaller to any of the previous observed.

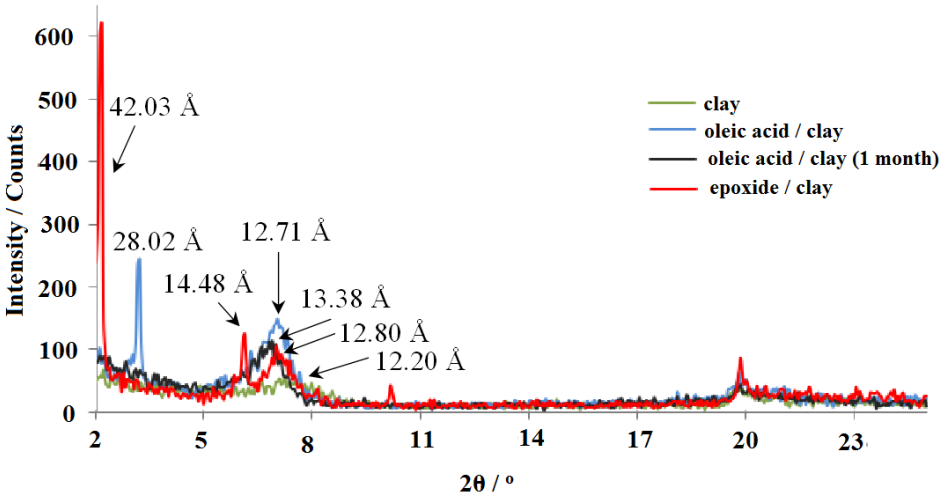

Figure 82. X-ray traces of pure clay, oleic acid-clay and epoxide-clay.

5.5.2 XRD study of monomers with DET, ALA and PPD modified clay

In Figure 83 the XRD traces for the modified clay and their interactions with epoxidized oleic acid are shown. These modified clays were chosen according to the results from Johnson's work.[344]

The DET modified clay interaction with the epoxide presented the higher interlayer spacing of 44.14 Å, which indicated an enlargement of 237% compared with the 13.08 Å of the DET-clay. However, not all epoxide interacted as two other peaks at 15.49 and 13.08 Å are also observed. As for ALA-clay interaction with the monomer, the distance was only increased by 1.52 Å while for PPD-clay it could be said that no interaction was observed as the interlayer space increased only by 0.21 Å.

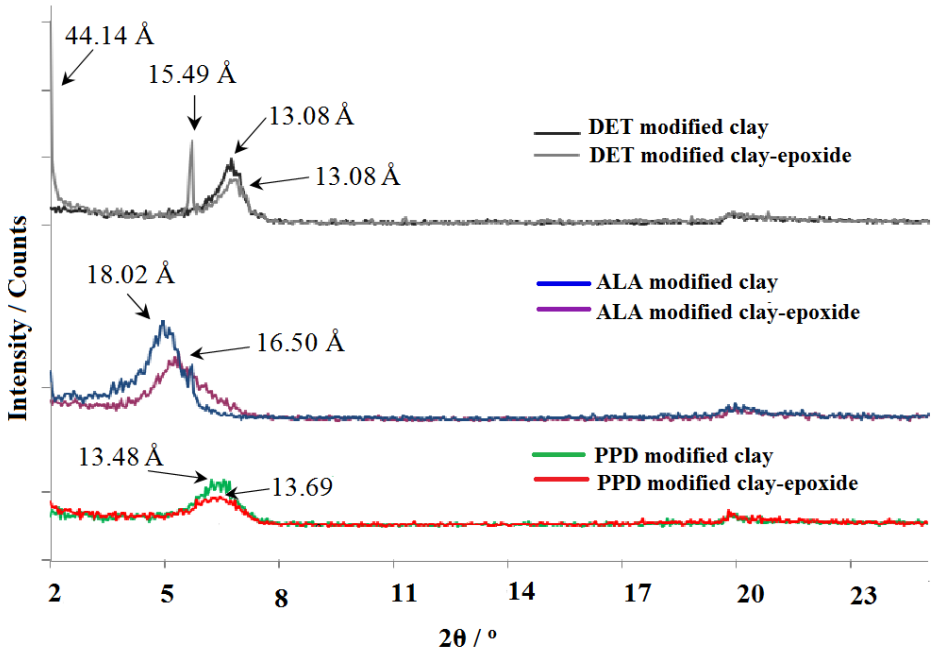

Figure 83. X-ray traces of modified clays and their mixture with epoxidized oleic acid.

5.5.3 XRD study of monomers with L-lysine modified clay

As attempted previously in section 3.3.2, the clay was modified with L-lysine in order to increase the interlamellar space and to create a stronger interaction between the clay and the monomer. The use of an aminoacid as a linking agent supports the aim of this project to have a mineral oil-free final product.

The XRD traces of the L-lysine modified clay with oleic acid and the epoxide are shown in Figure 84. It was observed that no interaction between the L-lysine modified clay with epoxidized oleic acid took place as the interlamellar space increased the minimum amount of 0.54 Å (from 14.13 to 13.59 Å). As for the interaction with oleic acid, three peaks are observed, corresponding to 42.03, 21.27 and 14.26 Å. The maximum enlargement was by 209 % compared to the 13.59 Å of the L-lysine modified clay.

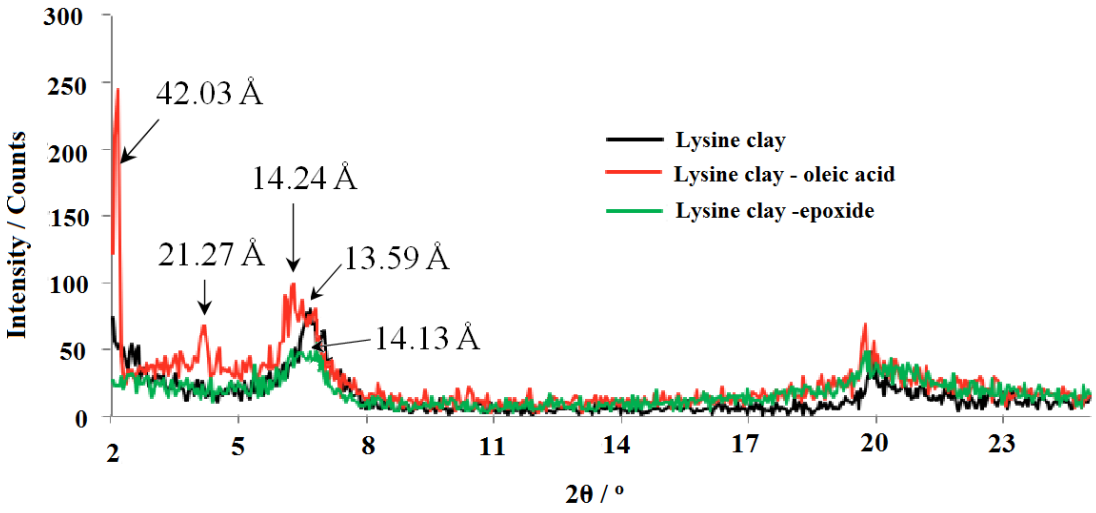

Figure 84. X-ray diffraction traces of L-lysine modified clay with oleic acid and epoxide

5.5.4 XRD study of oleic acid with Cloisite 10A

The use of an organophilic clay to increase the interaction between oleic acid and clay showed a positive result. As observed in Figure 85, the XRD trace shows the increase of the interlamellar space of the clay from 18.02 Å to a maximum distance of 42.03 Å. This indicated an enlargement of 133%. However a peak corresponding to 14.84 Å indicated a decrease of the spacing between layers. This behaviour between the organoclay and monomer was also observed in section 3.3.3 with d-limonene experiments, where it is suggested that all quaternary ammonium salt was used for the interaction and during the interaction some salt was extracted from a small percentage of the layers which therefore retracted to the natural basal space.

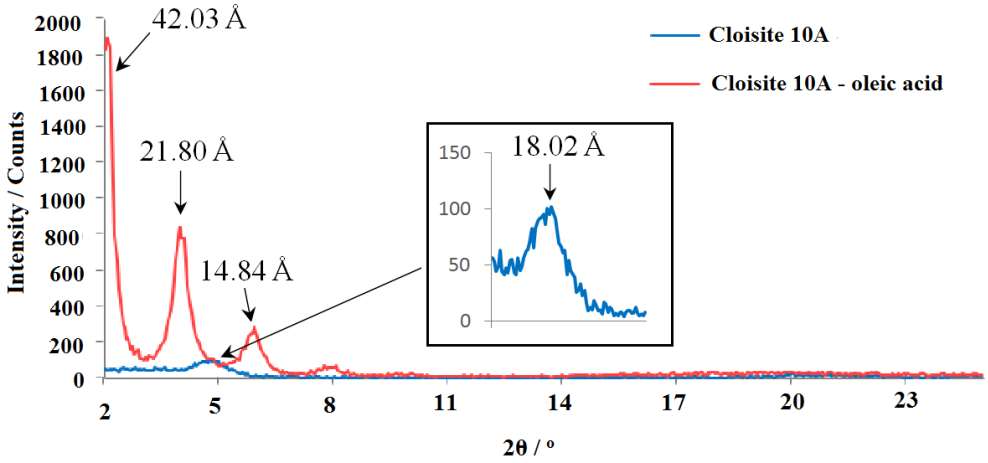

Figure 85. X-ray trace of organoclay with oleic acid.

5.5.5 Summary of results

A summary of the monomer interactions with the different modified clays is shown in Table 60.

From the results, it can be concluded that DET modified clay with epoxidized oleic acid presents the higher interaction with an interlayer spacing of 44.14 Å. As for (i) unmodified montmorillonite clay with epoxidized oleic acid, (ii) L-lysine modified clay with oleic acid and (iii) Cloisite 10A with oleic acid present an interlayer spacing of 42.03 Å. However the use of reagent montmorillonite clay is more suitable for an industrial procedure, as no further modification has to be done, hence the total price of a process would decrease.

Table 60. Summary of results for clay interaction with oleic acid and epoxidized oleic acid.

Clay	Monomer	Interlayer spacing Å
MMT	-	12.20
MMT	Oleic acid	28.02, 12.71
MMT	Oleic acid epoxide	42.03, 14.48
L-lysine	-	13.59
L-lysine	Oleic acid	42.03, 21.27, 14.24
L-lysine	Oleic acid epoxide	14.13
Organoclay	-	18.02
Organoclay	Oleic acid	42.03, 21.80, 14.84
ALA	-	16.50
ALA	Oleic acid epoxide	18.03
DET	-	13.08
DET	Oleic acid epoxide	44.14, 15.49, 13.08
PPD	-	13.48
PPD	Oleic acid epoxide	13.69

6. Conclusion

From the introductory part of this thesis it can be understood that three factors are likely to displace the polymer and composite materials market towards biomass resources and away from mineral oil feedstock. They are (i) the upward drift in mineral oil price, (ii) regulatory interventions intended to address climate change and (iii) consumer preference for "eco-products". This may have an impact on land-use, exacerbating the existing conflict between biofuel and food production. The intelligent redeployment of food waste materials extinguishes this conflict and potentially realigns the agricultural and industrial economic sectors: sectoral integration is sometimes seen as a source of economic stability. If these projections are correct, companies that have positioned themselves with the technology to exploit biomass resources are well placed to take advantage of a plentiful supply of food waste. A clear link between food producers, food processors and materials producers thus unfolds. At present, bio-polymers are starting to participate in the market as commercial PLA and PHA (Nodax®) are already an accepted part of the plastics industry.

Although there are many agricultural species which yield food production wastes, the raw materials that issue from them are few in number, principally fatty acids and terpenes, sugars, celluloses, starches, lignin, proteins, polyphenols and fibres. The limited range is however, compensated by the high tonnage of food wastes available, annually worldwide from the food-processing industry.

The main sources which could be deployed in biopolymer production are potato waste, mango seed, citrus peel, coffee waste, straw, sugar bagasse, pumpkin seed, banana peel, avocado seed, corn stover, carrot waste and peanut husk. Grape waste is also a candidate but its waste products are reasonably well integrated into the economy already. These types of food waste are the most viable and they are produced, processed and commonly used in the majority of countries in the world, even though the quantity varies according to the region, Human Developed Index of the country and consumer social behaviour.

There are three strategic pathways for biopolymer production: (i) chemical derivation from biomass, (ii) biochemical modification of the components or (iii) polymer precursor production in genetically modified transgenic plants. All provide a polymer product with added value. Furthermore, the characteristics of the bio-polymers thus obtained could be improved by using reinforcements themselves sourced from

natural resources such as plant fibres and smectite clays.

In the possibility of using citrus waste as a resource, the first part of this project demonstrates that it is possible to obtain dimethylstyrene from D-limonene without by-products such as terpinolene, γ-terpinene, α-terpinene, carvone, ρ-cymene, ρ-menthene and ρ-menthane. This make separation of product DMS from reactant limonene easier and opens up the possibility of recirculatory flow reactors in an industrial operation to produce this hydrophobic polymer precursor from food waste.

The road to commercialisation is made easier by the demonstration in this work that 2,6-lutidine in preference to the more expensive 2,6-*t*Bu$_2$Py functions as an effective base.

The reaction time has been reduced from 144 ks (40 hours) to 14.4 ks (4 hours) by changing the base and the proportions of reactants.

The results emphasise the need to use anhydrous reactants. Although five alternative solvents were tested, they did not favour the production of limonene. However the solvent had a major effect on the selectivity of the reaction path. For example anhydrous DMSO produced only γ-terpinene while using CPME 34 wt.% of only ρ-cymene was produced, findings of benefit to the use of these oils in the pharmaceutical and fragrance industries. Clearly there is scope to explore other solvents that favour conversion to DMS.

From the poly-dimethylstyrene obtained, only 31% was soluble in organic solvent. These waxes and low molecular weight fraction had an average M_w of 3800. At present, crosslinked polystyrene is commercially sold under the trade name ‘Rexolite’ and it is mainly used as a dielectric material with applications such as switch housings, capacitors, lenses, X-ray equipment, radiation detectors and non-destructive material testing devices as it presents stable electrical and high radiation properties.

The second part of this work focused in the use of phenolic compounds obtained from potato waste. By applying three different methods for the polymerization of phenol, it was possible to polymerise chlorogenic acid. Studies on the position of the chemical groups in the structure indicated that those with adjacent hydroxyl groups allowed enzymatic polymerization to take place while separated hydroxyl groups required extra energy or inhibit the polymerization. Also it was observed that the presence of alcohol and a water soluble polymer in the reaction medium encouraged the conversion into polymers. The highest conversion of poly-chlorogenic acid (5.2%) was obtained by the using PEG as a water soluble polymer. In the case of poly-phenol best results were obtained when methanol and water or phosphate buffer were being used

during the polymerization process, obtaining in average 70 % conversion. And finally, the best conversion into poly-caffeic acid was a 23 % conversion by using an aqueous solution with methanol.

As a third part of this project, the use of oleic acid obtained from mango butter for the production of polymers was explored. By using low temperatures, -25 °C, the oleic acid was purified from the commercial mango seed butter with an efficiency of 32%. The esterification of two oleic acid molecules using 1,3-propanediol, resorcinol and orcinol to form ester linkages was achieved and the structures were confirmed by FT-IR and ^{1}H NMR analysis. The further epoxidation reaction of each di-ester previously formed was achieved with a yield of 93% for orcinol, 66% for resorcinol and 50% for 1,3-propanediol.

Subsequently, the epoxidized monomers were reacted with amine and anhydride curing agents. When cis-1,2-cyclohexanedicarboxylic anhydride was used as curing agent with epoxidized oleic acid, a non-crosslinked polymer was obtained with a yield of 67%. For this reason further experiment with di-esters were attempted only with amine curing agents. When diethylenetriamine (DET) was used, soluble waxes were obtained and reaction efficiencies of 100, 94 and 62.5 % were obtained with di-ester of 1,3-propanediol, resorcinol and orcinol, respectively. With phenylenediamine (PPD) as curing agent, two soluble waxes were obtained in a yield of 98 % with di-ester 1,3-propanediol and 30% for di-ester orcinol, as for di-ester resorcinol a partial insoluble wax was obtained which indicated the presence of crosslinking in its structure.

Finally a study of the monomers' natural interaction with montmorillonite clay was made. Results indicated that chlorogenic acid and oleic acid were able to intercalate between the clay layers while D-limonene and DMS needed the clay to be chemically modified in order to create an interaction as the hydrophobic and non-polar nature of the monomers prevented their intercalation in the pure clay. Oleic acid was also able to intercalate with L-lysine modified clay and organoclay Cloisite 10A, while the epoxidized oleic acid interacted only with pure and DET-modified clay.These results are helpful indetermining how to create a nano-composite polymer

This PhD project therefore takes us closer to the realisation of materials that have low embodied fossil carbon.

7. Future work

Future work, following the results from this project, will involve the production of biopolymer nanocomposites by the addition of nanoscale reinforcements at the polymer matrix for the improvement of its physical properties. For instance, in the case of poly-DMS, the organoclay Cloisite 10A, an organophilic clay, can be used while for poly-chlorogenic acid natural montmorillonite clay, an hydrophilic clay, is commercially suitable. Furthermore, other reinforcements like graphene (electrical and optical properties), nano-calcium carbonate (mechanical), nano-zinc oxide (ultraviolet radiation), nano-barium sulphate (X-ray opaque), carbon nanotobes (mechanical and electrical) among others, could be added and studied for many conventional and specific applications as their improving properties emerge. It is also important to study which concentration of reinforcement added is the best for improve the properties of the biopolymer. In the case of oleic acid, first of all, stiffer crosslinked polymers should be achieved by testing aromatic anhydride agents and by increasing temperature in the amine curing agent reactions.

Each biopolymer obtained from the experiments could be tested through different measurement methods to know their mechanical, physical, chemical and thermal properties. At the end, properties will be compared between the biopolymers with and without reinforcements to asses the benefits of reinforcement. An economical, environmental and sustainable study must take place to find suitable applications for theses new nano-biopolymers in the food, technological, medical, packaging and automobile industry.

Moreover, in this study the author found that both fossil-based polymer nanocomposites and biopolymer nanocomposites have the same drawback in physical properties caused by poor dispersion and distribution of the nanoparticles throughout the whole polymer matrix. To surpass this phenomena, the author proposes, for future work, ultrasonic treatment on the processing to generate cavitation and large shear flows able to destroy particle agglomerates and rendering exfoliated biopolymer nanocomposites.

In the longer term it is expected to have biopolymers which will be fully competitive in the market by price, properties and availability against mineral oil-based polymers because in the latter, the process of extraction and refinement is each day more expensive indicative of an impending market transition. Therefore, a feasible

development within the polymer chemical industry and research project proposals in the academic area should be implemented once the oil price achieves parity. Furthermore, finding a way to make biopolymers more economically viable, maybe by using cheaper experimental transformation processing than the mineral oil polymers and making them high proprity in the options for industry will become important.

Changes in regulatory measures addressing climate change and environmental laws will also encourage the use of biomass as a resource for biomaterials. Governments will have to invest in biopolymers research in preparation for the increase in oil price and to ensure their future raw material security.

Looking at the future, the use of biomass as a resource for bio-fuel and biomaterials might create conflict over land use and increase the price for human consumption. Therefore the use of food waste material will solve part of this problem and also realign the industrial and agricultural sectors. An agreement between industries has to be made in order to assure availability and therefore sustainability for this project.

Appendix 1. Physico-chemical properties of D-limonene.[345]

Acid Number	0.4
Aldehyde Content	0.37% to 1.50%
Auto-ignition Temperature	Unknown
Boiling Point	176 °C
Coefficient of Expansion	0.761 mL/L/°C
Color	Colorless
Copper Strip Number	0
Dielectric Constant	2.3
Dielectric Strength	4.8 mv m^{-1}
Temperature Coefficient of Entropy	0.2032 at 20.2°C (ds/dt) ρ
Ester Content	0.07% to 2.46%
Evaporation Residue	0.03% to 0.80%
Flash Point	50 °C
Freezing Point	-96.7 °C
Hanus Iodine Number	79.1
Heat Capacity	0.438 cal/g/°C
Heat of Combustion	6130.8 kJ mol^{-1}
Heat of Formation	-54.2 kJ mol^{-1} at 25°C
Heat of Vaporization	44 kJ mol^{-1}
Heat Transfer Coefficient	0.142 W $(m^2 K)^{-1}$
Kauri-Butanol Number	67
Liquid Density	844 g/mL @ 20 °C
Melting Point	-74.35° C
Molecular Formula	$C_{10}H_{16}$
Molecular Weight	136.23 g/mol
Odor	Clean citrus odor
Optical Rotation	+96° to +104°
Peroxide Value	Not more than 2.0
Refractive Index	1.4710 to 1.4740
Saponification Number	1.5
Specific Gravity at 20° C	0.84 - 0.85
Specific Gravity at 25° C	0.838 to 0.843
Specific Heat	59.62 cal · g/mol @ 20.2°C
Viscosity at 25° C	0.9 mPas
Vapor Pressure	133.32 Pa - 14°C
	266.64 Pa - 20°C
	1.3332 KPa - 54°C
	5.3328 KPa - 84°C
	13.332 KPa - 108°C
	53.328 KPa - 151°C
	101.323 KPa - 178°C
VOC Content	95%, 850 g/L
Vapor Density	0.015 g/L @ 20°C

Appendix 2. Ways to produce limonene oxide

Here are listed the possible ways for the alkene epoxidation of limonene in order to produce limonene oxide:

1. With polymer polybenzimidazole supported Mo(VI) as catalysts and tert-butyl hydroperoxide as oxidant. It is an exothermic reaction which produces 50:50 mixture of *cis*- and *trans*- diastereosiomers. The reaction takes place in a batch reactor with stirring speed of 400 rpm producing a 94% selectivity of 1,2-limonene epoxide after 60 min.[346]
2. Using polymer-supported Schiff base complexes. Polymer supported Mn(III)salophen-PSI produces 92% conversion after 2.5 h with a 65% yield of limonene oxide when used as catalyst. Whereas the unsupported polymer Mn(III)salophen as catalysts produces 83% conversion after 0.5 h with a 55% yield of epoxide.[347]
3. Via V_2O_5/TiO_2 (vanadia-titania) catalysts using t-butyl hydroperoxide (t-BHP) as oxidant. This reaction has two possible pathways; it can produce limonene oxide (limonene 1,2-epoxide) by epoxidation or produce carveol and carvone by allylic oxidation (Figure 86). In acidic reaction media, the limonene oxide may be hydrolysed to form limonene glycol. During the reaction some polymerization make take place, depending on the reaction condition the polymer can be form from the epoxide initiated on acid sited proceeding via cationic mechanism or directly from limonene after a long induction period.[348]

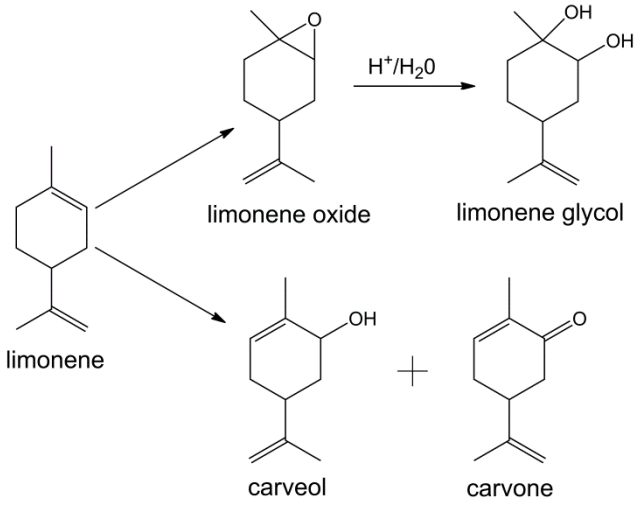

Figure 86. Possible pathways for the oxidation of limonene with V_2O_5/TiO_2 catalyst.[348]

4. With MCM-41 anchored manganese salen complexes as catalysts**,** t-butyl hydroperoxide (t-BHP) as oxidant and 1,4-butanediisocyanate as linking agent. From this reaction limonene oxide, carveol, carvone and polymer are obtained. The polymer obtained if formed by polymerization via free radicals pathways as shown on Scheme 14.[349]
5. By microbiological degradation of D-limonene.[350-352] This route was first studied by the Indian National Chemical Laboratory in Poona by Dhavalikar and Bhattacharyya in 1966 (339). They proposed three routes for D-limonene biotransformation by isolated *Pseudomonas*. (Scheme 40)

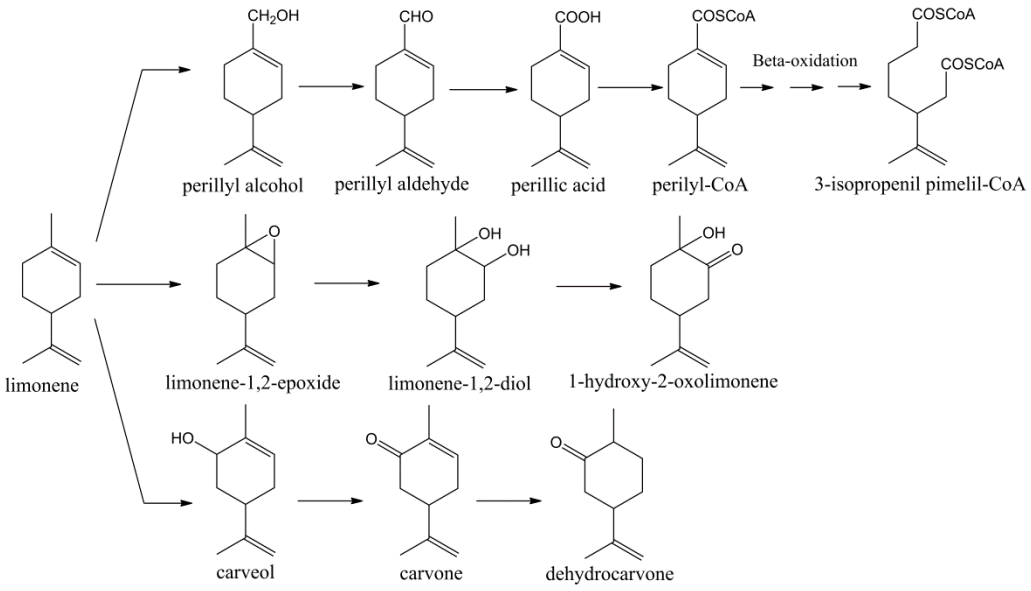

Scheme 40. Proposed routes for limonene biotransformation by Dhavalikar and Bhattacharyya in 1966.[351]

From different studies it is known that limonene-1,2-epoxide is an intermediate for 1-hydroxy-2-oxolimonene and does not accumulate. In Table 61 are shown the organisms that produce this reactive.

Table 61. Epoxidation of D-limonene by microbial biotransformation.[352]

Product	**Substrate (D or L)**	**Organism**	**Main references**
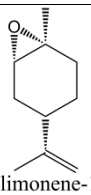 limonene-1,2 epoxide	D, L	Diplodia gossypina ATCC 10936	Abraham et al. 1986.[353]
	D, L	Corynespora cassiicola DSM62474/5	Abraham et al. 1986.[353]
	D	Rhodococcus erythropolis DCL14	Van der Werf and De Bont 1998.[354]

Appendix 3. Diagram of the ink-jet printer valve

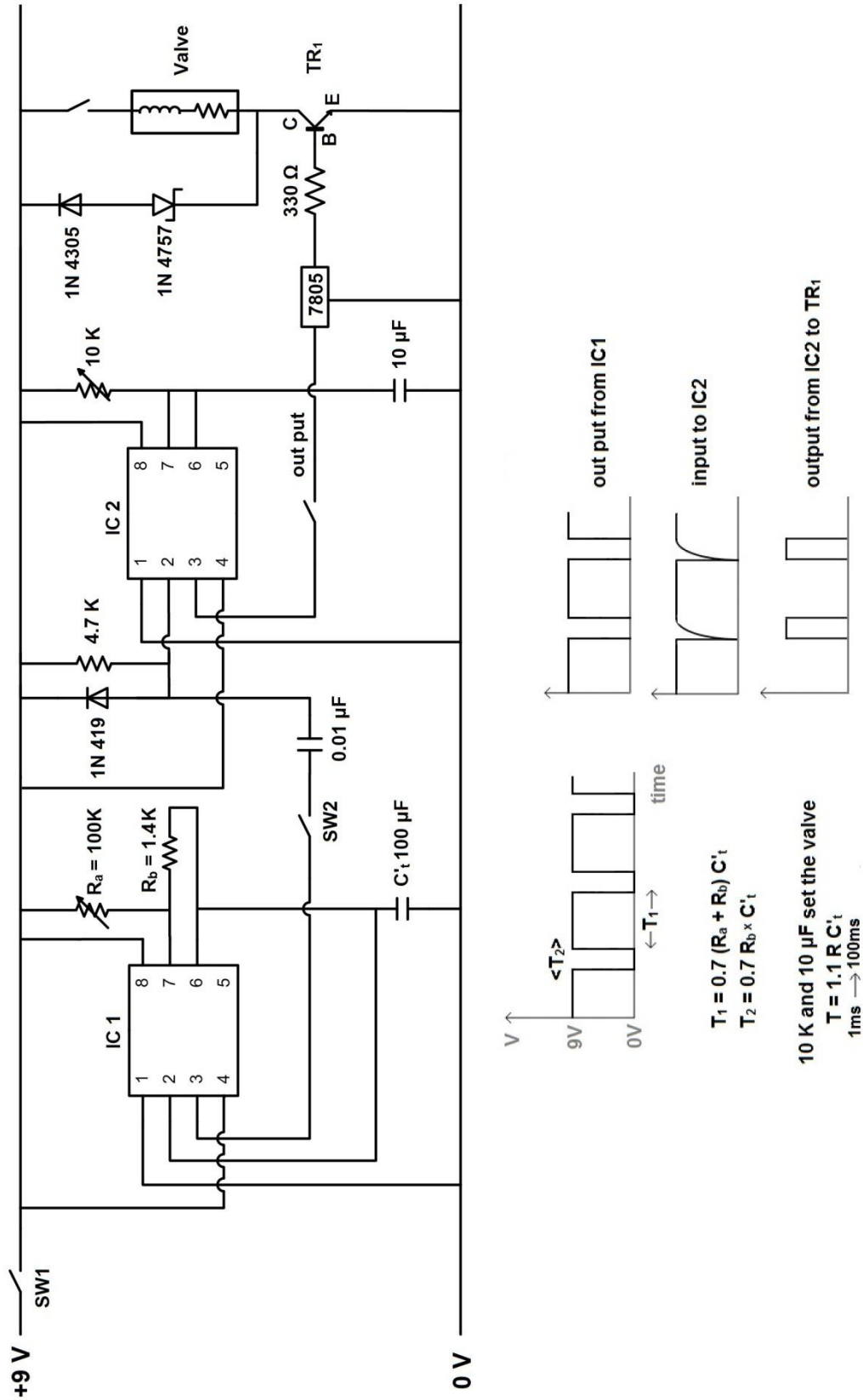

Appendix 4. Mango butter specifications.[355]

BioChemica INTERNATIONAL

Mango Butter - Ultra Refined ™

INCI = Mangifera Indica {Mango} Seed Butter

Product Code: MB001

The Mango Butter supplied by BioChemica has been extracted from the fruit kernels of the Mango tree (Mangifera indica). The "butter" is carefully refined and deodorized to obtain a product which meets the stringent requirements for cosmetic applications. The Mango Butter contains a high content of C18:0 and C18:1 fatty acids. It is a soft solid at room temperatures, but melts on contact at skin temperatures and disperses evenly. Mango Butter may be used for cutaneous dryness to assist in moisturization after exposure to sun and other harsh elements. **Suggested uses:** Creams, lotions, balms. Use from 3% to 100% pure (as a butter-like balm).

SPECIFICATIONS		TYPICAL RESULTS
Appearance:		Pale yellow solid fat
Odor		Slight Fatty Odor
Iodine Value (Wijs)		39 - 50
Saponification Value:		183 - 198
Peroxide Value (meq/kg):		5.0 maximum
Color (lovibond 5 1/4")		5.0 R maximum
Unsaponifiables:		0.7 % minimum
% Free Fatty Acid:		0.50 maximum
Melting Point:		31 - 39° C
Typical Fatty Acid Profile:		**Range %**
Palmitic	C16:0	5-8
Stearic	C18:0	40-45
Oleic	C18:1	40-50
Linoleic	C18:2	2-4
Arachidic	C20:0	1-4
Total Saturated		46-57
Total Monounsaturated		40-50
Total Polyunsaturated		2-4

Keep in cool (preferably below 25°C) storage away from light and moisture in unopened container.

The above specifications are offered in good faith, and are accurate to the best of our knowledge; however, no guarantee or warranties are offered or implied. It is recommended that your laboratories perform their own analysis to ensure that the product specifications and results meet your specific requirements, and those of your local and national governmental standards.

BioChemica International
875 Creel Street - Melbourne, FL 32935 USA
Tel: 321-254-3444 Fax: 321-242-9507 E-mail: techhelp@biochemica.com
Web Site: http://www.biochemica.com

06/07

Appendix 5. Wacker type process

It this process the oxidation of ethylene into acetaldehyde by the oxygen in water in the presence of Palladium as catalyst ($PdCl_2$) and copper(II) chloride ($CuCl_2$) as an oxidizing agent takes place.

The $CuCl_2$ intercepts the precipitation of Pd(0) by oxidizing it and reducing itself to cuprous chloride (CuCl). Air oxidises the resultant CuCl back to $CuCl_2$, allowing the cycle to repeat.

$$PdCl_2 + C_2H_4 + H_2O \rightarrow CH_3CHO + Pd + 2\ HCl$$

$$Pd + 2\ CuCl_2 \rightarrow PdCl_2 + 2\ CuCl$$

$$2\ CuCl + 1/2\ O_2 + 2\ HCl \rightarrow 2\ CuCl_2 + H_2O$$

$$C_2H_4 + 1/2\ O_2 \rightarrow CH_3CHO \qquad \Delta G = -197 kJ/mol$$

Appendix 6. Techniques deployed in this research

1. Gas Chromatography (GC)

This is a separation technique based in the distribution of compounds between a stationary and a mobile phase which provides information on the number of components in a mixture, as well as their quantity. Subsequently, identification of each component can be achieved by mass spectroscopy attached to the gas chromatography equipment.

In a gas chromatograph system the sample is introduced through an injector into the mobile phase (gas) which transports the vaporized components along a column. Here separation of the components takes place due to a rapid mass transfer between the mobile phase (solid or liquid) and the stationary phase. Finally the mobile phase carries the separated solutes into a detector. (Figure 87)

The detector records the separated component bands in a chromatograph as a function of time. The chromatograph provides the residence time and quantitative information of each substance in the sample. The residence time of the components depends on the vapour pressure of the solutes which is affected by the temperature and intermolecular interaction between the solutes and the stationary phase.[356]

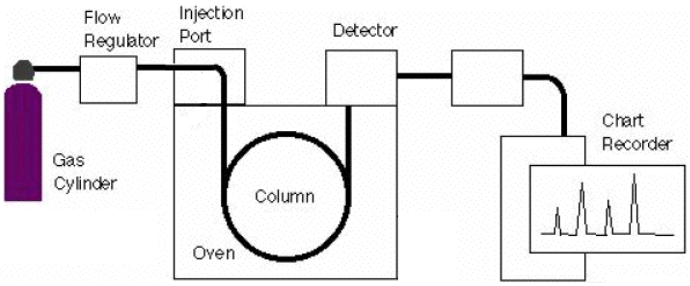

Figure 87. Schematic diagram of gas chromatography system components.[357]

2. Fourier Transformation – Infrared (FT-IR) spectroscopy

FT-IR is an analytical and potentially quantitative technique based on the interaction between an electromagnetic field with a molecule such that, the dipole moment of the molecule changes as a consequence of a molecular vibration. This study can be applied to organic and inorganic compounds. The structural features of a molecule produce characteristic and reproducible molecular vibrations absorptions frequencies, making the vibrational spectrum a unique physical property. The different absorptions can indicate if the molecule has linear or branched chains, unsaturations, aromatic rings and functional groups. Depending on the number of functional groups attached to the molecular structure, additional bands are observed. It is possible to determine their location and orientation in the backbone structure of the molecule. The adsorption peaks of specific functional groups may occasionally displaced from the theoretical ranges due to influences from other functional groups in the molecular structure, spatial orientations and entropy related effects.

The infrared spectrum is formed as a consequence of the electromagnetic radiation adsorption at frequencies which correlate to the chemical bond vibrations within a specific molecule. The greater number of electrons involved in the chemical bond, the higher the energy needed for its excitation. The energy applied is proportionally related to the frequency, therefore stretching absorptions of a vibrational chemical bond are observed at higher frequencies (wavenumbers) than the corresponding bending deformation vibrations. Likewise, symmetric vibrations are easier to excite than those which are asymmetric. In the case of mass, the frequency is inversely proportional hence light elements vibrate at higher frequencies than heavy elements.

The infrared spectrometer consists of an infrared radiation source, a beam splitter, fixed and movable mirrors (in order to change the frequency) and a detector as shown in Figure 88. The infrared radiation is produced by a thermal source and sent to a beam

splitter (BS) which separates the radiation in two. One half is reflected into fixed mirror M1 traveling the distance *L* twice (one going and one coming back) while the other half of the radiation is transmitted to the movable mirror M2. This M2 mirror can be moved by an additional distance *x* making the radiation tray a total distance of *2L+x.* After this, the beam is directed to the sample to pass through it and finally land in a detector. The detector registers the intensity of the radiation measured as a function of the displacement *x*. Later, a computer provides the respective spectrum by using the mathematical transformation of Fourier transform.

In FT-IR, the spectrum is scanned several times in order to reduce the noise and provide greater sensitivity. The resolution depends on (i) the distance displacement by the mirror and (ii) the apodization function used in computing the spectrum. The identification of most unknown substances is accomplished by comparison with previous recorded spectra in computer databases.[356]

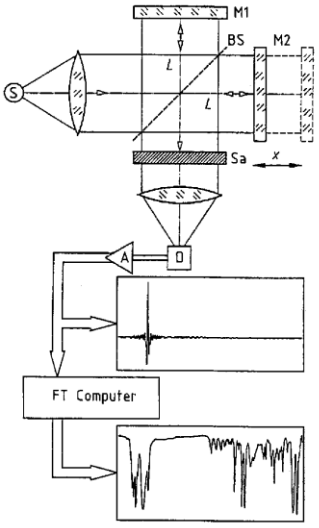

Figure 88. Schematic diagram of an FT-IR instrument. S = radiation source, BM = bean splitter, M1 = fix mirror, M2 = movable mirror, L = fix distance, X = movable distance, D = detector, Sa = sample, A = amplifier and FT = fourier transformation.[356]

3. Nuclear Magnetic Resonance (NMR)

Nuclear magnetic resonance spectroscopy is one of the most important instrumental measuring techniques in chemistry for the determination of molecular structures. It is a quantitative technique based on the fundamental properties of magnetic resonance. According to quantum mechanics, the separation between energy levels are quantized and from this resonance frequency information about the chemical structure and local

magnetic environment can be obtained, and by its disturbance from equilibrium it is possible to obtain information about the spin system.

In order to exhibit magnetic resonance, the system must have a magnetic moment which is provided in the NMR by a nucleus with non-zero nuclear spin. Subsequently the magnetic moments tend to align in magnetic fields which are applied in the form of ratio frequencies pulses.

Therefore, during the experiment, the sample is exposed to electromagnetic waves of varied frequencies and when it matches the characteristic frequency of the nuclei or the electron, an electric signal is sent to a detector. These signals are recorded as plots of voltage as a function of time and through the Fourier Transform mathematical procedure the time domain signals are converted into peaks as a function of frequency. The most common nuclei studied are the hydrogen and carbon, known as ^{1}H NMR and ^{13}C NMR, respectively.

Samples are studied in solution of deuterated solvent and placed in 5 or 10 mm glass tubes. These tubes are placed in the cryomagnet probe which is positioned between the poles of an electro- or permanent magnet or inside a solenoid of a superconducting magnet under liquid helium conditions. The scheme of the NMR machine is in Figure 89.

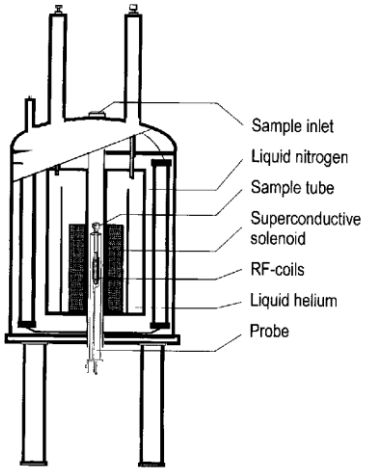

Figure 89. Schematic diagram of an NMR instrument.[356]

The probe as indicated in Figure 90 is integrated by radio-frequency transmitter and receiver coils and a spinner which spins the tube sample in its vertical axis in order to average out the magnetic field inhomogeneity across all sample.

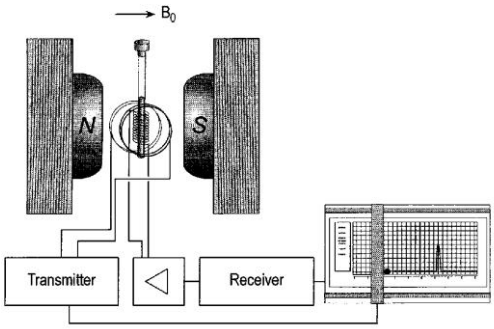

Figure 90. Schematic diagram of the probe inside the NMR instrument.[356]

The NMR spectroscopy is used as a quantitative method as the time domain signals are directly related to the peak intensities in the frequency spectrum. Furthermore, each frequency component corresponds to a peak at a specific frequency and amplitude and its own line-width. The resolution of a NMR spectrum depends on the atomic motions, i.e. faster molecular motions lead to sharper lines and higher resolutions. As well, impurities like solid particles or viscous solutions can cause peak broadening and degrade the quality of the spectrum.[356,358]

4. X-ray Diffraction (XRD)

X-ray diffraction studies are used for determining crystal structures and the spacing between the atomic planes. It is a technique based in the Bragg's law (Equation 5) which assumes that the scattering from atoms produces reflections from atomic planes (Figure 91); it relates the wavelength of the X-rays to the spacing of atomic planes.

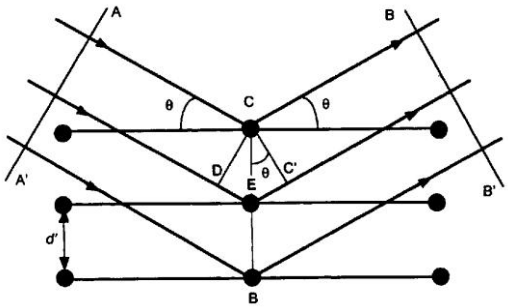

Figure 91. Bragg's law.[359]

Assuming that the diffracted wave from the plane makes the same angle that the incident wave and that all reflected waves are in phase, then the path lengths between wavefront AA' & BB' must differ by exactly an integral number (n) of wavelengths (λ).

$$\delta = n\lambda \tag{6}$$

This path difference can also be written in terms of CC' and CD wavefronts as,

$$\delta = DE + EC' = 2EC' \tag{7}$$

From the geometry,

$$\sin\theta = \frac{EC'}{CE} = \frac{\frac{\delta}{2}}{CE} = \frac{\delta}{2CE} \tag{8}$$

As result, Equation 1 can be expressed in terms of CE; which is the spacing *d'*,

$$\delta = 2CE\sin\theta = 2d'\sin\theta \tag{9}$$

and finally, by combining Eqs. 1 and 4 Bragg's law is obtained.

$$n\lambda = 2d'\sin\theta \tag{10}$$

An X-ray diffractometer is formed by three basic components; an X-ray source, the specimen and the X-ray detector. They are arranged in two circles, one where the specimen is centered while the X-ray source and the detector lie on the circumference and the other one where the three parts lie on the circumference; they are known as the diffractometer and the focusing circle, respectively (Figure 92). The diffractometer circle is fixed while the focusing circle increases as the angle 2θ decreases by moving the detector.

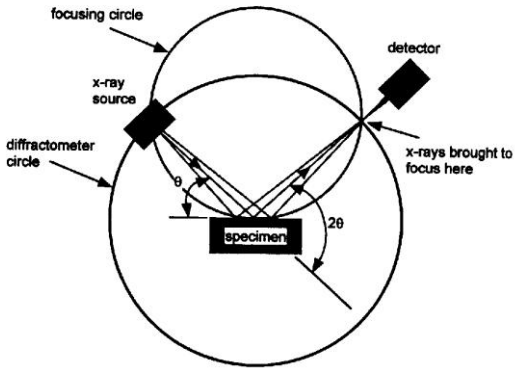

Figure 92. X-ray diffractometer configuration.[359]

X-rays are high-energy electromagnetic radiation produced by interactions between an external source of electrons and electrons in the shells of an atom. X-rays are produced in a vacuum chamber when a beam of electrons, created from heating a tungsten filament cathode, is accelerated towards a water-cooled anode. The loss of energy due to the collision is manifested as X-rays.

X-rays wavelength range is from 0.1 to 10nm but the useful range for X-ray diffraction studies is between 0.05-0.25nm. X-ray diffraction studies use a monochromatic beam, i.e. X-rays of a single wavelength, mainly from K_α and K_β energy lines because they are very energetic and therefore the less strongly absorbed by the studied specimen.

To define and collimate the incident beam of electrons parallel metal plates of molybdenum or tantalum, for which the absorption edge of X-rays lies between K_α and K_β components of the spectrum, are used. Moreover, to obtain a monochromatic beam, a graphite crystal is placed at the end of the diffracted beam and arranged in known lattice spacing oriented way to diffract only K_α and K_β radiation, as shown in Figure 93.

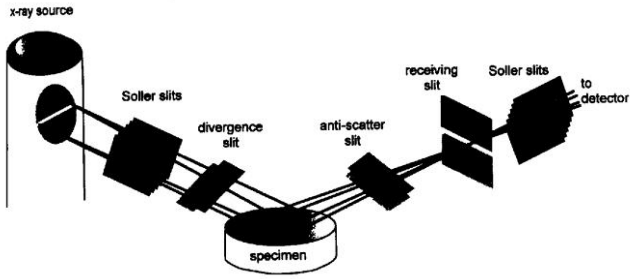

Figure 93. Optical arrangement in the X-ray diffractometer.[359]

The detectors interpret the energy of the incoming X-ray as pulses and present the count rate as a series of peaks. Each peak corresponds to an X-ray diffracted from a specific set of planes in the specimen while their intensities are proportional to the number of X-ray photons of a particular energy that have been counted by the detector for each angle 2θ. The position of the peaks depends on the crystal structure while their quantity increases as the symmetry of the crystal decreases. Peak broadening of X-rays occurs when the crystallite or grain size of the studied material is <0.1μm and it increases with the decrement of crystallite size.[359]

5. Differential Scanning Calorimetry (DSC)

This technique measures energy changes. A sample and a reference material are subjected to a temperature programme and the difference in temperature (ΔT) between them is measured and monitored. The basic squeme of a differential scanning calorimetry instrument is shown in Figure 94 .

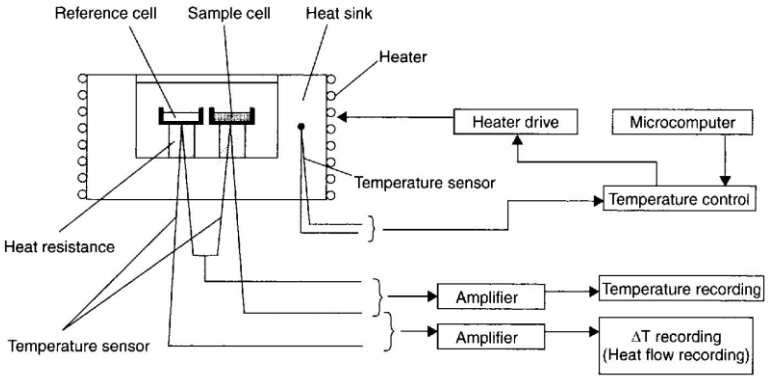

Figure 94. Schematic diagram of an DSC instrument.[360]

It is used to study endothermic and exothermic reactions, to deduce the heat capacity of the sample by measuring the difference of energy input between the sample and the reference material, to study relaxation processes and glass transition temperatures. It can also be used to determine absolute thermodynamic quantities as the peak area is related to the energy change and the sample size according to the following equation where ΔH is enthalpy, m the sample mass and k is a proportionality constant which is temperature-dependent.[361]

The difference in temperature (ΔT) remains constant if no reaction takes place but if an endothermic reaction starts the sample temperature lags behind and the difference in temperature (ΔT=Ts-Tr) becomes negative producing a concave peak in the DSC curve while an exothermic reaction works vice versa and produces a convex peak, as seen on Figure 95.

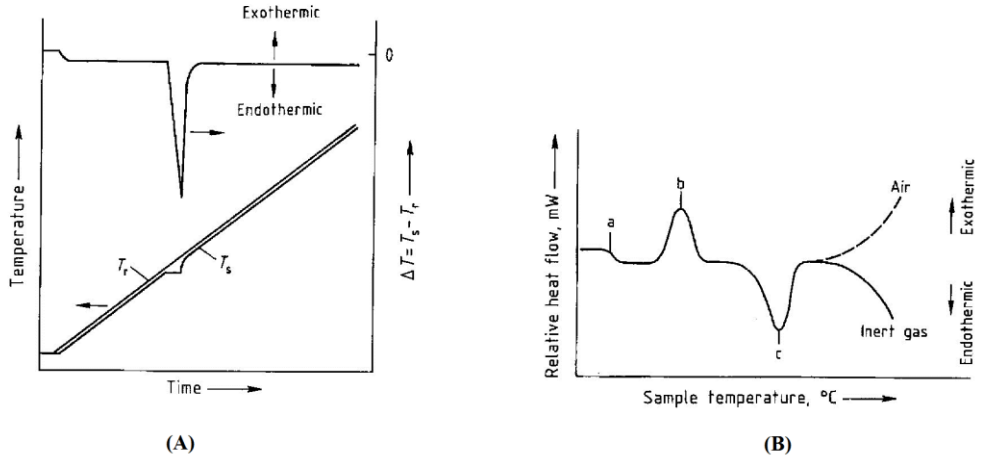

Figure 95. (A) DSC curve example where Tr = temperature reference and Ts = temperature sample (B) Generalized DSC curve for a polymer where a) glass transition, b) crystallization, c) melting and subsequent reactions.[362]

References

1. Berner, R.A.; Petcsch, S.T.; Lake, J.A.; Beerling, D.J.; Popp, B.N.; Laws, E.A.; Westley, N.Cassar, M.B.; Woodward, F.I.; Quick, W.P. "Isotope fractionation and atmospheric oxygen: implications for phanerozoic O_2 evolution", Science. 2000, 287,1630-1633.
2. Berner, R.A. "The carbon cycle and CO_2 over phanerozoic time: the role of land plants", Phil. Trans. Roy. Soc. Lond. 1998, B-353,75-82.
3. Smil, V. Oil, Oneworld; Oxford. 2008, Chp. 5, pp 159-188.
4. Pollastro, R.M.; Cook, T.A.; Roberts, L.N.R.; Schenk, C.J.; Lewan, M.D.; Anna, L.O.; Gaswirth, S.B.; Lillis, P.G.; Klett, T.R.; Charpentier, R.R. "Assessment of undiscovered oil resources in the Devonian-Mississippian Bakken Formation, Williston Basin Province, Montana and North Dakota" U.S. Geological Survey Fact Sheet. 2008, 2008–3021.
5. Smil, V. "Energy in nature and society" MIT Press, MA. 2008, 212-217.
6. Aguilera, R.F.; Ripple, R.D. "Technological progress and the availability of European oil and gas resources" Applied Energy. 2012, 96, 387–392.
7. Liu, Z.Y.; Shi, S.D.; Li, Y.W. "Coal liquefaction technologies-development in China and challenges in chemical reaction engineering" Chem. Eng. Sci. 2010, 65, 12-17.
8. Boswell, R.; Collett, T.S. "Current perspectives on gas hydrate resources" Energy & Environ. Sci. 2011, 4, 1206-1215.
9. Mejean, A. ; Hope, C. "Modelling the costs of non-conventional oil: A case study of Canadian bitumen" Energy Policy. 2008, 36, 4205–4216.
10. Hearps, P.; McConnell, D. "Renewable energy technology cost review" Melbourne Energy Institute Technical Paper Series. March 2011.
11. IEA, International Energy Agency. Monthly oil market reports. January 1987- January 2013. http://omrpublic.iea.org/ (last accessed April 23, 2013)
12. Winstone, R.; Boulton, P.; Gore, D. "Energy security, House of Commons Research Paper 07/42" House of Commons Library. May 2007, 1-38.
13. Anon. "Oil and gas security: emergency response of IEA countries: Uninted Kingdom" International Energy Agency,Paris. 2010, 1-10.
14. Isaksen, I.S.A.; Gauss, M.; Myhre, G.; Anthony, K.M.W.; Ruppel, C. "Strong atmospheric chemistry feedback to climate warming from Arctic methane emissions" Global Biogeochemical Cycles. 2011, 25, Art. No. GB2002.
15. Scambos, T. "Earth's ice: Sea level, climate, and our future commitment" Bull. Atomic Sci. 2011, 67, 28-40.
16. Bekryaev, R.V.; Polyakov, I.V.; Alexeev, V.A. "Role of polar amplification in long-term surface air temperature variations and modern arctic warming" J. Climate. 2010, 23, 3888-3906.
17. Costello, A. and 29 others. "Managing the health effects of climate change" The Lancet. 2009, 373, 1693-1733.

18. Sullivan, G.R. and 10 others. “National security and the threat of climate change, Report of military advisory board” CNA Corporation, Alexandria, Virginia, USA. 2007, 1-63.
19. Williams, C.K.; Hillmyer, M.A. “Polymers from renewable resources: A perspective for a special issue of polymer reviews” Polymer Reviews. 2008, 48, 1-10.
20. Bledzki, A.K.; Gassan, J. “Composites reinforced with cellulose based fibres,” Prog. Polym. Sci. 1999, 24, 221-274.
21. Zuhri, M.Y.M.; Sapuan, S.M.; Ismail, N. “Oil palm fibre reinforced polymer composites: a review” Prog. Rubb. Plast. Recycling Tech. 2009, 25, 233-246.
22. Summerscales, J.; Dissanayake, N.P.J.; Virk, A.S.; Hall, W. “A review of bast fibres and their composites. Part 1-Fibres as reinforcements” Composites Part A-Applied Science and Manufacturing.2010, 41, 1329-1335.
23. Summerscales, J. ; Dissanayake, N.P.J.; Virk, A.S.; Hall, W. “A review of bast fibres and their composites. Part 2-Composites,” Composites Part A-Applied Science and Manufacturing. 2010, 41, 1336-1344.
24. Rouilly, A.; Rigal, L. “Agro-materials: A bibliographic review, Polymer Reviews” Journal of Macromolecular Science. Part C - Polymer Reviews. 2002, C42, 441-479.
25. Mooney, B.P. “The second green revolution? Production of plant-based biodegradable plastics” Biochem. J. 2009, 418, 219-232.
26. Jain, J.P.; Sokosky, M.; Kumar, N.; Domb, A.J. “Fatty acid based biodegradable polymer” Polymer Reviews. 2008, 48, 156-191.
27. Tong, X.; Ma, Y.; Li, Y. “Biomass into chemicals: Conversion of sugars to furan derivatives by catalytic processes” Applied Catalysis A:General. 2010, 385, 1-13.
28. Ford, H. “Automotive body construction” US Patent No 2269451. 1940.
29. Firbank, L.G. “Assessing the ecological impacts of bioenergy projects” Bioenergy Res. 2008, 1, 12-19.
30. Prins, A.G.; Eickhout, B.; Banse, M.; Van-Meijl, H.; Rienks, W.; Woltjer, G. “Global impacts of european agricultural and biofuel policies” Ecology and Society. 2011, 16, Art. No. 49.
31. Patzek, T.W. “Can the earth deliver the biomass-for-fuel we demand? Biofuels, solar and wind as renewable energy systems”, D. Pimental: Springer, 2008, 19-55.
32. IBIB.2012-13. “International business directory for innovative bio-based plastics and composites” Nova-Institute GmbH Huerth, Ger. & Bioplastics Magazine. 2012, ISBN 978-3-9812027-5-5.
33. Endres, H.J.; Siebert-Raths, A. “Engineering biopolymers. Market, manufacturing, properties and applications” Hanser Publications, 2011.
34. British Plastics Federation. “Oil Consumption” http://www.bpf.co.uk/Press/Oil_Consumption.aspx. (last accessed February 10, 2014)
35. U.S. Energy Information Administration. “Independent Statics & Analysis” http://www.eia.gov/tools/faqs/faq.cfm?id=34&t=6 (last accessed January 29, 2014)

36. Institute for Ecology and Innovation, NOVA. “Bio-based polymers - Production capacity will triple from 3.5 million tonnes in 2011 to nearly 12 million tonnes in 2020” Press release-long version. March 06, 2013.
37. Institute for Ecology and Innovation, NOVA. “Production capacities for bio-based polymers in europe - Status Quo and trends towards 2020” Press release. July 24, 2013.
38. Wolf, O.; Crank, M.; Marscheider-Weidemann, F. “Techno-economic feasibility of large-scale production of bio-based polymers in Europe. Technical Report Series » European Commision, Joint Reserach Centre. EUR 22103 EN, 2005.
39. Institute for Ecology and Innovation, NOVA. “Growth in PLA bioplastics: a production capacity of over 800,000 tonnes expected by 2020” Press release. August 06, 2012.
40. Andresen, C.; Demuth, C.; Lange, A.; Stoick, P.; Pruszko, R. “Biobased automobile parts investigation. A report developed for the USDA Office of energy policy and new uses” Iowa State University, 2012
41. Bolck, C. “Biobased performance materials programme introduction.”Biobased performance materials, 2011.
42. Institute for Ecology and Innovation, NOVA. “Market study on bio-based polymers in the world. Capacities, production and applications: Status Quo and trends towards 2020.” www.bio-based.eu/market_study. (last accessed January 31,2014)
43. Chandra, R.; Rustigi, R. “Biodegradable polymers” Prog.Polym.Sci. 1998, 23, 1273-1335.
44. Morschbacker, A. “Bio-ethanol based ethylene” Polymer Reviews. 2009, 49, 79-84.
45. Nyambo, C.; Mohanty, A.K.; Misra, M. “Polylactide-based renewable green composites from agricultural residues and their hybrids” Biomacromolecules. 2010, 11, 1645-1660.
46. Firn, R.D.; Jones, C.G. “A darwinian view of metabolism: molecular properties determine fitness” J. Expt. Botany . 2009, 60, 719-726.
47. Gustavsson, J.; Cederberg, C.; Sonesson, U.; Van Otterdijk, R.; Meybeck, A. “Global food losses and food waste. Extent, causes and prevention” Food and Agriculture Organization of the United Nations (FAO), Rome 2011.
48. Akinfemi, A. “Bioconversion of peanut husk with white rot fungi: Pleurotus ostreatus and Pleurotus pulmonarius”. Livestock Research for Rural Development. http://www.lrrd.org/lrrd22/3/akin22049.htm (last accessed April 23, 2013)
49. Furst-McNess company. “Commodity nutrient profile, potato processing waste, use and application”. http://www.mcness.com/sites/default/files/file_attach/PotatoWasteUSE03.pdf (last accessed April 23, 2013)
50. Karim,M.S.; Percival,G.C.; Dixon,G.R. “Comparative composition of aerial and subterranean potato tubers” J. Sci. Food. Agric. 1997, 75, 251-257.
51. Kittiphoom, S. “Utilization of mango seed” Int. Food Res. J. 2012, 19, 1325-1335.
52. Templeton, D.W.; Scarlata, C. J.; Sluiter, J.B.; Wolfrum, E.J. “Compositional analysis of lignocellulosic feedstocks. 2. Method uncertainties” J. Agric. Food Chem. 2010, 58, 9054–9062.

53. Sinclair, W.B. “The grapefruit. Its composition, physiology and products; Division of Agricultural Sciences”. University of California : ANR Publications, 1972. p.514.
54. Oluremi, O.I.A.; Andrew, I.A.; Ngi, J. “Evaluation of the nutritive potential of the peels of some citrus fruit varieties as feedingstuffs in livestock production”. Pakistan J. Nutrition, 2007, 6, 653-656.
55. Marín, F. R.; Soler-Rivas, C.; Benavente-García, O.; Castillo, J.; Pérez-Alvarez, J. A. “By-products from different citrus processes as a source of customized functional fibres” Food Chemistry. 2007, 100, 736–741.
56. Palmquist, D.L.; Jenkins, T.C. “Challenges with fats and fatty acid methods” J. Animal Science. 2003, 81, 3250-3254.
57. Berghe, E. V.; Dhont, J. Laboratory of Aquaculture & Artemia Reference Center. “Analytical techniques in aquaculture research. Proximate analysis: Nitrogen Free Extract (NFE)”.http://www.aquaculture.ugent.be/Education/coursematerial/online%20courses/ATA/analysis/NFE.htm (last accessed April 23, 2013)
58. Pandey, A.; Soccol, C. R.; Nigam, P.; Brand, D.; Mohan, R.; Roussos S. “Biotechnological potential of coffee pulp and coffee husk for bioprocesses” Biochem. Eng. J. 2000, 6, 153–162.
59. Production., Food and Agriculture Organization of the United Nations (FAOSTAT) and United State Department of Agriculture (USDA)” in the “Foreign Agricultural Service” http://faostat.fao.org. (last accessed April 23, 2013)
60. Ishizaki, Y.; Kondo, M.; Kamal, M.U.; Isowa, Y.; Matsui, H.; Karita, S. “Fermentation characteristics, nutrient composition and in vitro ruminal degradability of whole crop wheat and wheat straw silage cultivated at dried paddy field” J. Food, Agriculture & Environment. 2013, 11, 664 - 668.
61. Essien, J.P.; Akpan, E.J.; Essien, E.P. “Studies on mould growth and biomass production using waste banana peel” Bioresource Technology. 2005, 96, 1451–1456.
62. Hongzhang, C. ; Hongqiang, L.; Liying, L. “The inhomogeneity of corn stover and its effects on bioconversion” Biomass and Bioenergy. 2011, 35, 1940-1945.
63. Chau, C.F.; Chen, C.H.; Lee, M.H. “Comparison ofthe characteristics, functional properties, and in vitro hypoglycemic effects of various carrot insoluble fiber-rich fractions” Swiss Society of Food Science and Technology. 2004, 37, 155–160.
64. Chantaro, P.; Devahastin, S.; Chiewchan, N. “Production of antioxidant high dietary fiber powder from carrot peels” Food Sci. Tech. 2008, 41, 1987-1994.
65. Pereiae, G.I.S.; Pereira, R.G.F.A.; Barcelos, M.F.P.; Morais, A.R. “Carrot leaf, chemical evaluation aiming its use in human feeding” Ciênc. Agrotec, Lavras. 2003, 27, 852-857.
66. Fox, T. “Global food waste not, want not” Inst. Mech. Engnrs. Lon. U.K. 2013; pp 2-31.
67. FAOSTAT. Food and Agriculture Organization of the United Nations, “International year of the potato” 2008. http://www.potato2008.org/en/ (last accessed April 23, 2013)
68. Friedman, M. “Chemistry, biochemistry and dietary role of potato polyphenols. A review” J. Agric. Food Chem. 1997, 45, 1523-1540.

69. Greenbiz news. Potato Power for Homes, Factories on McD's New Best Practices List.http://www.greenbiz.com/news/2010/05/04/potato-power-homes-factories-on-mcdonalds-new-best-practices-list (last accessed April 23, 2013).
70. The carbon caputre report. “Thirty thousand tonnes of potato waste converted into renewable energy”. http://www.freshplaza.com/news_detail.asp?id=54469 (last accessed April 23, 2013.)
71. Bilanovic, D.D.; Malloy, S.H.; Remeta, P. “Solid or semi-solid state fermentation of xanthan on potato or potato waste”Assgn: Bemidji State University Foundation. June 2010, US Patent Number: 07727747.
72. Bemidh State University, Minnesota Public Radio. “Horizons” Summer/Fall. 2006, 6, 6-8.
73. Mackean, D.G.; Mackean, I. “Biology teaching and learning resources. Plants: flower structure. http://www.biology-resources.com/plants-flowers.html (last accessed April 23, 2013)
74. Liao, W.J.; Heijungs, R.; Huppes, G. “Is bioethanol a sustainable energy source? An energy-, exergy-, and emergy-based thermodynamic system analysis” Renewable Energy. 2011, 36, 3479–3487.
75. Agbogbo, F; Haagensen, F.;Wenger, K. “Fermentation of acid pretreated corn stover to ethanol using Pichia stipitis” Applied Biochemistry & Biotechnology. 2008, 145, 53-58.
76. Zambare, V.P.; Bhalla, A.; Muthukumarappan, K.; Sani, R.K.; Christopher, L.P. “Bioprocessing of agricultural residues to ethanol utilizing a cellulolytic extremophile” Extremophles. 2011, 15, 611-618.
77. Ryu, S. ; Karim, M.N. “A whole cell biocatalyst for cellulosic ethanol production from dilute acid-pretreated corn stover hydrolyzates” Appl. Microbiol. Biotechnol. 2011, 91, 529-542.
78. Dale, S.K.; Bruce, E. “Life cycle assessment study of biopolymers (polyhydroxyalkanoates) derived from no-tilled corn” Int. J. Life Cycle Assess. 2005, 10, 200-210.
79. Fei, Y.; Yuhuan, L.; Xuejun, P.; Xiangyang, L. “Liquefaction of corn stover and preparation of polyester from the liquefied polyol” Appl. Biochem. Biotechnol. 2006, 129, 564-585.
80. Tipeng, W.; Lianhui, Z.; Dong, L.; Jun, Y.; Sha, W.; Zhihuai , M. “Mechanical properties of polyurethane foams prepared from liquefied corn stover with PAPI” Bioresource Technol. 2008, 99, 2265-2268.
81. Solis-Fuentes, J.A.; Durán-de-Bazua, M.C. “Mango seed uses: thermal behaviour of mango seed almond fat and its mixtures with cocoa butter” Bioresource Technol. 2004, 92, 71–78.
82. Nilani, P.; Raveesha, P.; Kasthuribai.N.R.N.; Duraisamy, B.; Dhamodaran, P.; Elango, K. “Formulation and evaluation of polysaccharide based biopolymer– An ecofriendly alternative for synthetic polymer” J. Pharma. Sci. Res. 2010, 2, 178-184.
83. Hosni, K.; Zahed, N.; Chrif, R.; Abid, I.; Medfei, W.; Kalle, M.; Brahim, N. B.; Sebei, H. “Composition of peel essential oils from four selected tunisian citrus species: evidence for the genotypic influence” Food Chemistry. 2010, 123, 1098–1104.
84. Marin, F. R.; Soler-Rivas, C.; Benavente-Garcia, O.; Castillo, J.; Perez-Alvarez, J. A. “By-products from different citrus processes as a source of customized functional fibres” Food Chemistry. 2007, 100, 736-741.

85. Ladaniya, M.S. Citrus Fruit. Biology, technology and evaluation. USA : Academic Press, 2008, pp. 170-180.
86. Mamma, D.; Kourtoglou, E.; Christakopoulos, P. “Fungal multienzyme production on industrial by-products of the citrus-processing industry” Bioresource Technol. 2008, 99, 2373–2383.
87. Chowdhury, S.D.; Hassin, B.M.; Das, S.C. “Evaluation of marigold flower and orange skin as source of xanthophyll ogment for the improvement of egg yolk color” J. Poultry Sci. 2008, 45, 265-272.
88. Boluda-Aguilar, M.; García-Vidal, L.; González-Castañeda, F.P.; López-Gómez, A. “Mandarin peel wastes pretreatment with steam explosion for bioethanol production” Bioresource Technol. 2010, 101, 3506–3513.
89. Cho, C.W.; Lee, D.Y.; Kim, C.W. “Concentration and purification of soluble pectin from mandarin peels using crossflow microfiltration system” Carbohydrate Polymers. 2003, 54, 21–26.
90. Organisation Internationale de la Vigne et du Vin (OIV). World Vitivinicultural Statistics 2007, Structure of the World Vitinicultural Industry in 2007.
91. Wine Institute. World Wine Production by Country 2010. http://www.wineinstitute.org/resources/worldstatistics/article87 (last accessed April 23, 2013)
92. Private comment from Robert Tinlot, ex-president and honorary general manager and director of the “Office International de la Vigne et du Vin” (OIV) , president of the the Amorim Academy and present honorary head of Chateau Changyu AFIP Global.
93. Arvanitoyannis, I.S.; Ladas, D.; Mavromatis, A. “Potential uses and applications of treated wine waste: a review” Int. J. Food Sci. & Technol. 2006, 41, 475–487.
94. Musee,N.; Lorenzen,L.; Aldrich,C. “Cellar waste minimization in the wine industry: a systems approach” J. Cleaner Production. 2007, 15, 417-431.
95. Fernández, C.M.; Ramos, M.J.; Perez, A.; Rodríguez, J.F. “Production of biodiesel from winery waste: Extraction, refining and transesterification of grapes seed oil” Bioresource Technology. 2010, 101, 7019–7024.
96. Luque-Rodríguez, J.M.; Luque de Castro, M.D.; Pérez-Juan, P. “Dynamic superheated liquid extraction of anthocyanins and other phenolics from red grape skins of winemaking residues” Bioresource Technol. 2007, 98, 2705–2713.
97. Szterk, A.; Roszko, M.; Sosinska, E.; Derewiaka, D.; Lewicki, P. P. “Chemical composition and oxidative stability of selected plant oils” J. Am. Oil Chem. Soc. 2010, 87, 637–645.
98. Australian Cane Farmers Association. Sugar Milling. http://www.acfa.com.au/. (last accessed April 23, 2013)
99. Almazan, O.; Gonzalez, L.; Galvez, L. “The sugar cane, its by-products and co-products”; Asociacion de tecnicos azucareros de cuba, Food and Agricultural Research Council, Mauritius, 1998, pp. xiii-xxv.
100. Cardona, C.A.; Quintero, J.A.; Paz, I.C. “Production of bioethanol from sugarcane bagasse: Status and perspectives” Bioresource Technology. 2010, 101, 4754–4766.

101. Demirbas, A. “Bioethanol from cellulosic materials: A renewable motor fuel from biomass” Energy Sources. 2005, 27, 327-337.
102. International Coffee Organization. Methods for coffee extraction. http://www.ico.org/field_processing.asp (last accessed April 23, 2013)
103. Rojas, J.B.U.; Verreth, J.A.J.; Van-Weerd, J.H.; Huisman, E.A. “Effect of different chemical treatments on nutritional and antinutritional properties of coffee pulp” Animal Feed Sci. & Technol. 2002, 99, 195-204.
104. Bekalo, S.A.; Reinhardt, H.W. “Fibers of coffee husk and hulls for the production of particleboard” Materials and Structures. 2010, 43, 1049–1060.
105. Espíndola-Gonzalez, A.; Martínez-Hernández, A. L. “Novel crystalline SiO_2 nanoparticles via annelids bioprocessing of agro-industrial wastes” Nanoscale Res Lett. 2010, 5, 1408–1417.
106. Agri-Food Business Development Centre via Nation Master. Agriculture Statics. “Banana production by country 2000”. http://www.nationmaster.com/graph/agr_ban_pro-agriculture-banana-production (last accessed April 23, 2013)
107. Mohapatra, D.; Mishra, S.; Sutar, N. “Banana and its by-products utilisation: an overview” J. Sci. & Indust. Res. 2010, 69, 323-329.
108. Emaga, T. H.; Robert, C.; Ronkart, S. N.; Wathelet, B. ; Paquot, M. “Dietary fibre components and pectin chemical features of peels during ripening in banana and plantain varieties” Bioresource Technol. 2008, 99, 4346–4354.
109. Bardiya, N.; Somayaji, D.; Khanna, S. “Biomethanation of banana peel and pineapple waste” Bioresource Technol. 1996, 58, 73-76.
110. Joshi, S.; Bhopeshwarkar, R.; Jadhav, U.; Jadhav, R.; D'souza , L.; Dixit, J.”Continuous ethanol production by fermentation of waste banana peels using flocculating yeast” Indian J. Chem. Technol. 2001, 8, 153-156.
111. Annadurai, G.; Juang, R.S.; Lee, D.J. “Adsorption of heavy metals from water using banana and orange peels” Water Sci. &Technol. 2002, 47, 185-190.
112. Lopez, V.M.G. “Characterization of avocado (Persea americana Mill.) Varieties of very low oil content” J. Agric. Food Chem. 1998, 46, 3643-3647.
113. Pushkar, S.B.; Narain, N. ; Rocha, R.V.M.; Paulo, M.Q. “Characterization of the oils from the pulp and seeds of avocado (cultivar: Fuerte) fruits” Grasas y Aceites. 2001, 52, 171-174.
114. Rodriguez-Carpena, J.G.; Morcuende, D.; Andrade, M.J.; Kylli, P.; Estevez, M. “Avocado (Persea americana Mill.) phenolics, in vitro antioxidant and antimicrobial activities, and inhibition of lipid and protein oxidation in porcine patties” J. Agricultural and Food Chem. 2011, 59, 5625-5635.
115. Mueller, R. ; Seidel, K. ; Hollenberg, A. ; Matzik, I. “Skin and hair aerosol foam preparations containing an alkyl polyglycoside and vegetable oil” Official Gazette of the United States Patent and Trademark Office Patents. 2000, 1233.
116. Rosenblat, G.; Werman, M.J.; Yudicky, E.; Itzhak, O.; Neeman ,I. “Hepatic collagen solubility in growing rats following oral administration of a lysyl oxidase inhibitor from avocado seed oil” Med. Sci. Res. 1995, 23, 813-814.

117. Werman, M.J.; Mokady, S.; Nimni, M.E.; Neeman, I. “The effect of various avocado oils on skin collagen-metabolism, “ Connective Tissue Research. 1991, 26, 1-10.
118. Werman, M.J.; Neeman, I.; Mokady, S. “Avocado oils and hepatic lipid-metabolism in growing rats” Food and Chem. Toxicol. 1991, 29, 93-99.
119. Chen, B. H.; Tang, Y. C. “Processing and stability of carotenoid powder from carrot pulp waste” J. Agric. Food Chem. 1998, 46, 2312-2318.
120. Liessens, B.; Grootaerd, H.; Verstraete, W. “Utilization of carrot pulp/pomace as alternative RACOD-source enhancing granulation and sludge bed stability in UASB reactors” Eleventh Forum for Applied Biotechnology, Faculty of Agricultural and Applied Biological Sciences. 1997, 62, 1553-1555.
121. Garg, N.; Hang, Y.D. “Microbal-production of organic-acids from carrot processing waste” J. of Food Sci. & Technol. 1995, 32, 119-121.
122. Yoon, K.Y.; Cha, M.; Shin, S.R.; Kim, K.S. “Enzymatic production of a soluble-fibre hydrolyzate from carrot pomace and its sugar composition” Food Chemistry. 2005, 92, 151-157.
123. Bhatti, H.N.; Nasir, A.W.; Hanif, M.A. “Efficacy of Daucus carota L. waste biomass for the removal of chromium from aqueous soluions” Desalination. 2010, 253, 78-87.
124. Jamshidian, M.; Tehrany, E.A.; Imran, M.; Jacquot, M.; Desobry, S. “Poly-lactic acid: production, applications, aanocomposites, and release studies” Comp. Revs. Food Sci. & Food Safety. 2010, 9, 552-571.
125. Nepote, V.; Grosso, N.R.; Guzman, C. A. “Extraction of antioxidant components from peanut skins”. Grasas y Aceites. 2002, 53, 391-395.
126. Woodroof, J.G. “Peanuts. Production, processing, products”; The AVI Publishing: Western Conneticut, 1983. p. 141.
127. Yeboah, Y.D.; Bota, K.B.; Wang, Z. “Hydrogen from biomass for urban transportation. hydrogen, fuel cells and infrastructure technologies”; Program Review Meeting: Berkeley, CA, 2003, pp. 18-22.
128. NPRL National Peanuy Research Laboratory, USDA United States Department of Agriculture. Peanuts-Other uses. http://www.ars.usda.gov/Main/site_main.htm?modecode=66-04-00-00 (last accessed April 23 , 2013)
129. Chang, E. “Peanut shells, corn stalks: China's alternative to coal?” CNN World. http://articles.cnn.com/2009-12-06/world/china.alternative.energy.coal_1_chinese-government-boilers-low-carbon?_s=PM:WORLD (last accessed April 23, 2013).
130. Evans, R.J. “Renewable hydrogen production by catalytic steam reforming of peanut shells pyrolysis products” Clark Atlanta University: Fuel Chemistry Division Preprints. 2002, 2, 757-758.
131. Bieak, N.; George, B.R. “Utilization of peanut shell fibers in nonwoven erosion control materials” Int. Nonwoven J. 2003, 60-65.

132. Chamarthy, S.; Seo, C.W.; Marshall, W.E. “Adsorption of selected toxic metals by modified peanut shells” J. Chem. Technol. & Biotechnol. 2001, 76, 593-597.
133. Asubiojoa, O. I.; Ajelabia, O. B. “Removal of heavy metals from industrial wastewaters using natural adsorben” Toxic. & Environ. Chem. 2009, 91, 883–890.
134. ScienceDaily. “Peanut Husks Could Be Used Clean Up Waste Water”. http://www.sciencedaily.com/releases/2007/11/071108080114.htm (last accessed April 23, 2013).
135. Bauder, J. “Cereal crop residues and plant nutrients”. Montana State University Communications Services. http://www.montana.edu/cpa/news/wwwpb-archives/ag/baudr230.html (last accessed April 23, 2013)
136. Deswarte, F.E.I.; Clark, J.H.; Hardya, J.J.E.; Rose, P.M. “The fractionation of valuable wax products from wheat straw using CO_2” Green Chemistry. 2005, 8, 39-42.
137. Sleaford renewable energy plant. “The Sleaford project technology”. http://www.sleafordrep.co.uk/?page_id=10. (last accessed April 23, 2013)
138. Mantanis, G.; Berns, J. “Strawboards bonded with urea-formaldehyde resins” Presentation made at the 35th Int. Particleboard/Composite Mat. Symp. WSU, Pullman, USA, 2001.
139. Daizhong, S.; Quingbin, Z.; Shifan, Z. “Technical parameters of rice-straw board with fire-retardant of wood” Key Eng. Mat. 2010, 419-420, 549-552.
140. King, B. “Design of straw bale buildings”; Green Building Press, 2006.
141. Department for environment food and rural affairs, Controls on animal by-product. Guidance on Regulation (EC) 1069/2009 and accompanying implementing regulation (EC) 142/2011, enforced in England by the animal by-products (Enforcement) (England) Regulations 2011. 2011, pp. 1-26.
142. Verheijen, L.A.H.M.; Wiersema, D.; Pol, L.W.H. Food and Agriculture Organization of the United Nations. “Management of waste from animal product processing.” http://www.fao.org/WAIRDOCS/LEAD/X6114E/x6114e00.htm#Contents. (last accessed April 23, 2013)
143. United States Department of Agriculture, Office of Global Analysis. “Livestock and Poultry: World Markets and Trade”. Foreign Agricultural Service, 2012, pp 1-25.
144. Feddern, V. ; Cunha Jr., A.; Pra, M.C.; Abreu, P.G.; Filho, J.I.S.; Higarashi, M.M.; Sulenta, M.; Coldebella, A. “Animal Fat Wastes for Biodiesel Production”, In Biodiesel - Feedstocks and Processing Technologies; Montero, G.; Stoytcheva, M.; InTech, 2011, pp. 45-70.
145. Jin, E.; Reddy, N.; Zhu, Z.; Yang, Y. “Graft polymerization of native chicken feathers for thermoplastic applications” J. Agric. Food Chem. 2011, 59, 1729–1738.
146. Mazik, K.; Burdon, D.; Elliott. M. “Seafood-waste disposal at sea – a scientific review”; Institute of Estuarine and Coastal Studies, Hull, U.K., 2005, pp 13-14.
147. Thirunavukkarasu, N.; Dhinamala, K.; Inbaraj, R.M. “Production of chitin from two marine stomatopods Oratosquilla spp. (Crustacea)” J. Chem. Pharm. Res. 2011, 3, 353-359.
148. Beilen, J.B.V.; Poirier, Y. “Production of renewable polymers from crop plants” Plant Journal. 2008, 54, 684-701.

149. Ramesg, H.P.; Tharanathan, R.N. “Carbohydrates-The renewable raw materials of high biotechnological value” Critical Revs. in Biotechnol. 2003, 23, 149-173.
150. Cunha, A.G.; Gandini, A. “Turning polysaccharides into hydrophobic materials: a critical review” Cellulose. 2010, 17, 875-889.
151. Gandini, A. “Perspective, polymers from renewable respurces: A challenge for the future of macromolecular materials” Macromolecules. 2008, 41, 9491-9504.
152. Tester, R. F.; Karkalas, J.; Qi., X. “Starch-composition, fine structure and architecture” J. Cereal Sci. 2004, 39, 151-165.
153. Buleon, A.; Colonna, P.; Planchot, V.; Ball, S. “Starch granules: structure and biosynthesis” Int. J. Biol. Macromol. 1998, 23, 85-112.
154. Singh, N.; Singh, J.; Kaur, L.; Sodhi, N.S.; Gill, B.S. “Morphological, thermal and rheological properties of starches frok different botanical sources” Food Chemistry. 2003, 81, 219-231.
155. Fredriksson, H.; Silverio, J.; Andersson, R.; Eliasson, A.C.; Aman, P. “The influence of amylose and amylopectin characrteristics on gelatinization and retrogradation properties of different starches” Carbohydrate Polymers. 1998, 35, 119-134.
156. Vroman, I.; Tighzert, L. “Biodegradable Polymers” Materials. 2009, 2, 307-344.
157. Angellier-Coussy, H.; Putaux, J.L.; Molina-Boisseau, S.; Dufresne, A.; Bertoft, E.; Perez, S. “The molecular structure of waxy maize starch nanocrystals” Carbohydrate Research. 2009, 344, 1558-1566.
158. Hoover, R. “The impact of heat-moisture treatment on molecular structures and properties of starches isolated from different botanical sources” Critical Revs. in Food Sci. & Nutrition. 2010, 50, 835-847.
159. Rahmat, A.R.; Rahman, W.A.W.A.; Sin, L.T.; Yussuf, A.A. “Aproches to improve compatibility of starch filled polymer system: A review” Mat. Sci.& Eng. C. 2009, 29, 2370-2377.
160. Averous, L. “Biodegradable multiphase systems based on plasticized starch: A review” Journal of Macromolecular Science. Part C - Polymer Reviews. 2004, C44, 231-274.
161. Tang, X.; Alavi, S. “Review. Recent advances in starch, polyvinyl alcohol based polymer blends, nanocomposites and their biodegradability” Carbohydrate Polymers. 2011, 85, 7-16.
162. Paul, H. “Enzymatic digestion of polysaccharides. Part II: Optimization of polymer digestion and glucose production in microplates”; BioTek., Biofuel Res., Winooski, USA, 2013, pp 1-5.
163. Blazek, J.; Gilbert, E.P. “Effect of enzymatic hydrolysis on native starch granule structure” Biomacromolecules. 2010, 11, 3275-3289.
164. Krassig, H. “Cellulose-morphology, structure, accessibility and reactivity” Papier. 1990, 44, 617-623.
165. Bergue, L.E.R.; Pettersson, L.G. “The mechanism of enzymatic cellulose degradation, purification of a cellulolytic enzyme from Trichoderma viride active on highly ordered cellulose” Eur. J. Biochem. 1973, 37, 21-30. Vol. 37.

166. Garrain, D.; Vidal, R.; Franco, C.; Martinez, P. Global warming impact of biodegradable polymers and biocomposites upon disposal; 1st International Conference on Biodegradable Polymers and Sustainable Composites, Alicante, Spain, 2007, pp 2-33.
167. Hirano, S.; Tsuchida, H.; Nagao, N. "N-acetylation in chitosan and the rate of its enzymatic hydrolysis" Biomaterials. 1989, 10, 574-576.
168. Franca, E.F.; Freitas, L.C.G.; Lins, R.D. "Chitosan molecular structure as a function of N-acetylation" Biopolymers. 2011, 95, 448-460.
169. Pillai, C.K.S.; Paul, W.; Sharma, C.P. "Chitin and chitosan polymers: Chemistry, solubility and fiber formation" Prog. Polym.Sci. 2009, 34, 641-678.
170. Zohuriaan-Mehr, M.J. "Advances in chitin and chitosan modification through graft copolymerization: A comprehensive review" Iranian Polymer J. 2005, 14, 235-265.
171. Jayakumara, R.; Selvamurugana, N.; Nair, S.V.; Tokurab, S.; Tamura, H. "Preparative methods of phosphorylated chitin and chitosan - An overview" Int. J. Biol. Macromol. 2008, 43, 221–225.
172. Kurita, K. "Chitin and chitosan: functional biopolymers from marine crustaceans" Marine Biotechnol. 2006, 8, 203-226.
173. Souza, V.C.; Monte, M.L.; Pinto, L.A.A. "Preparation of biopolymer film from chitosan modified with lipid fraction" Int. J. Food & Technol. 2011, 46, 1856-1862.
174. Hirano, S. "Chitin and chitosan as novel biotechnological materials" Polymer Int. 1999, 48, 732-734.
175. Sashiwa, H.; Aiba, S. "Chemically modified chitin and chitosan as biomaterials" Prog.Polym. Sci. 2004, 29, 887-908.
176. Aranaz, I.; Mengíbar, M.; Harris, R.; Paños, I.; Miralles, B.; Acosta, N. "Functional characterization of chitin and chitosan" Current Chemical Biology. 2009, 3, 203-230.
177. Prashanth, K.V.H.; Tharanathan, R.N. "Chitin/chitosan: modifications and their unlimited application potential - an overview" Trends in Food Sci. & Technol. 2007, 18, 117-131.
178. Kumar, M.N.V.R. "A review of chitin and chitosan applications" Reactive & Functional Polymers. 2000, 46, 1-27.
179. Khoushab, F.; Yamabhai, M. "Chitin research revisted" Marine Drugs. 2010, 8, 1988-2012.
180. Ren, D. ; Yi, H.; Wanga, W.; Ma, X. "The enzymatic degradation and swelling properties of chitosan matrices with different degrees of N-acetylation" Carbohydrate Research. 2005, 340, 2403–2410.
181. Boerjan, W.; Ralph, J.; Baucher, M. "Lignin biosynthesis" Annu. Rev. Plant Biol. 2003, 54, 519-546.
182. Lebo Jr., S.E.; Gargulak, J.D.; McNally, T.J. "Lignin" Kirk-Othmer Encyclopedia of Chemical Technology. 2001, 15, 1-32.
183. Gandini, A.; Belgacem, M.N. "Monomers, polymers and composites from renewable resources.Lignins as components of macromolecular materials"; Elsevier, 2008, Chp. 11, pp. 243-272.

184. Jeffries, T.W. “Biodegradation of lignin and hemicelluloses”, In Biochemistry of Microbial Degradation, Ratledge C.; Kluwer Academic Publisher, Hull, U.K. 1994, pp 233-277.
185. Ko, J.J.; Shimizu, Y.; Ikeda, K.; Kim, S.K.; Park, C.H.; Matsui, S. “Biodegradation of high molecular weight lignin under sulfate reducing conditions: Lignin degradability and degradation by-products” Bioresource Technol. 2009, 100, 1622-1627.
186. Okuda, K.; Man, X.; Umetsu, M.; Takami, S.; Adschiri, T. “Efficient conversion of lignin into single chemical species by solvothermal reaction in water–p-cresol solvent” J. Phys.Condens. Matter. 2004, 16, S1325-S1330.
187. Kishimoto, T.; Uraki, Y.; Ubukata, M. “Chemical synthesis of b-O-4 type artificial lignin” Organic & Biomol. Chem. 2006, 4, 1343–1347.
188. Crestini, C.; Melone, F.; Saladino, R. “Novel multienzyme oxidative biocatalyst for lignin bioprocessing” Bioorganic & Med. Chem. 2011, 19, 5071-5078.
189. Andresen, C.; Demuth , C.; Lange, A.; Stoick , P.; Pruszko, R. “Biobased automobile parts investigation”. A report developed for the USDA Office of energy policy and new uses; Iowa State University, 2012.
190. Raquez, J.M.; Veléglise, M.; Lacrampe, M.F.; Krawczak, P. “Thermosetting (bio)materials derived from renewable resources: A critical review” Progress in Polym. Sci. 2010, 35, 487-509.
191. Martucci, J.F.; Ruseckaite, R.A.; Vazquez, A. “Creep of glutaraldehyse-crosslinked gelatin films” Mat. Sci. & Eng. A. 2006, 435-436, 681-686.
192. Swain, S.N.; Biswal, S.M.; Nanda, P.K.; Nayak, P.L. “Biodegradable soy-based plastics: opportunities and challenges” J. Polym. & Environment. 2004, 12, 35-42.
193. West, J.I.; Hubbell, J.A. “Polymeric biomaterials with degradation polymeric biomaterials with degradation” Macromolecules. 1999, 32, 241-244.
194. Wik, R.M. Henry Ford and Grass-roots America; Univ. Michigan Press., 1992, pp. 148-152.
195. Scrimgeour, C. “Chemistry of fatty acids” Bailey's Industrial Oil and Fat Products. 2005, 6, 1-44.
196. O'Brien, R.D. “Fats and oils: formulating and processing for applications”; Taylor & Francis group, Abingdon, U.K., 2009. p. 212.
197. Desroches, M.; Escouvois, M.; Auvergne, R.; Caillol, S.; Boutevin, B. “From vegetable oils to polyurethanes: synthetic routes to polyols and main industrial products” Polymer Reviews. 2010, 52, 38-79.
198. Petrovic, Z.S. “Polyurethanes from vegetable oils” Polymer Reviews. 2008, 48, 109-155.
199. Zeitsch, K.J. “The chemistry and technology of furfural and its many by-products”; Elsevier, 2000, pp. 3-7.
200. Lewkowski, J. “Synthesis , chemistry and applications of 5-hydroxymethylfurfural and its derivatives” Arkivoc.2001, (i), 17-54.
201. Tong, X.L.; Ma, Y.; Li, Y.D. “Biomass into chemicals: Conversion of sugars to furan derivatives by catalytic processes” Applied Catalysis A-General. 2010, 385, 1-13.

202. Gandini, A. “Furans as offspring of sugars and polkysaccharides and progenitors of a family of remarkable polymers: a review of recent progress” Polymer Chemistry. 2009, 1, 245-251.
203. Averous, P.L. Bioplastics. Biodegradable polyesters. “Biodegradable and biobased polymer, biopolymer, agro-polymer, bioplastic, biomaterial, compostable packaging”. University of Strasbourg.http://www.biodeg.net/index.html (last accessed April 23, 2013)
204. Preethi, R.; Sasikala, P.; Aravind, J. “Microbial production of polyhydroxyalkanoate (PHA) utilizing fruit waste as a substrate” Research in Biotechnol. 2012, 3, 61-69.
205. Marham, P.J.; Keller, A.; Wills, H.H. “The relationship between microstructure and mode of fracture in polyhydroxybutyrate” J. Polym. Sci. Polym.Phys. Edition. 1986, 24, 69-77.
206. Noda, I.; Green, P.R.; Satkowski, M.M.; Schechtman, L.A. “Preparation and properties of a novel class of polyhydroxyalkanoate copolymers” Biomacromolecules. 2005, 6, 580-586.
207. Kessler, B.; Witholt, B. “Perspective of medium chain lenght poly(hydroxyalcanoates), a versatileset of bacterialbioplastics” Curr. Opin. Biotechnol. 1999, 3, 279-285.
208. Mochizuki, M.; Hirami, M. “Structural effects on the biodegradation of aliphatic polyesters” Polymers for Advance Technologies. 1997, 8, 203-209.
209. Philip, S.; Keshavarz, T.; Roy, I. “Polyhydroxyalkanoates: biodegradable polymers with a range of applications” J. Chem. Technol. Biotechnol. 2007, 82, 233-247.
210. Barham, P.J.; Keller, A. “The relationship between microstructure and mode of fracture in polyhydroxybutyrate” J. Polym. Sci. Polym. Phys. Edition. 1986, 24, 69-77.
211. Mohanty, A.K.; Misra, M.; Hinrichsen, G. “Biofibres, biodegradable polymers and biocomposites: An overview” Macro.Mater.Eng. 2000, 276, 1-24.
212. Federle, T.W.; Barlaz, M.A.; Pettigrew, C.A.; Kerr, K.M. “Anaerobic biodegradation of aliphatic polyesters: poly(3-hydroxybutyrate-co-3-hydroxyoctanoate) and poly(E-caprolactone)” Biomacromolecules. 2002, 3, 813-822.
213. Bernd, H.A.R.; Steinbüchel, A. “Polyhydroxyalkanoate (PHA) synthases: the key enzymes of PHA synthesis” Biopolymers Online. 2008, 173-180.
214. Ohkouchi, Y.; Inoue, Y. “Direct production of L(+)-lactic acid from starch and food wastes using Lactobacillus manihotivorans LMG18011” Bioresource Technology. 2006, 97, 1554–1562.
215. John, R.P.; Nampoothiri, K.M. “Fermentative production of lactic acid from biomass: an overview on process developments and future perspectives” Appl Microbiol Biotechnol. 2007, 74, 524-534.
216. Jamshidian, M.; Tehrany, E. A.; Imran, M.; Jacquot, M.; Desobry, S. “Poly-lactic acid: production, applications, nanocomposites, and release studies” Comp. Revs. in Food Sci. & Food Safety. 2010, 9, 552-571.
217. Nampoothiri, K.M.; Nair, N.R.; John, R.P. “An overview of the recent developments in polylactide (PLA) research” Bioresource Technol. 2010, 101, 8493-8501.
218. Zenkiewicz, M.; Richert, J.; Rytlewski, P.; Moraczewski, K.; Stepczynska, M.; Karasiewicz, T. “Characterisation of multi-extruded poly(lactic acid)” Polymer Testing. 2009, 28, 412-418.

219. Geuss, M. “Enzymatic catalysis in the synthesis of new polymer architectures and materials”; Dissertation, Technische Universiteit Eindhoven, 2007. p. 6.
220. Kobayashi, S.; Uyama H.; Kimura S. “Enzymatic polymerization” Chemical Reviews. 2001, 101, 3793-3818.
221. Wu, Y.M.; Mao, X.; Wang, S.J.; Li, R.Z. “Improving the nutritional value of plant foods thorugh transgenic approaches” Chinese J. Biotechnol. 2004, 20, 471-476.
222. Ahmad, P.; Ashraf, M.; Younis, M.; Hu, X.; Kumar, A.; Akram, N.A.; Al-Qurainy, F. “Role of transgenic plants in agriculture and biopharming” Biotechnology Advances. 2012, 30, 524-540.
223. Shewry, P.R.; Jones, H.D.; Halford, N.G. “Plant Biotechnology: Transgenic Crops” Adv. Biochem. Engin./Biotechnol. 2008, 111, 149-186.
224. Newmann, K.; Stephan, D.P.; Ziegler, K.; Huhns, M.; Broer, I.; Lockau, W.; Pistorius, E.K. “Production of cyanophycin, a suitable source for the biodegradable polymer polyaspartate, in transgenic plants” Plant Biotechnol. J. 2005, 3, 249-258.
225. Snell, K.D.; Peoples, O.P. “Polyhydroxyalkanoate polymers and their production in transgenic plants” Metabolic Engineering. 2002, 4, 29-40.
226. Riesmeier, J.; Kobmann, J.; Trethewey, R.; Heyer, A.; Landschiitze, V.; Willmitzer, L. “Production of novel polymers in transgenic plants” Polym. Degrad. & Stabil. 1998, 59, 383-386.
227. Kurdikar, D.; Fournet, L.; Slater, S.C.; Paster, M.; Gerngross, T.U.; Coulon, R. “Greenhouse gas profile of a plastic material derived from a genetically modified plant” J. Ind. Ecol. 2001, 4, 107-122.
228. Devine, M.D. “Why are there not more herbicide-tolerant crops?” Pest. Manag. Sci. 2005, 61, 312-317.
229. Ku, H.; Wang, H.; Pattarachaiyakoop, N.; Trada, M. “A review on the tensile properties of natural fiber reinforced polymer composites” Composites: Part B. 2011, 42, 856–873.
230. Kalia, D.; Kaith, B.S.; Kaur, I. “Pretreatments of natural fibers and their application as reinforcing material in polymer composites-A review” Polym. Engng. &Sci. 2009, 49, 1253-1272.
231. Summerscales, J.; Dissanayake, N.; Virk, A.; Hall, W. “A review of bast fibres and their composites. Part 2 – Composites” Composites: Part A. 2010, 41, 1336–1344.
232. Khalil, H.P.S.A.; Bhat, A.H.; Yusra, A.F.I. “Green composites from sustainable cellulose nanofibrils: A review” Carbohydrate Polymers. 2012, 87, 963– 979.
233. Lotus cars, Engineering. 2012 Group Lotus PLC. http://www.lotuscars.com/engineering/eco-elise (last accessed April 23, 2013)
234. Chaudhary, D.S.; Jollands, M.C.; Cser, F. “Recycling rice hull ash: A filler material for polymeric composites?” Advances in Polymer Technology. 2004, 23, 147-155.
235. Lee, J.G.; Culter, I.B. “Formation of silicon carbide from rice hulls” Bull. Amer. Ceram. Soc. 1975, 54, 195-198.

236. Petchwattana, N.; Covavisaruch, S. “Influences of particle sizes and contents of chemical blowing agents on foaming wood plastic composites prepared from poly(vinyl chloride) and rice hull” Mater. & Design. 2011, 32, 2844-2850.
237. Ndazi, B.S.; Karlsson, S. “Characterization of hydrolytic degradation of polylactic acid/rice hulls composites in water at different temperatures” Express Polym.Lett. 2011, 5, 119-131.
238. Dimzoski, B.; Bogoeva-Gaceva, G.; Gentile, G.; Avella, M.; Grozdanov, A. “Polypropylene-based eco-composites filled with agricultural rice hulls waste” Chemical and Biochemical Engineering Quarterly. 2009, 23, 225-230.
239. Wang, W.H.; Wang, Q.W.; Xiao, H.; Morrell, J.J. “Effects of moisture and freeze-thaw cycling on the quality of rice-hull-PE composite” Pigment and Resin Technol. 2007, 36, 344-329.
240. Dixit, N.; Kortschot, M.T.; Sain, M.; Gulati, D. “Effect of interactions between interface modifiers and viscosity modifiers on the performance and processibility of the rice hulls-HDPE composites” J. Reinforced Plast. & Comps. 2006, 25, 1691-1699.
241. Chollakup, R.; Tantatherdtam, R.; Ujjin, S.; Sriroth, K. “Pineapple leaf fiber reinforced thermoplastic composites: effects of fiber length and fiber content on their characteristics” J. Appl. Polym. Sci. 2011, 119, 1952-1960.
242. Santafe, H.P.G.; Lopes, F.P.D.; Costa, L.L.; Monteiro, S.N. “Mechanical properties of tensile tested coir fiber reinforced polyester composites” Revista Materia. 2010, 15, 113-118.
243. Chattopadhyay, S.K.; Singh, S.; Pramanik, N.; Niyogi, U.K.; Khandal, R.K.; Uppaluri, R.; Ghoshal, A.K. “Biodegradability studies on natural fibers reinforced polypropylene composites” J. Appl.Polym. Sci. 2011, 21, 2226-2232.
244. Run-Cang, S. “Cereal straw as resource for sustainable biomaterials and biofuels”; Elsevier,Oxford, U.K., 2010.
245. Belgacem, M.N.; Gandini. A. “Furan-based adhesives”, In Handbook of ahesives technology,revised and expanded, 2nd Edition ; Pizzi, A. ; Mittal, K.L. Eds: CRC Press, 2003, pp 615-634.
246. Okada, A.; Usuki, A. “Twenty years of polymer-clay nanocomposites” Macromolecular Mater. Eng. 2006, 291, 1449-1476.
247. Chen, B.; Evans, J.R.G.; Greenwell, H.C.; Boulet, P.; Coveney, P.V.; Bowden, A.A.; Whiting, A. “A critical appraisal of polymer-clay nanocomposites” Chem. Soc. Revs. 2008, 37, 598-594.
248. Chen, B. “Polymer–clay nanocomposites: an overview with emphasis on interaction mechanisms” Br. Ceram. Trans. 2004,103, 241-249 .
249. Woodruff, M.A.; Hutmacher, D.W. “The return of a forgotten polymer-polycaprolactone in the 21st century” Prog. Polym. Sci. 2010, 35, 1217-1256.
250. Szekely, J.; Evans, J.W.; Sohn, H.Y. “Gas-solid reactions”; Academic Press NY, 1976.
251. Kung S.D.; Yang S.F. “Discoveries in Plant Biology, Volume I”; World Scientific Publishing: USA, 1998; pp 333-338.
252. Florida Chemical Company Inc., Inside Florida Chemical http://www.floridachemical.com/whatisd-limonene.htm (last accessed March 12, 2013)

253. Grau, R.J.; Zgolicz, P.D.; Gutierrez, C.; Taher, H.A. “Liquid phase hydrogenation, isomerization and dehydrogenation of limonene and derivatives with supported palladium catalyst” Journal of Molecular Catalysis A:Chemical. 1999, 148, 203-214.
254. Weyrich, P.A.; Holderich, W.F. “Dehydrogenation of limonene over Ce promoted, zeolite supported Pd catalysts” J. Mol. Catal. A: General. 1996, 158, 145-162.
255. Martin-Luego, M.A.; Yates, M.; Domingo, M.J.M.; Casal, B.; Iglesias, M.; Esteban, M.; Ruiz-Hitzky, E. “Synthesis of p-cymene from limonene, a renewable feedstock” J. Mol. Catal. B: Environmental. 2008, 81, 218-224.
256. Neumann, R.; Liseel, M. “Aromatization of hydrocarbons by oxidative dehydrogenation catalyzed by the mixed addenda heteropoly acid H5PMo10V2040” J.Org.Chem. 1989, 54, 4607-4610.
257. Fernandes, C.; Catrinescu, C.; Castillo, P.; Russo, P.A.; Carrot, M.R.; Breen, C. “Catalytic conversion of limonene over acid activated Serra de Dentro (SD) bentonite” J. Mol. Catal. A: General. 2007, 318, 108-120.
258. Bueno, A.C.; Brandao, B.B.N.S.; Gusevskaya, E.V. “Aromatization of para-menthenic terpenes by aerobic oxidative dehydrogenation catalyzed by p-benzoquinone” J. Mol. Catal. A: General. 2008, 351, 226-230.
259. Takeuchi, M.; Kuramoto, M. “Process for producing styrene-based polymer”; United State Patent, 1991, No. 5023304.
260. Lenz, R. W.; Sutherland, J. E.; Westfelt, L. C. “Cationic polymerization of p-substituted α-methylstyrenes” Die Makromolekulare Chemie. 1976, 177, 653-662.
261. Luinstra, G.; Becker, F.; Muller, M.; Meckelnburg, D.; Assmann, J. “Copolymers of ρ-α-dimethylstyrene and thermoplastic compositions”; Unites States Patent, 2010. No. 0261831.
262. Powers, P.O. “Copolymers of dimethylstyrene vinyl fatty esters with butadiene” Ind.& Eng. Chem. 1946, 38, 837-389.
263. Seymour, R.B.; Harris, Jr. F.F.; Branum ,Jr.I. “Copolymers of vinyl compounmds and maleic anhydride” Industrial and Engineering Chemistry. 1949, 41, 1509-1513.
264. Moderna, M.; Bates, R.B.; Marvel, C.S. “Some low molecular weight polymers of d-limonene and related terpenes obtained by Ziagler-type catalysts” Journal of Polymer Science: Part A. 1965, 3, 949-960.
265. Marve, C.S.; Olson, L.E. “Polyalkylene sulfides. XVIII. Polymers from 4-Vinyl-1-cyclohexene and d-limonene” Journal of Polymer Science. 1957, 26, 23-28.
266. Sharma, S.; Srivastava, A.K. “Radical copolymerization of limonene with acrynolitrile: kinetics and mechanism” Polymer-Plastics Technology and Engineering. 2003, 42, 485-502.
267. Sharma, S.; Srivastava, A.K. “Alterning copolymers of limonene with methyl methacrylate: Kinetics and mechanism” Journal of Macromolecular Science Part A: Pure and Applied Chemistry. 2003, 40, 593-603.
268. Douchi, T.; Yamaguch, H.; Minoura, Y. “Cyclocopolymerization of d-limonene with maleic anhydride” European Polymer Journal. 1981, 17, 961-968.

269. Satoh, K.; Matsuda, M.; Nagai, K.; Kamigaito, M. “AAB-sequence living radical chain copolymerization of naturally occurring limonene with maleimide: an end-to-end sequence-regulated copolymer” J.Am.Chem.Soc. 2010, 132, 10003-10005.
270. Byrne, C.M.; Allen, S.D.; Lobkovsky, E.B.; Coates, G.W. “Alternating copolymer of limonene oxide and carbone dioxide” J. Am. Chem. Soc. 2004, 126, 11404-11405.
271. Sawalha, H.; Schroen, K.; Boom, R. “Addition of oils to polylactide casting solutions as a tool to tune film morphology and mechanical properties” Polymer Engineering and Science. 2010, 50, 513-519.
272. Mathers, R.T.; Damodaran, K.; Rendos, M.G.; Lavrich, M.S. “Functional hyperbranched polymers using ring-opening metathesis polymerization of dicyclopentadiene with monoterpenes” Macromolecules. 2009, 42, 1512-1518.
273. Comino, C.; Lanteri, S.; Portis, E.; Acquadro, A.; Romani, A.; Hehn, A.; Larbat, R.; Bourgaud, F. “Isolation and functional characterization of a cDNA coding a hydroxycinnamoyltransferase involved in phenylpropanoid biosynthesis in *Cynara cardunculus L*” BMC Plant Biology. 2007, 1-14.
274. Lewis, C.E.; Walker, J.R.L.; Lancaster, J.E.; Sutton, K.H. “Determination of anthocyanins, flavonoids and phenolic acids in potatoes. I: coloured cultivars of *Solanum tuberosum* L” J. Sci. Food Agric. 1998, 77, 45-57.
275. Brown, C.R. “Antioxidants in potato” Amer. J. of Potato Res. 2005, 82, 163-172.
276. Friedman, M. “Chemistry, biochemistry, and dietary role of potato polyphenols. A review” J. Agric. Food Chem. 1997, 45, 1523-1540.
277. Voigt, J.; Noske, R. “On the question of chlorogenic acid content of raw and stewed potatoes” Aus dem Institut fur Ernahrung. 1964, 8, 19-27.
278. Liu, J.J.; Zhao, G.L.; Wang, H.; Zhang, X.H. “Extraction process of chlorogenic acid in flos Ionicerae by enzymatic treatment” Journal of Central South University of Technology. 2002, 9, 246-249.
279. Li, H.; Chen, B.; Yao, S. “Application of ultrasonic technique for extracting chlorogenic acid from *Eucommia ulmodies Oliv. (E. ulmodies)*” Ultrasonics Sonochemistry. 2005, 12, 295-300.
280. Chen, Y.; Yu, Q.J.; Li, X.; Luo, Y.; Liu, H. “Extraction and HPLC characterisation of chlorogenic acid from tobacco residuals” Separation Science and Technology. 2007, 42, 3481-3492.
281. Siwawej, S.; Jaisaard, N. “Extraction of phenolic compounds from potato peel” Kasetsart University Annual Conference of Bangkok. 2003, 12-19.
282. Andrich, G.; Stevanin, E.; Zinnai, A.; Venturi, F.; Fiorentini, R. “Extraction kinetics of natural antioxidants from potato industry” International Society for Advancement of Supercritical Fluids.
283. Rodriguez, D.S.D.; Hadley, M.; Holm, E.T. “Phenolics in aqueous potato peel extract: Extraction, identification and degradation” Journal of Food Science. 1994, 59, 649-651.

284. Singh, A.; Sabally, K.; Kubow, S.; Donnelly, D.J.; Gariepy, Y.; Orsat, V.; Raghavan, G.S.V. "Microwave-assisted extraction of phenolic antioxidants from potato peels" Molecules. 2011, 16, 2218-2232.
285. Singh, P.P.; Saldaña, M.D.A. "Subcritical water extraction of phenolic compounds from potato peel" Food Research International. 2011, 44, 2452–2458.
286. Li, H.; Liu, Y.; Zhang, Z.; Liao, H.; Nie, L.; Yao, S. "Separation and purification of chlorogenic acid by molecularly imprinted polymer monolithic stationary phase" Journal of Chromatography A. 2005, 1098, 66–74.
287. Maslak, A. "Einfluss erhoohter atmospharischer CO_2-konzentrationen auf den sekundarstoffwechsel und pathogenabwehrmechanismen von nicotina tabacum" Dissertation zur Erlangung des akademischen Grades doctor rerum naturalium. Martin-Luther-Universität Halle-Wittenberg, 2002.
288. Pierpoint, W.S. "The enzymic oxidation of chlorogenic acid and some reactions of the quinone produced" Biochem. Journal. 1966, 98, 567-580.
289. Richard-Forget, F.C.; Rouet-Mayer, M.A.; Goupy, P.M.; Philippon, J.; Nicolas, J.J. "Oxidation of chlorogenic acid, catechins, and 4-methylcatechol in model solutions by apple polyphenol oxidase" J. Agric. Food Chem. 1992, 40, 2114-2122.
290. Horrilo-Martinez, P.; Virolleaud M.A.; Jaekel C. "Selective palladium-catalyzed dehydrogenation of limonene to dimethylstyrene" Chem. Cat. Chem. 2010, 2, 175-181.
291. British Standars Institution. "Methods for determination of the viscosity of liquids" Vol. BS 188, 1977.
292. Kaye & Laby. "Tables of physical and chemical constants." National Physical Laboratory, 16th edition, 1995.
293. Kim, Y.; Uyama, H.; Kobayashi, S. "Enzymatic template polymerization of phenol in the presence of water-soluble polymers in an aqueous medium" Polymer J. 2004, 36, 992-998.
294. Oguchi, T.; Tawaki, S.; Uyama, H.; Kobayashi, S. "Enzymatic synthesis of soluble polyphenol" Bull.Chem.Soc.Jpn. 2000, 73, 1389-1396.
295. Xu, P.; Uyama, H.; Whitten, J.E.; Kobayashi, S.; Kaplan, D.L. "Peroxidase-catalyzed in situ polymerization of surface oriented caffeic acid" J.Am.Chem.Soc. 2005, 127, 11745-11753.
296. Mularczyk, E.; Drzymala, J. "Separation of oleic acid from fatty acid impurities" Separation Science and Technology. 1989, 24, 151-155.
297. Haraldsson, G. "Separation of saturated/unsaturated fatty acids" Journal of the American Oil Chemists' Society. 1984, 61, 219-222.
298. Zuo, J.; Shaojun, L.; Bouzidi, L.; Suresh, S.N."Thermoplastic polyester amides derived from oleic acid" Polymer. 2011, 52, 4503-4516.
299. Gan, L.H.; Goh, S.H.; Ooi, K.S. "Kinetic studies of epoxidation and oxirane cleavage of palm olein methyl esters" Journal of the American Oil Chemists Society. 1992, 69, 347-351.
300. Martini, D.S.; Braga, B.A.; Samios, D. "On the curing of linseed oil epoxidized methyl esters with different cyclic dicarboxylic anhydrides" Polymer. 2009,50, 2919-2925.

301. Nicolau, A.; Mariath, R.M.; Martini, E.A.; Martini, D.S.; Samios, D. "The polymerization products of epoxidized oleic acid and epoxidized methyl oleate with cis-1,2-cyclohexanedicarboxylic anhydride and triethylamine as the initiator: Chemical structures, thermal and electrical properties" Materials Science and Engineering: C. 2010, 30, 951-962.
302. Rosch, J.; Mulhaupt, R. "Polymers from renewable resoureces: polyester resins and blends based upon anhydride-cured epoxidized soybean oil" Polymer Bulletin, 1993, 31, 679-685.
303. Bykov, V.V.; Bumagin, N.A. "Effect of water on the palladium-catalyzed reaction of styrene with iodobenzene" World Russ.Chem.Bull. 1997, 46, 1401-1404
304. Ohtsuka, H.; Tabata, T. "Effect of water vapor on the deactivation of Pd-zeolite catalysts for selective catalytic reduction of nitrogen monoxide by methane" Applied Catalysis B: Environmental, 1999, 21, 133-139.
305. Long, G.; Meek, M.E.; Lewis M. "Concise International Chemical Assessment Document 31, N,N-Dimethylformamide" World Health Organization, International Programme on Chemical Safety, Geneva, 2001.
306. Steinhoff, B.A.; King, A. E.; Stahl, S.S. "Unexpected roles of molecular sieves un palladium-catalyzed aerobic alcohol oxidation" J. Org. Chem. 2006, 71, 1861-1868.
307. Nyquist, A.S.; Kropa, E.L. "Method of preparing polymeric materials from isopropenyl toluene" United State Patent Office, Vol. 2,490,372A. 1949
308. Harris, K.R. "Temperature and density dependence of the viscosity of toluene" J. Chem. Eng. Data. 2000, 45, 893-897.
309. McLinden, M.O.; Splett, J.D. "A liquid density standard over wide ranges of temperature and pressure based on toluene" J. Res. Natl. Inst. Stand. Technol. 2008, 113, 29-67.
310. Burge, D.E.; Bruss, D.B. "Preparation and properties of some poly-α-methylstyrenes" Journal of Polymer Science: Part A. 1963, 1, 1927-1935.
311. American Polymer Standards Corporation. Mark-Houwink Parameters for Polymers. http://www.ampolymer.com/a%20&%20K.html (last accessed July 24, 2013)
312. Cuadros, J.; Aldega, L.; Vetterlein, J.; Drickamer, K.; Dubbin, W. "Reactions of lysine with montmorillonite at 80 ◦C: Implications for optical activity, H^+ transfer and lysine–montmorillonite binding" Journal of Colloid and Interface Science. 2009, 333, 78-84.
313. Kitadai, N.; Yokoyama, T;, Nakashima, S. "*In* situ ATR-IR investigation of L-lysine adsorption on montmorillonite" Journal of Colloid and Interface Science. 2009, 338, 395–401.
314. Parbhakar, A.; Cuadros, J.; Sephton, M.A.; Dubbin, W.; Coles, B.J., Weiss, D. "Adsorption of L-lysisne on montmorillonite" Colloids and Surfaces A: Physicochem. Eng. Aspects. 2007, 307, 142-149.
315. Lubbert, A.; Nguyen, T.Q.; Sun, F.; Sheiko, S.S.; Klok, H.A. "L-lysine dendronized polystyrene" Macromolecules. 2005, 38, 2064-2071.
316. Tsuchida, E.; Nishide, H.; Ishimaru, N.; Montgomery, D.D.; Anson, F.C. "Electrochemical response of electrodes coated with lysine-styrene block copolymers with microphase-separated structures" J.Phys.Chem. 1987, 91, 2898-2902.

317. Timochenco, L.; Grassi, V.G.; Pizzol, M.D.; Costa, J.M.; Castellares, L.G.; Sayer, C.; Machado, R.A.F.; Araujo, P.H.H. "Swelling of organoclays in styrene. Effect on flammability in polystyrene nanocomposites" Polymer Letters. 2010, 4, 500-508.
318. Fu, X.A.; Qutubuddin, S. "Swelling behavior of organoclays in styrene and exfoliation in nanocomposites" Journal of Colloid and Interface Science. 2005, 283, 373–379.
319. Liauw, C.M.; Lees, G.C.; Rothon, R.N.; Wilkinson, A.N.; Limpanapittayatorn, P. "Evaluation of an alternative modification route for layered silicates and synthesis of poly(styrene) layered silicate nanocomposites by in-situ suspension polymerisation" Composite Interfaces. 2007, 14, 361-386.
320. Arioli, R.; Goncalves, O.H.; Castellares, L.G.; da Costa, J.M.; Araujo, P.H.; Machado, R.; Bolzan, A. "Effect of foster swelling degree in polystyrene/clay nanocomposites obtained by *in situ* incorporation." Macromol. Symp. 2006, 245-246, 337-342.
321. Fu, X.A.; Qutubuddin, S. "Polymer–clay nanocomposites: exfoliation of organophilic montmorillonite nanolayers in polystyrene" Polymer. 2001, 42, 807-813.
322. Cayman Chemical Company. "Product information of caffeic acid" catalog No. 70602, 2010.
323. Inoue, K. "Functional dendrimers, hyperbranched and star polymers" Prog. Polym. Sci. 2000, 25, 453-571.
324. Yang, J. "Modifications of epoxy resins with functional hyperbranched poly(arylene ester)s" Dissertation submitted to the faculty of the Virginia Polytechnic Institute and State University, 1998.
325. Hult, A.; Johansson, M.; Malmstrom, E. "Hyperbranched polymers" Advances in Polymer Science. 1999, 143, 1-34.
326. Kricheldorf H.R., Bolender, O.; Stukenbrock, T. "Hyperbranched poly(ester-amide)s derived from 3,5-dihydroxybenzoic acid and 3,5-diaminobenzoic acid" Macromol. Chem. Phys. 1997, 198, 2651-2666.
327. Aktas, N.; Tanyolac, A. "Kinetics of laccase-catalyzed oxidative polymerization of catechol" J. Mol. Catalysis B: Enzymatic. 2003, 22, 61–69.
328. Aktas, N.; Sahiner, N.; Kantogly, O.; Salih, B.; Tayolac, A. "Biosynthesis and characterization of laccase catalyzed poly(catechol)" J. Polym. & Environ. 2003, 11, 123-128.
329. Kim, S.; Silva, C.; Evtuguin, D.V.; Gamelas, J.A.F.; Cavaco-Paulo, A. "Polyoxometalate/laccase-mediated oxidative polymerization of catechol for textile dyeing" Appl. Microbiol. Biotechnol. 2011, 89, 981–987.
330. Dubey, S.; Singh, D.; Misra, R.A. "Enzymatic synthesis and various properties of poly(catechol)" Enzyme and Microbial Technology. 1998, 23, 432–437.
331. Nabid, M.R.; Zamiraei, Z.; Sedghi, R.; Nazari, S. "Synthesis and characterization of poly(catechol) catalyzed by porphyrin and enzyme" Polym. Bull. 2010, 64, 855-865.
332. Hong, L.; Cui, Y.; Wang, X.; Tang, X. "Synthesis of a novel one-pot approach of hyperbranched polyurethanes and their properties" Journal of Polymer Science Part A. 2001, 40, 344-350.

333. Haifeng, L.; Yuwen, L.; Xiaomin, C.; Zhivong, W.; Cunxin, W. “Effects of sodium phosphate buffer on horseradish peroxidase thermal stability” Journal of Thermal Analysis and Calorimetry, 2008, 93, 569-574.
334. Ryu, K.; Dordick, J.S. “Kinetic behaviour and substrate specificity horseradish peroxidase in water-miscible solvents” Resources, Conservation and Recycling, 1990, 3, 177-185.
335. Tonami, H.; Uyama, H.; Kibayashi, S.; Kubota, M. “Peroxidase-catalyzed oxidative polymerization of m-substituted phenol derivatives” Macromol. Chem. Phys. 1999, 200, 2365–2371.
336. Kobayashi, S.; Uyama, H.; Ushiwata, T.; Uchiyama, T.; Sugihara J.; Kurioka H. “Enzymatic oxidative polymerization of bisphenol-A to a new class of soluble polyphenol” Macromol. Chem. Phys. 1998, 199, 777-782.
337. Uyama, H.; Kuiorka, H.; Sugihara, J.; Kobayashi, S. “Enzymatic synthesis and thermal properties of a new class of polyphenol” Bull. Chem. Soc. Jpn., 1996, 69, 189-193.
338. Zhang, L.; Zhang, Y.; Xue, Y.; H., Duana; Cui, Y. “Enzymatic synthesis of soluble phenol polymer in water using anionic surfactant as additive.” Soc. Chem. Ind., 2013, 62, 1277-1282.
339. Zhang, L.; Zhao, W.; Ma, Z.; Nie, G.; Cui, Y. “Enzymatic polymerization of phenol catalyzed by horseradish peroxidase in aqueous micelle system.”European Polymer Journal, 2012, 48, 580-585.
340. Junming, X.; Jianchun, J.; Jing, L. “Preparation of polyesterpolyols from unsaturated fatty acid.” Journal of Applied Polymer Science. 2012, 126, 1377-1384.
341. Tillet, G.; Boutevin, B.; Ameduri, B. “Chemical reactions of polymer crosslinking and post-crosslinking at room and medium temperature” Progress in Polymer Science. 2011, 36, 191-217.
342. Chen, B.; Evans, J.R.G.; Greenwell, H.C.; Boulet, P.; Coveney, P.V.; Bowden, A.A.; Whiting, A. “A critical appraisal of polymer –clay nanocomposites” Chemical Society Reviews. 2008, 37, 568-594.
343. Pielichowska, K.; Glowinkowski, S.; Lekki, J.; Binias, D.; Pielichowski, K.; Jenczyk, J. “PEO/fatty acid blends for thermal energy storage materials. Structural/morphological features and hydrogen interactions” European Polymer Journal. 2008, 44, 3344-3360.
344. Johnson, B. “Polymer nanocomposites by intercalation into self-assembled clays” University College London, 2013
345. Simian Networks, Inc. Customer Technical Support. “Chemical Constants” http://www.floridachemical.com/dlimonenechemical_constants.htm (last accessed August 07, 2013)
346. Ambroziak, K., Mbeleck, R., Saha, B., Sherrington, D. “Greener and sustainable method for alkene epoxidations by polymer-supported Mo(VI) catalysts” International Journal of Chemical Reactor Engineering. 2010, 8, 1-13.
347. Gupta, K.C.; Sutar, A.K.; Lin, C.C. “Polymer-supported Schiff base complexes in oxidation reactions” Coordination Chemistry Reviews. 2009, 253, 1926-1946.

348. Oliveira P.; Rojas-Cervantes, M.L.; Ramos, A.M.; Fonseca, I.M.; Botelho, A.M.; Vital J. "Limonene oxidation over V_2O_5/TiO_2 catalysts" Catalysis Today. 2006, 118, 307-314.
349. Oliveira P.; Machado, A.; Ramos, A.M.; Fonseca, I.M.; Fernnandes, F.M.B.; Botelho, A.M.; Vital, J. "MCM-41 anchored manganese salen complexes as atalysts for limonene oxidation" Microporous and Mesoporous Materials. 2009, 120, 432-440.
350. Dhavalik, R.S.; Bhattacharyya, P.K. "Microbiological transformations of terpenes. XVIII Fermentation of limonene by a soil pseudomonad" Indian Journal of Biochemistry. 1966, 3, 144-157.
351. Lerin, L.; Toniazzo, G.; Oliveira, D.; Rottava, L.; Dariva, C.; Cansain, R.L.; Treichel, H.; Padilha, F.; Antunes, O.A.C. "Microorganisms screening for limonene oxidation" Food Science and Technology (Campinas). 2010, 30, 399-405.
352. Duetz, W.A.; Bouwmeester, H.; Van Beilen, J.B. "Biotranformation of limonene by bacteria, fungi, yesasts and plants" Appl. Microbiol. Biotechnol. 2003, 61, 269-277.
353. Abraham, W.R.; Stumpf, B.; Kieslich, K. "Microbal transformations of terpenoids with 1-p-menthene skeleton" Appl. Microbiol. Biotechnol. 1986, 24, 24-30.
354. Van der Werf, M.J.; Keijzer, P.M., Van der Schaft, P.H. "*Xanthobacter sp*. C20 contains a novel bioconversion pathway for limonene" Journal of Biotechnology. 2000, 84, 133-143.
355. Gunzler, H.; Biochemia**.** "Mango Butter - Ultra Refined™ " http://biochemica.com (last accessed October 04, 2013)
356. Williams, A. "Handbook of Analytical Techniques -Vol. 1": Wiley-VCH, USA, 2001.
357. Bourne, D.W.A. PHAR 7633 Chapter 24 "Pharmaceutical Analysis." http://www.boomer.org/c/p4/c24/c24.pdf. (last accessed August 06, 2013)
358. Mirau, P.A. "A practical guide to understanding the NMR of polymers": Wiley, USA, 2005.
359. Suryanarayana, C.; Norton, M.G. "X-Ray Diffraction, A practical approach": Plenum Publishing Corporation, USA, 2010, pp. 1-94.
360. Sorai, M. "Calorimetry & Thermal Analysis". John Wiley & Sons, USA, 2005
361. Haines, P.J. "Principles of thermal analysis and calorimetry" RSC Paperbacks, Royal Society of Chemistry, Surrey, U.K., 2002.
362. Gunzel, H.; Williams, A. "Handbook of Analytical Techniques" Wiley-VCH, 2001. Vol. II, Germany, 2001.